ANALYTICA CHIMICA ACTA

International monthly devoted to all branches of analytical chemistry
Revue mensuelle internationale consacrée à tous les domaines de la chimie analytique
Internationale Monatsschrift für alle Gebiete der analytischen Chemie

ELSEVIER PUBLISHING COMPANY
AMSTERDAM

Anal. Chim. Acta, Vol. 53, No. 1, 1–224, January 1971
Published monthly

Publication Schedule for 1971

In the interests of rapid publication it has been found necessary to schedule 5 volumes for appearance in 1971. Since monthly publication will be maintained, this implies that 2 of the volumes will each consist of three issues, while 3 of the volumes will each consist of only 2 issues. The following provisional schedule applies:

Vol. **53**, No. **1**	January 1971	
Vol. **53**, No. **2**	February 1971	**(completing Vol. 53)**
Vol. **54**, No. **1**	March 1971	
Vol. **54**, No. **2**	April 1971	
Vol. **54**, No. **3**	May 1971	**(completing Vol. 54)**
Vol. **55**, No. **1**	June 1971	
Vol. **55**, No. **2**	July 1971	**(completing Vol. 55)**
Vol. **56**, No. **1**	August 1971	
Vol. **56**, No. **2**	September 1971	
Vol. **56**, No. **3**	October 1971	**(completing Vol. 56)**
Vol. **57**, No. **1**	November 1971	
Vol. **57**, No. **2**	December 1971	**(completing Vol. 57)**

Subscription price: $17.50 or Dfl. 63.— per volume plus postage. Total subscription price for 1971: $87.50 or Dfl. 315.— plus postage. Additional cost for copies by airmail available on request. For subscribers in the U.S.A. and Canada, 2nd class postage paid at New York, N.Y. For advertising rates apply to the publishers.

Subscriptions should be sent to:

ELSEVIER PUBLISHING COMPANY P.O. Box 211, Amsterdam, The Netherlands

---

GENERAL INFORMATION

Languages

Papers will be published in English, French or German.

Submission of papers

Papers should be sent to:

PROF. PHILIP W. WEST,
Coates Chemical Laboratories,
College of Chemistry and Physics,
Louisiana State University,
Baton Rouge 3,
La. 70803 (U.S.A.)

or to:

DR. A. M. G. MACDONALD,
Department of Chemistry,
The University,
P.O. Box 363
Birmingham B15 2TT (Great Britain)

Reprints

Fifty reprints will be supplied free of charge. Additional reprints (minimum 100) can be ordered at quoted prices. They must be ordered on order forms which are sent together with the proofs.

Journal of Mass Spectrometry and Ion Physics

Editors:
J. FRANZEN (Dortmund)
A. QUAYLE (Chester)
H.J. SVEC (Ames, Iowa)

the journal has 6 issues per volume and approx. two volumes appear per year. Subscription price per volume Dfl. 90.00 plus Dfl. 18.00 postage or equivalent
US$25.00 plus US$5.00

Subscriptions may be placed with your usual supplier or direct with the publisher

Elsevier
Publishing
Company

P.O. BOX 211,
AMSTERDAM, THE NETHERLANDS

CONTENTS VOLUME 5 NO. 1/2

A new single-stage mass spectrometric method for studying charge transfer reactions (D.L. Smith, Salt Lake City, Utah, U.S.A. and L. Kevan, Detroit, Mich., U.S.A.)
General method for computing the statistics of charge amplification in particle and photon detectors used for pulse counting (L.A. Dietz, (Schenectady, N.Y., U.S.A.)
Computer analysis of low resolution mass spectra. Correction for natural abundance of ^{13}C, ^{2}H, ^{15}N, ^{17}O and ^{18}O.(B. Boone, R.K. Mitchum and S.E. Scheppele Stillwater, Okla., U.S.A.)
Ion-optical properties of magnetic prisms with axially symmetric r^{-1} fields and spiral main paths (D. Ioanoviciu, Cluj, Romania)
Calculation of sector-shaped mass spectrometric analysers with curvilinear boundaries (A.A. Sysojev and G.A. Samsonov, Moscow, U.S.S.R.)
Calculation of the current - voltage characteristics of a field ion microscope (V.A. Nazarenko, Kiev, U.S.S.R.)
Ionization, attachement and ion-molecule reactions in oxygen (P.R. Kinsman and J.A. Rees, Liverpool, Great Britain)
Relative sensitivities of twenty elements in the iron matrix for spark-source mass spectrometry (J.M. McCrea, Monroeville, Pa., U.S.A.)
Ionisation and dissociation of carbonyl fluoride and trifluoromethyl hypofluorite by electron impact (J.C.J. Thynne and K.A.G. MacNeil, Edinburgh, Great Britain)
Study of ion-neutral reactions with a time-of-flight double mass spectrometer (J.F. Paulson, F. Dale and S.A. Studniarz, Bedford, Mass., U.S.A.)
Mass-spectrometric observations of uranium and plutonium monohydrides formed by ion-molecule reaction (P.E. Moreland, Jr., D.J. Rokop and C.M. Stevens, Argonne, Ill., U.S.A.)
A study of Penning ionization reactions using a single-source mass spectrometer (E.G. Jones and A.G. Harrison, Toronto, Ontario, Canada)
Ionization potentials of pentaborane(9) derivatives by electron impact and molecular orbital calculations (C.B. Murphy; Jr., Syracuse, N.Y., U.S.A. and R.E. Enrione, Cincinnati, Ohio, U.S.A.)
Electron impact excitation by the SF_6 scavenger technique. II. Benzene and ethylene (M.-J. Hubin-Franskin and J.E. Collin, Liege, Belgium)
Short Communications
Resonant charge transfer reactions in neon, argon and krypton (E.G. Jones and A.G. Harrison, Toronto, Ontario, Canada)
Comment on the rule concerning rearrangement peaks in field ionization mass spectra (H.D. Beckey, Bonn, Germany)

CONTENTS VOLUME 5 NO. 3/4

Current-voltage characteristics and angular distribution of the ions in field ionization (I.V. Goldenfeld and V.A. Nazarenko, Kiev, U.S.S.R.)
Theoretical analysis of a cylindrical time-of-flight mass spectrometer with radial ion paths (M.F. Zabielski, H.T. Diem and B.R.F. Kendall, University Park, Pa., U.S.A.)
A multiple trajectory ion beam analyzer (J.D. Stein and F.A. White, Troy, N.Y., U.S.A.)
Magnet and controller for a fast scanning mass spectrometer (G. Haertel, J.D. Morrison and J.F. Smith, Bundoora, Vic., Australia)
A proposed technique for signal multiplexing in mass spectrometry (C.J. Eckhardt and M.L. Gross, Lincoln, Nebr., U.S.A.)
The interpretation of double resonance signals in ion cyclotrom resonance mass spectrometry (G.C. Goode, A.J. Ferrer-Correia and K.R. Jennings, Sheffield, Great Britain)
On-line acquisition of ionization efficiency data (R.A.W. Johnstone, F.A. Mellon and S.D. Ward, Liverpool, Great Britain)
Multiply charged cluster ions of nitrogen (W. Henkes and G. Isenberg, Karlsruhe, Germany)
Electron impact excitation by the SF_6 scavenger technique. III. Carbon monoxide (M.-J. Hubin-Franskin and J.E. Collin, Liege, Belgium)
Hochempfindlicher Nachweis metastabiler Ein- und Zweistufenzerfälle (U. Löhle und Ch. Ottinger, Freiburg, Deutschland)
Kinetische Energie von Produktionen aus Ionen-Molekül-Reaktionen bei thermischen Energien (P.-J. Bauer und H.-J. Drewitz, Braunschweig und Berlin, Deutschland)
Cryogenic mass spectrometry of reactive fluorine-containing species. I. The mass spectra of sulfur hexafluoride, chlorine trifluoride, chlorine monofluoride, nitrosyl fluoride and tetrafluorohydrazine. II. Applications to synthesis via pyrolysis, photolysis and microwave discharge (S.S. Cristy and G. Mamantov, Knoxville, Tenn., U.S.A.)
Ionisation of tetrafluoroethylene by electron impact (J.C.J. Thynne and K.A.G. MacNeil, Edinburgh, Great Britain)
Short Communications
Determination of background-to-signal ratio in a molecular-beam sampling system (A. Tessier and W. Forst, Quebec, Canada)
Threshold ionization of acetylene by monoenergetic electron impact (F.P. Lossing, Ottawa, Canada)
Bimolecular reactions of trapped ions. II. Reactions in vinyl fluoride (N.A. McAskill and A.G. Harrison, Toronto, Ontario, Canada)
Announcements

A new NORTH-HOLLAND publication in

Biochemistry, Pharmacology, Organic Chemistry, Pathology

Research Progress in Organic, Biological, and Medicinal Chemistry

volume 2

Editors: U. GALLO and L. SANTAMARIA, Societa Editoriale Farmaceutica, Milan, Italy.

1970. 350 pages. Hfl. 60.– (140 s.) ISBN 0 7204 4064 5

This is the second volume in a series publication designed to appeal to medicinal as well as organic and biological chemists. Volume I was published in 1964, and the next volume in the series will be devoted to the chemical, biological, pharmacological and physiophathological aspects of natural and synthesized pigments and dyes.

CONTENTS: Chemistry and pharmacology of hydroxamic acids: *N. P. Buu-Hoi, G. Lambelin, Cl. Gillet.* Structure and biosynthesis of ophiobolins: *L. Canonica, A. Fiecchi.* The biochemistry of human cells in culture: *V. J. Cristofalo, B. V. Howard, D. Kritchevsky.* Chemistry and pharmacology of 3,8-diazabicyclo (3.2.1.) octanes: *G. Cignarella, E. Testa, G. Maffii.* Some recent advances in the field of synthetic steroids, *R. Deghenghi.* Acute toxicities of drugs, solvents and related compounds in laboratory animals: edited by *G. Maffii, G. Schott, M. G. Serralunga.*

Previously published:

Volume 1 – 1964. 599 pages. Hfl. 68.50 (160 s.) ISBN 0 7204 4013 0

AMSTERDAM
P.O. BOX 3489 **NORTH** N·H·C **HOLLAND** PUBLISHING CO.
NETHERLANDS

Sole distributors for the U.S.A. and Canada: American Elsevier Publishing Company, Inc., 52 Vanderbilt Avenue, New York – N.Y. 10017

ANALYTICA CHIMICA ACTA

Vol. 53 (1971)

ANALYTICA CHIMICA ACTA

International monthly devoted to all branches of analytical chemistry
Revue mensuelle internationale consacrée à tous les domaines de la chimie analytique
Internationale Monatsschrift für alle Gebiete der analytischen Chemie

Editors
PHILIP W. WEST *(Baton Rouge, La., U.S.A.)*
A. M. G. MACDONALD *(Birmingham, Great Britain)*

ELSEVIER PUBLISHING COMPANY
AMSTERDAM

Anal. Chim. Acta, Vol. 53 (1971)

PRINTED IN THE NETHERLANDS

Analytica Chimica Acta
Elsevier Publishing Company, Amsterdam
Printed in The Netherlands

THE LIQUID-STATE, IODIDE–SELECTIVE ELECTRODE

J. RŮŽIČKA
Chemistry Department A, The Technical University of Denmark, Building 207, Lyngby (Denmark)
AND K. RALD
Chemical Laboratory D, The Royal Danish School of Pharmacy, Universitetsparken 2, 2100 Copenhagen Ø (Denmark)

(Received August 7th, 1970)

The liquid-state electrode, developed in our laboratory about a year ago[1-4], is a very simple device, consisting of a graphite rod (B), impregnated with the organic phase and placed in a Teflon tube (A) in the manner shown in Fig. 1. While one end of the graphite cylinder (B) is immersed in the measured aqueous sample (E), the other end is covered by the organic phase (C), which is also contained in the reservoir within the Teflon tube. The stainless steel wire (F), which is screwed into the graphite rod serves as a lead to the electronic voltmeter. The organic phase, which penetrates from the reservoir through the pores in the graphite rod, forms at its lower end a nearly invisible, very thin, but continuous layer (D), which prevents direct physical contact between the measured aqueous solution and the graphite rod.

There are several requirements regarding the properties of the organic phase, which must be fulfilled if the electrode is to function properly. First, the organic liquid used must be immiscible with water and preferably should have a low vapour pressure so that it does not appreciably evaporate during use of the electrode. It has also been established that the composition of the organic phase is the controlling factor for the electrode function. If the organic phase consists of a very pure "inert" organic solvent such as carbon tetrachloride, benzene, mesitylene, etc., no definite potential will be established and the electrode will not respond to activity of any particular ion in the measured sample[3]. However, the organic phase can be "doped" by electroactive species, which will "activate" the electrode so that it becomes sensitive to a certain ion in the solution. Thus, for example, mercury(II) ion-selective electrodes can be made by using a solution of mercury(II) dithizonate in carbon tetrachloride, silver(I) ion-selective electrodes by means of a silver dithizonate solution in carbon tetrachloride or in xylene, etc. It has also been established that the higher is the extraction constant of the metal chelate used for "doping" of the organic phase, the more selectively the electrode responds to the activity of the particular ion in the solution[3]. There are, however, other compounds than metal chelates, suitable for making liquid-state electrodes of various types. Thus, recently two potassium ion-selective electrodes were prepared in this laboratory[4]. One employs a solution of valinomycine[5,6] (a cyclic polypeptide) in mesitylene, while the other one utilizes a solution of dicyclohexyl-18-crown-6 (a macrocyclic polyether)[6] in mesitylene. Both electrodes exhibit Nernstian response down to 10^{-5} M potassium(I), but the valinomycine electrode has better selectivity for potassium ions over sodium ions.

In the present paper, an iodide ion-selective electrode, based on solutions of iodine in carbon tetrachloride, benzene and mesitylene, is described. The iodine, which determines the electrode function, is in redox equilibrium with iodide ion in measured aqueous solution and the corresponding redox potential is

$$E = E_0 + (RT/2F) \ln a_{I_2}/(a_{I^-})^2 \qquad (1)$$

where: a_{I_2} is the activity of iodine in aqueous solution, a_{I^-} is the activity of iodide ion in the aqueous solution, and E_0 is the standard potential.

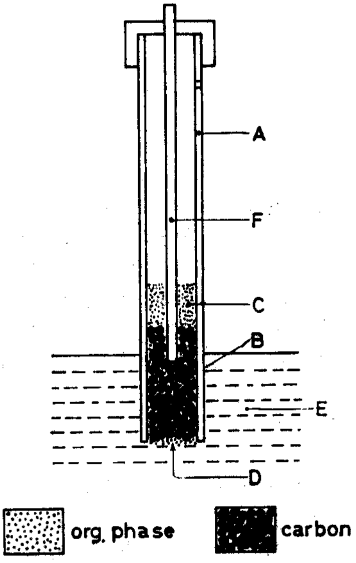

Fig. 1. Construction of the liquid-state electrode. (A) Teflon tube, (B) porous graphite rod, (C) organic phase, (D) the ion-sensitive surface, (E) sample solution, (F) lead off to the potentiometer.

The standard potential E_0 of this iodine electrode of the first kind can be measured by means of a platinum electrode immersed in an *aqueous* solution of iodine, which contains defined quantities of iodide and triiodide ions. The present liquid-state electrode, however, employs solutions of iodine in the *organic* phase, and it is considered that its potential should therefore be:

$$E = E'_0 + (RT/2F) \ln (a_{I_2})_o/(a_{I^-})^2_w \qquad (2)$$

where: $(\ )_o$ denotes the activity in the organic phase and $(\ )_w$ denotes the activity in the aqueous phase. If the discussion is confined to dilute solutions, activities can be replaced by concentrations, so that

$$E = E'_0 + 0.0296 \log [I_2]_o - 0.0592 \log [I^-]_w \quad \text{(at 25°)} \qquad (3)$$

where: $[\ ]_o$ denotes the concentration in the organic phase and $[\ ]_w$ denotes the concentration in the aqueous phase.

From eqn. (3), it follows that the potential of this liquid-state electrode depends on the concentration of iodine in the organic phase as well as on the concentration of the iodide ion in the aqueous sample. Clearly, if both E'_0 and $[I_2]_o$ can be kept constant, an iodide ion-sensitive electrode suitable for practical purposes could be obtained. A comparison of electrodes containing different quantities of iodine in the organic phase is interesting from a theoretical viewpoint, and provides a better understanding of the basic properties of the liquid-state electrodes.

EXPERIMENTAL

Apparatus

The liquid-state electrode. This was constructed as shown in Fig. 1. The materials used, as well as the dimensions of the graphite rod, Teflon tube, etc. were the same as described previously[3]. Each rod was machined to the required size, furnished with a coil, and heated to about 600° for *ca.* 1 min. After it had cooled to room temperature, it was mounted into the Teflon tube as previously described[3]. The open end of the Teflon tube was then connected to a slight vacuum and the other end, containing the carbon rod, was immersed in the solution of iodine in the organic phase. In order to obtain electrodes with reproducible properties, it was found necessary to suck the organic solutions of iodine through the mounted graphite rod for at least 30 min. With shorter treatment, electrodes with differing potentials were occasionally obtained, while longer evacuation periods had no further effect on the electrode potential. This indicates that 30 min is sufficient for reproducible impregnation of graphite rods by means of iodine solutions. The inner resistance of these prepared electrodes varied between 100 and 500 kΩ.

The electrodes, made according to the above procedure, were normally used for several weeks. In order to avoid the evaporation of the organic solvent and consequent changes of iodine concentration in the electrode liquid, the electrodes were stored immersed in the same organic solutions of iodine, with which they were originally impregnated and which was also contained in the electrode cavity. Shortly before the measurement the electrodes were rinsed with redistilled water.

The instruments and glass electrodes used for measurement as well as for automated recording of the potential–pH curves were the same as described previously[1]. As the reference electrode, a saturated calomel electrode (S.C.E.) (K401, Radiometer A/S, Copenhagen) was used. In order to avoid variations of junction potentials, which could be greater than the precision of the measurements, most of the experiments were carried out in $1 \cdot 10^{-3} M$ nitric acid.

Reagents

The chemicals used were of a.r. grade quality, and doubly-distilled water was used in all experiments. All organic solvents were tested for impurities which might eventually reduce iodine so that its concentration in the organic phase would gradually decrease.

RESULTS

Calibration curves

Calibration curves for the liquid-state electrodes impregnated with $1 \cdot 10^{-4} M$,

$1 \cdot 10^{-3}M$ and $1 \cdot 10^{-2}M$ solutions of iodine in benzene are shown in Fig. 2 (curves 1–3). They were prepared by measuring the potentials of these electrodes in $1 \cdot 10^{-3}M$ nitric acid solutions, containing known quantities of sodium iodide. The observed potentials correspond to eqn. (3) down to $1 \cdot 10^{-5}M$ iodide. Below this level the calibration curve forms a plateau and just below $10^{-7}M$ iodide the electrode no longer responds to changes in the iodide ion activity.

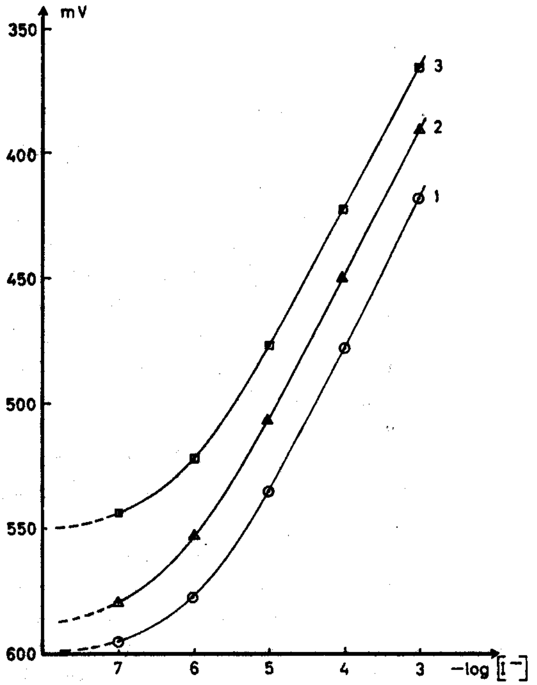

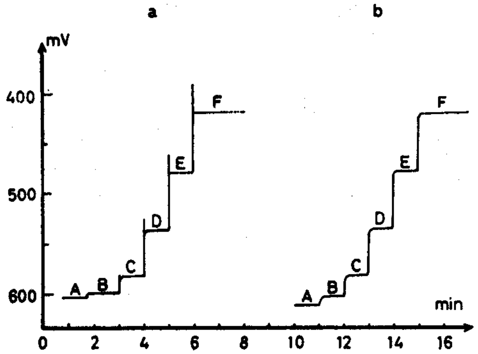

Fig. 2. Calibration curves for the iodide-selective electrodes, with various solutions of iodine in benzene as the organic phase. (○) $1 \cdot 10^{-2}M$ I_2 in C_6H_6, (△) $1 \cdot 10^{-3}M$ I_2 in C_6H_6, (□) $1 \cdot 10^{-4}M$ I_2 in C_6H_6.

Fig. 3. The response of the iodide-selective electrode, with $1 \cdot 10^{-2}M$ I_2 solution in benzene as the organic phase. (A) $1 \cdot 10^{-7}M$ NaI, (B) $1 \cdot 10^{-6}M$ NaI, (C) $1 \cdot 10^{-5}M$ NaI, (D) $1 \cdot 10^{-4}M$ NaI, (E) $1 \cdot 10^{-3}M$ NaI all in $1 \cdot 10^{-3}M$ HNO_3. The maxima, as seen on the first record (a) indicate that the electrode response is much faster than the rate of the mixing of the solution.

Response time

The response of this iodide-sensitive electrode is very fast at all levels of the iodide activities. This was confirmed by adding small volumes of sodium iodide solutions to 100 ml of rapidly stirred $1 \cdot 10^{-3}M$ nitric acid. The potential of the liquid-state electrode (containing $1 \cdot 10^{-2}$ M I_2 in benzene) was measured *versus* the S.C.E. and recorded. In Fig. 3 two consecutive experiments with the same electrode are shown. In the first run (a), the tip of the pipette was always placed close to the liquid-state electrode. The "over-shoots" seen in the recording so obtained reflect the higher activity of iodide ions in the "cloud" of more concentrated solution which was momentarily present at the electrode surface. The next record (b) was made under the same conditions, except that the solution of sodium iodide was pipetted into the stirred solution as far away as possible from the electrode surface. The plateau potentials, however, are the same in both experiments, except of the lowest levels (A, $1 \cdot 10^{-7}$ *M* iodide) where the difference reflects the uncertainty of the measurement at this detection limit.

EFFECT OF PH

The influence of pH was investigated by recording the potential of the liquid-state electrode (containing $1 \cdot 10^{-2} M$ iodine in benzene) in 100 ml of an aqueous sample, containing known amounts of sodium iodide. To this rapidly stirred solution, which was initially $1 \cdot 10^{-3}$ *M* in nitric acid, 0.25 *M* potassium hydroxide was automatically added in precisely controlled increments so that the pH of the solution increased linearly at the rate of 0.5 pH unit per min. The results obtained (Fig. 4) show that the electrode should be used in acidic solutions, because its sensitivity is higher than in more alkaline media. This behaviour indicates that the lower limit of measurement in alkaline solutions is primarily caused by the decrease of iodine concentration in the organic phase and consequently also by the increase of iodide ion concentration in the aqueous phase. This process can be described by the following reactions:

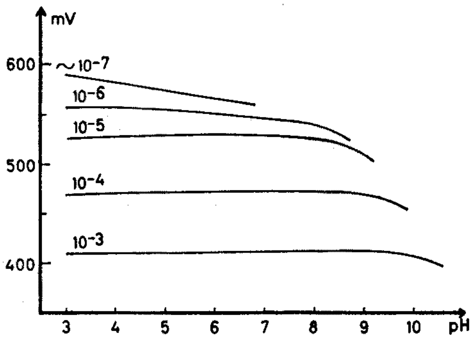

Fig. 4. The potential–pH dependence of the iodide-selective electrode, employing $1 \cdot 10^{-2} M$ solution of iodine in benzene as the organic phase. The influence of pH increases with decreasing concentration of iodide ions in the sample.

$$I_2 + 2\,OH^- = IO^- + I^- + H_2O$$

$$3\,IO^- = 2\,I^- + IO_3^-$$

In this connection it is interesting to note that a change in the organic solvent from benzene to carbon tetrachloride or xylene has no significant effect on the potential–pH dependence, in spite of the fact that the partition coefficient of iodine between water and these solvents is not the same. These observations and also the redox sensitivity of the electrode (see below) indicate that the redox properties of the iodine–iodide–triiodide system are the main factors determining the electrode behaviour.

Reproducibility of measurements

Various electrodes employing benzene, mesitylene or carbon tetrachloride as the organic solvent were tested for reproducibility in $1 \cdot 10^{-3} M$ nitric acid media, in order to avoid interference from hydroxyl ion and traces of reducing species (Tables I–III). Initially, the reproducibility of preparation of the electrodes was investigated. Five electrodes (A–E, Table I) were made by the procedure mentioned, with $1 \cdot 10^{-2} M$ iodine in benzene as the organic phase. Each electrode was first placed in $1 \cdot 10^{-3} M$ nitric acid (first column) and then used in solutions with increasing concentrations of iodide ions. When the first run of measurements was completed, the electrode was rinsed with distilled water and used again, starting from the sample of pure $1 \cdot 10^{-3} M$ nitric acid (first column, second line).

The long-term stability of electrode "C" from Table I was investigated over a period of 5 weeks. The mean values of about twenty measurements made with this electrode (Table II), do not differ at all from the values of the second set of measurements in Table I, thus confirming, together with the low values of the standard deviations, the absence of drift and reasonable precision of measurements.

TABLE I

THE REPRODUCIBILITY OF PREPARATION OF THE LIQUID-STATE IODIDE-SELECTIVE ELECTRODES

(All results given in mV measured against S.C.E.)

Electrode[b]	$1 \cdot 10^{-3} M\ HNO_3$	*Concentration of iodide in sample*				
		$0.97 \cdot 10^{-7}$	$1.06 \cdot 10^{-6}$	$1.06 \cdot 10^{-5}$	$1.05 \cdot 10^{-4}$	$1.04 \cdot 10^{-3}$
A 1[a]	585	584	575	537	479	421
2	595	592	578	533	476	418
B 1	589	587	575	536	477	417
2	587	585	573	532	474	414
C 1	—	579	565	534	479	420
2	597	595	581	539	481	420
D 1	605	602	586	541	482	422
2	608	605	586	539	480	420
E 1	610	607	588	542	483	423
2	598	596	582	538	480	419

[a] Numbers 1 and 2 refer to the very first and the second run of measurements.
[b] $1 \cdot 10^{-2} M\ I_2$ in benzene.

TABLE II

LONG-TERM STABILITY OF THE LIQUID-STATE IODIDE-SELECTIVE ELECTRODE

(All measurements performed with one electrode ("C", Table I) over a period of 5 weeks. The values of potentials are expressed in mV followed by standard deviations and by the number of measurements (in brackets). All E values *versus* S.C.E.)

		Concentration of iodide in sample				
	$1 \cdot 10^{-3} M\ HNO_3$	$0.97 \cdot 10^{-7}$	$1.06 \cdot 10^{-6}$	$1.06 \cdot 10^{-5}$	$1.05 \cdot 10^{-4}$	$1.04 \cdot 10^{-3}$
E	597 ± 6 (17)	594 ± 6 (20)	581 ± 6 (21)	539 ± 4 (21)	480 ± 4 (21)	420 ± 4 (21)

TABLE III

REPRODUCIBILITY OF MEASUREMENT WITH THE LIQUID-STATE IODIDE-SELECTIVE ELECTRODE

(All potentials measured *versus* S.C.E. The mean value is followed by standard deviation of a single measurement and by number of measurements in brackets)

Organic solvent	*Concn. of I_2 in solvent (M)*	$1\cdot10^{-3}$ *M* HNO_3	*Concentration of iodide in sample*				
			$0.97\cdot10^{-7}$	$1.06\cdot10^{-6}$	$1.06\cdot10^{-5}$	$1.05\cdot10^{-4}$	$1.04\cdot10^{-3}$
Benzene	10^{-2}	599 ± 9 (51)	596 ± 8 (62)	580 ± 8 (62)	536 ± 6 (66)	477 ± 6 (63)	417 ± 6 (68)
	10^{-3}	598 ± 29 (2)	580 ± 16 (4)	553 ± 8 (6)	507 ± 8 (8)	448 ± 4 (7)	390 ± 4 (8)
	10^{-4}	560 ± 10 (6)	544 ± 19 (6)	522 ± 11 (7)	477 ± 5 (9)	423 ± 3 (9)	365 ± 3 (9)
Mesitylene	10^{-2}	602 ± 14 (20)	591 ± 10 (28)	563 ± 7 (29)	513 ± 5 (33)	457 ± 5 (31)	398 ± 5 (31)
	10^{-3}	584 ± 18 (6)	569 ± 16 (7)	535 ± 9 (8)	483 ± 6 (10)	426 ± 7 (11)	367 ± 5 (12)
	10^{-4}	558 ± 18 (6)	538 ± 13 (6)	509 ± 7 (7)	459 ± 6 (7)	403 ± 5 (8)	346 ± 5 (8)
Carbon tetrachloride	10^{-2}	608 ± 16 (19)	602 ± 15 (19)	580 ± 10 (20)	531 ± 9 (21)	473 ± 8 (21)	413 ± 7 (21)
	10^{-3}	606 ± 33 (15)	589 ± 26 (21)	557 ± 15 (20)	508 ± 8 (22)	451 ± 6 (22)	392 ± 6 (25)
	10^{-4}	582 ± 21 (12)	566 ± 13 (13)	534 ± 5 (14)	483 ± 3 (14)	426 ± 4 (14)	367 ± 3 (14)

Finally, Table III summarizes the measurements with a number of electrodes employing different solvents, and different concentrations of iodine over a period of several months. They therefore reflect all possible variables, such as preparation of electrodes, drift, effect of temperature, storage, etc. The standard deviation of potentials as measured in 10^{-5}–$10^{-3} M$ iodide solutions undoubtedly reflects these factors. The larger values of the standard deviations in "blank" and $10^{-7} M$ solutions are most probably due to the changing level of iodide ion impurities in the nitric acid, apparatus and redistilled water.

Selectivity of the electrode

The selectivity was studied by investigating the influence of redox systems as well as of foreign anions. It was found that any reducing species which brought the redox potential of the sample below +315 mV (measured by means of a bright platinum electrode *versus* S.C.E. at pH 3 in $1 \cdot 10^{-3} M$ iodide), would interfere with the measurement. Moreover, any oxidizing agent which oxidized iodide to iodine

TABLE IV

SELECTIVITY OF THE LIQUID-STATE IODIDE-SENSITIVE ELECTRODE

Foreign anion	*(M)*	*Iodide (M)*	*Ionic strength*	*Activity coeff.*[a]	*Activity of iodide*	*Potential in mV*		*Selectivity constant*[b]
						Measured	*Calculated*	
Perchlorate	0	$1.04 \cdot 10^{-3}$	$2 \cdot 10^{-3}$	0.964	$1.00 \cdot 10^{-3}$	418	—	—
	10^{-2}	$1.04 \cdot 10^{-3}$	$1.2 \cdot 10^{-2}$	0.920	$0.96 \cdot 10^{-3}$	420	419	$< 10^{-5}$
	10^{-1}	$1.04 \cdot 10^{-3}$	$1.02 \cdot 10^{-1}$	0.80	$0.83 \cdot 10^{-3}$	424	423	$< 10^{-5}$
	0	$1.05 \cdot 10^{-4}$	$1.1 \cdot 10^{-3}$	0.975	$1.02 \cdot 10^{-4}$	478	—	—
	10^{-2}	$1.05 \cdot 10^{-4}$	$1.1 \cdot 10^{-2}$	0.923	$0.97 \cdot 10^{-4}$	481	479	$< 10^{-5}$
	10^{-1}	$1.05 \cdot 10^{-4}$	$1.01 \cdot 10^{-1}$	0.81	$0.85 \cdot 10^{-4}$	483	483	$< 10^{-5}$
Nitrate	0	$1.04 \cdot 10^{-3}$	$2 \cdot 10^{-3}$	0.964	$1.00 \cdot 10^{-3}$	420	—	—
	10^{-2}	$1.04 \cdot 10^{-3}$	$1.2 \cdot 10^{-2}$	0.920	$0.96 \cdot 10^{-3}$	422	421	$< 10^{-5}$
	10^{-1}	$1.04 \cdot 10^{-3}$	$1.02 \cdot 10^{-1}$	0.80	$0.83 \cdot 10^{-3}$	423	425	$8 \cdot 10^{-5}$
	0	$1.05 \cdot 10^{-4}$	$1.1 \cdot 10^{-3}$	0.975	$1.02 \cdot 10^{-4}$	481	—	—
	10^{-2}	$1.05 \cdot 10^{-4}$	$1.1 \cdot 10^{-2}$	0.923	$0.97 \cdot 10^{-4}$	483	482	$< 10^{-5}$
	10^{-1}	$1.05 \cdot 10^{-4}$	$1.01 \cdot 10^{-1}$	0.81	$0.85 \cdot 10^{-4}$	485	486	$4 \cdot 10^{-5}$
Chloride	0	$1.04 \cdot 10^{-3}$	$2 \cdot 10^{-3}$	0.964	$1.00 \cdot 10^{-3}$	416	—	—
	10^{-2}	$1.04 \cdot 10^{-3}$	$1.2 \cdot 10^{-2}$	0.920	$0.96 \cdot 10^{-3}$	416	417	$4 \cdot 10^{-3}$
	10^{-1}	$1.04 \cdot 10^{-3}$	$1.02 \cdot 10^{-1}$	0.80	$0.83 \cdot 10^{-3}$	422	421	$< 10^{-5}$
	0	$1.05 \cdot 10^{-4}$	$1.1 \cdot 10^{-3}$	0.975	$1.02 \cdot 10^{-4}$	476	—	—
	10^{-2}	$1.05 \cdot 10^{-4}$	$1.1 \cdot 10^{-2}$	0.923	$0.97 \cdot 10^{-4}$	475	477	$8 \cdot 10^{-4}$
	10^{-1}	$1.05 \cdot 10^{-4}$	$1.01 \cdot 10^{-1}$	0.81	$0.85 \cdot 10^{-4}$	482	481	$< 10^{-5}$
Bromide	0	$1.04 \cdot 10^{-3}$	$2 \cdot 10^{-3}$	0.964	$1.00 \cdot 10^{-3}$	415	—	—
	10^{-2}	$1.04 \cdot 10^{-3}$	$1.2 \cdot 10^{-2}$	0.920	$0.96 \cdot 10^{-3}$	417	416	10^{-5}
	10^{-1}	$1.04 \cdot 10^{-3}$	$1.02 \cdot 10^{-1}$	0.80	$0.83 \cdot 10^{-3}$	412	420	$4 \cdot 10^{-3}$

[a] *Cf.* ref. 8.

[b] Values lower than 10^{-5} could be calculated, but they would not be significant owing to the uncertainty of the measurements.

influenced the electrode potential. It was therefore decided to use $1 \cdot 10^{-3}M$ nitric acid as a medium for any further interference studies. However, sulfuric and hydrochloric acid of similar normalities could be used as well. From the values of the potentials measured in the presence and absence of various quantities of foreign anions, the selectivity of the electrode was evaluated by means of the equation:

$$E = \text{const.} - 0.0592 \log (a_{I^-} + K \cdot a_X) \quad (\text{at } 25°) \tag{4}$$

where const. involves both E'_0 and $[I_2]_0$, a_{I^-} is the activity of the iodide ion, and a_X is the activity of the foreign monovalent anion.

The results summarized in Table IV show, that perchlorate, nitrate and chloride ions have no influence on the measurements. The slight interfering effect of bromides might possibly have been due to iodide impurities in the potassium bromide used.

Because light sensitivity is a problem when iodide-sensitive solid-state electrodes are used for measurement of activities of iodide ions below $10^{-4}M$, it was decided to investigate the influence of illumination on the electrode potential. It was found that there is no difference in between the potentials measured in sunlight, artificial light or in darkness, at any level of iodide activities studied. This is, of course, not surprising, as all solid-state iodide-sensitive electrodes contain either pure, or a certain proportion of, light-sensitive silver iodide, while here the electroactive species is elemental iodine.

DISCUSSION

The measurements made with different electrodes, as summarized in Tables I–III, confirm that for practical purposes eqn. (3) can be written as

$$E = \text{const.} - 0.0592 \log [I^-] \quad (\text{at } 25°) \tag{5}$$

The value of const. which combines both E'_0 and $[I_2]_0$ is reasonably stable with time, can be readily reproduced when a series of electrodes is prepared and also does not change very much during the lifetime of the electrode. Thus, if for example, $1.04 \cdot 10^{-3}M$ sodium iodide in $1 \cdot 10^{-3}M$ nitric acid is chosen as a reference solution, a comparison of the potentials for five different electrodes (A–E, Table I), prepared in the same manner and used for the first time, shows that the maximum observed difference in the potentials is only 5 mV. Moreover the differences between the first and second runs of measurements performed with freshly prepared electrodes indicate that they can be used immediately after preparation. With regard to long-term stability, the values of potentials (as measured in $1.04 \cdot 10^{-3}$ M iodide) over a period of five weeks show only a slight random scattering, so that no drift can be observed. The differences in potentials in the range 10^{-3}–$10^{-5}M$ are to some extent due also to the changes of temperature, which varied from 22° to 24°. The large values of the standard deviations at $10^{-7}M$ are due to changing levels of iodide impurities in the measured samples; to what extent the impurities originated from the water and acid used, or from the electrode itself has not yet been established. However, in a solution of $10^{-3}M$ silver(I) potentials as positive as +950 mV were measured. Because this potential is not far from that which one might expect in solutions containing an iodide activity of 10^{-13} (assuming a slope of 59 mV/pI and $S_{AgI} = 10^{-16}$), it appears that the electrode might function properly even in solutions of much lower activities than those investigated in this work, provided that they are buffered by iodide compounds of low solubility.

From the theoretical viewpoint, the most significant result of this work is the verification of the dependence of the potential of the liquid-state electrode on the concentration of iodine in the organic phase (Table III, Fig. 2). This demonstrates the difference between liquid-state and liquid–liquid membrane electrodes, which was not proved by the previous work[3]. While the concentration of the electroactive species in the organic phase of the membrane electrode has no effect on the potential, here the differences in potentials caused by different concentrations of iodine in the organic solvent have precisely the influence predicted by eqn. (3).

Another interesting fact is that the values of potentials as shown in Table III depend not only on the concentration of iodide ions and of iodine, but also on the type of the organic solvent used. The differences between the mean values of the potentials of the electrode employing mesitylene or benzene and carbon tetrachloride are significantly larger than the standard deviations, which confirms that the E'_0 value depends also on the type of the solvent used. In order to explain this effect, it would be interesting to investigate other solvents, the properties (*e.g.* viscosity, polarity and vapour pressure) of which differ considerably from those used in the present work.

CONCLUSION

The liquid-state iodide-selective electrode is very easy to make, and possesses good precision, reasonable long-term stability, a very low inner resistance and a selectivity comparable to that of the solid-state AgI/Ag_2S membrane electrode; it is not sensitive to illumination. On the other hand it is unfavourably affected by reducing species, which deplete the electrode of iodine. For the same reason, the sensitivity of the electrode is limited in alkaline solutions. Although the last two drawbacks can be overcome by suitable buffering of the samples, the practical utility of this electrode has yet to be tested and its selectivity further investigated.

From the theoretical viewpoint, the iodide ion–iodine system is very interesting because it allows a simple comparison of the properties of liquid-state and liquid–liquid membrane electrodes. This may prove to be very useful because very little is known about how the porous conducting material influences the potential and the stability of the liquid-state electrodes. So far, only one type of graphite has been used in these experiments, but different sorts of this material as well as charcoal and active coal are available. Different types of carbon pastes, like those used in organic polarography, might also be used for making the electrodes. Finally, the preliminary treatment of the graphite, which enhances or diminishes its own ion-exchange qualities[7] should be kept in mind. Potentiometric studies with organic solutions of iodine, performed with various porous conducting supports, as well as with membranes, will further contribute to the development of ion-selective electrodes.

The authors express their sincere thanks to Professor N. Hofman-Bang for his interest in this work and to Chemistry Department A for providing facilities and instrumentation for one of us (K.R.).

SUMMARY

The ion-sensitive surface of the liquid-state electrode is formed by a very thin layer of an organic liquid, adsorbed at the surface of porous graphite. The composition of this organic phase, which must be immiscible with water, can be chosen so that the electrode responds only to the activity of a certain ion in the measured aqueous sample. The performance and construction of a liquid-state electrode with solutions of iodine in carbon tetrachloride, benzene and mesitylene as the organic phase is described. The electrode is suitable for measurement of iodide activities down to $10^{-6}M$; it has selectivity ratios for iodide over bromide of about 10^{-3} and over chloride ion of better than 10^{-4}. In contrast to the solid-state iodide-selective electrode (AgI/Ag_2S membrane), the liquid-state electrode is not sensitive to light at any level of the iodide activities studied, but it is sensitive to species which would reduce iodine to iodide.

RÉSUMÉ

La surface ionique sensible des électrodes sélectives liquides est formée par une couche très mince d'un liquide organique, adsorbé à la surface de graphite poreux. La composition de cette phase organique, qui doit être non miscible à l'eau, peut être choisie pour que l'électrode réponde seulement à l'activité d'un certain ion dans l'échantillon aqueux mesuré. On décrit une de ces électrodes permettant de déterminer des activités de iodure jusqu'à 10^{-6} M, en présence de bromure et de chlorure. L'électrode à l'état liquide, contrairement à l'électrode solide sélective (à membrane AgI/Ag_2S) n'est pas sensible à la lumière. Par contre elle est sensible à des substances pouvant réduire l'iode en iodure.

ZUSAMMENFASSUNG

Die ionenempfindliche Oberfläche der Flüssig-Elektrode wird durch eine sehr dünne Schicht einer organischen Flüssigkeit gebildet, die an der Oberfläche von porösem Graphit adsorbiert ist. Die Zusammensetzung dieser organischen Phase, die mit Wasse unmischbar sein muss, kann so gewählt werden, dass die Elektrode nur auf die Aktivität eines bestimmten Ions in der zu messenden wässrigen Probe anspricht. Es werden Leistung und Aufbau einer Flüssig-Elektrode mit lösungen von Jod in Kohlenstofftetrachlorid, Benzol und Mesitylen als organischer Phase beschrieben. Die Elektrode ist für Messungen von Jodidaktivitäten bis zu 10^{-6} M herab geeignet. Das Selektivitätsverhältnis für Jodid ist etwa 10^{-3} gegenüber Bromid und besser als 10^{-4} gegenüber Chlorid. Im Gegensatz zur jodidselektiven Fest-Elektrode (AgJ/Ag_2S-Membran) ist die Flüssig-Elektrode bei keiner der untersuchten Jodidaktivitäten lichtemfindlich; sie ist jedoch empfindlich gegenüber Stoffen, die Jod zu Jodid reduzieren.

REFERENCES

1 J. Růžička and J. Chr. Tjell, *Anal. Chim. Acta*, 47 (1969) 475.
2 J. Růžička and J. Chr. Tjell, Patents appl. No. 3789/69 and further, Denmark.

3 J. Růžička and J. Chr. Tjell, *Anal. Chim. Acta*, 51 (1970) 1.
4 J. Růžička, *Proceedings of the VIth Intern. Symp. on Microtechniques*, Graz,1970.
5 L. A. R. Pioda, V. Stankova and W. Simon, *Anal. Letters*, 2 (12) (1969) 665.
6 G. Eisenman, *Proc. Symp. on Ion-Selective Electrodes*, National Bureau of Standards, Washington, 1969, p. 1–54.
7 G. W. Murphy, J. L. Copper *et al.*, U.S. Dept. of Interior Progress Report No. 399, 1969.
8 J. Kielland, *J. Amer. Chem. Soc.*, 59 (1937) 1675.

Analytica Chimica Acta
Elsevier Publishing Company, Amsterdam
Printed in The Netherlands

A STANDARD ADDITION TITRATION METHOD FOR THE POTENTIOMETRIC DETERMINATION OF FLUORIDE IN SEA WATER

TORBJÖRN ANFÄLT AND DANIEL JAGNER
Department of Analytical Chemistry, University of Gothenburg, Fack, S-402 20 Göteborg 5 (Sweden)

(Received August 3rd, 1970)

The total concentration of fluoride in sea water, which is approximately 0.07 m*M* at $35^{0}/_{00}$ salinity, is normally determined spectrophotometrically[1], the lanthanum–alizarin–complexone method[2-4] modified for sea water analysis by Greenhalgh and Riley[5], yielding the most accurate results. The method is, however, time-consuming and salinity corrections have to be applied. Much attention has thus recently been paid to the possibility of using the fluoride-selective electrode for direct potentiometric measurement[6-8] or null-point potentiometric titration[9] of fluoride in natural waters. In sea water approximately half the total fluoride content is, however, bound as the magnesium and calcium complexes[9,10], and direct potentiometric measurements would consequently have to be modified in order to be applicable to the analysis of sea water. This may be done[8] with standards of known salinity and fluoride concentration or by adding a known amount of fluoride to the sample[13]. It is also possible to liberate bound fluoride by complexing[7] magnesium and calcium with HEDTA or EDTA. Alternatively, the total fluoride concentration could be calculated from the potentiometrically measured free fluoride concentration, with known values of the stability constants of the magnesium and calcium complexes together with known values for the free magnesium and calcium concentrations. Since the addition of a large amount of a strongly complexing agent would, however, interfere with the working of the electrode[11,12] and since accurate values of the stability constants are not available for all sea water salinities and temperatures, neither of these methods is particularly satisfactory.

In this paper a standard addition titration method is described for the fluoride-selective membrane electrode. In order to take full advantage of the suggested technique, it has been adapted to the semi-automatic titrator previously described[14].

EXPERIMENTAL

Reagents

Standard fluoride solution was prepared by dissolving the sodium salt, dried at 100°, in doubly distilled water.

Standard sea water of chlorinity $19.3745^{0}/_{00}$ was purchased from I.A.P.S.O., Standard Sea Water Service, Charlottenlund Slot, Denmark. Sea water of lower chlorinity was obtained by volumetric dilution.

Apparatus

Electrodes. The fluoride concentration was measured by means of a single crystal fluoride electrode (Orion, Model 94-09) and an Orion single junction reference electrode (Orion, Model 90-01).

Titrator. The titrations were performed with a semi-automatic titrator[14] which operates with discrete increments of titrant of pre-chosen magnitude; it is possible to preset the time interval between each new addition of titrant. The titration data, E mV and v ml titrant added, were obtained on punched tape ready for subsequent computing.

Buffer system

Since many buffering agents might cause erroneous e.m.f. readings[11,12], it was considered to be more satisfactory to make use of the carbonate buffer system inherent in sea water. In sea water of normal ionic composition, most of the total carbonate is in the hydrogen carbonate form, the concentration of which is in the order of magnitude of 2.4 mM at $35^0/_{00}$ salinity. By the addition of *ca.* 0.5 mmol of hydrochloric acid to 100 ml of sea water, the buffering region of the carbonic acid–carbonate system is attained, the corresponding pH value of approximately 6.6 lying within the optimum working range of the fluoride electrode. For sea water samples of lower salinity less hydrochloric acid would of course be required. The slight increase in pH during a titration caused by the evolution of carbon dioxide has been shown to have no discernible effect on the potentiometric determination of the fluoride content.

Recommended titration procedure

To a sample of *ca.* 150 g of sea water accurately weighed into a polyethylene beaker, 0.5–0.75 ml of 0.1 M hydrochloric acid is added and the potential reading obtained after 1 min is registered. Titrant increments of 0.05 ml of 0.01 M sodium fluoride are then added until the e.m.f. reading is *ca.* −75 mV, the total volume of added titrant being *ca.* 2 ml. The time interval between one titrant addition and the next should not be less than 15 sec. The same titration procedure is used in both automatic and manual titrations. Representative data for the titration of 140 g of standard sea water are shown in Table I which also illustrates the form of the data tape obtained from the titrator; this can be used directly as input for the computer program applied to evaluate the equivalence point. Algol or Basic versions of the computer program can be obtained from the authors.

THEORY

To v_0 ml of a sea water sample with a total fluoride concentration of x M, increments of v ml of t M sodium fluoride are added. If the pH value of the solution is greater than 6, which means that proton fluoride complexes (HF and HF_2^-) can be neglected[15], then

$$(v_0+v)([F^-]+[MgF^+]+[CaF^+]) = vt+v_0x \qquad (1)$$

provided that no solid fluoride phase (*e.g.* CaF_2) is formed. Since

$$[CaF^+] = \beta_{CaF}[Ca^{2+}][F^-] \qquad (2)$$

and

$$[MgF^+] = \beta_{MgF}[Mg^{2+}][F^-] \qquad (3)$$

TABLE I

EXPERIMENTAL DATA AND FORM OF INPUT DATA TAPE FOR THE TITRATION OF 140 g OF STANDARD SEA WATER WITH v ml OF 0.01 M SODIUM FLUORIDE

(The first 6 lines are punched manually and the subsequent data are punched automatically in an actual data tape)

140 gram standard sea water;		(Title)
140		(grams of sample)
23		(T°C)
0.01		(concentration of sodium fluoride)
35		(sample salinity)
1		(number of titrations run parallel)
87-0000	89-1000	
87-0050	89-0988	(Measuring channel number (87) followed by ml titrant ×1000
87-0100	89-0977	Measuring channel number (89) followed by $10 \times E$ mV)
87-0150	89-0965	
87-0200	89-0954	
87-0250	89-0943	
87-0300	89-0933	
87-0350	89-0923	
87-0400	89-0913	
87-0450	89-0904	
87-0500	89-0895	
87-0550	89-0886	
87-0600	89-0878	
87-0650	89-0870	
87-0700	89-0862	
87-0750	89-0855	
87-0800	89-0848	
87-0850	89-0841	
87-0900	89-0834	
87-0950	89-0828	
87-1000	89-0822	
87-1050	89-0815	
87-1100	89-0809	
87-1150	89-0804	
87-1200	89-0798	
87-1250	89-0792	
87-1300	89-0787	
87-1350	89-0781	
87-1400	89-0777	
87-1450	89-0771	
87-1500	89-0766	
87-1550	89-0761	
87-1600	89-0756	
87-1650	89-0751	
87-1700	89-0746	
/	(End of titration)	

eqn. (1) can be rewritten as

$$(v_0+v)(1+\beta_{\mathrm{MgF}}[\mathrm{Mg}^{2+}]+\beta_{\mathrm{CaF}}[\mathrm{Ca}^{2+}])[\mathrm{F}^-]=v_0x+vt \tag{4}$$

or

$$k(v\ \ +v)[\mathrm{F}^-]=v_0x+vt \tag{5}$$

where

$$k = 1 + \beta_{\mathrm{MgF}}[\mathrm{Mg}^{2+}] + \beta_{\mathrm{CaF}}[\mathrm{Ca}^{2+}] \tag{6}$$

k is constant provided that the amounts of magnesium and calcium present as fluoride complexes are neglected and the ionic medium is not changed to any great extent. Such a change would, for example, shift the ion-pairing of magnesium(II) and calcium(II) with sulphate or the activity coefficients of the ions involved. Neglecting the dilution of magnesium and calcium the value of k can thus be considered to be constant throughout a titration.

At constant ionic strength and below pH 8, the electrode couple measures the fluoride concentration according to

$$E = E^0 + RTF^{-1} \ln 10 \log [\mathrm{F}^-] \tag{7}$$

where the activity coefficients and liquid junction potentials have been included in E^0. Thus,

$$[\mathrm{F}^-] \propto 10 \exp EF/RT \ln 10 \tag{8}$$

Thus, if

$$F_1 = (v_0 + v)\, 10 \exp EF/RT \ln 10 \tag{9}$$

is plotted against v ml of titrant added, an almost straight line will be obtained which, when extrapolated to zero, intersects the v-axis at $v = v_{\mathrm{eq}}$, where

$$v_{\mathrm{eq}} = -v_0 x/t \tag{10}$$

The total fluoride concentration in the sea water sample can then be calculated. The graphical evaluation of v_{eq} can be performed fairly rapidly. If, however, a computer is used to evaluate v_{eq} the F_1 plot can be corrected for the dilution of magnesium and calcium during the titration procedure according to

$$F_2 = F_1(1 + 1.07\, v_0 S/35\,(v_0 + v)) \tag{11}$$

where S is the salinity of the sea water sample.

The value 1.07 has been derived from

$$\beta_{\mathrm{MgF}}[\mathrm{Mg}^{2+}] + \beta_{\mathrm{CaF}}[\mathrm{Ca}^{2+}] = 18.8 \cdot 0.0544 + 4.22 \cdot 0.0105 = 1.07 \tag{12}$$

where 18.8 and 4.22 are the stability constants for the magnesium and calcium fluoride complexes[10], respectively, and 0.0544 and 0.0105 are the total magnesium and calcium concentrations at the salinity of $35^0/_{00}$. The total magnesium and calcium concentrations are assumed to be proportional to the sample salinities and the change in the stability constants of the magnesium and calcium fluoride complexes with salinity has been neglected.

From the evaluated v_{eq} value the total fluoride concentration in each titration point can, moreover, be calculated as

$$[\mathrm{F}]_{\mathrm{tot}} = t(v - v_{\mathrm{eq}})/(v_0 + v) \tag{13}$$

And an E_s^0 value can be defined in each titration point as

$$E_s^0 = E - RTF^{-1} \ln 10 \log [\mathrm{F}]_{\mathrm{tot}} \tag{14}$$

the mean value of E_s^0 in all titration points being denoted as $E_{s,\mathrm{mean}}^0$. The value of

E_s^0 is related to the E^0 value in eqn. (7) by

$$E_s^0 = E^0 - RTF^{-1} \ln 10 \log k \qquad (15)$$

The $E_{s,\text{mean}}^0$ value can then be used to determine the total fluoride concentrations in different sea water samples according to

$$[\text{F}]_{\text{tot}} = 10 \exp (E_1 - E_{s,\text{mean}}^0) F/RT \ln 10 \qquad (16)$$

where E_1 is the e.m.f. reading obtained in the sea water sample before the addition of titrant (*i.e.* at $v = 0$ ml). E_1 is 100.0 mV in Table I.

Computer calculation of the theoretical titration curve

In order to verify that the plots F_1 and F_2 can be used to evaluate the amount of fluoride in a sea water sample, the computer program Haltafall[16] was used to calculate the theoretical form of the titration curve. The calculation was performed as a titration of 150 ml of sea water of total fluoride concentration equal to 0.07 m*M* with v ml of 0.01 *M* sodium fluoride at pH 6 ($v_{eq} = -1.05$). The total concentrations of magnesium and calcium were 0.0544 and 0.0105 *M*, respectively, which corresponds to a sea water salinity of $35^0/_{00}$. The relevant stability constants for the magnesium and calcium fluoride complexes were taken from Elgqvist[10], *i.e.*:

$$\text{Ca}^{2+} + \text{F}^- \rightleftharpoons \text{CaF}^+ \qquad \beta_1 = 4.22$$

$$\text{Mg}^{2+} + \text{F}^- \rightleftharpoons \text{MgF}^+ \qquad \beta_1 = 18.8$$

Since no solid fluoride phases were formed during the actual titrations, the solubility products for magnesium and calcium fluoride were not included in the calculations. The calculation was performed with an accuracy[16] of 0.01% in the total concentration of all components.

The results of the calculation are shown in Fig. 1 in which the amounts of the dominant fluoride species have been plotted against v ml of titrant added. From the Figure, it can be seen that on addition of fluoride ions to the sea water approximately half of the fluoride ions will form either magnesium or calcium complexes while the

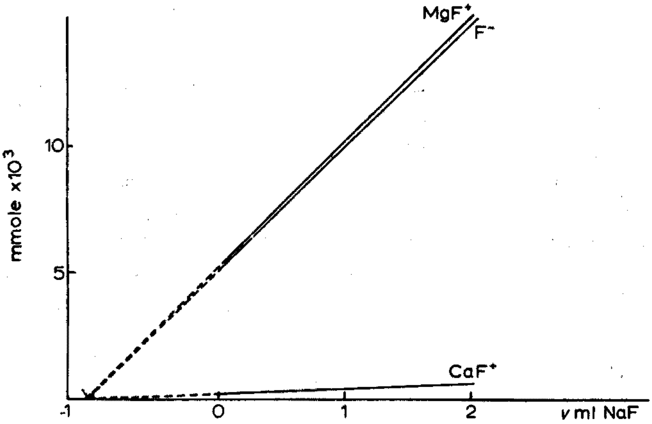

Fig. 1. Haltafall calculation of the concentrations of F^-, MgF^+ and CaF^+ formed by the addition of NaF to standard sea water.

other half will contribute to the increase in the free fluoride concentration. Moreover, from the intersection of the linear plot $F_1=(150+v)[F^-]$ on the v-axis at $v=-1.04 \pm 0.005$ ml, it can be concluded that F_1 can be used graphically to establish the total amount of fluoride without introducing a systematic error greater than 1.5%.

Computer evaluation of the equivalence point

The titration data, E mV and v ml, were used to evaluate the equivalence point with a computer program similar to that used to evaluate the chloride concentration in sea water[17], which has been described in detail by Dyrssen *et al.*[18]. This program calculates a value of F_2 in each titration point and then fits the best straight line through these points starting with the last five titration points. The standard deviation from the calculated line and the five titration points is then calculated, a new titration point is included, and the standard deviation is recalculated. This procedure is repeated until all titration points have been included and the set of titration data giving the smallest value for the standard deviation is then used for the straight line regression and the subsequent extrapolation of v_{eq}. In fluoride titrations all registered titration points are normally included on the best straight line since even for $v=0$ ml relevant e.m.f. values are registered.

In order to verify that the computer program does not introduce significant systematic errors the theoretically calculated data, pF_{calc}, *vs.* v ml of titrant added, were converted into e.m.f. data according to

$$E_{calc} = -RTF^{-1} \ln 10 \, pF_{calc} \tag{17}$$

and fed into the computer program. The equivalence point thus obtained, −1.0496 ml, differed from the theoretical value of −1.05 ml by less than 0.1% thus showing the systematic error to be negligible in comparison with the precision obtained in the titration procedure. The total fluoride concentration evaluated from the computed E_1 and $E^0_{s,mean}$ value (eqn. 16) was found to be 0.0699 mM which is in good agreement with the theoretical value of 0.0700 mM.

RESULTS

High-saline sea water

The results from several titrations of different amounts of undiluted standard sea water are shown in Table II. The mean value of 0.0734 mmol kg^{-1} (1.394 mg kg^{-1} or $F^-/Cl=7.20 \cdot 10^{-5}$ g/kg per $^0/_{00}$) for the total concentration of fluoride in $35^0/_{00}$ standard sea water is in good agreement with the values obtained spectrophotometrically[1]. From Table II it is also apparent that the titration procedure gives a slightly higher precision when the data are calculated from F_2 than from E_1 and $E^0_{s,mean}$. The same mean value for the total fluoride concentration is obtained in both cases. This indicates that the fluoride electrode is very satisfactory in high-saline sea water samples.

Low-saline sea water

The results from titrations in dilute standard sea water samples are summarized in Table III. In these titrations weighed amounts of sea water samples were diluted to a total volume of 150 ml and five titrations were performed for each salinity. From

TABLE II

RESULTS FROM 24 TITRATIONS OF UNDILUTED STANDARD SEA WATER WITH v ml OF 0.01 M SODIUM FLUORIDE

Evaluated from F_2 with eqns. (9)–(11)				*Evaluated from E_1 and $E^0_{s,mean}$ with eqn.* (16)	
No. of titrations	*Sample weight (g)*	*$[F]_{tot}$ (mmol kg^{-1})*	*Mean deviation (%)*	*$[F]_{tot}$ (mmol kg^{-1})*	*Mean deviation (%)*
8	80	0.0733	0.81	0.0733	1.21
8	100	0.0737	0.76	0.0736	0.76
8	120	0.0734	0.41	0.0733	0.62
8	140	0.0733	0.38	0.0732	0.91
Mean values		0.0734	0.59	0.0734	0.88

TABLE III

RESULTS FROM 30 TITRATIONS OF 150-ml SAMPLES OF DILUTED STANDARD SEA WATER WITH v ml OF 0.01 M SODIUM FLUORIDE

			Evaluated from F_2 with eqns. (9)–(11)		*Evaluated from E_1 and $E^0_{s,mean}$ with eqn.* (16)	
No. of titrations	*Salinity (‰)*	*$[F]_{tot,calc}$ (mM)*[a]	*$[F]_{tot}$ (mM)*	*Mean deviation (%)*	*$[F]_{tot}$ (mM)*	*Mean deviation (%)*
5	25	0.0524	0.0521	0.78	0.0523	0.76
5	15	0.0315	0.0312	1.20	0.0313	0.81
5	10	0.0210	0.0211	1.56	0.0209	0.63
5	7	0.0147	0.0143	2.10	0.0147	0.81
5	3.5	0.00734	0.00703	3.81	0.00715	4.3
5	2.33	0.00489	0.00460	7.11	0.00482	8.2

[a] Calculated from dilution of weighed amounts of sea water with a total fluoride concentration equal to 0.0734 mmol kg^{-1}.

Table III it may be concluded that the fluoride-selective electrode can be used to measure the total fluoride concentration in sea water down to a salinity of *ca.* 5‰ from E_1, provided that a relevant $E^0_{s,mean}$ value is evaluated by a titration procedure. In more dilute sea water samples the free fluoride concentration is too low for the electrode to show Nernstian behaviour. Moreover, Table III shows that for sea water salinities between 25 and *ca.* 5‰, the fluoride concentration determined from E_1 and $E^0_{s,mean}$ is slightly more than the value determined from F_2.

Another item of great interest is whether a calibration curve $E^0_{s,mean}$ *vs.* salinity will be sufficient to evaluate the total fluoride concentration by a single point measurement thus ruling out the necessity of a titration of each sample. From Fig. 2, obtained from the computer evaluation of v_{eq}, where $E^0_{s,mean}$ has been plotted against salinity at 23°, it can be deduced that even if the sample salinity is accurately known, the $E^0_{s,mean}$ value cannot be estimated to better than ±1 mV. The precision will thus be considerably reduced, especially at high salinities but on the other hand, measurements can be made very much more rapidly. Such a calibration curve must, of course, be relevant to the temperature of the sample.

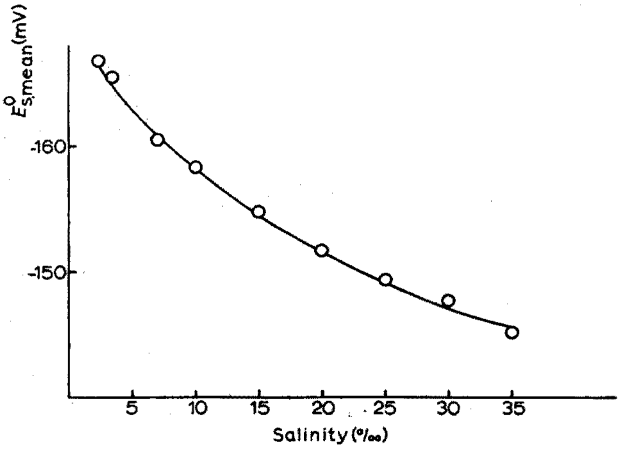

Fig. 2. E^0 for the fluoride electrode as a function of the salinity at 23°.

DISCUSSION

Interferences

Minor constituents of sea water which form highly stable fluoride complexes might interfere in the fluoride determination. However, the formation constant of fluoroborate is much too low above pH 6 for interference in sea water of normal ionic composition. The formation of AlF^{2+} above pH 6 is completely negligible at the concentrations of aluminium normally found in sea water.

Accuracy

The computer calculations have proved that the evaluation of the equivalence point is free from systematic errors. The main systematic error, no doubt, originates from the preparation of the standard sodium fluoride solution. It is, however, not possible to find a standardization procedure which gives a better accuracy than 0.2% which is approximately the accuracy obtained when the dried sodium fluoride is weighed in.

Precision

The precision is governed mainly by the errors in the volume measurements. In the future the semi-automatic titrator[13] will therefore be equipped with a motor-driven syringe buret of 2 ml instead of 10 ml. It is obvious from Table II which shows that the greater the amount of fluoride titrated, *i.e.* the greater the value for v_{eq}, the better is the precision obtained. It ought thus to be possible to obtain an increased precision, especially for low saline samples, by titrating a very large sample. Since, however, large volumes are difficult to handle this procedure is recommended only in cases where the demand for precision is extremely high. Another way of increasing the equivalence volume is, of course, to use a more dilute sodium fluoride solution. This will, however, cause an increase in the dilution of magnesium, calcium and sulphate concentrations during a titration. Since in the computer program the plot F_2, used to evaluate the total fluoride concentration, is corrected for dilution of magnesium and calcium by means of stability constants for the fluoride concentrations which are relevant only at $35^0/_{00}$, an increased dilution might introduce systematic errors. Moreover, very dilute fluoride solutions are often difficult to store.

The authors are indebted to the head of the department, Professor David Dyrssen, for valuable discussions and to Mrs Kerstin Årén for experimental assistance. Grants from the Swedish Natural Research Council and Carl Tryggers Stiftelse, the latter to cover the cost for the automatic titrator, are also gratefully acknowledged.

SUMMARY

A standard addition titration method for the potentiometric determination of the total fluoride concentration in sea water with a lanthanum fluoride electrode is described. The fluoride concentration of standard sea water was found to be 0.0734 ±0.0004 mmol kg^{-1}. Equations for the computer treatment of the titration data are given. The calibration of the electrode for single point potentiometric measurements at different sea water salinities is discussed.

RÉSUMÉ

On décrit une méthode de titrage avec étalon interne pour le dosage potentiométrique de fluorure total dans l'eau de mer, à l'aide d'une électrode au fluorure de lanthane. La concentration en fluorure d'une eau de mer standard est de 0.0734± 0.0004 mmol kg^{-1}. Des équations dont données pour utilisation d'un ordinateur. On examine également le calibrage des électrodes pour des mesures potentiométriques d'eaux de salinité différente.

ZUSAMMENFASSUNG

Es wird eine Standard-Additionstitrationsmethode für die potentiometrische Bestimmung der Gesamt-Fluoridkonzentration in Meerwasser mit einer Lanthanfluoridelektrode beschrieben. Die Fluoridkonzentration von Standard-Meerwasser wurde zu 0.0734±0.0004 mmol kg^{-1} ermittelt. Es werden Gleichungen für die Auswertung der Titrationsergebnisse durch einen elektronischen Rechner vorgelegt. Die Eichung der Elektrode für potentiometrische Einpunktmessungen bei verschiednenen Meerwasser-Salzgehalten wird diskutiert.

REFERENCES

1 F. CULKIN, in J. P. RILEY AND G. SKIRROW, *Chemical Oceanography*, Academic Press, London and New York, 1965.
2 R. BELCHER, M. A. LEONARD AND T. S. WEST, *Talanta*, 2 (1959) 92.
3 R. BELCHER, M. A. LEONARD AND T. S. WEST, *J. Chem. Soc.*, (1959) 3577.

4 M. A. LEONARD AND T. S. WEST, *J. Chem. Soc.*, (1960) 4477.
5 R. GREENHALGH AND J. P. RILEY, *Anal. Chim. Acta*, 25 (1961) 179.
6 J. E. HARWOOD, *Water Res.*, 3 (1969) 273.
7 M. S. FRANT AND J. W. ROSS, *Science*, 154 (1966) 1553.
8 P. G. BREWER, D. W. SPENCER AND P. E. WILKNISS, *Contrib. No. 2343*, Woods Hole Oceanographic Institution.
9 R. A. DURST, *Anal. Chem.*, 40 (1968) 931.
10 B. ELGQVIST, *J. Inorg. & Nucl. Chem.*, 32 (1970) 937.
11 T. ANFÄLT AND D. JAGNER, *Anal. Chim. Acta*, 47 (1969) 483.
12 T. ANFÄLT AND D. JAGNER, *Anal. Chim. Acta*, 50 (1970) 23.
13 E. W. BAUMAN, *Anal. Chim. Acta*, 42 (1968) 127.
14 D. JAGNER, *Anal. Chim. Acta*, 50 (1970) 15.
15 C. CULBERSON, R. M. PYTKOWICZ AND J. E. HAWLEY, *J. Marine Res.*, 28 (1970) 15.
16 N. INGRI, W. KAKOLOWICZ, L. G. SILLÉN AND B. WARNQVIST, *Talanta*, 14 (1967) 1261.
17 D. JAGNER AND K. ÅRÉN, *Anal. Chim. Acta*, 52 (1970) 491.
18 D. DYRSSEN, D. JAGNER AND F. WENGELIN, *Computer Calculation of Ionic Equilibria and Titration Procedures*, Almqvist & Wiksell, Stockholm, 1968.

Anal. Chim. Acta, 53 (1971) 13–22

Analytica Chimica Acta
Elsevier Publishing Company, Amsterdam
Printed in The Netherlands

DIRECT POTENTIOMETRIC DETERMINATION OF FLUORIDE IN WATER AFTER 8-HYDROXYQUINOLINE EXTRACTION*

PAUL J. KE** AND LLOYD W. REGIER
Fisheries Research Board of Canada, Halifax Laboratory, Halifax, Nova Scotia (Canada)

(Received July 16th, 1970)

The chemical analysis of water for fluoride has become increasingly important, owing to the growing need for potable water from various sources and the increase of pollution studies. The usual colorimetric methods for fluoride determination are time-consuming, and may yield erroneous results in highly polluted waters. The fluoride ion-selective membrane electrode[1], which uses a lanthanum fluoride membrane and responds to fluoride ion activity, offers rapid methods of fluoride determination. Johnson and Daugherty[2] used this electrode directly to determine the fluoride content of polluted river water, but were discouraged by inconsistent results caused by interferences from the high level of calcium and magnesium ions in the sample. Warner[3] developed a direct method for fluoride determination in seawater based on the assumption of a constant composition in seawater. However, the method can only be used for the deep seawater samples without much change in their composition, and would not fully meet the requirements for coastal seawater, especially for some polluted water samples.

The use of this electrode on water samples has also been studied by other workers[4-6]. However, the interaction of fluoride with polyvalent cations limits the usefulness of the electrode, particularly in most seawater and polluted water samples, even when such complexing agents such as citrate or DCTA (1,2-diaminocyclohexane-N,N,N′,N′-tetraacetic acid) are incorporated in the buffer system[3,4].

This report presents a modified technique based on the removal of interfering ions by extraction. In a recent study on the development of a method for fluoride in biological materials, the characteristic concentration limits of these interfering ions, at which the fluoride determination by the ion-selective electrode would be affected significantly, were reported[7]. These results suggested that removal of the major portions of the polyvalent cations would suffice to allow application of the lanthanum fluoride electrode to most samples. The extraction of the cations as complexes of 8-hydroxyquinoline[8] under slightly basic conditions was selected for study. The organic solvent used for the extraction was a mixture of ethylene glycol monobutyl ether and chloroform[9,10].

---

* Presented at the American Chemical Society (159th) and the Chemical Institute of Canada (25th) joint conference in Toronto, Canada, May 25–29, 1970.

** Present address: Department of Chemistry, University of Windsor, Windsor, Ontario, Canada.

EXPERIMENTAL

Apparatus

The Orion model 401 Specific Ion Meter, with an Orion model 94-09 fluoride solid-membrane electrode and a standard calomel reference electrode, was used for the direct measurement of fluoride activity in solution.

Reagents

Potassium fluorosilicate was prepared by the AOAC procedure[11]. Merck reagent-quality sodium fluoride was further purified[12] for use as a standard.

8-Hydroxyquinoline in chloroform and butyl cellosolve. This was prepared by dissolving 40 g of 8-hydroxyquinoline (oxine) in 1 l of a 1+9 mixture of ethylene glycol monobutyl ether (butyl cellosolve) and chloroform both freshly distilled.

Glycine buffer. This was prepared by mixing 56.4 ml of 2 *M* glycine and 100 ml of 1 *M* sodium hydroxide and diluting to 1 l with distilled water, after which the pH was adjusted with 1 *M* sodium hydroxide to between 10.5 and 10.8.

Total ionic strength adjustment buffer (*TISAB*). This was prepared by dissolving 340 g of sodium nitrate, 10 g of DCTA and 120 ml of anhydrous acetic acid in 500 ml of distilled water and diluting to 1 l after adjustment of the pH to 5.5 with 12 *M* sodium hydroxide solution.

All other reagents were prepared from stock ACS-grade chemicals without any treatment, but each material was tested for fluoride content using an internal fluoride standard[7].

Water used throughout this study was distilled twice in all-glass apparatus.

Samples

Four samples (A–D) of seawater were used in this study. Samples A and B were taken from the two inlets to seawater supply of the Halifax Laboratory of the Fisheries Research Board of Canada. Samples C and D were obtained from a bay which was receiving the effluent from a phosphate reduction plant. Samples E and F were taken, respectively, from fluorinated city water, and from a potable water well in Hants County, Nova Scotia. Samples G, H and I were taken from the effluent of the phosphate reduction plant noted in samples C and D above. Only samples A and B were filtered through Whatman No. 50 paper by suction, but all samples were made alkaline to phenolphthalein with 1 *M* sodium hydroxide solution to prevent loss of fluoride by vaporization. All the samples were stored in polyethylene bottles.

Recommended extraction procedure

Double 8-hydroxyquinoline extraction. Place 90 ml of the oxine solution and 20 ml of glycine buffer in a 250-ml separatory funnel. Add 50 g of the water sample and shake vigorously for 2 min. Remove the bottom organic layer as rapidly as the phases separate. If more than 10 min elapses before the organic layer is removed, a precipitate of some of the complexes tends to form on the glass, and introduces a slight error. Make a second extraction with 50 ml of oxine solution. Combine the organic phases from the two extractions in a second 250-ml separatory funnel. Wash the organic phase with 15–20 ml of distilled water. Transfer the aqueous phase from both funnels to a 100-ml volumetric flask, using the water wash to help rinse the principal sample into the flask. Dilute the extracted water sample to volume with distilled water, as sample stock solution.

Single 8-hydroxyquinoline extraction. Use same extraction volumes and procedure as in the first extraction described above. No further washing or extraction is made before the sample is diluted to the 100-ml volume.

Comparative pF methods

Modified distillation. To provide a basis for comparison, a distillation procedure for separation of fluoride from the interfering ions was used. Carry out the distillation essentially as reported previously[7], but do not place the sample, which has been made slightly alkaline, in the distillation flask. The large amount of silver chloride precipitate that forms with seawater samples causes serious bumping during the distillation. To avoid this, add the sample dropwise from an addition funnel; rapid distillation at slightly above 140° is then facilitated. Use additional distilled water to rinse all the sample into the distilling flask and to ensure that the fluoride has all been distilled into the receiver. Dilute the distillate to 250 ml in a volumetric flask as a sample stock solution.

Direct determination. For additional comparison, the water samples were diluted directly with the TISAB and the pF was measured directly.

pF measurement

Dilute the sample stock solution from the above treatment with TISAB and distilled water as previously reported[7]. Determine the fluoride activity directly with a precalibrated fluoride electrode.

RESULTS AND DISCUSSION

The results of the analyses on the nine samples by the pF method directly and after extraction or distillation are presented in Table I. The double extraction technique yielded results which were quite close to those obtained by distillation, but the

TABLE I

FLUORIDE CONTENT OF SEVERAL WATER SAMPLES AS DETERMINED BY THREE METHODS

Sample	*F content (p.p.m. ± S.D.)*			
	Distillation–pF method	*Direct pF method*	*Extraction–pF method*	
			Single extr.	*Double extr.*
A (seawater)	0.915 ± 0.006	0.891 ± 0.025	0.913 ± 0.008	0.916 ± 0.004
B (seawater)	0.853 ± 0.006	–	0.852 ± 0.007	0.855 ± 0.002
C (seawater)	1.208 ± 0.007	1.081 ± 0.041	1.211 ± 0.011	1.209 ± 0.006
D (seawater)	0.976 ± 0.008	0.935 ± 0.028	0.973 ± 0.010	0.980 ± 0.003
E (city water)	1.049 ± 0.012	1.042 ± 0.010	1.038 ± 0.014	1.049 ± 0.008
F (well water)	0.176 ± 0.003	0.172 ± 0.004	0.170 ± 0.005	0.175 ± 0.002
G (waste water)	5.701 ± 0.020	3.604 ± 0.081	–	5.711 ± 0.010
H (waste water)	3.004 ± 0.014	1.890 ± 0.060	2.890 ± 0.032	2.996 ± 0.010
I (waste water)	4.906 ± 0.018	2.540 ± 0.080	–	4.913 ± 0.012

extraction method had a consistently smaller standard deviation. Even the single extraction technique gave quite good results and although these were generally slightly lower than those obtained by the distillation method, their standard deviations were within 1.5% of the reference values.

The direct pF method gave results which were consistently lower than by the other two methods. The difference was especially pronounced in the analysis of the waste water samples which had a much higher concentration of dissolved material. The double extraction technique allows one operator to complete at least 4 determinations per h, whereas the distillation technique[7], which must be watched closely to ensure temperature control, requires at least 1 h per sample even when two or three are done simultaneously. The single extraction technique is even more rapid. When combined with the battery operated specific-ion meter, the latter method could be used quite easily in the field for routine analyses.

The results of a study of the recovery of standards of sodium fluoride and potassium fluorosilicate standards added to seawater after the extraction technique are shown in Fig. 1. Only at fluoride concentrations above about 6 p.p.m. were there significant decreases in the recovery of the added fluoride. The extraction technique can thus be used without dilution, on samples up to this concentration. Although the working limit for the single extraction procedure is lower, it can be used satisfactorily on sea and fresh water, as the usual fluoride contents are below 2 p.p.m.[13-16].

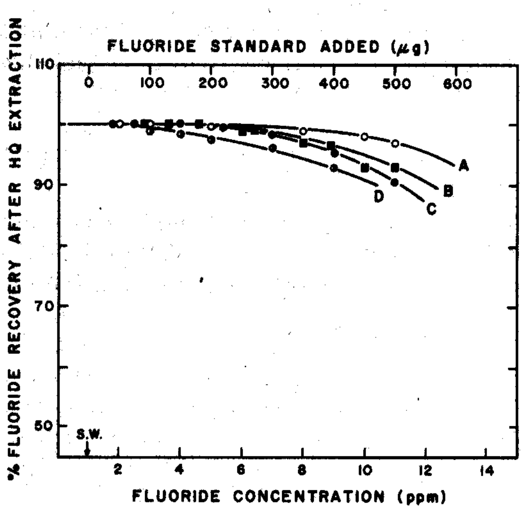

Fig. 1. Recovery of fluoride in the 8-hydroxyquinoline extraction method. (A) NaF standard, double extraction (○); (B) K_2SiF_6 standard, double extraction (☒);(C) Sample A (50 g) with NaF (●) or K_2SiF_6 (■) standards, double extraction; (D) Sample A (50 g) with NaF (◑) standard, single extraction.

The main natural interfering ions in water samples, magnesium(II) and calcium(II), and the potential pollutants as aluminum(III), iron(II) and iron(III), were reduced by the 8-hydroxyquinoline extraction to levels at which they no longer interfered with the pF determination[7]. At the pH of 10.5 used here, 8-hydroxyquinoline forms complexes with most polyvalent cations, such as the transition metals, as well as the alkaline earths[8]. Also, the DCTA used in the buffer is a strong complexing agent and forms soluble stable complexes with the small amounts of polyvalent cations that may remain after the extraction[17,18].

The effects of adding an excess of 50–250% of the major ions in seawater on the results of the extraction pF method were investigated with the results as shown in Table II. The method works well with 50% excess of chloride, magnesium(II) and calcium(II). With sulfate, silicate, iodide and borate, 100% or even 200% excess still caused no significant error. The presence of up to a 1 *M* concentration of sulfate was without significant effect.

TABLE II

EFFECTS OF ADDED FOREIGN IONS ON THE FLUORIDE DETERMINATION IN SEAWATER (50 g OF SAMPLE A) BY THE DOUBLE EXTRACTION–pF METHOD

Ion	*Added as*	*Ion added (mg)*	*% Excess*[a]	*F content (p.p.m.)*	*Rel. error (%)*
Cl^-	NaCl	600	50	0.912	−0.43
		1,200	100	0.861	−6.10
Mg(II)	$Mg(NO_3)_2$	32	50	0.899	−1.85
		64	100	0.745	−18.5
Ca(II)	$Ca(NO_3)_2$	12	50	0.918	0.28
		24	100	0.905	−1.21
SO_4^{2-}	Na_2SO_4	78	50	0.914	−0.28
		156	100	0.909	−0.76
BO_3^{3-}	H_3BO_3	0.02	100	0.914	−0.28
		10.04	200	0.917	0.14
SiO_3^{2-}	Na_2SiO_3	130.14	100	0.920	0.44
I^-	KI	0.01	250	0.915	−0.14
Al(III)	$AlCl_3$	1.0	—	0.916	0.00
		10.0	—	0.915	−0.14
Fe(III)	$FeCl_3$	2.0	—	0.915	−0.14
		20.0	—	0.915	−0.14

[a] $\% \text{ Excess} = \dfrac{\text{amount added} \cdot 100}{\text{maximum in normal seawater}^{18}}$

The synthesized samples with high contents of aluminum(III) and iron(III), up to 200 p.p.m., were also tested (Table II). It is believed that the recommended procedure can be effectively employed for fluoride determination in this kind of polluted water.

The amount of polyvalent ions in solution which can be complexed by citrate or DCTA in the TISAB is limited[6]. At pH 6.5 which is commonly used for pF measurements, the DCTA complexes with the ions such as calcium and magnesium[18,19] are significantly dissociated and it is not possible to dissolve a sufficient amount of DCTA to lower these metals to tolerable levels. In waters containing more than trace amounts of other ions such as aluminum(III) or iron(III), similar difficulties will be encountered. The effective removal of the 8-hydroxyquinoline complexes by the mixed solvent extraction technique presents a practical solution to this problem.

The direct pF procedure would work well for fluoride determination only in some fresh waters and most drinking waters. The extraction–pF method is recommended for the determination of fluoride in coast and surface seawaters[5], and most polluted natural and waste water. When the fluoride content is below 2 p.p.m., a single extraction procedure would work satisfactorily for general analysis of water samples.

We wish to express our sincere appreciation to Dr. R. G. Ackman and Mr. H. E. Power for their continuous encouragement and advice. This research was supported in part by Industrial Development Service of the Department of Fisheries and Forestry of Canada.

SUMMARY

A rapid method for fluoride determination in natural and waste water with a fluoride ion-specific electrode is described. This method involves a preliminary extraction of the interfering polyvalent cations, as their 8-hydroxyquinoline complexes, into a butyl cellosolve–chloroform mixture. The procedure is directly usable for water samples containing fluoride in the 0.2–6.0 p.p.m. range, with an overall error of less than 0.5%. The method can be successfully employed for fluoride determination in most polluted water samples which contain a high level of Ca, Mg, Fe and Al ions.

RÉSUMÉ

On décrit une méthode rapide pour le dosage des fluorures dans les eaux naturelles et les eaux résiduaires, à l'aide d'une électrode spécifique au fluorure. Elle comprend une extraction préliminaire des cations polyvalents gênants, sous forme de leur complexe avec l'hydroxy-8-quinoléine, dans un mélange butycellosolve–chloroforme. Ce procédé est directement applicable pour des échantillons d'eau contenant 0.2 à 6.0 p.p.m. de fluorure, avec une erreur inférieure à 0.5%. Il est utilisé aussi avec succès pour le dosage de fluorure dans la plupart des échantillons d'eau polluée contenant des teneurs élévées en Ca, Mg, Fe, et Al.

ZUSAMMENFASSUNG

Es wird eine schnelle Methode für die Fluoridbestimmung in natürlichem Wasser und Abwasser mittels einer fluoridspezifischen Elektrode beschrieben. Störende mehrwertige Kationen werden vorher als 8-Hydroxychinolin-Komplexe mit einem Butylcellosolve–Chloroform-Gemisch extrahiert. Das Verfahren ist unmittelbar auf Wasserproben mit einem Fluorid-Gehalt von 0.2–6.0 p.p.m. anwendbar; der Gesamt-Fehler ist kleiner als 0.5%. Die Methode kann mit Erfolg auf die Fluoridbestimmung in stark verunreinigtem Wasser mit einem hohen Gehalt an Ca-, Mg-, Fe- und Al-Ionen angewendet werden.

REFERENCES

1 M. S. Frant and J. W. Ross, Jr., *Science*, 154 (1966) 1553.
2 J. D. Johnson and E. D. Daugherty, *Dept. of Environ, Sci. and Eng., Univ. of N. Carolina, Chapel Hill, U.S.A., Publication No. 177*, 1968.
3 T. B. Warner, *Science*, 165 (1969) 178.
4 J. E. Harwood, *Water Res.*, 3 (1969) 273.

5 N. T. Crosby, A. L. Dennis and J. G. Stevens, *Analyst*, 93 (1968) 643.
6 E. F. McFarren, B. J. Moorman and J. H. Parker, *Water Fluoride No. 3*, U.S.P.H.S. Publication No. 1895, 1969.
7 P. J. Ke, L. W. Regier and H. E. Power, *Anal. Chem.*, 41 (1969) 1081.
8 R. Belcher and C. L. Wilson, *New Methods of Analytical Chemistry*, 2nd Edn., Reinhold, New York, 1964, p. 255.
9 C. L. Luke and M. E. Campbell, *Anal. Chem.*, 28 (1956) 1443.
10 F. Umland and K. U. Mechkenstock, *Z. Anal. Chem.*, 165 (1959) 161.
11 *Official Methods of Analysis*, 10th Edn., Assoc. Offic. Agr. Chemists, Washington, D.C., U.S.A., 1965, p. 360.
12 J. J. Lingane, *Anal. Chem.*, 39 (1967) 881.
13 E. G. Young, D. G. Smith and W. M. Langille, *J. Fisheries Res. Board Can.*, 16 (1959) 7.
14 T. Murakami and K. Uesugi, *Japan Analyst*, 14 (1965) 235.
15 A. Massoumi and J. Caraptian, *J. Dental Res.*, 46 (1967) 532.
16 R. Greenhalgh and J. P. Riley, *Nature*, 197 (1963) 371.
17 G. Schwarzenbach, R. Gut and G. Anderegg, *Helv. Chim. Acta*, 37 (1954) 937.
18 G. Anderegg, *Helv. Chim. Acta*, 46 (1963) 1833.
19 E. Bellack and P. J. Schouboe, *Anal. Chem.*, 30 (1958) 2032.

Analytica Chimica Acta
Elsevier Publishing Company, Amsterdam
Printed in The Netherlands

THE COULOMETRIC DETERMINATION OF AMYLASE IN SERUM*

JOHN R. MOODY AND WILLIAM C. PURDY
Department of Chemistry, University of Maryland, College Park, Md. 20742 (U.S.A.)

(Received August 3rd, 1970)

Historically, most saccharogenic and amyloclastic procedures, as well as the units for amylase activity, may be traced to Somogyi[1]. Several studies and improvements have been made on the saccharogenic procedure[2-4]. For sample sizes less than 100 μl, most methods involve modifications of the amyloclastic procedure, such as the one proposed by Street and Close[5]. Henry and Chiamori[3] reported a normal range of 34 to 141 Somogyi units but admitted that this is somewhat lower than values reported by other authors.

The present investigation on the determination of amylase was undertaken as a continuation of the application of coulometric titrations to clinical analyses[6,7]. A serum sample is incubated with starch and the reducing sugars produced are treated with the copper reagent of Nelson[8]. The copper(I) so formed is coulometrically titrated with generated bromine. Since a constant current is used, the titration time is directly proportional to the reducing power of the sugars present.

EXPERIMENTAL

Apparatus

Constant-current coulometric titrations were carried out with a ChrisFeld Microcoulometric Quantalyzer or the equivalent. The titration cell employed was similar to that previously described[9]. Biamperometric end-point detection was employed by imposition of 200 mV between two platinum-foil electrodes with a Sargent Model XV Polarograph. At the beginning of the titration, the presence of copper(I) and copper(II), a reversible couple, causes a current to flow between the indicator electrodes. As the copper(I) is titrated, the current decreases to a minimum. Beyond the equivalence point, the excess of bromine causes a sharp rise in the indicator current. All titrations were carried out to the same indicator current level or excess of bromine. The system was similar to that described by Lingane and Anson[10], who gave a more detailed description of the titration curve.

Reagents

Alkaline copper reagent (Nelson–Somogyi). Prepare before use by diluting 4 ml of copper solution B to 100 ml with copper solution A.

Copper reagent, Solution A. Dissolve 50 g of anhydrous sodium carbonate, 50

---

* Taken in part from the Ph.D. Dissertation of John R. Moody, University of Maryland, College Park, Md., 1970.

g of Rochelle salt, 40 g of sodium hydrogen carbonate, and 400 g of anhydrous sodium sulfate in 1600 ml of boiled, distilled water, and dilute to 2 l.

Copper reagent, Solution B. Dissolve 150 g of copper sulfate pentahydrate in 1 l of boiled, distilled water and add 0.5 ml of concentrated sulfuric acid.

Arsenomolybdate color reagent. Dissolve 50 g of ammonium molybdate in 900 ml distilled water. Add 42 ml of concentrated sulfuric acid and mix. Dissolve 6 g of disodium hydrogen arsenate heptahydrate in 50 ml of distilled water and add to the molybdate solution with stirring. Incubate the solution at 37° for 24–48 h. The reagent is stable when protected from light.

Benzoate buffer, 0.02 *M*, *pH* 5.5. Add 2.44 g of benzoic acid to 800 ml of distilled water and heat to boiling. When cooled, add 1 *M* sodium hydroxide until the pH is 5.5, and then dilute with water to 1 l. This reagent is good as a preservative in preparing glucose standards.

Deproteinizing reagents. Approximately 0.45 *N* barium hydroxide and 8% zinc sulfate are used. More important than the concentration of the reagents is that the reagents must exactly neutralize each other. The titers of the reagents should be determined by titration and adjusted until 10.00 ml of zinc sulfate is equivalent to 10.00 ± 0.05 ml of barium hydroxide. The barium hydroxide must be protected from carbon dioxide. Millipore filters can be used to produce reagents free of turbidity.

Generating reagent, 1.6 *M bromide and* 0.32 *M sulfuric acid.* Dissolve 164 g of sodium bromide in 800 ml of distilled water, add 17.8 ml of concentrated sulfuric acid, and dilute with water to 1 l.

Glucose standards. Reagent-grade dextrose is weighed in amounts between 50 and 1500 mg as desired. Dissolve the weighed samples and make up to 100 ml in 0.02 *M* benzoate buffer, pH 5.5.

Phosphate buffer, 0.1 *M*. Dissolve 4.55 g of potassium dihydrogen phosphate and 9.35 g of disodium hydrogen phosphate in boiled, distilled water and dilute to 1 l. Adjust the pH as needed to 7.0 with acid or base.

Starch solution. It is recommended that available commercial starch solutions be screened for stability. Potato starch and Somogyi's corn starch (Harleco) may be used with the 0.1 *M* phosphate buffer to prepare a starch substrate by the procedure of Henry and Chiamori[3]. Stability of the prepared reagent is a problem that is best prevented by preparing fresh starch solutions weekly.

Control sera. Versatol-E and Versatol-EN (Warner-Chilcott, Morris Plains, N.J.), or similar commercial sera, are prepared as directed and may be mixed to provide a set of control sera with different levels of amylase activity.

Procedures

Incubation step. For each serum sample, add 0.5 ml of starch solution to each of two test tubes (10-ml capacity). Incubate the first test tube, the control, for 40 min at 40° and then perform the deproteinizing step. Incubate the other test tube for 10 min at 40° to allow equilibration. Add 50 µl of serum, mix, incubate for exactly 30 min at 40° and then perform the deproteinizing step. Incubate an additional pair of test tubes containing 0.5 ml of starch solution for 40 min at 40° for each standard desired.

Deproteinizing step. After the incubation step, the enzyme reaction is stopped by preparing a protein-free filtrate. For each test tube add, in order, 1 ml of zinc sulfate reagent, 2.5 ml of water, and 1 ml of barium hydroxide reagent. Mix well after the addition of each reagent. Finally, cap the test tubes and allow the contents to settle for 10 min. Centrifuge for 5 min. After the addition of the zinc sulfate reagent, add 50 μl of serum to each control and 50 μl of glucose standard to each standard test tube and proceed with the rest of the procedure.

Copper reduction step. Remove a 2-ml aliquot from each test tube and transfer to a clean 10-ml test tube. Dilute 100 ml of freshly prepared alkaline copper reagent to 200 ml with boiled, distilled water and add 4 ml of the dilute copper reagent to each test tube[4].

Cap the test tubes and place in a boiling water bath for 40 min. Then remove the samples and place in cold water for several minutes to cool. Avoid shaking or vibration in handling the test tubes.

Colorimetric measurement step. After cooling, remove the caps from the test tubes and add 2 ml of arsenomolybdate color reagent to each test tube. Agitate each test tube until the evolution of carbon dioxide stops. Transfer the contents to a larger test tube using 4 ml of water to dilute. The color produced is stable indefinitely. The absorbance is measured at 540 nm. Samples of high amylase content may be diluted and re-read. The net absorbance of the standard is the absorbance of the standard less the absorbance of the blank.

$$\underset{\text{(Somogyi units)}}{\text{Amylase activity}} = \frac{\text{net absorbance of sample}}{\text{net absorbance of standard}} \cdot \text{mg\% glucose standard}$$

Measurement by coulometric titration. Wash the electrode assembly with distilled water and fill the isolated compartment with generating reagent. Add a stirring bar, 5 ml of distilled water, and 10 ml of generating reagent to a 30-ml beaker. Insert the electrode assembly and titrate at a generating rate of 0.01 μeq sec^{-1} using indicator electrodes with an applied potential of 200 mV and a recorder sensitivity of 0.01 μA mm^{-1} of chart width. Shut off the generating current when the pen rises 1 cm above the minimum in the titration curve.

This pre-titration allows the controls on the coulometer to be adjusted and conditions the electrodes for titration. After the test tubes used in the copper-reduction step have cooled, remove one test tube at a time for titration. Use 10 ml of generating reagent to help dissolve and transfer the contents of the test tube into a 30-ml beaker. Rinse the electrodes in distilled water and immediately titrate the sample as in the pre-titration step. Record the titration time in sec and repeat this procedure for all samples. The difference in titration time between a sample and its control (the net titration time) is proportional to amylase activity. Similarly, for a standard, the net titration time is proportional to the mg% of reducing sugar present.

$$\underset{\text{(Somogyi units)}}{\text{Amylase activity}} = \frac{\text{net titration time of sample}}{\text{net titration time of standard}} \cdot \text{mg\% glucose standard}$$

RESULTS AND DISCUSSION

The greatest limitation in the procedure is the susceptibility of the reduced copper to air oxidation. Calibration curves were prepared with glucose standards.

These curves were used to optimize the heating time for the copper reagent in the boiling water bath and to determine the minimum feasible sample size. The dilute copper reagent, as employed by Sax and Trimble[4], was found to give better results than the usual proportion of reagents employed in the Nelson–Somogyi method.

The effect of the deproteinizing reagents was also studied. The high concentration employed was necessary to achieve final solutions which were not turbid. While turbid solutions did not appear to affect data obtained in the coulometric titration, corresponding data by the colorimetric method were obviously affected.

The most frequent cause of difficulty was in the preparation of a stable starch solution. The use of propyl *p*-hydroxybenzoate as a preservative produced a large blank. The TRIS–hydrochloric acid buffer used by Sax and Trimble[4] also produced a large blank as did many commercial starch solutions and all solutions prepared from soluble starch. The stability problem was minimized by weekly preparation of the reagent.

Another difficulty was found in the incomplete recovery of maltose from starch and the deproteinizing reagents when samples of less than 200 mg% were used. Recovery was found to improve in the presence of serum. The deproteinizing procedure was modified both to minimize this problem and to avoid turbidity. A limit of about 1100 Somogyi units was found through use of an amylase preparation of high activity. This limit is determined primarily by the amount of starch used and, to a lesser degree, by re-oxidation of the reduced copper before titration.

With the procedures presented, a large number of replicate determinations were performed on several different lots of Versatol-E and Versatol-EN sera over a period of several days. Determinations were made on the same samples by both the coulometric and the colorimetric procedures. Agreement between the two procedures was consistent with the standard deviations of the two procedures.

Tables I and II summarize results obtained by the coulometric and colorimetric methods, respectively. Quantitatively, it is of interest to note that the response of the two methods to the activity of the Versatol control sera is proportional to the activity of the amylase. This is expressed as a factor, *m*, which should be a constant for a linear calibration curve.

The average standard deviation for all samples run varied between 8.1 and 13.7 mg% on a day-to-day basis. The values for the same sample were 10.1 to 27.2

TABLE I

ANALYSIS OF VERSATOLS—COULOMETRIC DETERMINATION

Activity of Versatol (mg %)	*Total samples*	*Av. titration time (sec)*	$\frac{\textit{Titration time}}{\textit{Activity}}$	*Average daily standard deviation (mg %)*
82.8	19	47.9	0.579	9.9
144	9	85.5	0.596	12.3
188	10	122.0	0.649	11.3
205	9	126.5	0.617	8.1
266	9	155.8	0.586	12.8
293	10	204.6	0.698	11.4
327	9	196.5	0.601	13.7

TABLE II

ANALYSIS OF VERSATOLS–COLORIMETRIC DETERMINATION

Activity of Versatol (mg %)	*Total samples*	*Av. absorbance values (abs. units)*	$\frac{A\cdot 1000}{\textit{Activity}}$	*Average daily standard deviation (mg %)*
82.8	16	0.067	0.809	19.6
144	6	0.118	0.819	17.1
188	10	0.178	0.946	12.7
205	6	0.181	0.891	27.2
266	6	0.238	0.893	10.1
293	10	0.280	0.955	16.7
327	6	0.288	0.881	15.9

mg% by the colorimetric procedure. Results were also checked by running standard glucose samples. Owing to the smaller sample size, the standard deviation is poorer than usual. The advantage of the small samples is that sera of high activity (less than 1100 Somogyi units) may be analyzed without dilution of the sample and repetition of the test.

When the activity of the Versatol control sera was then calculated, the results were an average of 18% low whether performed by the coulometric or colorimetric method. The reason for this discrepancy is not clear but it was consistent throughout this study. A possibility is that the activity of the Versatol sera used was lower than normal.

TABLE III

COULOMETRIC AND COLORIMETRIC ANALYSIS OF SERUM

Serum	*No. of detns.*	*Reported (mg %)*	*Found*			
			Coulometric (mg %)	*Rel. error (%)*	*Colorimetric (mg %)*	*Rel. error (%)*
1	3	82	69	−15.9	—	
2	2	62	46	−25.8	—	
3	2	109	104	− 4.6	—	
4	2	79	52	−34.2	—	
5	3	324	368	13.6	—	
6	2	163	120	−26.4	—	
7	2	50	52	4.4	—	
8	2	140	151	7.9	—	
9	3	170	163	− 4.1	—	
10	2	67	67	0	—	
11	2	141	130	− 7.8	120	−14.9
12	3	73	85	16.5	83	13.3
13	2	51	49	− 3.2	53	3.2
14	2	107	113	5.6	118	10.3
15	2	71	86	21.1	87	22.6
16	2	161	181	12.4	178	10.5

Finally, sixteen serum samples were obtained from the clinical laboratory at Walter Reed Army Medical Center. These sera had previously been analyzed by the iodimetric procedure of Van Loon *et al.*[11]. The values reported were based on the use of Versatol control sera as a standard. The results obtained by the coulometric procedure are summarized in Table III.

The standard deviation averaged about 7 sec for all the sera. This corresponds to an average relative per cent standard deviation of 6% for the sera analyzed. This is slightly better than the results obtained from Versatol analyses. However, for all samples, there was an average error of 12.7% compared to the reported values.

Again the agreement between the coulometric and colorimetric procedures was good. Both procedures have an average per cent relative standard deviation of 10% or less. The largest errors and deviations by both procedures can be expected at low values of amylase activity; for such samples, the relative per cent error can be much larger than 10%.

The standard deviation of the Van Loon method was said to be as much as 10%, but usually somewhat less. A direct comparison of the two procedures must be made with an awareness of the uncertainty of each method. On the average, however, there was only a 2.5% difference between the coulometric and colorimetric data and the reported values. Once again, results calculated by the use of glucose standards were an average of 18% lower than results obtained using Versatol sera. All data in Table III are based on the use of Versatol-E control serum. The good agreement between coulometric and colorimetric data suggests that some of the difference with the reported (Van Loon) values may be due to differences in the basic procedures, *e.g.*, amyloclastic *vs.* saccharogenic, or aging of the serum samples between analyses as well as differences explainable on a purely statistical basis.

The authors are indebted to the U.S. Army Medical Research & Development Command for partial support of this work under Contract No. DADA17-67-C-7161.

SUMMARY

The saccharogenic procedure for serum amylase involves the determination of reducing sugars present both before and after incubation of the serum sample with starch substrate. The standard incubation conditions are those of Somogyi. Following the incubation period, a deproteinizing step is performed and the reducing sugars present are then determined. In the present method the reducing sugars are determined by coulometric titration with generated bromine. An analysis may be performed on as little as 100 μl of serum. Turbid solutions do not interfere in the coulometric procedure. The accuracy and precision of the coulometric and a colorimetric method are comparable. Both are limited by difficulties in the steps preceding measurement rather than in the measurement step itself.

RÉSUMÉ

Le procédé "saccharogénique" de l'amylase du sérum comprend le dosage de sucres réducteurs présents avant et après incubation de l'échantillon de sérum. Dans la méthode décrite, les sucres réducteurs sont dosés par titrage coulométrique à l'aide de brome électrogénéré. Une analyse peut être effectuée sur 100 μl de sérum. Des solutions troubles ne gènent pas. La précision et l'exactitude de cette méthode coulométrique est comparable à celle de la colorimétrie.

ZUSAMMENFASSUNG

Bei dem saccharogenen Verfahren für Serumamylase werden die reduzierenden Zucker bestimmt, die vor und nach Inkubation der Serumprobe mit Stärkesubstrat vorliegen. Die Standard-Inkubationsbedingungen sind jene von Somogyi. Auf die Inkubationsperiode folgt eine Deproteinisierungsstufe, und dann werden die reduzierenden Zucker bestimmt. Bei der vorliegenden Methode werden die reduzierenden Zucker durch coulometrische Titration mit Brom bestimmt. Für eine Analyse reichen 100 μl Serum aus. Trübe Lösungen stören bei dem coulometrischen Verfahren nicht. Sicherheit und Genauigkeit der coulometrischen und einer colorimetrischen Methode sind vergleichbar. Beide sind mehr durch Schwierigkeiten bei den Schritten begrenzt, die der Messung vorasugehen, als durch die Messung selbst.

REFERENCES

1 M. Somogyi, *J. Biol. Chem.*, 125 (1938) 399.
2 M. Somogyi, *Clin. Chem.*, 6 (1960) 23.
3 R. J. Henry and N. Chiamori, *Clin. Chem.*, 6 (1960) 434.
4 S. M. Sax and G. E. Trimble, *Clin. Chem.*, 9 (1963) 296.
5 H. V. Street and J. R. Close, *Clin. Chim. Acta*, 1 (1956) 256.
6 W. C. Purdy, *Z. Anal. Chem.*, 243 (1968) 17.
7 W. C. Purdy, *VIIth Intern. Congr. Clin. Chem., Geneva/Evian, 1969, Vol. 1, Methods in Clinical Chemistry*, S. Karger, Basel, 1970, pp. 82–97.
8 N. Nelson, *J. Biol. Chem.*, 153 (1944) 375.
9 G. D. Christian and W. C. Purdy, *Amer. J. Clin. Pathol.*, 46 (1966) 185.
10 J. J. Lingane and F. C. Anson, *Anal. Chem.*, 28 (1956) 187.
11 E. J. van Loon, M. R. Likins and A. J. Seger, *Amer. J. Clin. Pathol.*, 22 (1952) 1134.

Analytica Chimica Acta
Elsevier Publishing Company, Amsterdam
Printed in The Netherlands

ACID–BASE STRENGTHS IN PYRIDINE

M. BOS AND E. A. M. F. DAHMEN
Department of Chemical Technology, Twente University of Technology, Enschede (The Netherlands)

(Received July 21st, 1970)

Pyridine is an important solvent for acid–base titrations, but there are few systematic investigations about the equilibria that play a part in neutralization reactions in pyridine. It is generally accepted that ion pairs occur as intermediates in the dissociation of acids in solvents like pyridine[1-3]. Only overall dissociation constants of some acids have been measured in pyridine[1,2].

When ion-pair formation occurs these overall dissociation constants are not suitable for the comparison of the acid strengths of a compound in different solvents[4]. For this comparison the so-called ionization constants are needed. If the dissociation of an acid in pyridine is represented by the following equilibria

$$HX \leftrightharpoons H^+X^- \leftrightharpoons H^+ + X^- \tag{1}$$

this ionization constant is defined as

$$K_i^{HX} = [H^+X^-]/[HX] \tag{2}$$

The dissociation constant of the ion pair is given by

$$K_d^{H^+X^-} = [H^+][X^-]/[H^+X^-] \tag{3}$$

For acids of the ammonium type the dissociation can be represented by

$$BH^+ \leftrightharpoons B + H^+ \tag{4}$$

Here the dissociation constant can be defined as

$$K_d^{BH^+} = [B][H^+]/[BH^+] \tag{5}$$

In order to determine the ionization constant of an indicator acid, the method proposed by Kolthoff and Bruckenstein[4] can be used.

In this paper, besides the application of the method by Kolthoff and Bruckenstein, a method for the determination of dissociation constants of acids of the ammonium type from titration curves is discussed.

EXPERIMENTAL

Chemicals

Pyridine. Pyridine (Merck, reagent grade) was kept over an activated molecular sieve 3A for 48 h and was afterwards distilled over barium oxide. The pyridine (b.p. 115°) was collected and stored in an automatic burette. From this burette it was dispensed under pressure of carbon dioxide-free nitrogen. The water content was below 0.05% (Karl Fischer titration).

Perchloric acid. This was used as its pyridinium salt, which was prepared as described by Mukherjee *et al.*[1].

Hydrochloric acid. Solutions of hydrochloric acid in pyridine were prepared by passing a stream of dry hydrogen chloride gas through pyridine.

Sulfonphthaleins. The sulfonphthaleins, bromophenol blue, bromocresol purple, bromocresol green and chlorophenol red (indicator grade, Merck) were used as received.

Nitrophenols. The following samples were used: picric acid (Merck, reagent grade), 3-nitrophenol (Merck, indicator grade), 2,4-dinitrophenol (Merck and dried *in vacuo* at 40°), 2,5-dinitrophenol (Merck, indicator grade), 2,6-dinitrophenol (Merck, indicator grade). All the dinitrophenols were recrystallized twice from ether and dried *in vacuo* at 40°.

Bases. The bases used were *n*-butylamine, triethylamine and morpholine, all of which were reagent grade (Fluka).

Spectrophotometric technique

All measurements were carried out with a Zeiss spectrophotometer, type PMQ II, at a temperature of $20 \pm 2°$ in quartz cells with a light path of 1 cm.

Differential vapour pressure measurements

A Mechrolab model 301A osmometer was used for the differential vapour pressure measurements at 37°. The osmometer was calibrated for pyridine with benzil.

Potentiometric measurements

A Knick pH-meter, type 260, was used for the potentiometric measurements. The glass electrode was a Radiometer G222c electrode. As reference electrode an Ag/AgCl electrode filled with a saturated solution of tetramethylammonium chloride in pyridine was used. When not in use the glass electrode was kept in an aqueous buffer pH of 7. With this set of electrodes each potential measurement was continued until its change within 5 min became less than 2 mV. This took about 30 min. The resulting values are reproducible within ± 2 mV. The glass electrode was calibrated regularly in standard solutions of perchloric acid in pyridine.

Potentiometric titrations

The potentiometric titrations were recorded automatically with a Radiometer titration assembly composed of pH-meter PHM 28, burette ABU 2, recorder SBRC, and titrator TT 11. The electrode set was the same as the one described above. Titration curves were reproducible within ±5 mV.

RESULTS

Spectrophotometric measurements

If an ion pair occurs as an intermediate in the dissociation of an indicator acid, the ionization and dissociation constant of this acid can be determined spectrophotometrically by means of the method developed by Kolthoff and Bruckenstein[4]. This method is based on the equation

$$[\mathrm{HIn}]/\{\Sigma[\mathrm{base}]-K_{\mathrm{i}}[\mathrm{HI}]\}^{2}=(K_{\mathrm{i}}K_{\mathrm{d}})^{-1} \tag{6}$$

where [HIn] is the concentration of the indicator in the acid colour, and Σ[base] is the spectrophotometrically determined concentration of the indicator in the basic colour; K_{i} and K_{d} are the ionization and the dissociation constants, respectively.

In the case of the polynitrophenols and sulfonphthaleins application of eqn. (6) did not result in a single value for K_{i}. Instead, the results of the experiments, plotted according to eqn. (6) gave straight lines for a wide range of values for K_{i}. The results did, however, follow the equation for simple dissociation:

$$\{\Sigma[\mathrm{base}]\}^{2}/[\mathrm{HIn}]^{1}=K_{\mathrm{HX}} \tag{7}$$

For the determination of the dissociation constants of sulfonphthaleins, solutions of these compounds were used in which the first step of the acid was neutralized with tetramethylguanidine. Molar extinction coefficients were determined in solutions of the indicators to which an excess of tetramethylammonium hydroxide had been added.

The dissociation constants calculated from eqn. (7) are given in Table I.

TABLE I

SPECTROPHOTOMETRIC DETERMINATION OF K_{HX} FROM DILUTION SERIES OF INDICATOR ACIDS[a]

Indicator	$\lambda_{max.base}$ (*nm*)	ε_{base}	K_{HX}	pK_{HX}
Picric acid	380	$1.91 \cdot 10^{4}$[b]	$1.1 \cdot 10^{-3}$	3.0
2,6-Dinitrophenol	462	$1.07 \cdot 10^{4}$[b]	$5.9 \cdot 10^{-5}$	4.2
2,5-Dinitrophenol	470	$5.77 \cdot 10^{3}$[b]	$9.8 \cdot 10^{-6}$	5.0
Bromophenol blue[2]	607	$1.17 \cdot 10^{5}$	$5.6 \cdot 10^{-6}$	5.3
Bromocresol green[2]	633	$6.59 \cdot 10^{4}$	$3.4 \cdot 10^{-6}$	5.5
Bromocresol purple[2]	610	$1.09 \cdot 10^{5}$	$3.1 \cdot 10^{-8}$	7.5
Chlorophenol red[2]	597	$8.03 \cdot 10^{4}$	$8.4 \cdot 10^{-11}$	10.1

[a] Activity coefficients for ionic species were calculated from $-\log f=8.191\ \mu^{\frac{1}{2}}$, while the activity coefficients for non-ionic species were assumed to be unity.

[b] It was assumed that the acid is non-absorbing at this wavelength.

Differential vapour pressure measurements

The overall dissociation constant of an acid HX can be found by means of differential vapour pressure (DVP) measurements with the equation[1]

$$K_{\mathrm{HX}}=(m_{\mathrm{d}}-m_{\mathrm{s}})^{2}/(2m_{\mathrm{s}}-m_{\mathrm{d}}) \tag{8}$$

where m_{d} is the molarity measured by the DVP method and m_{s} is the stoichiometric concentration of HX.

The same equation can be applied in the determination of the dissociation constant of salts by this method (assuming that no acid–base dissociation occurs).

The results of the DVP measurements are given in Table II (acids) and Table III (salts).

TABLE II

DETERMINATION OF K_{HX} BY THE DIFFERENTIAL VAPOUR PRESSURE METHOD AT 37°

Acid	K_{HX}	pK_{HX}
Perchloric acid	$9.3\cdot10^{-4}$	3.0
Picric acid	$1.3\cdot10^{-3}$	2.9
2,5-Dinitrophenol	$2.8\cdot10^{-5}$	4.6
2,6-Dinitrophenol	$2.1\cdot10^{-4}$	3.7
2,4-Dinitrophenol	$1.0\cdot10^{-4}$	4.0

TABLE III

SALT DISSOCIATION CONSTANTS DETERMINED BY THE DIFFERENTIAL VAPOUR PRESSURE METHOD AT 37°

	Tetra-methyl-guanidine	n-*Butyl-amine*	*Morpho-line*	*Triethyl-amine*
Perchloric acid	$1.5\cdot10^{-3}$	$9.5\cdot10^{-4}$	$6.1\cdot10^{-3}$	$5.3\cdot10^{-4}$
Hydrochloric acid	$1.5\cdot10^{-4}$	$6.3\cdot10^{-5}$	$3.4\cdot10^{-5}$	$2.8\cdot10^{-6}$
Picric acid	$3.9\cdot10^{-4}$	$6.7\cdot10^{-4}$	$2.0\cdot10^{-3}$	$1.6\cdot10^{-3}$
2,5-Dinitrophenol	$2.6\cdot10^{-4}$			
2,6-Dinitrophenol	$4.0\cdot10^{-4}$			
2,4-Dinitrophenol	$5.2\cdot10^{-4}$			

Potentiometric measurements. Calibration of the glass electrode

At 25° the e.m.f. of the cell

glass electrode | solution HX | ref. electrode

is given by

$$E_{(\mathrm{mV})} = E_{\mathrm{ref}} + E_{\mathrm{l.j.}} + 29.5 \log K_{\mathrm{HX}} + 29.5 \log C_{\mathrm{HX}} \tag{9}$$

By measuring an acid with a known overall dissociation constant, one can find $E_{\mathrm{ref}}+E_{\mathrm{l.j.}}$. If it is assumed that $E_{\mathrm{ref}}+E_{\mathrm{l.j.}}$ is constant, one can determine pH values of unknown solutions from

$$\mathrm{pH} = \tfrac{1}{59}\,(E_{\mathrm{ref}} + E_{\mathrm{l.j.}} - E) \tag{10}$$

The behaviour of the glass electrode used can be represented by

$$-E_{(\mathrm{mV})} = 29.4 \log C_{\mathrm{HClO_4}} + 155$$

or, with $\mathrm{p}K_{\mathrm{HClO_4}} = 3.2^{1}$:

$$E_{(\mathrm{mV})} = 250 + 59 \log [\mathrm{H}^+]$$

This calibration with perchloric acid solutions was repeated for each set of potentiometric determinations. The results of the potentiometric determinations, calculated according to the equation for simple dissociation, are given in Table IV.

TABLE IV

K_{HX}, DETERMINED POTENTIOMETRICALLY

Acid	K_{HX}	pK_{HX}
Picric acid	$2.8\cdot10^{-4}$	3.5
2,6-Dinitrophenol	$1.9\cdot10^{-5}$	4.7
2,5-Dinitrophenol	$5.1\cdot10^{-6}$	5.3
3-Nitrophenol	$1.4\cdot10^{-13}$	12.5
2,4-Dinitrophenol	$4.1\cdot10^{-5}$	4.4

Potentiometric titrations

The following equilibria can be assumed to play a part in the titration of an acid HX with a nitrogen base B:

$$HX \overset{K_{HX}}{\rightleftharpoons} H^+ + X^-$$

$$H^+ + B \overset{1/K_d^{BH^+}}{\rightleftharpoons} BH^+$$

$$BH^+ + X^- \overset{1/K_d^{salt}}{\rightleftharpoons} BH^+X^-$$

If the equilibrium constants are known, the titration curve can be calculated by general methods of equilibrium calculations[5] with the aid of a fast digital computer. On the other hand equilibrium constants can be calculated from experimental titration curves by repeatedly entering the calculation procedure with various values for the constant to be determined until for one value of this constant, the experimental and the calculation curves give the best fit. In this way, the value of $K_d^{BH^+}$ for nitrogen bases can be determined when they are titrated with an acid of a known dissociation constant.

With the dissociation constants of the salts measured by the DVP method, $K_d^{BH^+}$ values were determined for tetramethylguanidine-H$^+$, morpholine-H$^+$, triethylamine-H$^+$ and *n*-butylamine-H$^+$ from the titrations of hydrochloric acid, perchloric acid and picric acid with the corresponding bases. The following p*K* values were used for the acids in the calculations: $pK_{HCl}=5.66$[1], $pK_{HClO_4}=3.2$[1], $pK_{picric\ acid}=3.0$. The results are summarized in Table V.

If homoconjugation does occur, the following set of equilibria must be used in the calculations:

TABLE V

$K_d^{BH^+}$ DETERMINED FROM POTENTIOMETRIC TITRATIONS

Acid used	$K_d^{BH^+}$			
	n-*Butylamine*	*Morpholine*	*Triethylamine*	*TMG*
Perchloric acid	$1.7\cdot10^{-6}$	$2.9\cdot10^{-4}$	$2.0\cdot10^{-4}$	$4.2\cdot10^{-10}$
Picric acid	$6.0\cdot10^{-6}$	$5.0\cdot10^{-4}$	$1.3\cdot10^{-4}$	$1.0\cdot10^{-10}$
Hydrochloric acid	$2.5\cdot10^{-6}$	$1.5\cdot10^{-4}$		$2.1\cdot10^{-10}$
Average	$3.5\cdot10^{-6}$	$3.1\cdot10^{-4}$	$1.7\cdot10^{-4}$	$2.4\cdot10^{-10}$

$$\mathrm{HX} \xrightleftharpoons{K_{\mathrm{HX}}} \mathrm{H^+ + X^-}$$

$$\mathrm{HX + X^-} \xrightleftharpoons{K_{\mathrm{HX_2}}} \mathrm{HX_2^-}$$

$$\mathrm{B + H^+} \xrightleftharpoons{1/K_d^{\mathrm{BH^+}}} \mathrm{BH^+}$$

$$\mathrm{BH^+ + X^-} \xrightleftharpoons{1/K_d^{\mathrm{salt}}} \mathrm{BH^+X^-}$$

With known values for K_d^{salt} and $K_d^{\mathrm{BH^+}}$, the dissociation constant, K_{HX}, as well as the homoconjugation constant, $K_{\mathrm{HX_2}}$, can be determined from the curves of the potentiometric titrations of 2,4-dinitrophenol, 2,5-dinitrophenol and 2,6-dinitrophenol with tetramethylguanidine. Here, it is necessary to vary both K_{HX} and $K_{\mathrm{HX_2}}$ until the best fit between experimental and calculated titration curve occurs. The results of these determinations are summarized in Table VI.

DISCUSSION

The results of the spectrophotometric determinations of the dissociation constants of polynitrophenols and sulfonphthaleins can be explained on the basis of

TABLE VI

K_{HX} AND $K_{\mathrm{HX_2}}$ FOR POLYNITROPHENOLS DETERMINED FROM POTENTIOMETRIC TITRATION CURVES[a]

Compound	K_{HX}	K_{HX_2}
2,4-Dinitrophenol	$5 \cdot 10^{-5}$	10
2,5-Dinitrophenol	$2.8 \cdot 10^{-7}$	100
2,6-Dinitrophenol	$1.1 \cdot 10^{-5}$	10^{-1}

[a] Calculations based on concentrations, not on activities.

TABLE VII

p*K* VALUES IN PYRIDINE

Compound	p*K*			
	Spectrophotom.	*DVP*	*Potentiom.*	*Titration*
Picric acid	3.0	2.9	3.5	
2,6-Dinitrophenol	4.2	3.7	4.8	4.7
2,4-Dinitrophenol		4.0	4.4	4.3
2,5-Dinitrophenol	5.0	4.6	5.3	6.5
Bromophenol blue[2]	5.3			
Bromocresol purple[2]	7.5			
Bromocresol green[2]	5.5			
Chlorophenol red[2]	10.1			
3-Nitrophenol			12.5	
n-Butylamine-H$^+$				5.5
Morpholine-H$^+$				3.5
Triethylamine-H$^+$				3.8
Tetramethylguanidine-H$^+$				9.6

simple dissociation. This indicates that no ion pairs occur as intermediates in the dissociation of these compounds in pyridine, although the dielectric constant of this solvent is rather low.

Homoconjugation can explain the typical form of the curves for the titrations of 2,4-dinitrophenol, 2,5-dinitrophenol and 2,6-dinitrophenol with tetramethylguanidine. It also explains the discrepancies in the pK values determined from the titration curves on the one hand and from spectrophotometric and potentiometric measurements on the other, for the latter are calculated on the basis of simple dissociation only.

The differences found by Mukherjee *et al.*[1] between pK values determined spectrophotometrically in solutions of pure 2,5-dinitrophenol and in mixtures of 2,5-dinitrophenol and a non-absorbing acid can be explained in the same way.

The pK values, determined in different ways, are summarized in Table VII.

A comparison of the pK values in water and in pyridine is given in Table VIII.

TABLE VIII

pK_a VALUES IN PYRIDINE COMPARED WITH pK_a VALUES IN WATER

Compound	$pK_{(pyr)}$	$pK_{(water)}$	ΔpK
Picric acid	3.0	0.4	2.6
2,6-Dinitrophenol	3.7	3.0	0.7
2,4-Dinitrophenol	4.2	3.5	0.7
2,5-Dinitrophenol	5.0	4.7	0.3
Bromophenol blue[2]	5.3	4.0	1.3
Bromocresol green[2]	5.5	4.7	0.6
Bromocresol purple[2]	7.5	6.1	1.4
Chlorophenol red[2]	10.1	6.1	4.0
3-Nitrophenol	12.5	7.2	5.3
n-Butylamine-H^+	5.5	10.6	−5.1
Morpholine-H^+	3.5	9.6	−6.1
Triethylamine-H^+	3.8	10.8	−7.0
Tetramethylguanidine-H^+	9.6	12.3	−2.7

It is interesting to note that the pK values for the protonated nitrogen bases are much lower in pyridine than in water. Undoubtedly, this is due to the greater basicity of pyridine compared with water. With uncharged or negatively charged acids the dielectric constant of the solvent has great influence on the dissociation. This could explain why for these acids $pK_{(pyridine)}$ is greater than $pK_{(water)}$.

The authors wish to thank Mr. H. Hof who carried out most of the potentiometric determinations and Miss A. L. Dekkers who prepared the manuscript.

SUMMARY

Although pyridine is a solvent with a low dielectric constant, spectrophotometric determinations show simple dissociation without ion pairs as intermediates for some sulfonphthaleins and polynitrophenols in pyridine.

The salts of a number of amines and hydrochloric acid, perchloric acid and picric acid are not completely dissociated in pyridine. Dissociation constants of these salts were determined from differential vapour pressure measurements. For the titrations in pyridine of an acid with an amine, calculations were based on the following reactions: $HX \rightleftharpoons H^+ + X^-$; $B + H^+ \rightleftharpoons BH^+$; $BH^+ + X^- \rightleftharpoons BH^+X^-$. With this reaction scheme it was possible to determine pK_a values for protonated amines in pyridine from the curves of titrations carried out with a calibrated glass electrode. Evidence for the occurrence of homoconjugation of some polynitrophenols in pyridine was found in the titration of these compounds with tetramethylguanidine. Homoconjugation constants were estimated from the titration curves.

RÉSUMÉ

Bien que la pyridine soit un solvant à faible constante diélectrique, des dosages spectrophotométriques montrent une dissociation simple pour quelques sulfophtaléines et polynitrophénols dans la pyridine. Les sels d'un certain nombre d'amines et acides chlorhydrique, perchlorique et picrique ne sont pas complètement dissociés dans la pyridine. Les constantes de dissociation de ces sels sont déterminées par des mesures de pression de vapeur différentielle. Pour les titrages d'un acide par une amine, dans la pyridine, des réactions sont données, permettent de déterminer les valeurs de pK_a.

ZUSAMMENFASSUNG

Obwohl Pyridin ein Lösungsmittel mit einer niedrigen Dielektrizitätskonstante ist, weisen spektrophotometrische Untersuchungen einiger Sulfonphthaleine und Polynitrophenole in Pyridin auf einfache Dissoziation ohne Ionenpaare als Zwischenstufen hin. Die Salze von einer Anzahl Amine und Salzsäure, Perchlorsäure und Pikrinsäure sind in Pyridin nicht vollständig dissoziiert. Dissoziationskonstanten dieser Salze wurden aus Differentialdampfdruckmessungen bestimmt. Berechnungen für die Titrationen einer Säure mit einem Amin in Pyridin gründeten sich auf folgende Reaktionen: $HX \rightleftharpoons H^+ + X^-$; $B + H^+ \rightleftharpoons BH^+$; $BH^+ + X^- \rightleftharpoons BH^+X^-$. Mit diesem Reaktionsschema konnten die pK_a-Werte für protonierte Amine in Pyridin aus den Titrationskurven bestimmt werden, die mit einer geeichten Glaselektrode erhalten wurden. Für einige Polynitrophenole in Pyridin wurden bei der Titration dieser Verbindungen Beweise für das Auftreten von Homokonjugation gefunden. Aus den Titrationskurven wurden Homokonjugationskonstanten ermittelt.

REFERENCES

1 L. M. Mukherjee, J. J. Kelly, W. Baranetzky and J. Sica, *J. Phys. Chem.*, 72 (1968) 3410.
2 L. M. Mukherjee and J. J. Kelly, *J. Phys. Chem.*, 71 (1967) 2348.
3 S. Bruckenstein and I. M. Kolthoff, *J. Amer. Chem. Soc.*, 78 (1956) 10.
4 I. M. Kolthoff and S. Bruckenstein, *J. Amer. Chem. Soc.*, 78 (1956) 1.
5 D. F. DeTar, *Computer Programs for Chemistry, Vol. II*, 1969, pp. 65–67.

Analytica Chimica Acta
Elsevier Publishing Company, Amsterdam
Printed in The Netherlands

THE PRECONCENTRATION OF VARIOUS TRACE ELEMENTS IN SEAWATER BY SOLVENT EXTRACTION AND THE RING OVEN*

BRUCE ARMITAGE AND HARRY ZEITLIN

Department of Chemistry and Hawaii Institute of Geophysics, University of Hawaii, Honolulu, Hawaii 96822 (U.S.A.)

(Received August 24th, 1970)

Problems in the areas of biochemistry, geochemistry, and environmental pollution in many cases require quantitative information concerning the concentration and distribution of trace metallic constituents in seawater samples. The determination of multiple elements in a single sample is, of course, desirable but poses two main obstacles: (*a*) the necessity of pretreatment to preconcentrate and separate the species of interest from its aqueous matrix, (*b*) the need for an analytical method that is sufficiently accurate, precise and selective for the satisfactory determination of a number of elements which may be present in the parts per billion range.

Commonly used preconcentration methods are ion-exchange, solvent extraction, co-crystallization, and co-precipitation, which have been discussed by Riley and Skirrow[1] and by Joyner *et al.*[2]. Multi-element analytical techniques applied to seawater include atomic absorption[3-5], neutron activation[6], and X-ray fluorescence[7,8], each of which has advantages and limitations.

In the analysis of seawater an additional set of problems arises when the sampling is carried out at sea where shipboard facilities rarely permit, routinely, preconcentration of seawater samples. Since considerable time may elapse between collection and shore analysis, precautions should be taken to "stabilize" original concentration levels and prevent changes caused by biological and chemical activity which may lead to spurious data. Chemical preservatives are hazardous because of risks of contamination and of doubt as to their effectiveness. Of the methods available the most reliable storage procedure is freezing in plastic containers which in all probability reduces changes to a minimum, although the possibility of chemical adsorption on the container walls should be faced.

A procedure has been developed for the preconcentration of various trace elements in seawater which possesses a number of advantages and avoids the difficulties alluded to above. The method permits the analysis of six trace elements uranium, copper, nickel, cobalt, iron, and manganese in a sample of seawater through a combination of solvent extraction with an 8-hydroxyquinoline–chloroform mixture and X-ray fluorescence spectrometry. No pH adjustment is required and the primary concentration step which may be carried out on board ship entails only three reagents and minimal minor equipment. Addition of a ring oven and a light portable pump makes possible the evaporation of extracted samples on filter-paper disks thus elimi-

---

* Hawaii Institute of Geophysics Contribution No. 366.

nating the danger of changes caused by storage and adsorption on walls of containers. The filter-paper disks may be stored indefinitely for analysis and future reference if desired.

With application of X-ray fluorescence and a sample volume of 100 ml a precision of 10% or better was achieved in the analysis for copper, nickel, iron, and manganese, and 20% and 30% for uranium and cobalt, respectively. The extraction procedure, however, does not limit the final analysis to the use of X-rays, since it should be possible to apply successfully either neutron activation or atomic absorption analysis to the dried primary extract if dissolved in a suitable organic solvent such as methanol. This paper is concerned primarily with the extraction and preconcentration procedure and its evaluation.

EXPERIMENTAL

Equipment

Equipment required for preconcentration were a kinetic clamp pump (Sigmamotor Inc.) and a ring oven (Scientific Industries, Inc.). The X-ray analysis was conducted with a Norelco vacuum X-ray tube and a lithium fluoride analyzing crystal.

Chemicals and standards

Chemicals used were redistilled reagent-grade chloroform, methanol, and 8-hydroxyquinoline. Analytical reagent-grade salts were used to prepare primary standards (Table I). Double distilled deionized water was used throughout.

TABLE I

COMPOUNDS USED IN PREPARATION OF PRIMARY STANDARDS

Compound	*Amount taken* ($g\ 2\ l^{-1}$)
$UO_2(C_2H_3O_2)_2 \cdot 2\,H_2O$	3.563
$CuSO_4 \cdot 5\,H_2O$	7.678
$NiSO_4 \cdot 6\,H_2O$	8.960
$Co(NO_3)_2 \cdot 6\,H_2O$	9.881
$MnSO_4 \cdot H_2O$	6.160
$Fe(NH_4)_2(SO_4)_2 \cdot 6\,H_2O$	14.040

Standards were prepared by dissolving known quantities of the salts in distilled water in order to furnish solutions containing 1 g of metal per 1 l of standard; 2 l of each standard were prepared (Table I). The secondary standard was prepared by diluting a mixture of appropriate volumes of primary standards to 1 l with absolute methanol. This standard was stable as long as it was protected from evaporation. The concentrations of each element in the secondary standard were: 2.00 μg U ml^{-1}, 10.0 μg Cu ml^{-1}, 2.00 μg Ni ml^{-1}, 1.00 μg Co ml^{-1}, 5.00 μg Fe ml^{-1}, 5.00 μg Mn ml^{-1}.

Preparation of standard curves

Standard curves which were used to evaluate the preconcentration and extraction efficiency were prepared by direct evaporation of known quantities of the secondary standard followed by X-ray analysis. The volume of solution added was controlled by pumping directly from a 5-ml calibrated buret which was connected by tubing to the pump and ring oven. The buret was also used to measure volumes of solution used in spiking water samples for the determination of extraction efficiency. Standards, with the exception of uranium, were checked by atomic absorption spectrophotometry, which was calibrated against independent standards prepared by dissolving known weights of the free metals. The uranium standard was checked gravimetrically. A known volume of the standard was treated with 8-hydroxyquinoline and the precipitated uranium–8-hydroxyquinolinate was dried and weighed. In all cases the standards agreed within experimental error (5%).

Preconcentration procedure

For the preliminary concentration the seawater sample was extracted directly without pretreatment as follows.

Place a 100-ml sample in a separatory funnel of appropriate size equipped with a Teflon stopcock and add 1 ml of 10% (w/v) 8-hydroxyquinoline in methanol. (This reagent should be kept in a glass bottle from which light is excluded in order to maintain its stability.) After mixing, allow the sample to stand for 5 min. The solution is yellow at this point.

Add 8 ml of chloroform and shake the mixture vigorously until there is a marked decrease in the yellow color of the aqueous phase, a change which requires 10–15 sec. After the chloroform layer has separated, drain it into a 7-dram glass vial. Then add another 6 ml of chloroform to the sample, shake, and drain into the vial. After the second extraction the aqueous phase should be colorless or milky white. Repeat the above treatment consisting of 8-hydroxyquinoline addition and two chloroform extractions, and collect all extracts in the glass vial.

Evaporate the combined extract to dryness on a hot plate maintained at 70–80°, speeding the evaporation by directing a gentle stream of air onto the surface of the extract. Do not leave the vial on the hot plate after evaporation of the chloroform, otherwise excess 8-hydroxyquinoline will be lost. This step requires less time than the preparation and extraction of the next sample. The total time for this primary concentration was 20–25 min. Three samples treated together required an additional 10 min.

Before cooling, the glass vial containing the dried sample is closed securely with a plastic cap. It may be stored for at least one month without change if kept away from light.

For the final concentration dissolve the sample in a minimum (<2 ml) of chloroform. Pump the solution by a kinetic clamp pump directly from the glass vial through Teflon tubing to a ring oven where it is evaporated as a spot on 37 mm No. 541 or 546 Whatman filter paper. Rinse the glass vial at least twice with chloroform. Use a pumping rate of 5–7 ml h^{-1} and operate the ring oven at 160°, at which temperature all unreacted 8-hydroxyquinoline is evaporated. Place the spotted filter-paper disks in 2-dram glass vials sealed with plastic caps where they may be stored indefinitely without change.

X-Ray fluorescence analysis

The disk of the size used fits the sample holders of the Norelco X-ray spectrometer. The following X-ray parameters were used in the analysis: pulse height analyzer, window 25 V, width 5 V; tungsten target X-ray tube, 45 kV and 45 mA, with a 0.002-in titanium filter; scintillation counter, 1000 V; gas flow proportional counter, 1590 V, with a P-10 gas flow rate of 1 standard cu. ft per h. The spectrometer was evacuated to 200 μm or better for all measurements. The scintillation counter was used to measure the L_α radiation intensity of uranium. The gas flow proportional counter was used for all other elements. All samples were rotated at 4 r.p.m. for uniform exposure to the primary beam. The samples were counted twice for 100 sec and the average used.

RESULTS AND DISCUSSION

Seawater samples are extracted without pretreatment. Limnological samples may be treated similarly provided that the pH is between 7 and 9. If the pH exceeds 9, magnesium– and aluminum–8-hydroxyquinolinates are formed and extracted which causes difficulty in the spotting step by the formation of deposits. Adjustment of the pH can be made if necessary with isopiestic hydrochloric acid and aqueous ammonia.

TABLE II

EXTRACTION EFFICIENCY OF THE 8-HYDROXYQUINOLINE–CHLOROFORM SYSTEM FOR SPIKED 100-ml DEIONIZED WATER SAMPLES

Element	*U*	*Cu*	*Ni*	*Co*	*Fe*	*Mn*
μg Added	2.0	10	2.0	1.0	5.0	5.0
μg Recovered	1.9	9.6	2.0	1.0	4.9	4.9
% Recovery[a]	95	96	100	100	98	98

[a] Mean of five determinations.

TABLE III

EXTRACTION EFFICIENCY OF THE 8-HYDROXYQUINOLINE–CHLOROFORM SYSTEM FOR SPIKED 100-ml SEAWATER SAMPLES

Element	*U*	*Cu*	*Ni*	*Co*	*Fe*	*Mn*
μg Added	2.0	10	2.0	1.0	5.0	5.0
μg Recovered[a]	2.0	9.7	2.0	1.0	5.0	4.8
% Recovery[b]	100	97	100	100	100	96

[a] Amount in seawater has been subtracted.
[b] Mean of five determinations.

Virtually complete extraction of the six elements was achieved for both distilled water and seawater spiked with the metals (Tables II and III). Although two additions of 8-hydroxyquinoline together with four chloroform extractions are recommended in the procedure, 95% or more recovery of the metals was realized in the first extraction with one exception. Only 60–70% of the manganese was removed by the first extraction with the remainder removed in succeeding extractions. The effect of time of contact on the percentage extraction of the various elements is shown in Table IV.

Accuracy was not determined with certainty since it can be measured only if the true value is known which is not the case in the analysis of natural waters. In this investigation accuracy was based upon extraction data from spiked seawater and distilled water samples (Tables II and III). Although information is provided concerning recovery of the spikes added, little actually may be contributed concerning the recovery of the chemical species originally present in the seawater since their speciation is not known. The speciation of the spikes chosen matched as closely as possible those given by Goldberg[9] for seawater and the assumption is made that the chemical

TABLE IV

EFFECT OF TIME DELAY AFTER ADDITION OF 8-HYDROXYQUINOLINE ON EXTRACTION EFFICIENCY (%)

Time (min)	*Element*					
	U	*Cu*	*Ni*	*Co*	*Fe*	*Mn*
0	81	96	47	46	77	88
1	100	100	69	60	92	—
5	99	98	100	101	98	100

TABLE V

SEA WATER ANALYSIS

Element	*Location*	*Concentration* ($\mu g\ l^{-1}$)
Uranium	North Central Pacific (NCP)	3.3
	Northwest Coast of United States (NCUS)	1.7
Copper	NCP	35
	NCUS	29
Nickel	NCP	3.2
	NCUS	1.1
Cobalt	NCP	0.24
	NCUS	0.13
Iron	NCP	6.1
	NCUS	5.4
Manganese	NCP	16
	NCUS	1.9

behavior of the trace species present was similar to that of the counterpart spikes added.

Table V shows that seawater values obtained are in general agreement with published values with the exception of mid-ocean manganese which is high. In the case of uranium, the agreement is within 5% for the overall averages of this element in both mid-ocean and coastal waters[10,11]. Other elements are not easily compared because of lack of agreement with values reported in the literature.

Although a sample volume of 100 ml is recommended in the procedure the precision of the determination can be improved markedly by increasing the volume to 500 ml. In this event a precision of 5% is obtained for iron, copper, manganese, and nickel, and 10% or less for cobalt and uranium.

The kinetic clamp pump was extremely useful in the deposition step. This pump permitted complete and facile control of the solution flow rate and was essential in the production of constant spot sizes using the ring oven. A combination of Teflon tubing and polyethylene was used in pumping chloroform solutions. A short, 3-inch section of polyethylene tubing, 3/16 inch o.d. (1/8 inch i.d.), was slipped over a 36-inch piece of Teflon tubing, 3/32 inch o.d. (3/16 inch i.d.). The polyethylene tubing was heated and stretched lengthwise about 100%. The stretching caused it to shrink snugly to the Teflon imparting the necessary resiliency to the Teflon tubing.

The ring oven was essential since, with its use, reproducible and uniform spots were formed. The oven consisted of a set of thermostatically heated rings between which the filter paper was placed, and a central air tube ending just below the filter paper. As the solution was deposited in the center of the filter paper and rings, it spread toward the hot rings and evaporated before reaching them with the result that the dissolved material was deposited in a spot of about 1 cm diameter in the center of the filter paper. In the operation of the oven at the optimal conditions, an air flow through the central tube was used which caused the filter paper just to flutter but not to float without the upper ring in place.

The extraction and concentration procedure has advantages when compared to that described by Morris[8],which uses a solution of ammonium pyrrolidine dithiocarbamate as the complexing agent and methyl isobutyl ketone as the extracting agent. An 800-ml seawater sample is required, the pH of which has to be adjusted. The procedure is relatively time-consuming since it involves a liquid–liquid extraction which takes 3 h. Following the extraction, cooling, distillation and evaporation, several nitric acid fumings to remove organic matter were required before the residue was mixed with powdered cellulose and the mixture pressed into pellets for X-ray analysis.

This investigation was supported in part by NSF Grant GU-3855.

SUMMARY

A procedure is described for the preconcentration from seawater without pretreatment of six trace elements uranium, copper, nickel, cobalt, iron, and manganese through solvent extraction with an 8-hydroxyquinoline–chloroform mixture. Extracted samples are deposited on filter-paper disks with the aid of a kinetic clamp pump and a ring oven, and the six elements are determined non-destructively by

X-ray fluorescence. Evaluation of the procedure with distilled water and seawater samples spiked with the metal ions shows that extraction of the trace metals is essentially quantitative.

RÉSUMÉ

On décrit une méthode de préconcentration d'éléments à l'état de traces dans l'eau de mer: uranium, cuivre, nickel, cobalt, fer et manganèse, par extraction dans un mélange hydroxy-8-quinoléine–chloroforme. Les échantillons extraits sont déposés sur des disques en papier filtre; les six éléments sont dosés sans destruction, par fluorescence aux rayons-X. On peut considérer cette technique comme essentiellement quantitative.

ZUSAMMENFASSUNG

Es wird ein Verfahren zur Anreicherung der sechs Spurenelemente Uran, Kupfer, Nickel, Kobalt, Eisen und Mangan in Meerwasser durch Extraktion mit einem Gemisch von 8-Hydroxychinolin und Chloroform beschrieben. Die extrahierten Proben werden mittels einer Pumpe und eines Ringofens auf Filterpaper abgeschieden und die sechs Elemente zerstörungsfrei durch Röntgenfluoreszenz bestimmt. Die Überprüfung des Verfahrens mit destilliertem Wasser und Meerwasserproben, die mit den Metallionen versetzt worden sind, ergibt, dass die Extraktion der Spurenmetalle praktisch quantitativ erfolgt.

REFERENCES

1 J. P. Riley and G. Skirrow, *Chemical Oceanography*, Vol. 2, Academic Press, London and New York, 1965, p. 325.
2 T. Joyner, M. L. Healy, D. Chakravarti and T. Koyanagi, *Environ. Sci. Tech.*, 1 (1967) 417.
3 R. R. Brooks, B. J. Presley and R. I. Kaplan, *Talanta*, 14 (1967) 809.
4 R. E. Mansell and H. W. Emmel, *At. Abs. Newsletter*, 4 (1965) 365.
5 C. E. Mulford, *At. Abs. Newsletter*, 5 (1966) 88.
6 D. F. Schutz and K. K. Turekian, *Geochim. Cosmochim. Acta*, 29 (1965) 259.
7 S. D. Natelson, D. Leighton and C. Calas, *Microchem. J.*, 6 (1962) 539.
8 A. W. Morris, *Anal. Chim. Acta*. 42 (1968) 397.
9 E. Goldberg, in M. N. Hill, *The Sea*, Vol. 2, Interscience, New York and London, 1966, p. 4.
10 R. L. Blanchard, *J. Geophys. Res.*, 70 (1965) 4055.
11 Y. Y. Miyake, Y. Sugimura and T. Uchida, *J. Geophys. Res.*, 71 (1966) 3083.

Analytica Chimica Acta
Elsevier Publishing Company, Amsterdam
Printed in The Netherlands

ETUDE DE L'EXTRACTION LIQUIDE–LIQUIDE DU CUIVRE(II) AU MOYEN DE L'OXYDE DE (CARBOXY-2-ETHYL)DIPHENYLPHOSPHINE

SEPARATION FER(III) ET CUIVRE(II)

J.-L. ROCCA ET M. PORTHAULT
Centre de Chimie Analytique, Faculté des Sciences de Lyon, 43, boulevard du 11 Novembre 1918, 69 Villeurbanne (France)

(Reçu le 1 août, 1970)

L'étude de l'extraction liquide–liquide de cations métalliques par différents acides carboxyliques a été faite par de nombreux auteurs[1-6]. En effet, de tels agents offrent, par la présence du groupement carboxylique, une sélectivité d'extraction fonction du pH de la phase aqueuse. Nous nous sommes intéressé à un dérivé de la phosphine, l'oxyde de (carboxy-2-éthyl)diphénylphosphine, présentant à la fois un groupement carboxylique, et un groupement oxyde de phosphine, devant lui conférer de bonnes propriétés extractantes.

Le partage de cet agent entre une phase aqueuse de force ionique 1 et le chloroforme a fait l'objet d'une précédente étude[7]. La connaissance des différentes constantes d'équilibre de dissociation, de partage et de polymérisation (Tableau I), nous permet désormais de mettre à profit les propriétés extractantes intéressantes de l'oxyde de (carboxy-2-éthyl)diphénylphosphine.

Cet agent s'est révélé assez efficace dans l'extraction de métaux de transition tels que le fer(III)[8,9]. En effet cette extraction peut être rendue quantitative pour des faibles pH (de l'ordre de 1.5 à 2.5), le fer est alors extrait en phase organique soit sous une forme monomère ($FeOHA_2 \cdot HA$) soit sous une forme trimère ($(FeOHA_2 \cdot HA)_3$), selon les conditions expérimentales de l'extraction (Tableau I).

Nous avons dans ce travail, envisagé l'extraction du cuivre(II) par l'oxyde de (carboxy-2-éthyl)diphénylphosphine. Nous avons ainsi déterminé une structure dimère du cuivre en phase organique du type $(Cu\,A_2 \cdot HA)_2$. Une telle structure avait déjà été suggérée soit par des études de partage par extraction liquide–liquide par des acides carboxyliques[10-12], soit par des mesures de moments magnétiques[13], soit par des mesures de poids moléculaires[14]. Le cuivre étant extrait pour des pH moins acides que le fer (de l'ordre de 3.5 à 4.5), nous avons pu envisager des séparations de couples fer–cuivre en fonction du pH de la phase aqueuse.

Etude théorique de la distribution du cuivre

L'étude de l'oxyde de (carboxy-2-éthyl)diphénylphosphine[7] (HA) a montré que cet agent existait principalement sous forme dimère dans le chloroforme. Dans les équilibres d'extraction qui suivent, nous ne faisons intervenir que cette forme (H_2A_2). De plus, nous supposons que le cuivre(II) est extrait en phase organique sous la forme la plus générale $(Cu\,A_2 \cdot (n-2)HA)_{j,o}$, j et $(n-2)$ étant respectivement les degrés de polymérisation et de solvatation de l'espèce extraite. Nous admettons aussi qu'aux

TABLEAU I

DIFFÉRENTES CONSTANTES RELATIVES AU PARTAGE DE L'OXYDE DE (CARBOXY-2-ÉTHYL)DIPHÉNYLPHOSPHINE ENTRE UNE PHASE AQUEUSE ($\mu=1$) ET LE CHLOROFORME, ET À L'EXTRACTION DE FER(III) ET DE CUIVRE(II) À L'AIDE DE CET AGENT EN SOLUTION DANS LE CHLOROFORME

	Nom des constantes	*Valeurs des constantes*	*Réf.*
Constantes relatives au partage de l'oxyde de (carboxy-2-éthyl)-diphénylphosphine entre une phase aqueuse de force ionique 1 et le chloroforme	Constante de dissociation de la forme HA en phase aqueuse	$K_a=(7.9\pm0.4)\cdot10^{-5}$	
	Constante de partage de la forme monomère HA	$K_d=3.5\pm0.2$	
	Constante de formation de l'espèce dimère	$K_2=(3.3\pm0.2)\cdot10^2$	7,9
	Constante de formation de l'espèce trimère	$K_3=(7.6\pm0.4)\cdot10^3$	
	Constante de formation de l'espèce tétramère	$K_4=(9.2\pm0.5)\cdot10^5$	
Constantes relatives à l'extraction de Fe(III) par l'oxyde de (carboxy-2-éthyl)-diphénylphosphine en solution dans le chloroforme	Constante d'extraction de la forme monomère ($FeOHA_2\cdot HA$)	$\log K_{1.1}=-0.7\pm0.2$	8,9
	Constante d'extraction de la forme trimère $(FeOHA_2\cdot HA)_3$	$\log K_{3.1}=8.4\pm0.2$	
Constante relative à l'extraction de Cu(II) par l'oxyde de (carboxy-2-éthyl)diphényl-phosphine en solution dans le chloroforme	Constante d'extraction de la forme dimère $(CuA_2\cdot HA)_2$	$\log K_{2.1}=-8.2\pm0.2$	Présent travail 9

pH auxquels nous avons travaillé, le cuivre(II) ne se trouve[15] en phase aqueuse que sous la forme Cu^{2+}. Dans ces conditions, si les indices a et o désignent respectivement les phases aqueuse et organique, l'équilibre d'extraction se traduit par les équations suivantes:

$$j\,Cu_a^{2+}+j(n/2)(H_2A_2)_o \rightleftarrows (CuA_2\cdot(n-2)HA)_{j,o}+2jH^+$$

la constante d'équilibre d'extraction $K_{j,n-2}$ est alors:

$$K_{j,n-2}=\frac{[(CuA_2\cdot(n-2)HA)_{j,o}][H^+]^{2j}}{[(H_2A_2)_o]^{j(n/2)}[Cu^{2+}]_a^j}$$

puisque $[Cu]_o=j[CuA_2\cdot(n-2)HA]_{j,o}$ et $[Cu]_a=[Cu^{2+}]_a+\Sigma[Cu(OH)_n^{(2-n)+}]=\alpha[Cu^{2+}]_a$.

Nous en déduisons l'expression générale:

$$[Cu]_o=\sum_{j=1}^{j}\sum_{n=2}^{n} jK_{j,n-2}[H_2A_2]_o^{j(n/2)}([Cu]_a/\alpha[H^+]^2)^j$$

Si une seule espèce est extraite, ce sera le cas du cuivre(II), la courbe log $[Cu]_o=f(\log[Cu]_a-\log\alpha+2pH)$ tracée pour $[H_2A_2]_o=$constante, est une droite de degré de polymérisation de l'espèce extraite. Puis la courbe $\log[Cu]_o-$

$j(\log[\mathrm{Cu}]_a - \log\alpha + 2\mathrm{pH}) = f(\log[\mathrm{H_2A_2}]_o)$ est une droite de pente $j(n/2)$, permettant ainsi la détermination du degré de solvatation $(n-2)$.

PARTIE EXPÉRIMENTALE

Technique de partage

L'extraction est étudiée à 25°: l'ensemble thermostaté a déjà été décrit[7-9]. Ces deux phases sont constituées de:

—25 ml de phase organique (chloroforme) dans laquelle est mis en solution, après pesée, l'oxyde de (carboxy-2-éthyl)diphénylphosphine (HA). Nous avons fait varier cette concentration de $3 \cdot 10^{-2} M$ à $10^{-1} M$.

—25 ml de phase aqueuse dont nous modifions le pH à l'aide de mélange soude–acide perchlorique (environ $10^{-2} N$), et dont la force ionique est ajustée à 1 par du perchlorate de sodium. Nous faisons varier la concentration initiale du cuivre(II) en phase aqueuse de $6.16 \cdot 10^{-5} M$ à $6.16 \cdot 10^{-4} M$ par dilution d'une solution $1.54 \cdot 10^{-1} M$ de sulfate de cuivre pentahydraté r.p.

L'étude cinétique de l'extraction a montré que 3 h d'agitation étaient suffisantes pour atteindre l'équilibre, puis nous laissons décanter pendant 30 min. Ces deux phases sont alors séparées. Nous déterminons le pH et la concentration en cuivre de la phase aqueuse. Pour pouvoir déterminer sa concentration dans la phase organique, le cuivre est réextrait quantitativement de 20 ml de cette phase organique dans 20 ml d'une solution d'acide chlorhydrique environ normale. Après 3 h d'agitation à 25° (même dispositif expérimental) et après décantation d'une demi-heure, le dosage du cuivre dans la phase acide chlorhydrique montre que la réextraction est bien quantitative.

Mesure du pH

Après l'équilibre d'extraction et après séparation des phases, nous déterminons le pH de la phase aqueuse. Pour cela nous utilisons une électrode de verre Metrohm type UX, et une électrode calomel Tacussel remplie d'une solution saturée en chlorure de sodium (pour éviter la cristallisation de perchlorate de potassium dans le poreux de l'électrode de référence). Nous mesurons les f.é.m. à l'aide d'un compensateur Metrohm type E 388. Les pH correspondants sont alors donnés par une courbe d'étalonnage pH = f (mV) tracée à l'aide de solutions titrées d'acide perchlorique de force ionique constante et ajustée à 1 par du perchlorate de sodium.

Dosages du cuivre et du fer

Les dosages sont faits par spectromètrie d'absorption atomique sur un appareil Techtron type AA4, directement dans le cas des phases aqueuses, indirectement dans le cas des phases organiques. Dans ce dernier cas une réextraction préalable par une phase aqueuse est nécessaire.

RÉSULTATS

Détermination du degré de polymérisation

Nous fixons à $10^{-1} M$ la concentration initiale totale $[\mathrm{HA}]_T$ en oxyde de (carboxy-2-éthyl)diphénylphosphine. Pour différentes concentrations initiales en cuivre(II) à extraire, nous faisons varier le pH de la phase aqueuse. Si nous traçons alors la courbe $\log[\text{Cu}]_o = f(\log[\text{Cu}]_a - \log\alpha + 2\text{pH})$, nous pouvons obtenir j à condition que $[H_2A_2]_o$ reste constante. Nous avons porté sur la fig. 1 la courbe $\log[H_2A_2]_o = f([\text{HA}]_T)$ pour différents pH, calculée à l'aide des différents coefficients d'équilibre de dissociation, de partage et de polymérisation de l'oxyde de (carboxy-2-éthyl)diphénylphosphine (HA)[7].

Nous voyons sur cette fig. 1, que pour une concentration initiale totale $[\text{HA}]_T = 10^{-1} M$, lorsque le pH varie de 3.50 à 4.20, $\log[H_2A_2]_o$ peut être considéré comme constant, compte tenu de l'imprécision sur la détermination de la constante k_2 de dimérisation de HA.

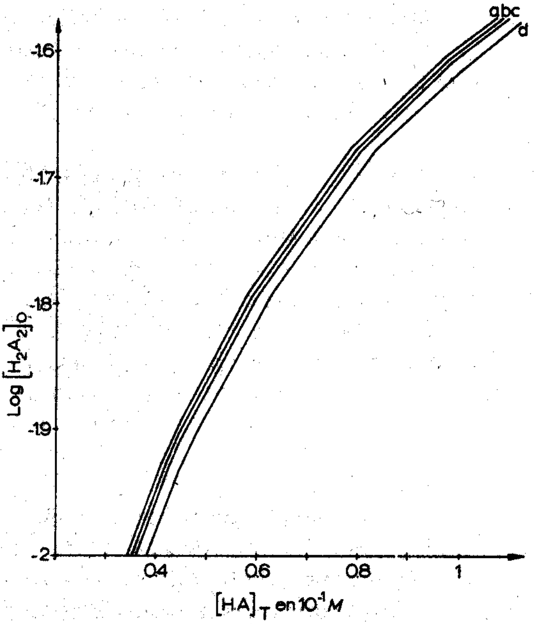

Fig. 1. Evolution de la forme dimère $(H_2A_2)_o$ en fonction du pH et de la concentration totale initiale $[\text{HA}]_T$ mise en solution dans le chloroforme; pH (a) 3.50, (b) 4, (c) 4.20, (d) 4.50.

Dans ces conditions, nous trouvons que la courbe $\log[\text{Cu}]_o = f(\log[\text{Cu}]_a - \log\alpha + 2\text{pH})$ (fig. 2) est une droite de pente 2. Ainsi pour des concentrations de cuivre(II) en phase organique de $4 \cdot 10^{-6} M$ à $4 \cdot 10^{-4} M$, l'espèce extraite est une forme dimère du type $(\text{CuA}_2 \cdot (n-2)\text{HA})_2$.

Détermination du degré de solvatation

Cette étude, pour deux concentrations aqueuses initiales de $1.54 \cdot 10^{-4} M$ et $2 \cdot 10^{-4} M$, est faite en faisant varier $[\text{HA}]_T$ de $10^{-1} M$ à $3.69 \cdot 10^{-2} M$ en phase organique. Après équilibre d'extraction, le pH de la phase aqueuse est déterminé et la fig. 1 nous permet de connaître $[H_2A_2]_o$ correspondant à chaque extraction. La fig. 3 représente la courbe $\log[\text{Cu}]_o - 2(\log[\text{Cu}]_a - \log\alpha + 2\text{pH}) = f(\log[H_2A_2]_o)$: c'est une droite de pente 3, d'où $j(n/2) = 3$ et puisque $j = 2$, $n = 3$, par suite $(n-2) = 1$. Ainsi, dans le domaine de concentration de cuivre(II) exploré, de $6.16 \cdot 10^{-5} M$

à $6.16 \cdot 10^{-4}$ *M*, le cuivre(II) est extrait en phase organique sous une seule forme dimère $(CuA_2 \cdot HA)_2$.

La constante d'équilibre d'extraction $\log K_{2,1}$, calculée à l'aide des courbes 2 et 3 est alors:

$$\log K_{2,1} = -8.2 \pm 0.2$$

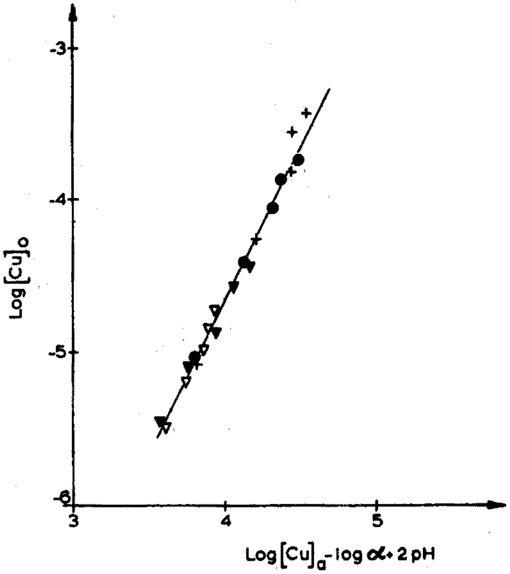

Fig. 2. Extraction du cuivre(II) pour $[HA]_T = 10^{-1}$ *M* dans le chloroforme. Détermination du degré de polymérisation *j*. $[Cu]_{initiale}$: (+) $6.16 \cdot 10^{-4}$, (●) $3.08 \cdot 10^{-4}$, (▼) $1.54 \cdot 10^{-4}$, (▽) $6.16 \cdot 10^{-5}$ *M*; pH: (+) 3.52 à 4.08, (●) 3.66 à 4.20, (▼) 3.70 à 4.05, (▽) 3.92 à 4.15.

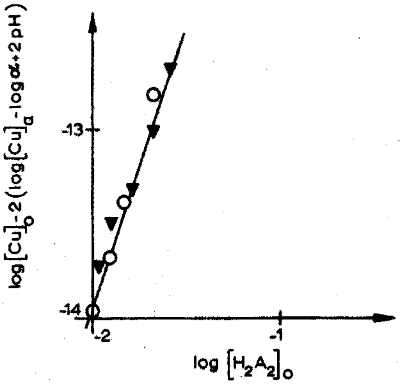

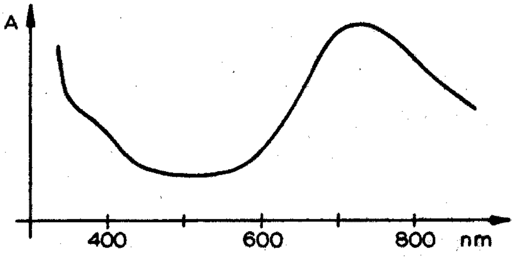

Fig. 3. Solvatation de la forme dimère. $[Cu]_{initiale}$: (▼) $1.54 \cdot 10^{-4}$, (○) $2 \cdot 10^{-4}$ *M*.

Fig. 4. Spectre visible du complexe $(CuA_2 \cdot HA)_2$ dans le chloroforme.

Spectre dans le visible

Par une méthode d'extraction liquide–liquide, nous avons identifié la forme extraite en phase organique à une forme dimère solvatée $(CuA_2 \cdot HA)_2$. Les études spectrales dans le visible de telles formes dimères[11,16] ont montré qu'il existait deux bandes caractéristiques d'absorption.

—Une bande à 650.0 nm, sensible aux changements de solvatation, se déplaçant vers les fortes longueurs d'onde (710.0 nm) lorsque celle-ci devient de plus en plus importante.

—Une bande (épaulement) vers 370.0 nm, attribuée à un recouvrement des orbitales des atomes de Cu voisins, avec formation de liaisons σ ou δ selon les auteurs[17].

Un spectre visible tracé à l'aide d'un appareil Beckman DK 2A (fig. 4) présente ces deux bandes caractéristiques d'absorption (725.0 nm et 370.0 nm). Ainsi la structure dimère proposée par extraction liquide–liquide $(CuA_2 \cdot HA)_2$ est en accord avec la forme du spectre observé.

SÉPARATIONS FER(III)–CUIVRE(II)

Nous avons représenté, sur la fig. 5, l'extraction du fer(III)[8,9] et celle du cuivre(II) en fonction du pH, pour une concentration initiale totale $[HA]_T = 10^{-1} M$ dans le chloroforme. Nous voyons qu'il peut exister des zones de pH permettant la séparation, sinon quantitative, du moins quasi totale, de ces deux éléments. De plus cette séparation doit être d'autant plus facile, que la concentration en fer(III) est plus élevée, et que celle en cuivre(II) est plus faible.

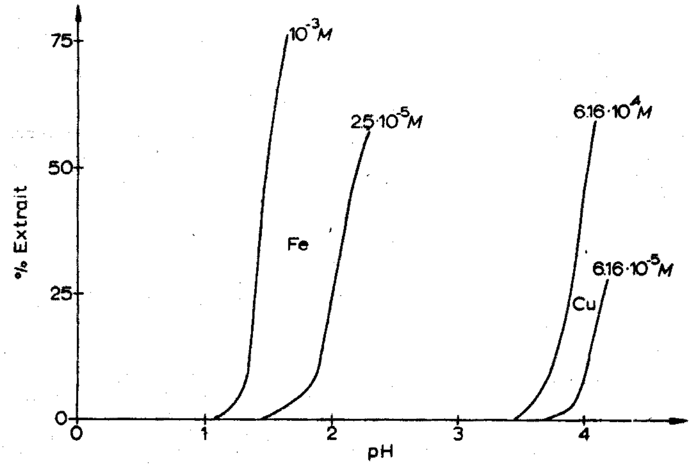

Fig. 5. Extraction de fer(III) et de cuivre(II) par $[HA]_T = 10^{-1} M$ dans le chloroforme. Extraction en fonction du pH pour différentes concentrations initiales en métal à extraire.

La séparation totale a pu être réalisée pour des concentrations en chacun des deux éléments de $3.08 \cdot 10^{-3} M$ (fig. 6). Pour des pH de 2.35 à 2.55, le fer(III) est totalement extrait en phase organique, alors que le cuivre se retrouve quantitativement en phase aqueuse.

Pour des solutions plus diluées en fer(III), la séparation totale nécessite le choix d'un pH élevé. Ainsi pour une solution à environ $1.5 \cdot 10^{-4} M$ en chacun des deux éléments, nous avons fixé un pH de 3.55 pour lequel l'extraction théorique du fer(III) est quantitative, alors que celle du cuivre(II) est faible. Nous constatons que le cuivre(II) est bien partiellement extrait (à 5%) en phase organique, mais que le fer(III) restant en phase aqueuse est d'environ 10%. De plus nous observons un défaut de fer(III) en phase organique, dû à une précipitation d'hydroxydes ferriques en phase aqueuse. Le même phénomène a été observé pour des solutions $3.08 \cdot 10^{-3} M$ en cuivre(II) et $1.54 \cdot 10^{-4} M$ en fer(III), (fig. 7). Lorsque le pH varie de 2.08 à 3.35, nous constatons que l'extraction du cuivre(II) reste toujours très faible jusqu'à pH 3.35, mais que le fer(III) restant en phase aqueuse est de l'ordre de 10%, avec un défaut en phase organique pouvant atteindre jusqu'à 50% pour les pH les plus élevés.

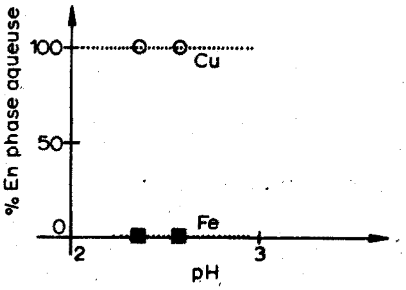

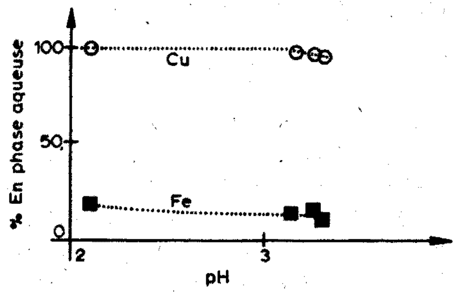

Fig. 6. Séparation fer(III)–cuivre(II) pour $[\mathrm{HA}]_T = 10^{-1}\,M$ dans le chloroforme: $[\mathrm{Cu}]_{\mathrm{initiale}} = [\mathrm{Fe}]_{\mathrm{initiale}} = 3.08 \cdot 10^{-3}\,M$.

Fig. 7. Séparation fer(III)–cuivre(II) pour $[\mathrm{HA}]_T = 10^{-1}\,M$ dans le chloroforme: $[\mathrm{Cu}]_{\mathrm{initiale}} = 3.08 \cdot 10^{-3}\,M$, $[\mathrm{Fe}]_{\mathrm{initiale}} = 1.54 \cdot 10^{-4}\,M$.

Ainsi la séparation de couples fer(III)–cuivre(II) est réalisable lorsque les conditions opératoires sont telles qu'il ne se produit pas de précipitation d'hydroxydes ferriques en phase aqueuse.

RÉSUMÉ

Nous avons étudié l'extraction liquide–liquide de Cu(II) par l'oxyde de (carboxy-2-éthyl)diphénylphosphine en solution dans le chloroforme. Pour des concentrations en phase organique de $4 \cdot 10^{-6} M$ à $4 \cdot 10^{-4} M$, le cuivre(II) se trouve sous une forme dimère solvatée $(\mathrm{CuA_2 \cdot HA})_2$. La constante d'extraction est alors $\log K_{2,1} = -8.2 \pm 0.2$. Nous avons testé la séparation de couples Fe(III)–Cu(II). Cette séparation est effectuée en fonction du pH de la phase aqueuse. Ainsi, pour des concentrations en fer(III) de l'ordre de $10^{-3} M$, une séparation a été possible. Cependant des solutions plus diluées en fer(III), de l'ordre de $10^{-4} M$, nécessitent le choix d'un pH élevé entraînant la précipitation d'hydroxydes ferriques en phase aqueuse, et rendant la séparation totale impossible.

SUMMARY

The extraction of copper(II) from an aqueous phase by carboxyethyldiphenylphosphine oxide in chloroform has been studied. For concentrations in the organic phase of $4 \cdot 10^{-6} M$–$4 \cdot 10^{-4} M$, the copper(II) complex is dimeric and has the constitution $(CuA_2 \cdot HA)_2$. The equilibrium extraction constant is $\log K_{2,1} = -8.2 \pm 0.2$. The separation of copper(II) from iron(III) is strongly dependent on the pH of the aqueous phase. For about $10^{-3}M$ iron(III) concentrations a complete separation is possible, but for more dilute iron(III) solutions ($10^{-4}M$), the more basic pH necessary for complete extraction leads to precipitation of iron(III) hydroxide in the aqueous phase and complete separation is impossible.

ZUSAMMENFASSUNG

Es wurde die Extraktion von Kupfer(II) mit Carboxyäthyl-diphenyl-phosphinoxid in Chloroform untersucht. Bei Konzentrationen von $4 \cdot 10^{-6}$ M–$4 \cdot 10^{-4}$ M in der organischen Phase hat der Kupfer(II)-Komplex die dimere Zusammensetzung $(CuA_2 \cdot HA)_2$. Die Verteilungskonstante ist $\log K_{2,1} = -8.2 \pm 0.2$. Die Trennung von Fe(III) und Cu(II) ist stark vom pH-Wert in der wässrigen Phase abhängig. Bei 10^{-3} M Fe(III)-Lösungen ist eine vollständige Trennung möglich. Verdünntere Lösungen (10^{-4} M Fe(III) erforndern jedoch einen grösseren pH-Wert, der zu einer Fällung von Eisenhydroxid führt und dadurch eine vollständige Trennung unmöglich macht.

BIBLIOGRAPHIE

1 A. W. Fletcher and D. S. Flett, *Solvent Extraction Chemistry of Metals*, MacMillan, Londres, 1965, p. 359.
2 G. K. Schweitzer and F. C. Clifford, *Anal. Chim. Acta*, 45 (1969) 57.
3 E. L. T. M. Spitzer, J. Radder and J. H. Siegmann, *Ind. Chim. Belge*, 32 (1967) 209.
4 A. W. Fletcher, D. S. Flett and J. C. Wilson, *Inst. Mining Met., Bull.*, 73 (1964) 765.
5 M. Tanaka, N. Nakasuka and S. Sasane, *J. Inorg. Nucl. Chem.*, 31 (1969) 2591.
6 M. Tanaka, N. Nakasuka and S. Sasane, *Solvent Extraction Chemistry*, North Holland Publishing Co, Amsterdam, 1967, p. 154.
7 J.-L. Rocca and M. Porthault, *Bull. Soc. Chim. France*, 5 (1970) 2036.
8 J.-L. Rocca and M. Porthault, *Bull. Soc. Chim. France*, à paraître.
9 J.-L. Rocca, *Thèse de Doctorat de spécialité (3e cycle)*, Lyon, 1970.
10 M. Tanaka and T. Niinomi, *J. Inorg. Nucl. Chem.*, 27 (1965) 431.
11 A. W. Fletcher and D. S. Flett, *J. Appl. Chem.*, 14 (1964) 250.
12 W. J. Haffenden and G. J. Lawson, *J. Inorg. Nucl. Chem.*, 3 (1964) 250.
13 M. Kishita, M. Inoue and M. Kubo, *Inorg. Chem.*, 3 (1964) 237.
14 A. K. Rai and R. C. Mehrotra, *J. Inorg. Nucl. Chem.*, 21 (1961) 311.
15 A. Ringbom, *Les Complexes en Chimie Analytique*, Dunod, Paris, 1967, p. 332.
16 D. P. Graddon, *J. Inorg. Nucl. Chem.*, 11 (1959) 337; *Nature*, (1960) 715.
17 *Transition Metal Chemistry, Vol. 5*, Marcel Dekker, New York, 1969, p. 105.

Analytica Chimica Acta
Elsevier Publishing Company, Amsterdam
Printed in The Netherlands

RATIONALISED SIZES OF SMALL MOLECULES IN GEL PERMEATION CHROMATOGRAPHY

A. LAMBERT
Shell Research Limited, Egham Research Laboratories, P.O.Box 11, Egham, Surrey (England)

(Received April 22nd, 1970)

About 680 independent observations of the elution behaviour of small molecules in gel permeation chromatography with porous polystyrene beads have been given in several papers[1-10]. Recently, the need for the rationalisation of these observations was discussed and a method of calculating reliable molar volumes was recommended[11]. Briefly, in this method all the data are recalculated in terms of molar volume after just one set of molar volume values has been used for the *n*-alkane calibration standards and the calibration curve has been drawn through the calibration points even when this meant introducing discontinuities in its slope. Only those data which do not require any extrapolation of the calibration outside the range of the calibration standards are considered reliable. The method has been applied to the 680 observations.

RESULTS

Table I shows that only about 380 observations lead to reliable molar volumes by the criteria recommended. Theoretical molar volumes not at 20° are followed by the temperature of measurement. Compounds containing more than one type of functional group are listed once under the group which occurs first in the Table; for instance, a glycol ether contains a hydroxyl and an ether group and is listed as a monohydric alcohol.

The 300 unreliable molar volumes, which are not listed, are unreliable mainly because the compounds eluted outside the range of the *n*-alkanes used in the appropriate work. If the *n*-alkanes are designated as the primary set of gel permeation chromatography standards, then other compounds with reliably known molar volumes can be used as secondary standards (in the same solvent only). However, when this idea was applied, the number of reliable results was increased by only two, *i.e.* *n*-nonanoic and *n*-decanoic acids (marked by an asterisk). It might be possible to make some of the other molar volumes reliable by experimentally measuring the elution behaviour of selected secondary standards in the various solvents.

DISCUSSION

The Table shows that some functional groups form hydrogen bonds with tetrahydrofuran and chloroform. The following conclusions can be drawn about the

TABLE I

RATIONALISED SIZES OF SMALL MOLECULES AT 20°

(The numbers in parentheses indicate the relevant reference; (a) indicates previously unpublished work)

Molecule	*Theoretical molar volume at 20° (cm^3 mole^{-1})*	*Recalculated experimental molar volume (cm^3 mole^{-1})*				
		Tetra-hydro-furan	*Chloroform + ethanol (Ref. 7)*	*Chloroform + amylenes (Ref. 7)*	*o-Dichloro benzene*	*Benzen (Ref. 9)*
Alkenes						
Heptene-1	141	140(1) 140(1)				146
Octene-1		155(1) 158(1)				
n-Decene-1	190		202	200		
Branched alkenes						
2-Methylpentene-1	122	123(1)			125(5)	179?
4-Methylpentene-1	126	130(1)			122(5)	186?
2,2,4-Trimethylpentene-1		152(1)				
Branched alkanes						
2-Methylpentane	132	134(1) 136(2)	135			
3-Methylpentane	128	128(1)			124(5)	
2,3-Dimethylpentane	144	142(1)				
2,2,4-Trimethylpentane	165	173(1)	170		153(5)	162
2-Methyloctane	181(25°)	184(2)				
3-Methyloctane	178	182(2)				
3-Ethyloctane	193(25°)	188(2)				
3-Methylnonane	195(25°)	191(2)				
4-Ethylnonane		207(2)				
4-Methyldecane		211(2)				
Monohydric alcohols						
Methanol	40	119(1)	81			
Triphenylcarbinol	217	228(1)				160
Ethanol	58	123(1) 138(6)	120			
β-Phenoxyethanol	125	162(1)				
β-Chloroethanol		140(1)				
n-Propanol	75	136(1) 144(6) 130(8)		117		
Isopropanol	77	142(1)	141	141		
1,3-Dichloropropanol	95	170(8)				
1,3-Dibromopropanol	103	160(8)				
2,3-Dichloropropanol	94	170(8)				
n-Butanol	91	146(8) 150(6)	138			
Isobutanol	91		139			
sec-Butanol			147			
tert-Butanol	94		156			

TABLE I (*continued*)

Molecule	*Theoretical molar volume at 20°* (*cm*^{3} *mole*$^{-1}$)	*Recalculated experimental molar volume* (*cm*^{3} *mole*$^{-1}$)				
		Tetra-hydro-furan	*Chloroform + ethanol* (*Ref.* 7)	*Chloroform + amylenes* (*Ref.* 7)	o-*Dichloro benzene*	*Benzene* (*Ref.* 9)
3-Methyl-1-butanol	109	158(8)				
n-Hexanol	125	172(8)			119(5)	
		184(6)				
Cyclohexanol		142(1)	152	143		
n-Heptanol	141	197(1)	204	183	136(5)	128
		203(6)				134
		185(8)				
3-Heptanol		194(1)				137
n-Octanol	158	200(8)				
		222(6)				
2,2,4-Trimethylpentanol						147
2,4,4-Trimethylpentanol		215(1)				
n-Nonanol	172	240(6)				
n-Decanol	191	260(6)				
		247(1)				171
n-Dodecanol	244	296(6)				
n-Tetradecanol	257	323(6)				
n-Hexadecanol		352(8)				
n-Octadecanol	324	372(6)				
Diethylene glycol monomethyl ether	116	157(1)				154
		165(10)				
Diethylene glycol monoethyl ether	132	177(10)				
Diethylene glycol monoisopropyl ether	153	205(10)				
Diethylene glycol monobutyl ether	169	215(1)				
Triethylene glycol monomethyl ether	156	200(10)				
Triethylene glycol monoethyl ether	175	220(10)				
Triethylene glycol monoisopropyl ether	192	247(10)				
Triethylene glycol mono-*n*-butyl ether	209	253(10)				
		246(8)				
β-Phenoxyethanol	125	162(1)				
Phenol	88	152(1)				
		146(8)				
p-Chlorophenol	98	178(1)				
o-Chlorophenol		162(1)				
Pentachlorophenol		173(1)				
2,6-Di-isopropylphenol						162
2,4,6-Trichlorophenol	132	173(1)				
2,6-Di*tert*-butyl-4-methylphenol		218(1)				
		233(a)				212
3-Ethoxy-1-propanol		158(8)				
Diacetone alcohol	125	172(8)				
		170(a)				
Acetoxyethanol	94	158(a)				

TABLE I (*continued*)

Molecule	*Theoretical molar volume at 20°* (*cm^3 mole^{-1}*)	*Recalculated experimental molar volume* (*cm^3 mole^{-1}*)				
		Tetrahydrofuran	*Chloroform + ethanol* (*Ref.* 7)	*Chloroform + amylenes* (*Ref.* 7)	o-*Dichloro benzene*	*Benzene* (*Ref.* 9)
Dihydric alcohols						
1,4-Butanediol	89		176			
Trimethylene glycol		180(1)				
Ethylene glycol	56	157(1)				
Diethylene glycol	94.5	185(10)				
Triethylene glycol	133	235(10) 208(8)				
Tetraethylene glycol	172	285(10)				208
Pentaethylene glycol		370(10)				
Propylene glycol		160(1)				
Dipropylene glycol	131	218(1) 225(10)				141
Tripropylene glycol		265(1) 270(10)				202
3-Chloro-1,2-propanediol	83	205(a) 192(8)				
Diphenylolpropane	216	315(a) 295(8)				
Tetrabromodiphenylolpropane		330(a) 341(8)				
Hydrogenated diphenylolpropane						160
1,4-Dihydroxybenzene	81	171(1) 200(8)				
1,2-Dihydroxybenzene	95	190(8)				
1,3-Dihydroxybenzene	86	182(8)				
Phenolphthalein	249	370(1)				
Trihydric alcohols						
Glycerol	73	190(8)				
Monocarboxylic acids						
Acetic acid	57	131(1)				
Trimethylacetic acid	113	185(a)				
n-Propanoic acid		140(6)				
Acrylic acid	68			115		
n-Butanoic acid	92	158(6)				
n-Pentanoic acid	116	168(6)		216		
n-Hexanoic acid	125			215		
2-Ethylhexanoic acid	160	200(8)				
n-Heptanoic acid	142	203(6)			131(5)	
n-Octanoic acid	156				142(5)	
n-Nonanoic acid	175	237(6)			156(3)*	
n-Decanoic acid					170(3)*	
n-Undecanoic acid	209				186(3)	
n-Dodecanoic acid	226	302(6)			202(3)	
n-Tetradecanoic acid		235(6)			232(3)	
n-Hexadecanoic acid		338(6)			254(3)	

ABLE I (*continued*)

olecule	*Theoretical molar volume at 20° (cm^3 $mole^{-1}$)*	*Recalculated experimental molar volume (cm^3 $mole^{-1}$)*				
		Tetra-hydro-furan	*Chloroform + ethanol (Ref. 7)*	*Chloroform + amylenes (Ref. 7)*	*o-Dichloro benzene*	*Benzene (Ref. 9)*
-Octadecanoic acid		365(6) 368(8)			303(3)	
leic acid	316	341(8)				
inoleic acid	310	337(8)				
icarboxylic acids						
Tetrahydrophthalic acid		245(a)				
Hexahydrophthalic acid		248(a)				
Sebacic acid	159	311(8)				
Anhydrides						
Phthalic anhydride	100	130(8)				
Tetrahydrophthalic anhydride		158(8)				
Hexahydrophthalic anhydride		158(8)				
Succinic anhydride	90	153(8)				
Halogenated compounds						
Chloroform	80	126(1)				
Tri-iodomethane	98	142(1)				
Tribromomethane	87	118(1)				
Carbon tetrachloride	96	138(8)				
1,1-Dichloroethylene			88	84		
sym-Tetrachloroethylene		175(1)				
Pentachloroethylene			81			
Pentachloroethane	120	146(1)				
Ethyl iodide	80		89	85		
Epichlorohydrin	78	98(a)				
1,4-Dichlorobutane	109	128(1)				
Hexachlorobutadiene	155	134(1)				
Ethyltrichloro acetate	138	135(1)				
Bromocyclohexane					112(5)	
1-Bromohexadecane	305	306(8)				
Chlorobenzene	102		88	84		
Bromobenzene	103		87			
Benzene hexachloride						124
p-Dichlorobenzene	96	119(2)				
p-Diiodobenzene		119(2)				
α,α'-Dichlorotoluene	128	143(8)				
Esters						
Ethyl acetate	98			173		
Propyl acetate	115	130(8)	206	197		
Butyl acetate	132	138(8)				
Ethylene glycol monoethyl ether acetate		100(10)				
Dimethyl adipate						168
Diethyl carbonate	121					126
Dimethyl terephthalate						137

TABLE 1 (*continued*)

Molecule	*Theoretical molar volume at 20°* (*cm^3 mole^{-1}*)	*Recalculated experimental molar volume* (*cm^3 mole^{-1}*)				
		Tetra-hydro-furan	*Chloroform + ethanol* (*Ref.* 7)	*Chloroform + amylenes* (*Ref.* 7)	*o-Dichloro benzene*	*Benzene* (*Ref.* 9)
Dibutyl phthalate	265	255(8)				
Dioctyl phthalate	(396)	362(8)				
Dinonyl phthalate	(390)	390(8)				
Diglycidyl phthalate	217	220(a)				
Diglycidyl hexahydrophthalate		220(a)				
Diglycidyl tetrahydrophthalate		220(a)				
Diglycidyl succinate		220(a)				
Glycidyl pivalate	158	173(a)				
Di-*n*-butyl-D-tartrate	(241)	310(8)				
Methyl oleate	339	322(8)				
Glyceryl monolinoleate		450(10)				
Glyceryl mono-oleate	376.5	475(10)				
Glyceryl monoricinoleate	362.4	500(10)				
Glyceryl dilinoleate		700(10)				
Glyceryl dioleate		666(10)				
Glyceryl diricinoleate		810(10)				
Glyceryl triricinoleate	960	1000(10)				
Ethers						
Dibutyl ether	169		220	212		
Diethyl ether	104		165	167		
Tetrahydrofuran	81		152	140		
			145			
Dioxane	85		167			
Di(*n*-dodecyl) ether		422(1)				
Di(*n*-octyl) ether	295	283(1)				
Butyl glycidyl ether						153
Isopropyl ether	(142)	146(8)				
Diglycidyl ether of diphenylol	293	290(a)				
propane		293(8)				
Diphenoxyethane		183(1)				159
Ketones and aldehydes						
Dimethyl ketone	73		167	162		
Diphenyl acetone		185(1)				
Isobutyl methyl ketone						128
Ethyl amyl ketone	156	162(8)				
2-Butanone	89		171			
2,5-Hexanedione	118	133(1)				
n-Heptaldehyde	134					150
Benzophenone	163	136(1)				
Anthraquinone	145	117(1)				
2-Ethylanthraquinone		143(1)				
Primary amines						
Isopropylamine	85	139(8)				
Butylamine	99	138(8)				

TABLE I (*continued*)

Molecule	*Theoretical molar volume at 20°* (cm^3 *mole*$^{-1}$)	*Recalculated experimental molar volume* (cm^3 *mole*$^{-1}$)				
		Tetra-hydro-furan	*Chloroform + ethanol* (*Ref.* 7)	*Chloroform + amylenes* (*Ref.* 7)	o-*Dichloro benzene*	*Benzene* (*Ref.* 9)
Octylamine	165	192(8)				
Aniline	91	136(8)	98	91		
		131(1)				
Benzylamine	109		208			
Ethylamine	65	106(a)				
1-Naphthylamine	128	145(8)				
2-Naphthylamine		163(1)				
o-Phenylenediamine		145(8)				
m-Phenylenediamine	95	170(8)				
p-Phenylenediamine		147(8)				
Diaminodiphenylsulphone		400(a)				
Diaminodiphenylmethane		260(a)				
Secondary amines						
Diethylamine	103	177(8)				
Dibutylamine	169	227(8)				
N-Ethylaniline	126	139(8)				
N-Butylaniline	160	172(8)				
N-Methyl-*p*-toluidene	(130)	138(8)				
Diphenylamine	145	165(8)				
		152(1)				
Dipropylamine	137		136			
Cyclohexylamine	173		155			
Piperidine	99		140			
Dibenzylamine	192	175(1)				
Tertiary amines						
Quinoline	118		151	137		
Dimethylaniline	127		163	147		
Tri-ethylenediamine		227(a)				
Tripropylamine	189	158(8)				
Tributylamine	238	200(8)				
Triamylamine	289	246(8)				
Trihexylamine		290(8)				
Tri-iso-octylamine		370(8)				
Dimethylaniline	127		163	153		
Diethylaniline	160	138(8)				
Amides						
Acetamide	59	120(1)				
Dicyandiamide		250(a)				
Imidazoles						
Imidazole		122(a)				
1-Methylimidazole		82(a)				
2-Methylimidazole		120(a)				
1-*n*-Butylimidazole		125(a)				
4 (or 5)-*tert*-Butylimidazole	127	175(a)				

TABLE I (*continued*)

Molecule	*Theoretical molar volume at 20°* (*cm*^{3} *mole*$^{-1}$)	*Recalculated experimental molar volume* (*cm*^{3} *mole*$^{-1}$)				
		Tetra-hydro-furan	*Chloroform + ethanol* (*Ref.* 7)	*Chloroform + amylenes* (*Ref.* 7)	o-*Dichloro benzene*	*Benzene* (*Ref.* 9)
1-Phenylimidazole	126.5	130(a)				
1-Benzylimidazole	139	137 (a)				
4,5-Diphenylimidazole	183	220(a)				
2,4,5-Triphenylimidazole	247	250(a)				
Benzimidazole		138(8)				
Nitriles						
Adiponitrile	114	180(1)				126
Hexanonitrile	120					138
Isocyanates						
Toluene diisocyanate	142.5	136(a)				
Diisocyanato diphenyl methane	210	220(a)				
Sulphur compounds						
Dimethyl sulphoxide	71		197	178		
Di-*n*-propyl sulphide	141	130(1)				
n-Dodecanethiol	239	214(1)				
Ring compounds						
Benzene	89		94	94		
Toluene	106	110(a)	119	114		
p-Xylene			139		119(5)	
m-Xylene	122				119(5)	
o-Xylene					116(5)	
Ethylbenzene	122			131	116(5)	
Nitrobenzene	102	117(1)				
Tetralin	136		142			
cis-Decahydronaphthalene	154	161(8)				
Biphenyl	130	117(1)	142	140		
Diphenylmethane	167					126
Phenanthrene	151	121(1)				
Anthracene	143	138(8) 122(1)				
2-Benzanthracene		182(1)				
Terphenyl		160(1)				
Hexaethylbenzene		134(1)				
Dicumyl peroxide						222
Cumene		125(1)				122
Triphenylmethane		158(8)				
Tetraphenylethylene	288	216(8)				
Triphenylphosphite	262	237(a)				

relationship between the theoretical and experimental molar volumes for different types of compound in tetrahydrofuran.

1. Alkanes, branched alkanes and branched alkenes have equal theoretical and experimental molar volumes.

2. One hydroxyl or carboxylic acid group causes the experimental molar volume to be larger than the theoretical molar volume by an average of 59 cm^3 $mole^{-1}$ (range 40–79). The hydroxyl group on glycol ethers, and each of the hydroxyl groups on dihydric alcohols, cause the experimental molar volume to be larger by about 47 cm^3 $mole^{-1}$.

3. One halogen atom causes the experimental molar volume to be larger by about 15 cm^3 $mole^{-1}$. For several chlorines the increase falls to about 5 cm^3 $mole^{-1}$ for each chlorine atom.

4. Ester groups and ketone groups cause a slight increase in the experimental molar volume of about 10 cm^3 $mole^{-1}$.

5. Ether groups cause no difference between the molar volumes.

6. Primary amines cause an average increase of 38 cm^3 $mole^{-1}$ in the experimental molar volume compared to the theoretical value, whereas secondary aliphatic amines cause an increase of only 10 cm^3 $mole^{-1}$. Tertiary aliphatic amines sorb onto the gel and cause the experimental molar volume to be less than the theoretical value by about 37 cm^3 $mole^{-1}$. The one tertiary aromatic amine causes a smaller decrease of 22 cm^3 $mole^{-1}$.

7. The pyrrole group on imidazole strongly solvates, leading to a larger experimental molar volume. The changes in the increase with the type of substitution indicate that the solvation is eliminated by substitution on the 1-position. Substitution on the 2- or 4(or 5)-position reduces the strength of the solvation and substitution on both the 2- and 4(or 5)-positions reduces it still further. Substitution on the 2-, 4- and 5- positions eliminates solvation.

8. A phenyl group causes a decrease of about 15 cm^3 $mole^{-1}$.

These results are similar to others[1,4,8] but are more consistent, although also more fragmentary.

No new conclusions can be drawn from the work in solvents other than tetrahydrofuran.

SUMMARY

680 independent observations of the elution behaviour of small molecules in gel permeation chromatography have been examined to see if reliable molar volumes can be calculated from them. For 380 observations this is possible, but for the other 300 it is not, mainly because the materials eluted outside the range of the calibration standards used in the appropriate work. The 380 reliable molar volumes are tabulated and the effects of the solvent are discussed.

RÉSUMÉ

On a examiné le comportement, lors de l'élution de petites molécules par chromatographie sur gel, de 680 cas, pour savoir si les volumes molaires peuvent ainsi être calculés. Cela est possible pour 380 observations. Les 380 volumes molaires trouvés sont donnés; l'influence du solvant est examinée.

ZUSAMMENFASSUNG

680 unabhängige Beobachtungen des Elutionsverhaltens kleiner Moleküle

bei der Gelchromatographie sind im Hinblick darauf geprüft worden, ob daraus zuverlässige Molvolumina berechnet werden können. Bei 380 Beobachtungen ist dies möglich, jedoch bei den 300 anderen nicht, hauptsächlich weil die Substanzen ausserhalb des Bereichs der in der eigenen Arbeit verwendeten Eichstandards eluierten. Die 380 zuverlässigen Molvolumina werden zusammengestellt und die Einflüsse des Lösungsmittels diskutiert.

REFERENCES

1 J. G. Hendrickson and J. C. Moore, *J Polymer Sci.*, A-1, 4 (1966) 167.
2 A. Kollmansberger and W. B. Smith, *J. Phys. Chem.*, 69 (1965) 4157.
3 J. Cazes and D. Gaskill, *Separation Sci.*, 2 (1967) 421.
4 J. G. Hendrickson, *Anal. Chem.*, 40 (1968) 49.
5 J. Cazes and D. Gaskill, *Separation Sci.*, 4 (1969) 15.
6 T.-L. Chang, *Anal. Chim. Acta*, 39 (1967) 519.
7 J. G. Hendrickson, *Reprints 4th International GPC Seminar*, Waters Associates Inc., 1967, p. 125.
8 G. D. Edwards and Q. Y. Ng, *J. Polymer Sci.*, C, 21 (1968) 105.
9 J. G. Hendrickson, *J. Chromatog.*, 32 (1968) 543.
10 A. Lambert, *J. Appl. Chem. (London)*, 20 (1970) 307.
11 A. Lambert, *J. Appl. Chem. (London)*, 20 (1970) 305.

Analytica Chimica Acta
Elsevier Publishing Company, Amsterdam
Printed in The Netherlands

SPECTROPHOTOMETRIC DETERMINATION OF URANIUM(VI) WITH 2-(5-BROMO-2-PYRIDYLAZO)-5-DIETHYLAMINOPHENOL

D. A. JOHNSON AND T. M. FLORENCE
Australian Atomic Energy Commission, Research Establishment, Lucas Heights, N.S.W. 2232 (Australia)

(Received June 30th, 1970)

An improved spectrophotometric method for the determination of uranium with the highly sensitive chromogenic reagent 2-(2-pyridylazo)-5-diethylaminophenol (PADAP) was recently described[1,2]. The bromo derivative of PADAP, 2-(5-bromo-2-pyridylazo)-5-diethylaminophenol (bromo-PADAP), used by Gusev and Shalamova[3] as a reagent for vanadium, has since been found to be more sensitive towards uranium(VI) than PADAP, with a greater iron tolerance, and easier to prepare in a pure state. The uranyl–bromo-PADAP complex has a practical molar absorptivity of 74,000 at 578 nm and pH 7.6, and in the presence of a mixed complexing solution[4] containing (1,2-cyclohexylenedinitrilo)tetraacetic acid (CyDTA), sulphosalicylate and fluoride, only chromium(III), vanadium(V), and phosphate interfere seriously. A preliminary extraction of uranium with tri-*n*-octylphosphine oxide followed by direct colour development in the organic phase with bromo-PADAP provides a highly sensitive and specific method for the spectrophotometric determination of uranium in a wide range of materials. Details are given in this paper for the determination of uranium in waters, ores, phosphoric acid and phosphate rocks, thorium oxide, and zirconium oxide.

EXPERIMENTAL

Apparatus and reagents

Hilger "Uvispek" and Cary 16 manual spectrophotometers were used for absorbance measurements. Wavelength–absorbance curves were recorded on a Hitachi EPS-3T spectrophotometer.

Complexing solution. Suspend 25 g of CyDTA (Fluka), 5 g of sodium fluoride, and 65 g of sulphosalicylic acid in 800 ml of water. Neutralize to pH 7.85 with 40% sodium hydroxide and dilute to 1 l.

Dilute complexing solution. Dilute one part of the complexing solution with an equal volume of water, and adjust the pH to 8.35 with 40% sodium hydroxide.

Buffer solution, pH 7.85 *or* 8.35. Dissolve 149 g of triethanolamine in 800 ml of water, neutralize to the required pH with perchloric acid and allow to stand overnight. Readjust to pH 7.85 or 8.35 with perchloric acid and dilute to 1 l.

Bromo-PADAP, 0.05%. Dissolve 0.05 g of recrystallized bromo-PADAP in 100 ml of reagent-grade ethanol.

TOPO solution, 0.1 *M*. Dissolve 19.3 g of tri-*n*-octylphosphine oxide (Eastman) in cyclohexane and dilute to 500 ml with cyclohexane.

Synthesis of 5-bromo-PADAP. For the diazotisation, place 1.56 g of sodium amide (Merck) as a 50% suspension in toluene into a dry 250-ml reaction flask fitted with a mechanical stirrer, a reflux condenser, a thermometer, and a tube for passing nitrogen. Add 20 ml of outgassed benzene and 6.92 g of 2-amino-5-bromopyridine (Aldrich) in 150 ml of outgassed benzene, with nitrogen passing through the flask. Maintain the thoroughly stirred suspension at 40°. After ammonia evolution has ceased (about 40 min; test with moist litmus) add isopentylnitrite (4.68 g) and continue stirring for another 90 min. Maintain the solvent volume by occasional additions of benzene. Filter the precipitated diazotate under suction, wash with ethyl ether and dry under vacuum. Store the hygroscopic product in an airtight container. For the coupling reaction, warm to 60° a solution of sodium 5-bromo-2-pyridyldiazotate (4.44 g) in 15 ml of water plus 20 ml of ethanol, and add dropwise to a solution of *m*-diethylaminophenol (3.3 g) in ethanol (10 ml) at 60°. Pass carbon dioxide through the solution during addition, and continue to pass the gas until all the ethanol has evaporated. Dissolve the oily residue in 10 *M* hydrochloric acid (8 ml) and then dilute with water (300 ml). Filter the precipitate under suction and wash with water. Recrystallize from 50% aqueous ethanol. The yield of 5-bromo-PADAP (burgundy-coloured crystals, m.p. 151–152°) is 20%.

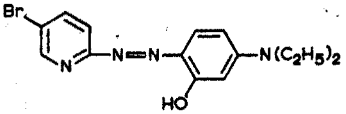

Elemental analysis. Calc. C 51.6%, H 4.9%, N 16.0%, O 4.6%, Br 22.9%; found C 51.6%, H 4.9%, N 16.2%, O 4.9%, Br 22.4%.

Recommended procedures

Uranium in waters. Pipette a sample aliquot containing 0.5–100 μg of uranium into a 25-ml volumetric flask. If the sample is strongly acidic, determine on a separate aliquot the volume of 1 *M* sodium hydroxide required for neutralization. Add, in the following order and with mixing, 2.0 ml of complexing solution, 2.0 ml of pH 7.85 buffer, the volume of 1 *M* sodium hydroxide required for neutralization, 10.0 ml of ethanol and 2.00 ml of 0.05% bromo-PADAP. Mix and dilute to volume with water. Allow to stand for at least 40 min, and then measure the colour at 578 nm against a reagent blank, using 1–5 cm cells. With a 1-cm cell 50 μg of uranium gives an absorbance of 0.62.

Uranium in ores. Weigh 0.1 g of ore (−200 mesh) into a platinum dish, add 5 ml of 15 *M* nitric acid and 5 ml of 40% hydrofluoric acid and evaporate to dryness on a water bath. Add a further 5 ml of 15 *M* nitric acid and 5 ml of 40% hydrofluoric acid and again evaporate to dryness on the water bath. Add 2 ml of 72% perchloric acid and fume on a hot plate until the volume of perchloric acid is less than 1 ml. Cool and dissolve the residue in 40 ml of 5 *M* nitric acid and filter through a small paper into a 100-ml volumetric flask. Wash the paper and dilute to volume with water.

Pipette an aliquot (5–100 ml) of the sample solution (1–150 μg uranium) into a separating funnel. Add 5.0 ml of 2% (w/v) sodium fluoride solution and 2.0 ml of freshly prepared 5% ascorbic acid solution, and mix. Pipette in 5.00 ml of 0.1 *M* TOPO and extract for 1 min. Allow the phases to separate and discard the aqueous phase.

Pipette 2.0 ml of the organic phase into a dry 25-ml volumetric flask. Add 1.0 ml of dilute complexing solution, 4.00 ml of 0.05% bromo-PADAP, and 1.0 ml of pH 8.35 buffer, in that order, mixing thoroughly after each addition. Stopper the flask and allow to stand for 10 min. Add 16.0 ml of ethanol and dilute to volume with water. Measure the colour at 574 nm against a reagent blank carried through the extraction procedure. Standards should be carried through the complete extraction procedure.

Uranium in phosphoric acid and phosphate rocks. Dissolve 0.5 g of phosphoric acid or phosphate rock in 50 ml of 2 *M* nitric acid and follow the extraction procedure given for uranium in ores.

Uranium in thorium oxide. Weigh 0.2 g of finely powdered thoria into a 100-ml beaker. Add 20 ml of 5 *M* nitric acid and 0.1 ml of 2 *M* hydrofluoric acid, place a watch glass over the beaker and boil gently until dissolution is complete. Cool, transfer to a separating funnel and add water to bring the volume to about 50 ml. Extract as described for uranium in ores, but use 0.3 g of sodium fluoride in place of the 5 ml of fluoride solution.

Uranium in zirconium oxide. Weigh 0.1 g of finely powdered zirconia into a platinum crucible. Add 1 g of sodium fluoroborate and fuse for 5 min. Cool, and use a total volume of 40 ml of 1.5 *M* nitric acid to dissolve the melt and to transfer the solution to a separating funnel. Add 20 ml of a solution which is 0.2 *M* in CyDTA and 2% in sodium fluoride, then add 2.0 ml of fresh 5% ascorbic acid solution and extract uranium with 5.00 ml of 0.1 *M* TOPO, as described for uranium in ores.

RESULTS AND DISCUSSION

Absorbance spectra, adherence to Beer's law, and stability

The absorbance spectra for bromo-PADAP and its uranyl complex are shown in Fig. 1. Introduction of the 5-bromo group into the pyridine ring produced an expected bathochromic shift, the wavelength of maximum absorbance for the uranyl bromo-PADAP complex being 578 nm compared to 564 nm for the PADAP complex[1]. There was also a concomitant increase of 12% in the practical molar absorptivity.

Beer's law was obeyed from zero to 1.3 absorbance units (0–4.2 μg U ml^{-1}) in both 48% and 80% ethanol, and the colour remains unchanged for at least 18 h.

Effect of pH

The effect of pH on bromo-PADAP and its uranyl complex was very similar to that found previously for PADAP, with the exception that maximum absorbance was obtained at a pH of 7.6 in 48% ethanol. A pH of 7.6 resulted when 2.0 ml of pH 7.85 triethanolamine buffer was used per 25 ml of final volume. The absorbance was almost constant in the pH range 7.1–8.1. In the TOPO extraction procedure, the effect of pH was investigated by changing the pH of the buffer solution[2]. Buffers of pH between 8.2 and 8.5 gave maximum absorbance.

Study of interferences

In the direct bromo-PADAP method (no extraction) the following elements

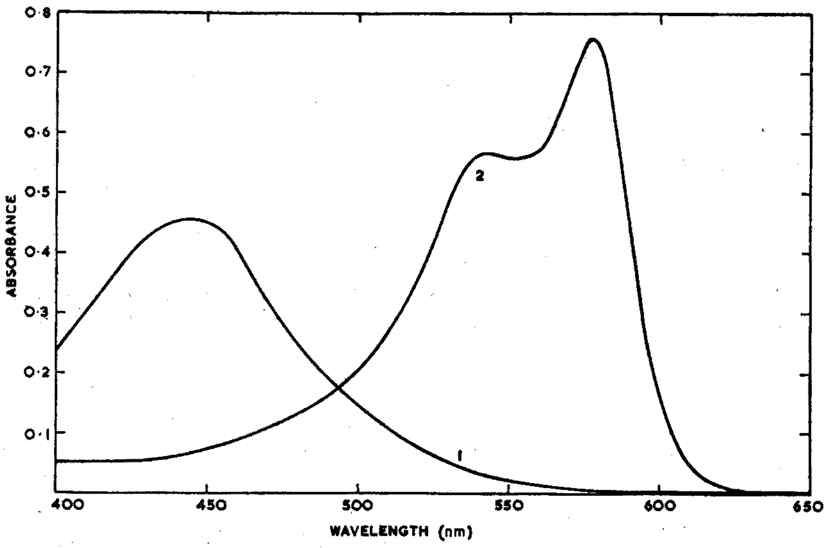

Fig. 1. Wavelength–absorbance curves. (1) Free bromo-PADAP ($1.00 \cdot 10^{-5}$ *M* *vs.* blank); (2) uranyl bromo-PADAP complex ($1.00 \cdot 10^{-5}$ *M* UO_2^{2+} *vs.* blank). Each solution contained 2 ml of complexing solution and 2 ml of buffer pH 8.75, per 25 ml. Measured in 1-cm cells.

TABLE I

INTERFERENCES IN THE DIRECT SPECTROPHOTOMETRIC METHOD FOR URANIUM WITH BROMO-PADAP

Ion	*Maximum permissible*[a] *amount (mg)*	*Ion*	*Maximum permissible*[a] *amount (mg)*
As(V)[b]	0.5	Ni(II)	3
Co(II)	4	V(V)	0.01
Cr(III)	0.2	V(IV)	1.0
Cr(VI)	3	Zr(IV)	0.5
Cu(II)	3	PO_4^{3-}[b]	0.5

[a] For less than 2% error in the determination of 50 μg of uranium.
[b] Negative error.

gave less than ±2% error at the 5-mg level in the determination of 50 μg of uranium: Al, Be, Bi, Ca, Cd, Cs, Fe(III), Hg(II), Li, Mg, Mn(II), Mo(VI), Nd, NH_4^+, Pb, Sn(II), Th, W(VI). Table I shows the maximum permissible amounts of ions which interfered to varying degrees in the direct method. The bromo-PADAP method could tolerate 6 mg of iron, *i.e.*, about five times as much as the PADAP method[1]. Vanadium interference could be decreased by reducing vanadium(V) to (IV) with ascorbic acid in hydrochloric acid media. To the sample aliquot 2.0 ml of 1 *M* hydrochloric acid and 2 ml of fresh 5% ascorbic acid were added followed by the complexing solution, buffer, and 2.0 ml of 1 *M* sodium hydroxide. This allowed up to 1 mg of vanadium(V) to be tolerated.

The TOPO extraction procedure utilized 2 *M* nitric acid containing 2 ml of 5% ascorbic acid and 5 ml of 2% sodium fluoride as a medium for extraction of uranium. Ascorbic acid reduced the higher valency states of cerium, vanadium, and iron, and prevented their extraction, while fluoride complexed zirconium and thorium. Under these conditions some extraction of molybdenum occurred, but this element did not react with bromo-PADAP. No interference was observed from 20 mg of the following elements in the determination of 100 μg of uranium: Al, As(V), Au(III), Ce(IV), Cr(III), Fe(III), Mo(VI), Nd, Pt(IV), Sb(III), Sn(IV), Th, Ti(IV), and V(V). In addition, 500 mg of phosphate, sulphate or chloride had no effect on uranium extraction. Sulphate and chloride, though, may enhance the extraction of some impurity metals, so these anions should preferably be absent. When the ascorbic acid was increased to 10 ml of 10% solution, 500 mg of iron(III) and 200 mg of vanadium(V) could be tolerated.

Analysis of various sample types

Uranium ores. The most generally applicable method for dissolution of ore samples is a double treatment with nitric and hydrofluoric acids, followed by fuming with perchloric acid. A small residue sometimes remained after this treatment, and occasionally it contained traces of uranium. Unless it has been previously established that the residue is uranium-free, it should be fused with 0.3 g of sodium carbonate. A more rapid dissolution technique for a small number of samples is fusion of the ore sample with a 5–10 fold weight excess of sodium fluoroborate. All ores tested were rapidly and completely dissolved by this flux, and the cooled melt dissolved readily in dilute nitric acid. A disadvantage of the sodium fluoroborate fusion was that fluorine was lost from the melt by reaction with silicon. The melt then consisted of a mixture of sodium fluoroborate and sodium metaborate, and when dissolved in nitric acid it consumed the fluoride added to complex thorium and zirconium before extraction with TOPO. Some thorium and zirconium were then free to extract, and high results were occasionally obtained for the uranium determination. This effect could be overcome by adding extra sodium fluoride before extraction.

Aluminium by itself had no effect on the TOPO extraction–bromo-PADAP method, even when present in gross amounts, but aluminium combined with thorium and/or zirconium could lead to high results; aluminium, like borate, consumed the fluoride added to prevent extraction of zirconium and thorium. The amount of fluoride added in the recommended procedure was sufficient to complex all the aluminium likely to be present in a 100-mg ore sample. However, if larger samples are used, and the ore is high in aluminium, more fluoride may be needed. Some care is needed in the addition of fluoride because very high concentrations depress the extraction of uranium (10% depression for 300 mg of sodium fluoride).

For convenience, the maximum sample weight of ore or rock was 0.25 g, and with this weight the limit of detection of uranium at the 95% confidence level was 2 p.p.m. of U_3O_8, with the Cary 16 manual spectrophotometer.

Phosphoric acid and phosphate rocks. There is an increasing interest in commercial phosphoric acid as a future source of uranium. Phosphate at the 500-mg level had no effect on the TOPO extraction–bromo-PADAP method, and 1 g of phosphate (as PO_4^{3-}) causes only a −7% error, hence these materials can be analyzed directly for uranium.

Thorium oxide. Ignited thoria dissolved rapidly in 5 *M* nitric acid containing a trace of fluoride catalyst, and when 300 mg of fluoride was used as masking agent, the spectrophotometric method tolerated 200 mg of thorium. With a 200-mg ThO_2 sample the limit of detection of uranium was 3 p.p.m. U_3O_8.

Zirconium oxide. Zirconium is perhaps the most difficult metal to mask completely in the bromo-PADAP method. The procedure recommended for uranium in ores tolerated 10 mg of zirconium, but 20 mg gave an error of +5%, and increasing the fluoride concentration did not entirely prevent extraction. Zirconium, however, formed a strong mixed complex with CyDTA and fluoride in 1 *M* nitric acid, which prevented extraction into TOPO and allowed amounts of zirconium up to 100 mg to be analyzed.

SUMMARY

A new reagent, 2-(5-bromo-2-pyridylazo)-5-diethylaminophenol (bromo-PADAP), is described for the spectrophotometric determination of uranium(VI). This reagent is highly sensitive towards uranium, the uranyl complex having a molar absorptivity of 74,000 at 578 nm and pH 7.6. In the presence of a mixed masking solution only a few ions interfere seriously, and the method can be made specific for uranium by a preliminary extraction of uranium into tri-*n*-octylphosphine oxide, and direct development of the bromo-PADAP colour in the organic phase. Details are given for the determination of uranium in waters, ores, phosphoric acid and phosphate rocks, thorium oxide, and zirconium oxide.

RÉSUMÉ

Un nouveau réactif, le 2-(5-bromo-2-pyridylazo)-5-diéthylaminophénol (bromo-PADAP), est proposé pour le dosage spectrophotométrique de l'uranium(VI). Ce réactif est très sensible pour l'uranium: coefficient d'extinction molaire 74.000 à 578 nm, au pH 7.6. Seuls quelques ions gênent en présence d'une solution de masquage; le dosage peut être rendu spécifique par extraction préliminaire de l'uranium à l'aide de tri-*n*-octylphosphine oxyde et développement direct de la couleur dans la phase organique. Des détails sont donnés pour le dosage de l'uranium dans les caux, les minerais, l'acide phosphorique et les roches phosphatées, l'oxyde de thorium et l'oxyde de zirconium.

ZUSAMMENFASSUNG

Es wird ein neues Reagenz, 2-(5-Brom-2-pyridylazo)-5-diäthylaminophenol (Brom-PADAP), für die spektrophotometrische Bestimmung von Uran(VI) beschrieben. Dieses Reagenz ist gegen Uran sehr empfindlich; der Uranylkomplex hat einen molaren Extinktionskoeffizienten von 74,000 bei 578 nm und pH 7.6. In Gegenwart einer gemischten Maskierungslösung stören nur wenige Ionen ernsthaft; die Methode wird für Uran spezifisch durch vorhergehende Extraktion des Urans mit Tri-*n*-octylphosphinoxid und unmittelbare Entwicklung der Brom-PADAP-Färbung in der organischen Phase. Es werden Einzelheiten angegeben für die Bestimmung von Uran in Wasserproben, Erzen, Phosphorsäure und Phosphatgesteinen, Thoriumoxid und Zirkoniumoxid.

REFERENCES

1 T. M. Florence, D. A. Johnson and Y. J. Farrar, *Anal. Chem.*, 41 (1969) 1652.
2 T. M. Florence and Y. J. Farrar, *Anal. Chem.*, 42 (1970) 271.
3 S. I. Gusev and G. G. Shalamova, *Zh. Analit. Khim.*, 23 (1968) 686.
4 T. M. Florence and Y. J. Farrar, *Anal. Chem.*, 35 (1963) 1613.

Anal. Chim. Acta, 53 (1971) 73–79

Analytica Chimica Acta
Elsevier Publishing Company, Amsterdam
Printed in The Netherlands

A METHOD FOR DETERMINING QUANTUM YIELDS FOR SOLID-STATE PHOTOCHEMICAL REACTIONS

E. LYNN SIMMONS AND W. W. WENDLANDT
Department of Chemistry, University of Houston, Houston, Texas 77004 (U.S.A.)

(Received July 29th, 1970)

Of the various methods which have been employed in the study of solid-state photochemical reactions, few enable the quantum yield to be determined. Methods involving reflectance spectroscopy[1-5], infrared spectra of potassium chloride pellets[6], and alcoholic slurries[4,5], serve only to identify photoproducts or determine reaction stoichiometries. Problems encountered experimentally in attempting to measure quantum yields of solid-state reactions mainly involve the variation of the radiation intensity and thus the concentration of reactant throughout the sample. These problems are further amplified in that solid-state reactions are heterogeneous surface reactions. Although these problems have been dealt with theoretically[7-10], it is often more convenient to select experimental conditions such that as many of them as possible can be neglected.

Quantum yield values for the solid-state reactions of $K_3[Co(C_2O_4)] \cdot 3\ H_2O$ and $K_3[Fe(C_2O_4)_3] \cdot 3\ H_2O$ have been measured by photolyzing thin layers of the compounds coated on glass plates[11] and chemically measuring the amount of photoproduct formed. This method is apparently applicable except that the absorption of radiation by the photoproducts usually introduces errors into the experimentally determined quantum yield values.

A similar method with some modifications is described here. Quantum yield values are determined using rate plots rather than chemical analyses of the photoproducts with corrections being applied for the absorption of radiation by the photoproducts. The method is applied to the solid-state photochemical reaction of $K_3[Mn(C_2O_4)_3] \cdot 3\ H_2O$ which undergoes an oxidation–reduction reaction when irradiated with ultraviolet light[4].

THEORY

A very thin layer of powdered compound, A, coated onto a glass plate, is illuminated with monochromatic radiation of constant intensity, *I*. On the absorption of radiation, A reacts to give product P.

After a certain length of time of reaction, the reflectance of the sample is *R* and the transmittance is *T*. All radiation not reflected or transmitted is absorbed either by the reactant, A, or the product, P. Thus,

$$1 - T - R = \alpha_A C_A + \alpha_P C_P \qquad (1)$$

where *C* is concentration in units of moles cm^{-2}, α is an absorption coefficient (cm^2

mole^{-1}), and A and P refer to reactant and product, respectively.
Since

$$C_A + C_P = C_0 \tag{2}$$

where C_0 is the initial concentration of reactant, then eqn. (1) may be written as

$$C_A = (1 - T - R - A_P C_0)/(\alpha_A - \alpha_P) \tag{3}$$

At $t = 0$,

$$1 - T_A - R_A = \alpha_A C_0 \tag{4}$$

and after completion of the reaction

$$1 - T_P - R_P = \alpha_P C_0 \tag{5}$$

where again A and P refer to values of the pure reactant and product, respectively.

Substituting eqn. (5) into eqn. (3) gives

$$C_A = (T_P + R_P - R - T)/(\alpha_A - \alpha_P) \tag{6}$$

and the time derivative of eqn. (6) is

$$\mathrm{d}C_A/\mathrm{d}t = (\alpha_A - \alpha_P)^{-1} \mathrm{d}(R + T)/\mathrm{d}t \tag{7}$$

The rate of reaction of A is also given by

$$\mathrm{d}C_A/\mathrm{d}t = -\alpha_A C_A \phi I \tag{8}$$

where ϕ is the quantum yield of the reactant. It is assumed that the layer of sample is thin enough that the variation in radiation intensity throughout the sample is negligibly small.

Equating eqns. (7) and (8) and substituting eqn. (6) into the resulting equation gives

$$\mathrm{d}(R + T)/\mathrm{d}t = \alpha_A \phi I [T_P + R_P - R - T] \tag{9}$$

which is equivalent to

$$\mathrm{d} \ln [T_P + R_P - R - T]/\mathrm{d}t = -\alpha_A \phi I\,. \tag{10}$$

Solving eqn. (4) for α_A and substituting the result into eqn. (10) gives the final equation,

$$\mathrm{d} \ln [T_P + R_P - R - T]/\mathrm{d}t = -[1 - T_A - R_A] C_0^{-1} \phi I\,. \tag{11}$$

Thus, when the indicated plot is prepared, a straight line should be obtained whose slope is related to the quantum yield and other easily measured parameters. The quantum yield can therefore be calculated from such a plot.

EXPERIMENTAL

Preparation of compounds

The compound, $K_3[Mn(C_2O_4)_3] \cdot 3\,H_2O$ was prepared and analyzed by previously described methods. The analysis of the compound was as follows: Mn found (11.6% theor.) 11.20%; C_2O_4 found (59.2% theor.) 58.58%.

Photolysis procedures

The photolysis procedure was carried out in the following manner. A small amount of an acetone slurry of the finely ground powdered compound was placed onto a weighed glass microscope slide which was allowed to dry and then weighed. The area of the resulting coating was measured by the use of planimeter so that C_0 could be calculated. The sample was then illuminated with monochromatic light from a Bausch and Lomb monochromator equipped with a mercury lamp source. A YSI-Kettering Model 65 radiometer was used to measure the radiation intensity. The output of the radiometer was recorded as a function of time of reaction on a strip-chart recorder. Periodically, the reaction was stopped and the reflectance of the sample was obtained by the use of a Beckman DK-2A spectroreflectometer. Black paper was placed behind the glass plate as the reflectance was measured to absorb all transmitted radiation. The reaction was carried to completion in order to determine the values of R_P and T_P.

Transmission values were calculated by $T = I/I_0$, where I_0 is the intensity of radiation passed through a clear glass plate.

RESULTS AND DISCUSSION

The plots of $\ln[R_P + T_P - R - T]$ *vs.* *t* are illustrated in Fig. 1 for the reaction of $K_3[Mn(C_2O_4)_3] \cdot 3\ H_2O$ at 400 nm and at three different intensities. As can be seen, reasonably straight lines were obtained. From the slopes of the plots, by means of eqn. (11), quantum yield values were calculated as given in Table I. No noticeable dependence of the quantum yield values on the radiation intensity was observed.

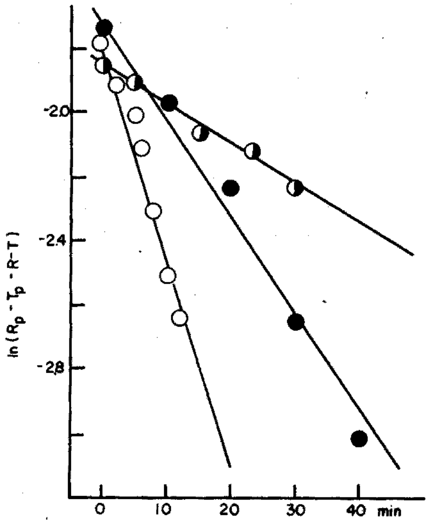

Fig. 1. Rate plots for $K_3[Mn(C_2O_4)_3] \cdot 3\ H_2O$ at a wavelength of 400 nm. (○) $I = 1.47 \cdot 10^{-8}$ einstein $cm^{-2}\ sec^{-1}$; (●) $I = 1.17 \cdot 10^{-8}$ einstein $cm^{-2}\ sec^{-1}$; (◑) $I = 0.74 \cdot 10^{-8}$ einstein $cm^{-2}\ sec^{-1}$.

The average value of about 0.52 is very close to the value of about 0.5 found[12] for the corresponding reaction in aqueous solutions at 400 nm. In contrast, quantum yield values found for other solid-state reactions were smaller than the corresponding reactions in aqueous solutions[11]. The larger quantum yield values found in this investigation may be due to the fact that radiation absorption by the photoproducts was taken into account in eqn. (11). This, in fact, is the major advantage of the method.

TABLE I

QUANTUM YIELDS FOR THE SOLID-STATE PHOTOCHEMICAL REACTION OF $K_3[Mn(C_2O_4)_3]\cdot 3\ H_2O$ AT 400 nm

I (*einstein cm*$^{-2}$)	C_0 (*moles cm*$^{-2}$)	ϕ (*mole einstein*$^{-1}$)
$1.47\cdot 10^{-8}$	$1.8\cdot 10^{-6}$	0.63
$1.17\cdot 10^{-8}$	$2.2\cdot 10^{-6}$	0.47
$0.74\cdot 10^{-8}$	$2.4\cdot 10^{-6}$	0.57
		Average 0.52
		Standard deviation ±0.09

A further advantage is that the experimental procedure is simple and rapid. The major difficulty encountered involved maintaining a constant radiation intensity, a particularly serious difficulty since very small changes in transmittance were involved (the largest change during reaction was in the sample reflectance). Numerous runs were carried out for each successful run in which the radiation intensity remained reasonably constant throughout the reaction. This problem, however, could probably be eliminated by suitable experimental techniques.

The method described for measuring solid-state quantum yields can only be accurate if the value of C_0 is small enough that the assumption that the radiation intensity remains reasonably constant throughout the sample is valid. In this investigation, C_0 values were about $2\cdot 10^{-6}$ moles cm^{-2} so that the fraction of the radiation absorbed was 10–25% during reaction. Thus, the errors introduced into the quantum yield values due to variations of radiation intensity throughout the sample were small, though probably not insignificant.

As can be seen, the standard deviation of the three quantum yield values from the mean is fairly large—about 20%. This is probably due to errors introduced by the previously-mentioned factors. Still, the method appears useful for rapidly determining reasonably good estimates of quantum yield values of solid-state photochemical reactions.

The financial support of this work by the Sandia Corporation, Albuquerque, N.M., is gratefully acknowledged.

SUMMARY

A method is described for determining the quantum yields of solid-state photochemical reactions. The major advantage of the method is that absorption of radiation by the photoproducts is taken into account. Use of the method for determining quantum yields for the solid-state photochemical reaction of $K_3[Mn(C_2O_4)_3]\cdot 3\ H_2O$ at 400 nm and various radiation intensities is discussed.

RÉSUMÉ

Une méthode est décrité pour déterminer les rendements quantiques de réactions photochimiques à l'état solide. Le principal avantage de cette méthode est qu'on tient compte de l'absorption des radiations par les photosubstances. On examine la réaction photochimique de $K_3[Mn(C_2O_4)_3] \cdot 3\ H_2O$ à 400 nm et diverses radiations.

ZUSAMMENFASSUNG

Es wird eine Methode für die Bestimmung der Quantenausbeute photochemischer Reaktionen im festen Zustand beschrieben. Der wesentliche Vorteil der Methode ist, dass die Strahlungsabsorption durch die Photoprodukte berücksichtigt wird. Die Anwendung der Methode auf die Bestimmung der Quantenausbeute der photochemischen Reaktion von $K_3[Mn(C_2O_4)_3] \cdot 3\ H_2O$ im festen Zustand bei 400 nm und verschiedenen Strahlungsintensitäten wird diskutiert.

REFERENCES

1 C. H. Stembridge and W. W. Wendlandt, *J. Inorg. & Nucl. Chem.*, 27 (1965) 129.
2 E. L. Simmons and W. W. Wendlandt, *J. Inorg. & Nucl. Chem.*, 27 (1965) 2317.
3 W. W. Wendlandt and E. L. Simmons, *J. Inorg. & Nucl. Chem.*, 27 (1965) 2325.
4 W. W. Wendlandt and E. L. Simmons, *J. Inorg. & Nucl. Chem.*, 28 (1966) 2420.
5 W. W. Wendlandt and J. H. Woodlock, *J. Inorg. & Nucl. Chem.*, 27 (1965) 259.
6 G. Lohmiller and W. W. Wendlandt, *Anal. Chim. Acta*, 51 (1970) 117.
7 W. A. Noyes and P. A. Leighton, *The Photochemistry of Gases*, Reinhold, New York, 1941.
8 J. E. Wilson, *J. Chem. Phys.*, 22 (1954) 334.
9 P. G. Barker, M. P. Halstead and J. H. Purnell, *Trans. Faraday Soc.*, 65 (1969) 2404.
10 T. R. Sliker, *J. Opt. Soc. Amer.*, 53 (1963) 454.
11 H. E. Spencer, *J. Phys. Chem.*, 73 (1969) 2316.
12 G. B. Porter, J. G. W. Poering and S. Karanka, *J. Amer. Chem. Soc.*, 84 (1962) 4027.

Analytica Chimica Acta
Elsevier Publishing Company, Amsterdam
Printed in The Netherlands

THE SUBSTOICHIOMETRIC DETERMINATION OF TUNGSTEN BY NEUTRON ACTIVATION AND ISOTOPE DILUTION ANALYSIS

N. K. BAISHYA AND R. B. HESLOP

Chemistry Department, The University of Manchester Institute of Science and Technology, Manchester, M60 1QD (England)

(Received September 1st, 1970)

Neutron activation methods of analysis have been developed by Brooksbank *et al.*[1] for the determination of trace amounts of tungsten in titanium, its alloys and compounds. Morrison and Cosgrove[2] analysed silicon for tungsten by direct γ-ray spectrometry, a technique which was also used by Jervis and Mackintosh[3] for the determination of tungsten in high-purity aluminium. Boganes *et al.*[4] determined tungsten in high-purity silicon by non-destructive activation analysis. Okada[5] used the short-lived nuclide formed by neutron activation for non-destructive analysis of tungsten. Subsequently, various other authors determined tungsten in rocks[6-8], sea water[9], ores[10] and steel[11,12]. Leliaert *et al.*[13], however, determined tungsten in high-alloy steels by isotope dilution. James and Richards[14] used a radiochemical method to determine tungsten as an impurity in silicon. Kalinin *et al.*[15] separated tungsten as its negative fluorocomplex on an anion-exchange column in the determination of tungsten impurity in silicon. Leliaert *et al.*[16] used decay-curve analysis for the determination of tungsten in steel, and resorted to a radiochemical separation to remove interfering elements. Activation analysis, with a neutron generator, has been used for the determination of tungsten in alloys[17]. Trace quantities of tungsten in biological materials[18], mine water[19], and plants[20] have also been determined by activation analysis.

The substoichiometric principle of neutron activation analysis has not previously been applied to the determination of tungsten. However, McClendon and DeVoe[21] determined tungsten in a molybdenum-containing alloy by substoichiometric isotope dilution, with toluene-3,4-dithiol as extractant. In the present investigation, attempts have been made to determine tungsten by activation analysis as well as by isotope dilution analysis, using various reagents such as α-benzoinoxime, 8-hydroxyquinoline, tetraphenylarsonium chloride, cupferron and toluene-3,4-dithiol in substoichiometric amounts. 8-Hydroxyquinoline, α-benzoinoxime and tetraphenylarsonium chloride could not be used because of poor and non-reproducible extraction. Although the extraction of tungsten with cupferron into an isoamyl alcohol–chloroform mixture seemed promising, many other metal ions interfered, and preliminary separation from these was difficult. However, toluene-3,4-dithiol was found to be satisfactory and was successfully used for the determination of tungsten in high-speed steel by isotope dilution, with the tungsten-185 isotope, and also in aluminium by neutron activation, with the radioisotope tungsten-187.

EXPERIMENTAL

Reagents

Tungsten carrier solution. A 0.1 *M* solution was prepared by dissolving 3.299 g of sodium tungstate in 100 ml of water.

Active tungsten solution. A 10.0-ml aliquot of 0.1 *M* sodium tungstate solution was taken to which 100 µCi of tungsten-185 was added. The solution was diluted to 100 ml.

Titanium(III) chloride solution. A 15% $TiCl_3$ solution (B.D.H) was used.

*Toluene-*3,4*-dithiol reagent*[22]. A carefully weighed amount (1.25 g) of toluene-3,4-dithiol was added to 100 ml of 2% sodium hydroxide solution. Dithiol was dissolved by warming to 35°. Thioglycollic acid (2.5 ml) was added after completion of the dissolution, and the volume was made up to 250 ml. The resulting solution, which was 0.5% (0.032 *M*) in dithiol was stored in a polythene bottle in a refrigerator.

Other compounds used to study the interferences were: $NH_4Fe(SO_4)_2 \cdot 12\,H_2O$, $CuSO_4 \cdot 5\,H_2O$, $CoSO_4 \cdot 7\,H_2O$, $NiSO_4 \cdot 6\,H_2O$, $ZnSO_4 \cdot 7\,H_2O$, $MnSO_4 \cdot 7\,H_2O$, $Al_2(SO_4)_3 \cdot 16\,H_2O$, $TiCl_4$, $Zr(NO_3)_4$, $(NH_4)_6Mo_7O_{24} \cdot 4\,H_2O$, NH_4VO_3.

Standard and test samples

The radioisotope tungsten-185 was obtained as sodium tungstate from the Radiochemical Centre, Amersham.

Tungstic oxide (99% pure) was used as the standard for neutron irradiation, and sheet aluminium, cut into small pieces, was used for tungsten analysis by neutron irradiation. A sample of high-speed steel B.C.S. No. 241/1 was used for isotope dilution analysis of tungsten.

Irradiation conditions and counting equipment

The standard and test samples were irradiated in the Universities Research Reactor, Risley, Warrington at a neutron flux of about $3.6 \cdot 10^{12}$ n cm^{-2} sec^{-1} for 4 h.

The γ-emission from tungsten-185 and tungsten-187 was counted by means of a Panax scintillation counter and a P7102 scaler. Experiments were designed to give at least 10,000 counts so that the standard deviation did not exceed 1%.

*Preliminary experiments on the extraction of tungsten with toluene-*3,4*-dithiol and the determination of the dithiol equivalent of tungsten*

A radiometric study of the extraction of tungsten(VI) with toluene-3,4-dithiol into chloroform was made. For this a 1.0-ml aliquot of 0.001 *M* tungstate, labelled with tungsten-185, was treated with 1.0 ml of 15% $TiCl_3$, and the resulting solutions were made 1 *M*, 3 *M*, 4 *M*, 5 *M*, 6 *M* and 9 *M* in hydrochloric acid in a total volume of 10.0 ml. Solutions were treated with 0.5 ml of 0.032 *M* dithiol, allowed to stand for about 30 min, and then shaken with 7.0 ml of chloroform for 5 min. The activity of 5.0 ml of the aqueous layer as well as 5.0 ml of the organic layer was measured. Extraction was found to be 99% from an aqueous solution 5–6 *M* in hydrochloric acid but to fall at higher or lower acidity.

For the determination of the dithiol equivalent of tungsten, to 1.0-ml aliquots of 0.01 *M* tungstate, labelled with tungsten-185, were added 1.0 ml of 15% $TiCl_3$ and

5.0 ml of concentrated hydrochloric acid; they were then diluted to 10.0 ml. The resulting solutions were then treated with 0.1, 0.2, 0.4, 0.6, 0.8, 1.0, 1.2, 1.4, 1.6 and 1.8 ml of 0.032 *M* dithiol respectively. Each solution, after 30 min, was shaken with 7.0 ml of chloroform for 5 min, and the activity of 5.0 ml of the organic layer was measured. A plot of the activity against the volume of 0.032 *M* dithiol (Fig. 1) shows the mole ratio of tungsten:dithiol in the tungsten-dithiol complex to be 1:4.

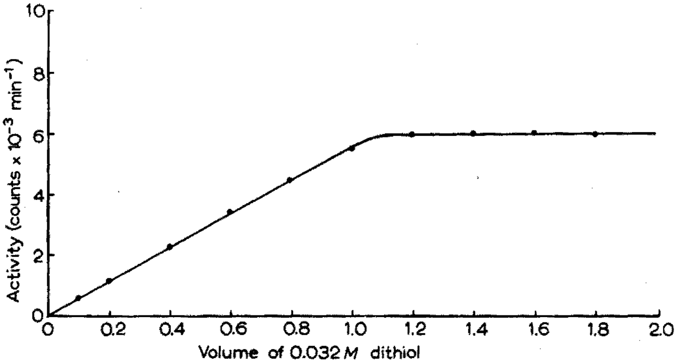

Fig. 1. Determination of the dithiol equivalent of tungsten. Volume of 0.01 *M* WO_4^{2-} used was 1.0 ml.

Preliminary experiments on the reproducibility of substoichiometric extraction of tungsten

Extraction of tungsten from solutions of different concentration with a fixed volume of dithiol reagent into chloroform. A series of 0.01 *M* tungstate solutions (1.0, 1.5, 2.0 and 2.5 ml), labelled with tungsten-185, were treated with 1.0 ml of 15% $TiCl_3$ and 5.0 ml of concentrated hydrochloric acid, and were then diluted to 10.0 ml. To each was added 0.5 ml of 0.032 *M* dithiol reagent. Solutions were then shaken, after 30 min, with 7.0 ml of chloroform for 5 min. The activity of 5.0 ml of the organic layer was measured in each case (Table I).

TABLE I

EXTRACTION OF TUNGSTEN FROM SOLUTIONS OF DIFFERENT CONCENTRATION WITH A FIXED VOLUME OF DITHIOL REAGENT

(0.5 ml of 0.032 *M* dithiol reagent was added in each case)

^{185}W-labelled 0.01 *M* WO_4^{2-} solution (ml)	1.0	1.5	2.0	2.5
Activity of ^{185}W isolated (counts min^{-1})	2841	2847	2850	2853

Extraction of tungsten from a fixed concentration with different substoichiometric amounts of dithiol reagent. Four different 1.0-ml portions of 0.01 *M* tungstate, labelled with tungsten-185, were treated as described immediately above, except that 0.2, 0.4, 0.6 and 0.8 ml of 0.032 *M* dithiol were used. The results are given in Table II.

Extraction of tungsten from solutions of increasing concentration with a fixed volume of dithiol reagent. A series of labelled 0.01 *M* tungstate solutions (0.1–1.0 ml) were treated as before, 0.5 ml of 0.032 *M* dithiol reagent being used. A plot of the activity against the volume of 0.01 *M* tungstate taken is shown in Fig. 2.

TABLE II

EXTRACTION OF TUNGSTEN FROM A FIXED CONCENTRATION WITH DIFFERENT SUBSTOICHIOMETRIC AMOUNTS OF DITHIOL REAGENT

(1.0 ml of ^{185}W-labelled 0.01 *M* tungstate solution was used in each case)

0.032 *M* dithiol reagent added (ml)	0.2	0.4	0.6	0.8
Activity of ^{185}W isolated (counts min^{-1})	1058	2064	3154	4105
Activity corresponding to 0.2 ml of 0.032 *M* dithiol reagent (counts min^{-1})	2106	2064	2102	2052

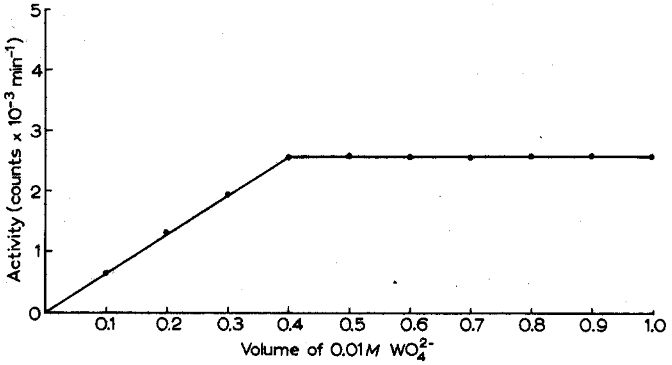

Fig. 2. Reproducibility of extraction of tungsten with dithiol into chloroform.

Interferences of other ions in the substoichiometric extraction of tungsten with dithiol

The effect of various cations on the substoichiometric extraction of tungsten was examined. To a series of 1.0-ml portions of 0.01 *M* tungstate solution, labelled with tungsten-185, 0.5 ml of a 0.02 *M* solution of Fe^{3+}, Cu^{2+}, Co^{2+}, Ni^{2+}, Cr^{3+}, Al^{3+}, Mn^{2+}, Zn^{2+}, Ti^{4+}, Zr^{4+}, V^{5+} or Mo^{6+} was added, followed by 1.0 ml of 15% $TiCl_3$ and 5.0 ml of concentrated hydrochloric acid. Solutions, after dilution to 10.0 ml, were treated with 0.5 ml of dithiol reagent and extracted as above. The activity of 5.0 ml of the organic layer was measured in each case and compared with the activity of an equal volume of the organic extract without interfering ions. A similar extraction was done in the presence of an equal volume of 0.01 *M* molybdate solution, labelled with molybdenum-99. Except for copper, titanium and zirconium, none of the metals interfered; titanium and zirconium formed precipitates (Table III). ^{99}Mo-labelled molybdate interfered, and the excess of activity over that from tungsten-185 decayed rapidly. In a separate experiment 1.0 ml of 0.01 *M* molybdate, labelled with molybdenum-99 was extracted in exactly the same way with dithiol and chloroform. The decay of the activity in an aliquot of the organic extract was followed and the half-life was found to be 6 h, the half-life of technetium-99m.

Preliminary experiments on isotope dilution analysis

To five different solutions, each containing 1.0 ml of 0.01 *M* tungstate, labelled with tungsten-185, were added, respectively, 0.0, 0.5, 1.0, 1.5 and 2.0 ml of inactive 0.01 *M* tungstate solution followed by 1.0 ml of 15% $TiCl_3$ and 5.0 ml of concentrated hydrochloric acid. Solutions were diluted to 10 ml and were extracted as before with

TABLE III

EFFECT OF OTHER IONS IN THE SUBSTOICHIOMETRIC EXTRACTION OF TUNGSTEN WITH DITHIOL (M/W = 1 : 1)

Interfering element	*Activity isolated in absence of diverse ions (counts min^{-1})*	*Activity isolated in presence of diverse ions (counts min^{-1})*	*% Interference*[a]
Fe(III)	2278	2251	—
Cu(II)	2278	1319	42
Co(II)	2278	2330	—
Ni(II)	2278	2313	—
Mn(II)	2278	2330	—
Zn(II)	2278	2307	—
Al(III)	2278	2257	—
Cr(III)	1835	1858	—
Ti(IV)	1835	872	52
Zr(IV)	1835	965	47
V(V)	1835	1799	—
Mo(VI)	1835	1865	—
Mo(VI)[b]	1719	3357	95

[a] The absence of a figure in the 4th column indicates that the two activities were within the range of statistical error.
[b] Molybdate, labelled with molybdenum-99.

TABLE IV

EFFECT OF ISOTOPIC DILUTION ON THE SUBSTOICHIOMETRIC EXTRACTION OF TUNGSTEN

(1.0 ml of ^{185}W-labelled 0.01 *M* tungstate solution was taken, and 0.8 ml of 0.032 *M* dithiol reagent was added in each case)

0.01 *M* inactive WO_4^{2-} solution added (ml)	0.0	0.5	1.0	1.5	2.0
Activity of ^{185}W isolated (counts min^{-1})	3590	2365	1829	1446	1223
Activity expected after dilution (counts min^{-1})	—	2393	1795	1436	1196

0.8 ml of the dithiol reagent. The activity of 5.0 ml of the organic layer was measured in each case (Table IV).

The substoichiometric determination of tungsten in high-speed steel by isotope dilution analysis

Accurately weighed steel samples were dissolved by heating in 8 *M* hydrochloric acid with 2–3 drops of concentrated nitric acid. To the cold solutions 2–3 drops of hydrofluoric acid were added to keep tungsten in solution. The resulting solutions were fumed off with 2.0 ml of 50% sulphuric acid. To each solution was then added 1.0 ml of 0.01 *M* tungstate solution, labelled with tungsten-185, followed by 1.0 ml of 15% $TiCl_3$. Solutions, after making 6 *M* in hydrochloric acid, were treated with 0.8 ml of 0.032 *M* dithiol reagent and were extracted as before. The activity (a) of 5.0 ml of the organic layer was measured in each case.

A standard 0.01 *M* ^{185}W-labelled tungstate solution (1.0 ml) was treated in exactly the same way and the activity (a_s) of 5.0 ml of the organic layer was measured. The amount of tungsten in each sample was calculated from the relation $Y = Y_s (a_s/a - 1)$, where Y and Y_s are the amounts of tungsten in the unknown and the standard. The results are given in Table V.

TABLE V

SUBSTOICHIOMETRIC ISOTOPE DILUTION ANALYSIS OF TUNGSTEN IN HIGH-SPEED STEEL

Sample	*Weight of sample (mg)*	*Activity from sample*[a] *(counts min*$^{-1}$*)*	*Activity from standard*[a] *(counts min*$^{-1}$*)*	*Amount of tungsten in the standard (mg)*	*W found (%)*	*Range of certified analysis (%)*
B.C.S.[b] No. 241/1	6.0	1818	2974	1.839	19.5	
	10.5	1402	2974	1.839	19.7	19.50–19.69
	14.6	1160	2974	1.839	19.6	

[a] The activity expressed is the average of three different counts on the sample, corrected for background.
[b] This high-speed steel alloy contains W 19.61%, Cr 5.03%, V 1.57%, Mo 0.52%, Co 5.67%, C 0.85%, Si 0.33%, S 0.033%, P 0.021%, Mn 0.30%, Sn 0.025%.

TABLE VI

SUBSTOICHIOMETRIC DETERMINATION OF TUNGSTEN IN ALUMINIUM BY NEUTRON ACTIVATION ANALYSIS

Weight of sample (mg)	*Activity from sample (counts min*$^{-1}$*)*	*Activity from standard (counts min*$^{-1}$*)*	*Amount of tungsten in standard (ng)*	*Tungsten found* ($\cdot 10^{-4}$%)
67.0	3711	3868	71.44	1.02
74.4	4676	3868	71.44	1.16
86.8	4502	3868	71.44	0.96
93.3	2468	1804	71.44	1.05
86.6	2104	1804	71.44	0.96

The substoichiometric determination of tungsten in aluminium by neutron activation analysis

An accurately weighed amount (9.1 mg) of irradiated tungstic oxide was dissolved in 10 ml of 5 *M* sodium hydroxide and the solution was diluted to 1 l. A 1.0-ml aliquot of this solution was further diluted to 100.0 ml for use as a standard solution.

Different weighed samples of aluminium irradiated under the same conditions were dissolved in 3–4 ml of 50% hydrochloric acid. Each solution was then added to a mixture of 1.0 ml of 0.01 *M* inactive tungstate and 1.0 ml 15% $TiCl_3$. The resulting solutions were made 6 *M* in hydrochloric acid, and were treated with 0.8 ml of 0.032 *M* dithiol reagent. Solutions were extracted after 30 min, with 7.0 ml of chloroform for 5 min. The activity (a) of 5.0 ml of the organic layer, due to tungsten-187, was measured in each case.

To 1.0 ml of 0.01 M inactive tungstate, 1.0 ml of standard active solution of tungsten was added followed by 1.0 ml of 15% $TiCl_3$. The solution was made 6 M in hydrochloric acid, and was extracted in exactly the same way with 0.8 ml of dithiol reagent. The activity (a_s) of 5.0 ml of the organic layer was measured. The amount of tungsten in aluminium was calculated from the relation $Y = Y_s \cdot a/a_s$, where Y and Y_s are the amounts of tungsten in the unknown and the standard. The results are given in Table VI.

The decay of the activity from the sample was followed and the half-life was found to be 24 h. The γ-energy, after calibration from ^{137}Cs and ^{60}Co, was found to be 0.688 MeV and 0.48 MeV; the values in the literature for ^{187}W are 0.686 MeV and 0.47 MeV.

DISCUSSION

When tungsten(VI) is reduced with titanium(III) chloride, it will form a blue-green complex with toluene-3,4-dithiol which can be extracted into chloroform. In adapting the complex for the isotope dilution analysis of tungsten with tungsten-181, McClendon and deVoe[21] used hot titanium(III) sulphate as reducing agent and allowed a cooling time of 90 min before any extraction was done. A reinvestigation of the use of dithiol with tungsten-185 appeared promising, with high percentage extraction (99%) and also with good reproducibility of substoichiometric separation. A 15% titanium(III) chloride solution was used as reducing agent and the time allowed was 30 min to ensure formation of the complex; no extra cooling time was necessary. Copper, titanium and zirconium interfered; the last two gave precipitates. Interference by molybdenum-99 was traced to the extraction by dithiol of ^{99m}Tc from the equilibrium mixture ^{99}Mo–^{99m}Tc. Tungsten in high-speed steel was determined by isotope dilution. Neutron activation analysis of tungsten in sheet aluminium was also attempted. The half-life and the γ-energies of the species extracted indicated that it was tungsten-187. An irradiation time of 4 h at a neutron flux of $3.6 \cdot 10^{12}$ n cm^{-2} sec^{-1} gave a precision of $\pm 10\%$ at the 0.1-p.p.m. level.

We thank the Manager and Staff of the Universities Research Reactor, Risley, Warrington for carrying out the irradiations and for helpful advice on the preparation of samples for irradiation.

SUMMARY

Extraction into chloroform with substoichiometric amounts of toluene-3,4-dithiol has been studied for the determination of tungsten. The effect of interfering metal ions has been investigated. Based on this, tungsten in high-speed steel has been determined by isotope dilution and in aluminium by neutron activation.

RÉSUMÉ

On propose un dosage du tungstène par extraction dans le chloroforme, contenant des quantités substoechiométriques de toluènedithiol-3.4. On examine l'influence de métaux étrangèrs. On décrit le dosage du tungstène dans l'acier rapide, par dilution isotopique et dans l'aluminium par activation neutronique.

ZUSAMMENFASSUNG

Für die Bestimmung von Wolfram wurde die Extraktion mit unterstöchiometrischen Mengen Toluol-3,4-dithiol in Chloroform erprobt. Der Einfluss störender Metallionen wurde untersucht. Hierauf gründete sich die Bestimmung von Wolfram in Schnelldrehstahl durch Isotopenverdünnung und in Aluminium durch Neutronenaktivierung.

REFERENCES

1 W. A. Brooksbank, W. G. Leddicotte and S. A. Reynolds, *Anal. Chem.*, 28 (1956) 1033.
2 G. H. Morrison and J. F. Cosgrove, *Anal. Chem.*, 27 (1955) 810.
3 R. E. Jervis and W. D. Mackintosh, *Proc. U.N. Int. Conf. Peaceful Uses At. Energy, 2nd, 1958*, 28 (1959) 470.
4 J. Boganes, P. Quittner and E. Sazlo, *At. Energy Aust.*, 24 (1968) 421.
5 M. Okada, *Tokyo Kogyo Shikensho Hokoku*, 61 (1966) 7.
6 H. Hamaguchi, R. Kuroda, T. Shimizu, R. Sugisita, I. Tsukahara and R. Yamamoto, *At Energy Soc. Japan*, 3 (1961) 800; *Nucl. Sci. Abstr.*, 16 (1962) 1712.
7 D. H. F. Atkins and A. A. Smales, *Anal. Chim. Acta*, 22 (1960) 462.
8 D. F. C. Morris and A. Olya, *Talanta*, 4 (1960) 194.
9 R. Fukai and W. W. Meinke, *Limmol. Oceanog.*, 7 (1962) 186.
10 G. W. Leddicotte, W. T. Mullins, L. C. Bate, J. F. Emery, R. E. Druschel and W. A. Brooksbank, *Proc. U.N. Int. Conf. Peaceful Uses At. Energy, 2nd, 1958*, 28 (1959) 478.
11 M. Okada, *Nature*, 196 (1962) 1088.
12 J. Hoste, *Pure Appl. Chem.*, 99 (1960).
13 G. Leliaert, J. Hoste and Z. Eeckhaut, *Rec. Trav. Chim.*, 79 (1960) 557.
14 J. A. James and D. H. Richards, *J. Electron. Control*, 3 (1957) 500.
15 A. I. Kalinin, R. A. Kuznetsov, V. V. Moiseev and A. A. Murin, *Dokl. Akad. Nauk SSSR*, 141 (1961) 98.
16 G. Leliaert, J. Hoste and J. Eeckhaut, *Talanta*, 2 (1959) 115.
17 A. Barwinsk, A. Buczek, L. Gorski, J. Janczyszyn, S. Kwiecinski, L. Loska and M. Geisler, *Isotopenpraxis*, 4 (1968) 15.
18 H. J. M. Bowen, *Biochem. J.*, 77 (1960) 79.
19 A. A. Abdullaev, A. Sh. Zakhidov and P. Kh. Nishanov, *Izv. Akad. Nauk Uz. SSR, Ser. Fiz.-Mat. Nauk*, 12 (1968) 60.
20 M. Neuburger and A. Fourcy, *J. Radioanal. Chem.*, 1 (1969) 225.
21 L. T. McClendon and J. R. DeVoe, *Anal. Chem.*, 41 (1969) 1454.
22 E. W. Hobart and E. P. Hurley, *Anal. Chim. Acta*, 27 (1962) 142.

Anal. Chim. Acta, 53 (1971) 87–94

Analytica Chimica Acta
Elsevier Publishing Company, Amsterdam
Printed in The Netherlands

DETERMINATION OF LEAD IN GASOLINE BY ATOMIC ABSORPTION SPECTROSCOPY

MASAYUKI KASHIKI, SEIGO YAMAZOE AND SHOZO OSHIMA
Maruzen Oil Co., Ltd., Research & Development Center, P.O. Box 1, Satte, Saitama 340-01 (Japan)

(Received July 20th, 1970)

The determination of lead in gasoline by atomic absorption spectroscopy was first described by Robinson[1]. The sample was diluted with iso-octane before being sprayed into the flame, and the absorbance was compared with the absorbance given by standards containing known amounts of tetraethyllead in iso-octane. Dagnall and West[2], using different equipment, preferred methyl ethyl ketone as the sample diluent, and found that standards prepared with lead nitrate or 8-hydroxyquinolinate were less satisfactory than those containing tetraethyllead. Trent[3] also investigated this analysis and obtained a precision of about 1% for the determination of either tetraethyl- or tetramethyllead in gasoline, with iso-octane as sample diluent. Mostyn and Cunningham[4] determined lead in gasoline by means of atomic absorption with a premix burner and iso-octane as a diluent. However, difficulties are encountered with all these methods, because different alkyllead compounds yield different responses.

The work described here includes the results of comparative tests made on tetraethyllead (TEL), tetramethyllead (TML) and mixed alkyllead compounds (MLA 250, MLA 500 and MLA 750) in gasolines. In the proposed method, iodine is added to the gasoline solution in methyl isobutyl ketone before its aspiration into an air–acetylene flame. By this means, lead can be determined in any of the alkyllead mixtures after calibration of the procedure against a single alkyllead standard. The effects of different additions of iodine and of various organic solvents are discussed.

EXPERIMENTAL

Instrumentation

The instrument used was a Perkin-Elmer Model 303 atomic absorption spectrophotometer. The source was a Perkin–Elmer neon-filled lead lamp, operated at 8 mA. The 283.3-nm resonance line was used, with a spectral slit width of 1.0 mm. An automatic null recorder readout was used with scale expansion and noise suppression. A burner with a 10-cm long slot was used. The detailed examination was carried out with an acetylene–air flame under the conditions listed in Table I.

Standard preparation

The following solutions were used; all lead compounds were supplied by the Ethyl Corporation.

1. 0.788 g of lead as tetraethyllead (TEL) per l of gasoline;

2. 0.715 g of lead as tetramethyllead (TML) per l of gasoline;
3. 0.819 g of lead as mixed alkyllead (MLA 250) per l of gasoline;
4. 0.841 g of lead as mixed alkyllead (MLA 500) per l of gasoline;
5. 0.755 g of lead as mixed alkyllead (MLA 750) per l of gasoline.

The lead stock solutions were standardized by the polarographic method[5].

Methyl isobutyl ketone (MIBK) and iodine were Wako chemical certified reagents.

TABLE I

OPERATING CONDITIONS FOR LEAD

Wavelength (nm)	283.3	Response time (sec)	1
Lamp current (mA)	8	Noise suppression	1
Air flow (l min^{-1})	23.8	Scale expansion	1
Acetylene flow (l min^{-1})	3.3	Slit width (mm)	1.0
Burner height (mm)	8.0 (0 division)		

Differences in TEL, TML, MLA 250, MLA 500 and MLA 750 gasoline

Early in the investigation of the feasibility of the determination of lead in gasoline, various gasoline samples were run against TEL standards. Although accurate values for lead content were obtained for most samples, very high values appeared in some cases. It was found that these samples contained TML as well as TEL, and an investigation of the differences between the five additives was therefore undertaken. The addition of iodine (above 3 mg I_2 per 50 ml MIBK) was found to have a remarkable effect on the results obtained for different lead compounds, each alkyllead compound showed the same absorbance for the same amount of lead (see Fig. 1).

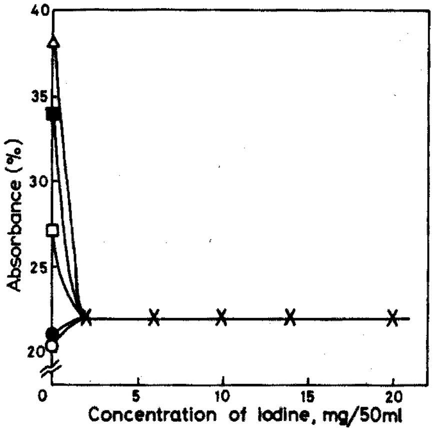

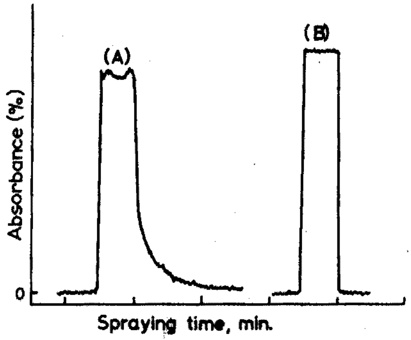

Fig. 1. Effect of iodine addition on absorption. All solutions contained 9 mg Pb l^{-1}. (○) TEL, (●) TML, (□) MLA 250, (■) MLA 500, (△) MLA 750, (×) TEL, TML, MLA 250–750.

Fig. 2. The "memory" effect. Recorder traces of lead in gasoline (as TEL). The solution contains 9.5 mg Pb l^{-1}. (A) No addition, (B) I_2 addition.

Each mixture of lead in gasoline (TEL, TML, MLA 250, MLA 500 and MLA 750) was diluted 1:50 with MIBK and burned.

TABLE II

INFLUENCE OF SOLVENTS ON RESULTS FOR ALKYLLEAD COMPOUNDS

(Results are given as % absorbance. Columns A show the results obtained with no addition of iodine. Columns B show the results with an addition of 3 mg of iodine per 50 ml. In all cases, the solutions contained 9 mg Pb l^{-1})

Solvent	*TEL*		*TML*		*MLA* 250		*MLA* 500		*MLA* 750	
	A	*B*	*A*	*B*	*A*	*B*	*A*	*B*	*A*	*B*
MEK	19.0	21.5	38.0	21.5	20.0	21.5	26.5	21.5	33.0	21.5
MIBK	20.5	22.0	38.3	22.0	21.0	22.0	27.0	22.0	34.0	22.0
Iso-octane	12.5	15.5	27.5	15.0	16.0	15.0	23.5	15.0	25.0	15.3
Toluene	14.0	15.5	27.0	16.0	16.0	16.0	19.5	16.0	22.0	16.0
Cyclohexane	19.0	13.5	24.0	13.0	22.0	13.0	23.0	13.0	23.5	13.0

Memory effect

The normal operating conditions for the determination of lead by atomic absorption are far too sensitive for undiluted gasoline samples to be used and dilution with an organic solvent is necessary to reduce the lead content of the test solution. In this case, a very distinctive "memory" effect was obtained when solutions of TEL, TML, MLA 250, MLA 500 and MLA 750 were analyzed. Dagnall and West[2] reported a slow rise to a maximum reading and showed that a long washing-out period with pure solvent was necessary between samples; Trent[3] reported that TEL standards required about 30 sec to reach a maximum reading, whereas TML standards reached almost instant equilibrium. In the present work, the same phenomena were found with TEL, TML, MLA 250, MLA 500 and MLA 750, but the addition of iodine removed the inconvenience.

The memory effect is illustrated in Fig. 2. Recorder trace A is from a gasoline containing 0.01 g Pb l^{-1} (TEL), diluted with MIBK. After spraying for 30 sec, no clear absorption plateau was reached; trace B, where iodine was added, shows no "memory" effect, the absorption reading leveling off after 1–2 sec and returning rapidly to zero when spraying was discontinued.

Effect of various organic solvents and iodine addition

To investigate the effect of various solvents on the relative sensitivities of the determinations of TEL, TML, MLA 250, MLA 500 and MLA 750, the burner with the 10-cm slot, supplied as standard equipment with the Model 303 spectrophotometer, was used. In each case, 1:50 dilutions of the gasoline with the particular solvent were prepared. Table II shows the relative sensitivities of TEL, TML, MLA 250, MLA 500 and MLA 750 in five different solvents. When iodine was added, methyl ethyl ketone (MEK) and MIBK produced similar sensitivities for all five lead compounds, and so were investigated further.

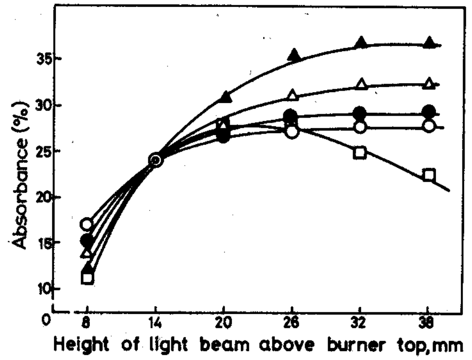

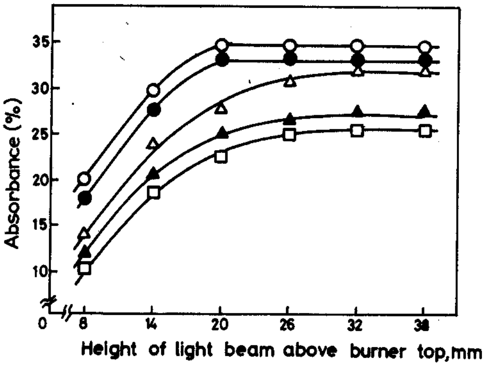

Fig. 3. Effect of variation of acetylene–air mixture and height of absorption path in the flame on the sensitivity for TEL. The air flow was constant at 23.8 l min^{-1} and the acetylene flow was varied as shown. Pb concentration 5 mg l^{-1}. Acetylene flow: (○) 2.2 l min^{-1}, (●) 2.5 l min^{-1}, (△) 3.3 l min^{-1}, (▲) 4.2 l min^{-1}, (□) 4.6 l min^{-1}.

Fig. 4. Effect of variation of acetylene–air mixture and height of absorption path in the flame on the sensitivity for TEL. The acetylene flow and air flow were varied as shown. Pb concentration 5 mg l^{-1}. (○) Acetylene flow 2.2 l min^{-1}, air flow 18.5 l min^{-1}; (●) acetylene flow 2.5 l min^{-1}, air flow 21.0 l min^{-1}; (△) acetylene flow 3.3 l min^{-1}, air flow 23.8 l min^{-1}; (▲) acetylene flow 4.2 l min^{-1}, air flow 26.2 l min^{-1}; (□) acetylene flow 4.6 l min^{-1}, air flow 29.0 l min^{-1}.

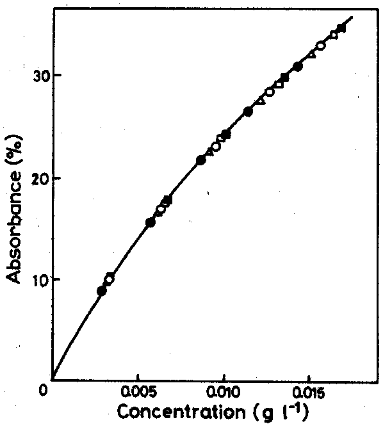

Fig. 5. Calibration curve. (○) TEL, (●) TML, (□) MLA 250, (■) MLA 500, (△) MLA 750.

Burner height and gas flow conditions

Six different burner settings were used, corresponding to heights of the center of the light beam above the burner top of 8, 14, 20, 26, 32 and 38 mm. Moving the burner so that the light center was below 8 mm resulted in blockage of the light beam. Plots of absorbance *vs.* concentration for these six positions are shown in Figs. 3 and 4 for different acetylene and air flow rates. On the basis of these results, the acetylene flow was selected as 3.3 l min^{-1} with an air flow of 23.8 l min^{-1}; stable flames and good sensitivity were found under these conditions. The optimal burner height was found to be 80 mm.

Calibration curve

The calibration curve shown in Fig. 5 was obtained by the iodine addition procedure, for standard TEL, TML, MLA 250, MLA 500 and MLA 750 solutions. The relationship between absorbance and concentration is sufficiently linear, and it is clear that all the alkyllead compounds tested give the same response.

RESULTS AND DISCUSSION

The results of a precision test are given in Table III; five independent dilutions and analyses were made for each single sample of gasoline.

TABLE III

DETERMINATION OF LEAD IN GASOLINE

(5 determinations were made on each sample)

Sample no.	*Sample concentration* ($g\,l^{-1}$)	*Average concentration found* ($g\,l^{-1}$)	*Relative error* (%)
1	0.157	0.154	1.91
2	0.310	0.306	1.29
3	0.470	0.467	0.64
4	0.630	0.632	0.32
5	0.790	0.788	0.25

The atomic absorption method, calibrated with polarographically analysed gasolines, is accurate and precise over the range 0.790–0.157 g Pb l^{-1}. Only 1 ml of sample, diluted to 50 ml with MIBK, is required and the average analysis time per sample is about 15 min, allowing triplicate readings on samples and reference standards. It should be emphasized, perhaps, that the lead content is measured, assuming gasoline standards of similar chemical composition, although considerable variation in the sulphur, phosphorus and nitrogen contents of the gasolines is permissible.

When bromine was added to the gasoline solutions instead of iodine, the different alkyllead compounds again showed the same absorbances (Table IV).

TABLE IV

COMPARISON OF IODINE WITH BROMINE AS ADDITIVE

(Results are given as % absorbance. All solutions contained 16 mg Pb l^{-1})

	No addition	*I_2 addition*	*Br_2 addition*
TEL	31.5	33.5	33.7
TML	54.0	33.8	34.0
MLA 250	32.0	33.5	33.5
MLA 500	40.0	33.5	34.0
MLA 750	48.0	33.5	33.5

Accordingly, addition of bromine is also possible in this analytical method. Applications of the method to other organometallic compounds should also be possible.

The authors wish to thank Mr. T. Kozuma and Dr. T. Amemiya for their encouragement throughout the work, and Dr. H. Hasegawa for his kind guidance.

SUMMARY

The rapid and accurate determination of lead in gasolines by atomic absorption spectroscopy is possible with a premix air–acetylene burner. Tetramethyllead, tetraethyllead and mixed alkyllead compounds can be determined by calibration of the method against a single standard alkyllead compound, if 3 mg of iodine is added to the 1-ml gasoline sample which is then diluted to 50 ml with MIBK before aspiration. The method is remarkably free from interference by other trace elements present, and is suitable for determination of 0.16–0.8 g Pb l^{-1} in gasoline.

RÉSUMÉ

Le dosage rapide et précis du plomb dans les essences, par spectroscopie d'absorption atomique est possible, à l'aide d'un bruleur "premix" air–acétylène. Le plomb-tétraméthyle, le plomb-tétraéthyle et des mélanges plomb-alcoyles peuvent être dosés par calibrage à l'aide d'un seul standard plomb-alcoyle, en ajoutant 3 mg d'iode à des échantillons de 1 ml d'essence, dilués ensuite à 50 ml avec MIBK, avant aspiration. Cette méthode est exempte d'intérférences et permet le dosage de 0.15 à 0.8 g Pb l^{-1} dans l'essence.

ZUSAMMENFASSUNG

Eine schnelle und sichere Bestimmung von Blei in Benzin durch Atomabsorptionsspektrometrie ist mittels einer vorgemischten Luft–Acetylen-Flamme möglich. Tetramethylblei, Tetraäthylblei und gemischte Alkylbleiverbindungen können durch Eichung der Methode mit einer einzigen Standard-Alkylbleiverbindung bestimmt werden, wenn 3 mg Jod zu der 1 ml-Benzinprobe hinzugefügt werden und diese dann vor der Zerstäubung mit MIBK auf 50 ml verdünnt wird. Die Methode wird durch andere Spurenelemente nicht gestört und eignet sich für die Bestimmung von 0.16–0.8 g Pb l^{-1} in Benzin.

REFERENCES

1 J. W. ROBINSON, *Anal. Chim. Acta*, 24 (1961) 451.
2 R. M. DAGNALL AND T. S. WEST, *Talanta*, 11 (1964) 1553.
3 D. J. TRENT, *Perkin-Elmer At. Abs. Newsletter*, 4 (9) (1965) 348.
4 R. A. MOSTYN AND A. F. CUNNINGHAM, *J. Inst. Petrol.*, 53 (1967) 101.
5 THE AMERICAN SOCIETY FOR TESTING AND MATERIALS, *D 1269-61*.

Analytica Chimica Acta
Elsevier Publishing Company, Amsterdam
Printed in The Netherlands

THE DETERMINATION OF RUTHENIUM BY ATOMIC ABSORPTION SPECTROPHOTOMETRY*

B. MONTFORD AND S. C. CRIBBS

Whiteshell Nuclear Research Establishment, Atomic Energy of Canada, Ltd., Pinawa, Manitoba (Canada)

(Received June 20th, 1970)

Certain ruthenium complexes catalyze hydrogen–deuterium exchange[1,2], which is being investigated in these laboratories in a search for a more economical way of producing heavy water. To assist this program, a suitable procedure for the analysis of the catalysts was required.

Ruthenium can be determined gravimetrically or colorimetrically[3], but little information is available on the atomic absorption spectrophotometry of ruthenium, which would offer a simpler technique. Allan[4] published detection limits for ruthenium, along with twenty-seven other elements, and Scarborough[5] has recently given details of the determination of fission-product ruthenium in uranium alloys. In the work described here, the atomic absorption behavior of ruthenium was found to be as complex as its solution chemistry. All of the forty ions examined interfered; the nitrous oxide–acetylene flame gave little improvement as regards interferences and generally provided lower sensitivity. Acid strength and oxidation state also affected the results. Attempts were made to correlate oxidation state with atomic absorption, by measuring the molecular spectra in solution concurrently with atomic absorption. As yet, no positive correlation has been possible, owing to the complexity of the molecular spectra.

While the volatility of ruthenium tetroxide permits simple and effective separation of ruthenium from complex mixtures, the separation is time-consuming, and a more direct approach would be advantageous. Scarborough[5] found that the inter-element effects of rhodium, palladium and molybdenum on the atomic absorption of ruthenium were eliminated by the presence of excess of uranium in the samples. Peterson and Smith[6] made similar observations.

Besides uranium, the following species were studied for suppression of interference: excess of lanthanum and strontium[7,8], which are effective for alkali earth metals, and hydroxylamine hydrochloride, the reducing agent in the distillation procedure. The effects of perchloric acid, sodium sulphite and sodium nitrate were also examined because of their enhancement of the atomic absorption of ruthenium. Of these, only uranium eliminated interferences, with the exception of that produced by titanium.

This paper describes the two procedures which were finally adopted: (*a*) the use of excess of uranium when titanium is absent; and (*b*) distillation of ruthenium tetroxide from perchloric acid–sulphuric acid mixtures into hydrochloric acid–hydroxylamine hydrochloride solution.

---

* This paper was presented at the 16th Spectroscopy Symposium of Canada, Montreal, October, 1969.

EXPERIMENTAL

Apparatus

A Techtron AA-4 atomic absorption spectrophotometer with both digital and chart recorder readouts was used. A cooled demountable shielded hollow-cathode lamp was used as the resonance source. The cathode was made by sintering spectrographically pure ruthenium powder in a graphite electrode. Details of the lamp, manufacture of cathodes and the vacuum control system have been given elsewhere[9]. Optimum operating conditions are given in Table I.

Schematic diagrams, specifications and operating procedures for the distillation apparatus have been published[10,11].

TABLE I

OPTIMUM OPERATING CONDITIONS OF RESONANCE SOURCE AND ATOMIC ABSORPTION SPECTROPHOTOMETER

Filler gas for lamp	Neon (5–6 mm Hg)
Current	30 mA (285 Hz)
Spectral line	349.89 nm
Slit-width	50 μm (bandpass, 0.17 nm)
Flame	Air–acetylene, slightly reducing
Burner	Techtron AB-41, 10 cm

Chemicals

All chemicals used were of reagent grade; demineralized distilled water was used throughout.

Ruthenium stock solution (60 mg Ru ml^{-1}) was prepared from ruthenium trichloride hydrate ($RuCl_3 \cdot x\ H_2O$) by dissolution in 3 *M* hydrochloric acid. The solution was standardized by a method similar to that used by Banks and O'Laughlin[10], aliquots being evaporated to dryness, reduced in hydrogen at 600° and weighed as metal. Triplicate analyses agreed within 10 μg on a mass of 10 mg. The stock solution was diluted as required. The atomic absorption results for diluted solutions made from 1-day old stock solutions were very variable, but consistent results were obtained after the stock solution had been stored for 2 days or more. Diluted solutions were prepared immediately before use.

A bulk 20% (w/v) uranium solution was prepared by dissolving 42 g of uranyl nitrate hexahydrate in 100 ml of water.

Procedures

Direct measurement when titanium is absent. Prepare standard and sample solutions of ruthenium in the concentration range 0–100 μg ml^{-1}, and add uranium solution to give 4% (w/v) uranium in the final solution. Compare the absorbances of standards and samples under the conditions given in Table I.

Prior distillation of ruthenium tetroxide when titanium is present. To the sample (containing 0–3.5 mg Ru) in the distillation flask, add 20 ml of concentrated sulphuric acid and 2 ml of concentrated perchloric acid. Place 15 ml of 10% (w/v) hydroxylamine hydrochloride in 3 *M* hydrochloric acid solution (receiving liquor) in the receiving flask, cool in ice, and connect the air carrier gas to the distillation flask. Regulate the gas flow to about 2 bubbles per sec. Then heat the flask and contents slowly to boiling and continue heating for 30 min. During this period ruthenium tetroxide is formed and distilled into the receiving solution. Warm the distillate until the colour changes from brown to colourless and make the volume up to 25 ml with the receiving liquor.

Prepare standards similarly and measure the absorbances. These standards are stable for a month.

Calibration and sensitivity

The procedures were calibrated in the concentration range 0–140 μg of ruthenium per ml. The calibration curves given in Fig. 1 were obtained for ruthenium in the presence of 4% uranium (as nitrate), or 10% hydroxylamine hydrochloride in 3 *M* hydrochloric acid, or 3 *M* hydrochloric acid. The final curve was included for comparison purposes to show that both the uranium and hydroxylamine hydrochloride solutions enhanced the atomic absorbance of ruthenium.

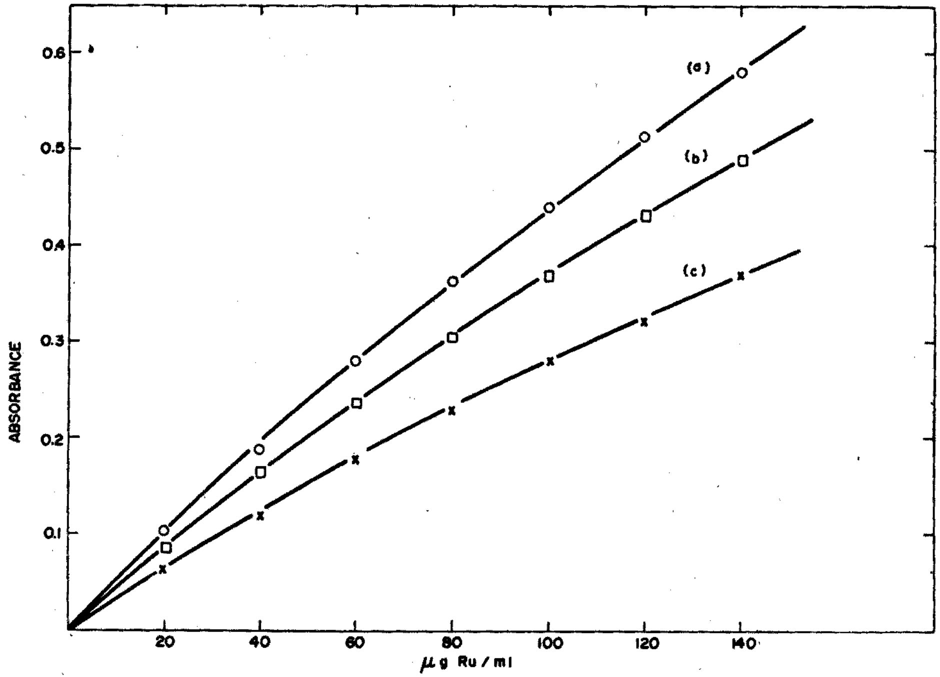

Fig. 1. Calibration curves for ruthenium with (a) 4% U, (b) 10% $NH_2OH \cdot HCl$ in 3 *M* HCl, (c) 3 *M* HCl.

The sensitivities for the three types of solution were 0.88, 1.0, and 1.4, all expressed as μg ml^{-1} for 1% absorbance.

RESULTS AND DISCUSSION

Interferences

Forty ions were examined for their effects on the atomic absorption of ruthenium standards containing 60 μg Ru ml^{-1}, in both air- and nitrous oxide-

TABLE II

ABSORBANCE OF RUTHENIUM IN THE PRESENCE OF VARIOUS ANIONS
(60 μg Ru ml^{-1}; 200 μg anion ml^{-1})

Salt added	*Air–acetylene*		*Nitrous oxide–acetylene*	
	$RuCl_3$ in H_2O	*$RuCl_3$ in 3 M HCl*	*$RuCl_3$ in H_2O*	*$RuCl_3$ in 3 M HCl*
None	0.140	0.179	0.061	0.067
NaCl	0.135	0.179	0.064	0.079
Na_2SO_4	0.208	0.228	0.081	0.094
$NaNO_3$	0.204[a]	0.241[a]	0.088	0.088
$NaNO_2$	0.206	0.217	0.081	0.086
NaH_2PO_4	0.164	0.186	0.059	0.062
$NaBrO_3$	0.007	0.048	0.005	0.033
Na_2SiO_3	0.075	0.155	0.054	0.061
Na_2MoO_4	0.053	0.166	0.034	0.058
Na_2SO_3	0.212	0.250	0.095	0.086
Na citrate	0.001	0.009	0.016	0.017
Na tartrate	0.001	0.015	0.025	0.025
Na oxalate	0.001	0.108	0.019	0.038
NaF	0.093	0.221	0.049	0.059
KBr	0.078	0.108	0.038	0.038
KI	0.049	0.072	0.035	0.028
$KSbO_2$	0.120	0.239	0.051	0.069
$KClO_4$	0.200	0.230	0.085	0.090

[a] Nitric acid at the 200 μg ml^{-1} level had virtually no effect on the ruthenium absorbance.

supported acetylene flames. The anions were added as their sodium or potassium salts, and the cations as chlorides, nitrates or sulphates. These effects are shown in Tables II and III.

All the ions examined affected the atomic absorbance of ruthenium in both types of flames. However, with the exception of EDTA, no spectral interferences were observed at the 349.89-nm wavelength. Presumably organic moieties from EDTA produced in the flame caused its interference. Banks and O'Laughlin[10] observed that ruthenium(III) and (IV), the common oxidation states in acid solution, form very slowly dissociated complexes with many anions. The present observations show that complex chemical interactions between ruthenium and both anions and cations also exist in flames. These interactions affect the atom population and so the subsequent atomic absorption measurement.

Effects of acid strength

The effects of the concentration of hydrochloric or nitric acid on the absorbance of ruthenium standards (60 μg ml^{-1}) were examined. These are given in Table IV.

The increase in absorbance produced by 3 *M* hydrochloric acid was possibly caused by the acid depolymerizing some ruthenium species[12]. No increase was observed with nitric acid. This may be due to the oxidizing nature of the acid affecting the subsequent formation of atoms in the flame.

TABLE III

ABSORBANCES OF RUTHENIUM IN THE PRESENCE OF VARIOUS CATIONS
(60 μg Ru ml^{-1}; 200 μg cation ml^{-1})

Salt added	*Air–acetylene*		*Nitrous oxide–acetylene*	
	$RuCl_3$ in H_2O	*$RuCl_3$ in 3 M HCl*	*$RuCl_3$ in H_2O*	*$RuCl_3$ in 3 M HCl*
None	0.140	0.179	0.061	0.067
$LiNO_3$	0.185	0.234	0.071	0.093
NaCl	0.140	0.179	0.061	0.067
KCl	0.139	0.195	0.055	0.072
RbCl	0.157	0.214	0.055	0.064
CsCl	0.161	0.218	0.057	0.068
$MgSO_4$	0.161	0.165	0.073	0.080
$Sr(NO_3)_2$	0.166	0.242	0.060	0.092
$BaCl_2$	0.161	0.222	0.064	0.083
$CoCl_2$	0.140	0.185	0.050	0.065
$MnCl_2$	0.164	0.216	0.057	0.081
$NiCl_2$	0.091	0.146	0.040	0.047
$Cr(NO_3)_3$	0.092	0.135	0.053	0.056
$FeSO_4$	0.052	0.058	0.038	0.046
$CuSO_4$	0.047	0.111	0.074	0.072
$Cd(NO_3)_2$	0.190	0.234	0.068	0.063
$UO_2(NO_3)_2$	0.190	0.205	—	—
$AlCl_3$	0.034	0.055	0.053	0.048
$SnCl_2$	0.058	0.170	0.044	0.066
$HgCl_2$	0.002	0.022	0.022	0.029
EDTA[a]	0.016	0.016	0.044	0.048
$LaCl_3$[a]	—	0.180	—	—
$TiCl_3$/HCl solution	—	0.010	—	—

[a] 1% in final volume.

TABLE IV

EFFECTS OF ACID STRENGTH ON THE ATOMIC ABSORPTION OF RUTHENIUM (60 μg ml^{-1})

Molarity	*HCl*	*HCl plus 4% (w/v) U*	*HNO_3*	*HNO_3 plus 4% (w/v) U*
0	0.140	0.280	0.144	0.288
3	0.180	0.285	0.054	0.280
6	0.128	0.278	0.028	0.285
9	0.080	0.180	0.017	0.175

Interference suppressors

The effects of possible interference suppressors, including lanthanum as chloride, strontium as nitrate, hydroxylamine hydrochloride and perchloric acid, and uranium as nitrate were examined. These effects are summarized in Table V. Sodium sulphite and nitrate were also examined, but were poor interference suppressors.

TABLE V

EFFECTS OF INTERFERENCE SUPPRESSORS ON THE ATOMIC ABSORPTION OF RUTHENIUM (60 μg ml^{-1})

Salt added[a]	*Interference suppressor*					
	3 M HCl	*La(III)*[b]	*Sr(II)*[b]	*$NH_2OH \cdot HCl$*[b]	*$HClO_4$*[b]	*U(VI)*[c]
None	0.180	0.180	0.240	0.239	0.230	0.283
Na tartrate	0.015	0.006	0.010	0.114	0.380	0.283
KBr	0.108	0.210	0.269	0.184	0.372	0.279
Na_2MoO_4	0.166	0.162	0.268	0.198	0.381	0.280
$HgCl_2$	0.022	0.100	0.116	0.169	0.100	0.285
$TiCl_3$/HCl solution	0.010	0.021	0.074	0.030	0.100	0.268
$NH_2OH \cdot HCl$ (2%)	0.239	—	0.263	—	0.201	—

[a] In all cases the solution contained 60 μg Ru ml^{-1}; 200 μg of interfering ion per ml was added.
[b] 2% (w/v) in the final solution.
[c] 4% (w/v) in the final solution.

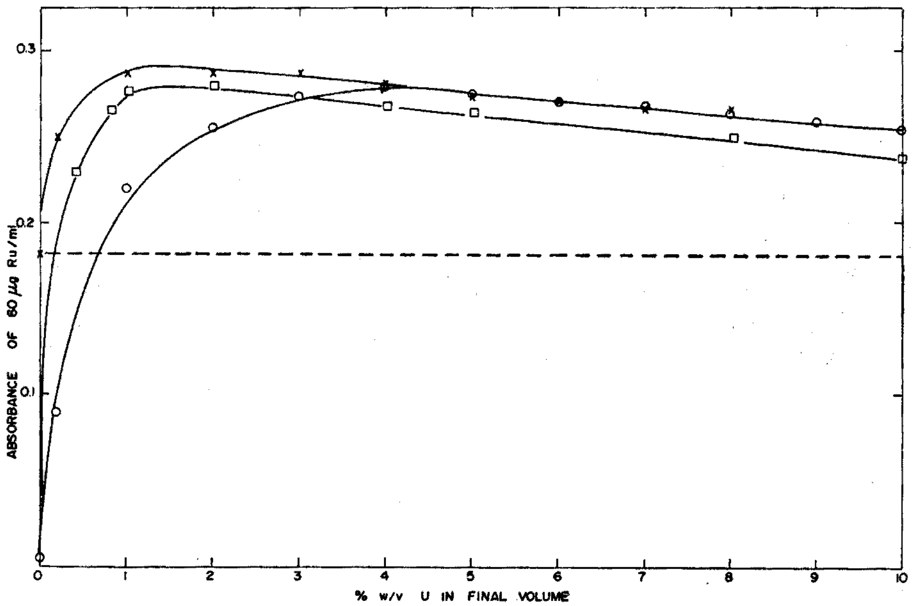

Fig. 2. Effects of uranium concentration on absorbance of 60 μg Ru ml^{-1} with and without interferents. (×) Ru+U, (○) Ru+U+interferent, (□) Ru+U+Ti. (---) 60 μg Ru ml^{-1} in 3 *M* HCl.

The effects of uranium concentration on the absorbance of ruthenium (60 μg ml^{-1}), with and without interfering species are shown in Fig. 2. The interferences (200 μg ml^{-1}) were sodium bromate, nitrate, iodide and tartrate in one experiment, and titanium chloride in the other.

Subsequently, the suppressing effects of uranium (VI) with all the ions present were examined. Uranium overcame the effects of almost all 40 ions, titanium being the only exception. The presence of uranium (4% w/v) also enhanced the atomic absorbance of ruthenium by 57%. Further, the addition of uranium (VI) eliminated the effects of varying acid strengths, up to 6 *M*, although greater acidities still caused a reduction in ruthenium absorbance (Table IV). It is not known why uranyl nitrate should be so effective in suppressing interferences and enhancing the absorption of ruthenium. No other uranium salts were examined.

Even with 4% (w/v) uranium solutions, no difficulties with burner clogging were encountered.

Distillation of ruthenium tetroxide from interferences

The volatility of ruthenium, as tetroxide, from oxidizing media[13] is well known; this property is commonly utilized in spectrophotometric procedures to separate ruthenium from interferences. The feasibility of using it in conjunction with atomic absorption was therefore examined.

The preliminary studies were made with a distillation apparatus essentially the same as that of Banks and O'Laughlin[10]. The recoveries obtained by distilling ruthenium tetroxide from sulphuric acid–perchloric acid into hydroxylamine hydrochloride–hydrochloric acid solution were 80%±2%; these values are similar to those quoted originally[10]. Under the same conditions but with an apparatus described by Chung and Beamish[11], the recoveries were 98%±1.5%. Recoveries were determined by comparing distilled standards to standards dissolved directly in 10% hydroxylamine hydrochloride–3 *M* hydrochloric acid solution.

Initially, the absorbances of the distillate changed with time, and it was concluded that this was due to changes in oxidation state. When the distillates were warmed until the solution became colourless, so that all the ruthenium was converted to a consistent oxidation state, no further changes then occurred. None of the ions examined interfered with the atomic absorption of ruthenium after distillation.

Conclusion

Of the interferences produced by 40 ions on the atomic absorption of ruthenium all except titanium were eliminated by the addition of excess of uranium. It is still possible to analyze for ruthenium by atomic absorption spectrophotometry in the presence of titanium, provided that the titanium concentrations of standards and samples are matched. However, the distillation of ruthenium tetroxide from oxidizing acid media provides an effective separation from all interfering species and should be used as an alternative to the uranium procedure when complex mixtures are encountered.

SUMMARY

The effects of some 40 ions and various acids on the atomic absorption spectrophotometry of ruthenium solutions have been studied. All produced interference; this was eliminated by the addition of uranium (4% (w/v)), or, in the case of titanium, by distillation of ruthenium tetroxide from oxidizing acid media. Lanthanum(III), strontium(II), hydroxylamine hydrochloride, perchloric acid, sodium sulphite and sodium nitrate proved ineffective as interference suppressors. Uranium(VI) also enhanced the absorbance of ruthenium; the sensitivity for ruthenium (expressed as

μg ml^{-1} for 1% absorbance) was found to be 0.88 in presence of uranium, and 1.0 after distillation. Recoveries of ruthenium by distillation were 98 ± 1.5%.

RÉSUMÉ

Les auteurs ont examiné l'influence de 40 ions et divers acides sur la spectrophotométrie par absorption atomique du ruthénium. Tous produisent des interférences, pouvant être éliminées par addition d'uranium (4% p/v), ou dans le cas du titane par distillation du tétroxyde de ruthénium, en milieu oxydant acide. Le lanthane, le strontium, le chlorhydrate d'hydroxylamine, l'acide perchlorique, le sulfite de sodium, et le nitrate de sodium ne permettent pas de supprimer ces interférences. D'autrepart l'uranium(VI) augmente l'absorption du ruthénium; la sensibilité du ruthénium (exprimée en μg ml^{-1}, pour une absorption de 1%) est de 0.88 en présence d'uranium et de 1.0 après distillation. Le rendement du ruthénium par distillation est de 98 ± 1.5%.

ZUSAMMENFASSUNG

Es wurde der Einfluss von etwa 40 Ionen und verschiedenen Säuren auf die Atomabsorptionsspektrophotometrie von Rutheniumlösungen untersucht. Alle riefen Störungen hervor; diese wurden eliminiert durch Zugabe von Uran (4% (Gew./Vol.)) oder im Falle von Titan durch Destillation von Rutheniumtetroxid aus oxidierendem, saurem Medium. Lanthan(III), Strontium(II), Hydroxylaminhydrochlorid, Perchlorsäure, Natriumsulfit und Natriumnitrat erwiesen sich für die Unterdrückung der Störungen als unwirksam. Uran(VI) erhöht auch die Absorption von Ruthenium; die Empfindlichkeit für Ruthenium (angegeben als μg ml^{-1} für 1% Absorption) war 0.88 im Gegenwart von Uran und 1.0 nach Destillation. Die nach Destillation wiedergewonnenen Anteile von Ruthenium betrugen 98 ± 1.5%.

REFERENCES

1 J. Halpern and B. R. James, *Can. J. Chem.*, 44 (1966) 671.
2 J. Halpern, J. F. Harrod and B. R. James, *J. Amer. Chem. Soc.*, 88 (1966) 5150.
3 F. E. Beamish, *Analytical Chemistry of the Noble Metals*, Pergamon Press, Oxford, 1966.
4 J. E. Allan, *Spectrochim. Acta*, 18 (1962) 259.
5 J. M. Scarborough, *Anal. Chem.*, 41 (1969) 250.
6 J. P. Peterson and F. R. Smith, *Soc. Appl. Spectrosc., Abs. 8th National Meeting, Anahem, Calif., October, 1969.*
7 *Analytical Methods for Atomic Absorption Spectrophotometry*, Perkin-Elmer, Sept., 1968.
8 T. V. Ramakrishna, J. W. Robinson and P. W. West, *Anal. Chim. Acta*, 36 (1966) 57.
9 B. Montford and S. C. Cribbs, *Report AECL-3292, Atomic Energy of Canada Limited*, 1969.
10 C. V. Banks and J. W. O'Laughlin, *Anal. Chem.*, 29 (1957) 1412.
11 K. S. Chung and F. E. Beamish, *Talanta*, 15 (1968) 823.
12 F. A. Cotton and G. Wilkinson, *Advanced Inorganic Chemistry*, 2nd Edn., Interscience, New York–London–Sydney, 1966, p. 998.
13 C. Claus, *Bull. de l'Académie Impériale des Sciences de St. Peterbourg*, 1 (1860) 97.

Analytica Chimica Acta
Elsevier Publishing Company, Amsterdam
Printed in The Netherlands

DOSAGE DU ZINC, DU FER ET DU PLOMB DANS UN COBALT DE TRES HAUTE PURETE

G. UNY, C. MATHIEN, J. P. TARDIF ET TRAN VAN DANH

Service de Physico-Chimie des Combustibles, Département de Métallurgie, Centre d'Etudes Nucléaires de Grenoble, 38-Grenoble (France)

(Reçu le 10 septembre, 1970)

Dans le cadre d'une étude générale entreprise sur le dosage des impuretés dans les métaux ultra-purs élaborés par fusion de zone[1-3], nous avons été amenés à mettre au point le dosage du zinc, du plomb et du fer dans le cobalt de très haute pureté.

Les concentrations présumées de chacun de ces éléments étant de l'ordre de $1 \cdot 10^{-6}$, la séparation de la matrice de cobalt est indispensable. Nous avons donc étudié pour chaque élément une méthode de séparation, soit par extraction par solvant, soit par échange d'ions. La séparation faite, les dosages du zinc et du fer par spectrophotométrie ne posent plus de difficultés particulières. Celui du plomb, par contre, que nous avons effectué par spectrométrie d'absorption atomique, nous a conduits à utiliser un four de préchauffage d'aérosol afin d'améliorer suffisamment la sensibilité.

Le présent travail rend compte des résultats obtenus.

SÉPARATION DU ZINC

Selon Scroggie et Dean[4], le zinc peut être séparé par extraction d'un bon nombre d'éléments métalliques à l'aide d'amines tertiaires dissoutes dans un solvant organique convenable. Nous utilisons cette méthode en nous servant de la tri-*n*-octylamine dissoute dans du trichloréthylène. Nous préférons le trichloréthylène à la méthylisobutylcétone car cette dernière se décante mal en milieu acide chlorhydrique 2 *M*.

Les résultats rassemblés au Tableau I rendent compte du comportement du zinc au cours des extractions en présence ou en l'absence d'environ 2 g de cobalt. La présence de Cu, Fe, Ni, Mn, Ti, Pb à des concentrations de 1 mg ml^{-1} ne perturbe pas le dosage.

L'ensemble de ces résultats montrent que l'extraction du zinc d'une matrice de cobalt par le tri-*n*-octylamine dans le trichloréthylène en milieu HCl est possible et que la méthode est parfaitement applicable au dosage de faibles traces de zinc dans le cobalt de très haute pureté.

LE DOSAGE DU ZINC

Mode opératoire

On transvase les 10 ml de la solution (HCl 2 *M*) résultant de l'attaque de 2 g environ d'échantillon dans une ampoule à décanter de 100 ml, on y ajoute 20 ml d'une solution de 5 g de tri-*n*-octylamine dans 100 ml de trichloréthylène. On agite l'ampoule pendant 3 min et on laisse décanter. On recueille la phase organique dans une nouvelle ampoule.

TABLEAU I

EXTRACTION DU ZINC EN PRÉSENCE OU EN ABSENCE DE COBALT

Zn introduit (µg)	*Zn trouvé après extraction (µg)*	*Ecart*
2.28	2.26	−0.02
4.56	4.50	−0.06
4.56	4.69	+0.13
6.84	6.88	+0.04
2 g Co ajouté		
2.28	2.35	+0.07
2.28	2.05	−0.23
4.56	4.60	+0.04

Dans la précédente on ajoute 2 ml de trichloréthylène et on l'agite pendant 30 sec. On lave deux fois les phases organiques réunies avec 10 ml HCl 2 *M* en agitant pendant 1 min. Après décantation la phase organique est agitée deux fois 2 min avec 10 ml de l'acide chlorhydrique 0.05 *M*. Le zinc repasse alors dans la phase aqueuse qu'on rince avec 5 ml de trichloréthylène. Après 30 min de décantation, on rejette la phase organique. On est alors en mesure de poursuivre le dosage du zinc directement sur la phase aqueuse en procédant à la spectrophotométrie de son complexe avec la dithizone.

TABLEAU II

LE DOSAGE DE ZINC DANS UN ÉCHANTILLON DE COBALT ET DANS UN SEL CONNU DE COBALT

Poids (g)	*Zn ajouté (µg)*	*Zn trouvé (µg)*	*Zn présent dans le Co (µg)*	*Zn (%)*
Echantillon de cobalt				
1.04	0	1.50	1.50	$14\cdot10^{-5}$
1.04	2.28	3.75	1.47	$14\cdot10^{-5}$
Sel de cobalt				
4.070	—	3.42	—	$84\cdot10^{-6}$
4.035	—	3.37	—	$84\cdot10^{-6}$
4.007	—	2.78	—	$70\cdot10^{-6}$

Résultats

Afin de vérifier la validité de cette méthode nous avons dosé quelques p.p.m. de zinc dans un sel connu de cobalt et dans un échantillon de cobalt réputé pur. Le Tableau II rend compte des résultats obtenus.

SÉPARATION DU FER

La spectrophotométrie du complexe formé par le fer(II) et la bathophénanthroline est utilisée pour doser quelques microgrammes de fer[5]. Cette méthode nécessite une séparation du fer du cobalt car la présence de plus d'un milligramme de ce dernier élément perturbe le dosage[6]. Nous adoptons la méthode de séparation du fer décrite par Claassen et Bastings[7].

Notre étude a consisté à déterminer le rendement de l'extraction de microquantités de fer de 2 g de cobalt et à vérifier que la quantité de cobalt entraînée avec le fer ne dépasse pas 1 mg.

Rendement de l'extraction

A 50 ml d'HCl 8 *M* contenant de 0 à 30 μg de fer(III), on ajoute 100 mg de potassium chlorate. On procède à deux extractions successives avec 50 ml d'un mélange 1+1 de méthylisobutylcétone et d'acétate d'amyle. Les deux phases organiques réunies sont lavées avec 50 ml d'HCl 8 *M*. On fait repasser ensuite le fer en solution aqueuse par agitation avec 100 ml d'eau distillée et on procède à son dosage avec le bathophénanthroline.

Les résultats obtenus figurent sur le Tableau III.

Détermination de la quantité de cobalt entraîné

Dans 50 ml d'une solution d'HCl 8 *M* contenant 2 g de cobalt environ, on ajoute 100 mg de potassium chlorate. Les extractions sont effectuées comme dans le paragraphe précédent. Le cobalt entraîné a été dosé par spectrophotométrie du complexe formé avec le nitroso-R[8].

Les résultats obtenus sont rassemblés au Tableau IV.

Les Tableaux III et IV montrent que les résultats obtenus sont très satisfaisants.

TABLEAU III

L'EXTRACTION DU FER

Fe soumis à l'extraction (μg)	*Fe retrouvé (μg)*	*Rendement de l'extraction en % (blanc déduit)*
0	1.5	
2.0	3.3	90
5.0	6.3	96
10.0	11.5	100
15.0	16.5	100
20.0	21.8	101
25.0	26.5	100
30.0	31.0	98

TABLEAU IV

LA QUANTITÉ DE COBALT ENTRAÎNÉ

Co introduit (mg)	*Co trouvé (µg)*		*Rendement de la séparation (%)*
	1 lavage	*2 lavages*	
2000	70	25	>99.99
2000	90	20	>99.99
2000	55	25	>99.99

La méthode convient donc pour le dosage de faibles traces de fer dans le cobalt. Nous l'avons mise en oeuvre pour le dosage du fer dans deux échantillons.

Résultats

Une prise d'essai de l'ordre de 2 g de cobalt en poudre est dissoute dans 40 ml d'acide chlorhydrique 8 *M*. Si le cobalt se présente sous forme massive, l'attaque est réalisée par dissolution anodique dans le même milieu. Dans un cas comme dans l'autre, le fer est oxydé par 100 mg de potassium chlorate. On porte à l'ébullition pour chasser le chlore. Si la quantité présumée du fer est faible, on peut ajouter des quantités connues de fer(III). Après refroidissement, on transvase la solution dans l'ampoule à décanter de 250 ml. On rince avec 10 ml de l'acide chlorhydrique 8 *M* et l'extraction

TABLEAU V

LE DOSAGE DU FER DANS LES ÉCHANTILLONS DE COBALT

Prise d'essai (g)	*Fer ajouté (µg)*	*Fer trouvé (µg)*	*Fe dans échantillon (10^{-4} %)*
Echantillon en poudre			
2.000	0	6.5	3.2
2.000	0	5.7	2.8
2.000	0	4.8	2.4
2.000	10.0	15.5	2.7
2.000	10.0	15.8	2.9
2.000	10.0	16.2	3.1
Moyenne $2.8 \cdot 10^{-4}$ %			
Echantillon massif			
2.045	0	14.5	7.1
2.045	0	14.7	7.2
2.045	10.0	24.5	7.2
2.045	10.0	24.2	6.9
1.736	0	10.6	6.1
1.736	0	10.4	6.0
1.736	10.0	21.0	6.3
1.736	10.0	20.7	6.2
1.736	10.0	20.7	6.2
Moyenne $6.6 \cdot 10^{-4}$ %			

du fer(III) est réalisée selon la technique décrite ci-dessus. Le fer extrait est ensuite dosé par la méthode à la bathophénanthroline.

Les différents résultats obtenus figurent au Tableau V.

L'ensemble des résultats obtenus montre bien l'intérêt que présente l'extraction en milieu HCl de faibles traces de fer par le mélange méthylisobutylcétone et acétate d'amyle. Elle permet de procéder ensuite à la détermination de $1 \cdot 10^{-6}$ à $15 \cdot 10^{-6}$ g de fer avec une précision de l'ordre de 10% en utilisant la méthode classique à la bathophénanthroline.

LE DOSAGE DU PLOMB

Séparation du plomb

D'après Andersen et Knutsen[9], Strelow et Von S. Toerien[10], et Klakl et Korkisch[11], on peut fixer le plomb en milieu acide bromhydrique de 0.1 à 4 *M* sur une résine anionique AGI-X8. Le cobalt qui n'est pas complexé à cette concentration en acide bromhydrique n'est pas retenu. La valeur maximale du coefficient de partage du plomb varie selon les auteurs de 500 à 1000.

Un essai effectué avec du plomb et du cobalt marqués permet de suivre par comptage γ la séparation du plomb contenu dans 3 g de cobalt en milieu acide bromhydrique 0.3 *M*. Nous avons utilisé une colonne ayant un diamètre intérieur de 12 mm et une hauteur de résine de 10 cm.

Le plomb n'apparaît pas dans l'effluent après passage de 350 ml de solution d'acide bromhydrique 0.3 *M*; ce cobalt par contre est totalement élué après passage de 1 à 2 volumes de colonne.

Le plomb fixé sur la résine est élué ensuite par de l'acide nitrique *M*. Du plomb marqué a été complètement élué par passage de 80 ml de l'acide nitrique 1 *M*.

Dosage du plomb par spectrophotométrie d'absorption atomique

La solution d'élution contenant le plomb peut être ramenée à 20 ml, ce qui donne une concentration présumée de 0.10 μg ml^{-1} à 0.15 μg ml^{-1} de plomb pour une prise d'essai de 3.g de cobalt.

Afin d'être en mesure d'effectuer correctement ce dosage, nous avons été amenés à améliorer la sensibilité de la méthode en employant un four de préchauffage de l'aérosol décrit par ailleurs[12]. Avant l'introduction dans le brûleur, l'aérosol est rapidement désolvaté sous rayonnement infra rouge et le solvant est condensé par un réfrigérant à la sortie du four. La sensibilité obtenue pour le plomb est de 0.034 μg ml^{-1} avec une limite de détection de 0.015 μg ml^{-1}. Nous pouvons ainsi doser 0.1 μg ml^{-1} de plomb avec une précision de 4 à 5%.

Nous avons dosé le plomb après séparation de la matrice de cobalt selon le mode opératoire décrit ci-dessous.

Mode opératoire

On attaque 3 g d'échantillon par 15 ml d'acide nitrique concentré en bécher pyrex. La solution est amenée à sec et laissée sur une plaque chauffante. Le nitrate se décompose en se transformant en oxyde. L'oxyde est repris deux fois par 25 ml d'acide bromhydrique concentré. Le bromure obtenu est dissous dans 80 ml d'acide bromhydrique 0.3 *M*.

Avant utilisation la résine Dowex AG 1-X8 (100–200 mesh), est lavée par l'acide nitrique 1 *M*, puis par de l'eau permutée. La résine est ensuite essorée. Elle est mise en contact durant 24 h avec l'acide bromhydrique 0.3 *M* et transvasée dans des colonnes de 12 mm de diamètre intérieur. La hauteur de la résine dans ces colonnes est de 10 cm. On fait passer la solution de cobalt à un débit de 1 ml min^{-1}.

Le cobalt retenu est élué par 50 ml d'acide bromhydrique 0.3 *M*, le plomb fixé sur la résine est élué par 100 ml d'acide nitrique 1 *M*.

La solution contenant le plomb est amenée à sec, puis reprise par 5 ml d'acide perchlorique et 15 ml d'acide nitrique concentré. Elle est à nouveau amenée à sec et reprise par l'acide nitrique 0.1 *M* et amenée au volume (20 ml).

Résultats

Nous avons dosé le plomb successivement dans du nitrate de cobalt et dans deux échantillons de cobalt réputé pur.

Le Tableau VI rend compte des résultats obtenus.

La pollution apportée par les réactifs chimiques utilisés limite à la fois la

TABLEAU VI

LE DOSAGE DU PLOMB

Prise d'essai g de cobalt	*Plomb ajouté (μg)*	*Plomb trouvé (μg)*	*Plomb (blanc soustrait) (μg)*	*Teneur (p.p.m.)*
Nitrate de cobalt				
3.078	0	10.9	8.2[a]	2.66
3.046	0	10.5	7.8[a]	2.56
3.098	20	30.8	8.1[a]	2.61
3.045	20	30.0	7.3[a]	2.40
3.047	30	40.0	7.3[a]	2.40
3.045	30	40.2	7.5[a]	2.46
			Moyenne	2.5±0.1
Cobalt réputé pur. Echantillon no. 1				
2.973	0	3.76	1.36[b]	0.46
	0	4.28	1.88[b]	0.63
	5	8.80	1.40[b]	0.47
	5	9.12	1.72[b]	0.58
			Moyenne	0.53±0.08
Echantillon no. 2				
3.104	0	3.90	1.25[c]	0.41
	0	3.55	0.90[c]	0.29
	5	9.20	1.55[c]	0.51
	5	8.50	0.85[c]	0.28
			Moyenne	0.37±0.1

[a] Blanc de réactif 2.70.
[b] Blanc de réactif 2.40.
[c] Blanc de réactif 2.65.

précision de ce dosage et la possibilité de déterminations inférieures à quelques dixièmes de p.p.m.

Néanmoins, la méthode décrite permet le dosage de 0.35 p.p.m. de plomb dans du cobalt avec une précision de 30%. Cette précision s'améliore très rapidement quand la teneur en plomb augmente.

CONCLUSION

L'ensemble des résultats obtenus au cours de cette étude montre qu'il est possible de doser les impuretés telles que le fer, le zinc et le plomb dans du cobalt de très haute pureté, à condition de procéder à la séparation préalable de la matrice.

Dans le cas du dosage du plomb par spectrométrie d'absorption atomique, l'amélioration de sensibilité apportée par l'utilisation d'un four de préchauffage de l'aérosol est telle que l'on peut encore doser 0.05 μg ml^{-1} de plomb avec une précision satisfaisante.

Cette étude montre enfin que la pollution due au réactifs chimiques utilisés, même lorsqu'ils sont réputés ultrapurs, au cours du traitement des échantillons, constitue une limitation à l'accroissement de la sensibilité de la méthode.

RÉSUMÉ

Des traces de zinc, de fer et de plomb dont les teneurs varient de 0.5 à 2 p.p.m., contenues dans du cobalt de très haute pureté sont, quantitativement, séparées de la matrice, soit par extraction par solvant, soit par fixation sur résine échangeuse d'ions. Le zinc est extrait par la tri-*n*-octylamine dissoute dans le trichloréthylène en milieu HCl 2 *M*. Le fer est extrait par un mélange de 1+1 de méthylisobutylcétone et d'acétate d'amyle en présence de chlorate. Le plomb est retenu sur résine anionique Dowex 1-X8 en milieu bromhydrique 0.3 *M*. On procède ensuite au dosage de ces éléments. Le zinc est dosé par la spéctrophotométrie de son complexe de dithizonate, le fer par la spectrophotométrie de son complexe de fer(II) avec la bathophénanthroline et enfin le plomb par spectrophotométrie d'absorption atomique.

SUMMARY

Trace impurities of zinc, iron and lead ranging from 0.5 to 2 p.p.m. in high-purity cobalt are quantitatively separated by solvent extraction or ion exchange before their determination. Zinc is extracted by tri-*n*-octylamine–trichloroethylene mixture from 2 *M* hydrochloric acid media. Iron is extracted with 1+1 methyl isobutyl ketone–amyl acetate from 8 *M* hydrochloric acid containing potassium chlorate. Lead is retained on a Dowex 1-X8 anion-exchange resin from 0.3 *M* hydrobromic acid media. After separation, zinc is determined spectrophotometrically as its dithizonate, iron spectrophotometrically with bathophenanthroline, and lead by atomic absorption spectrophotometry.

ZUSAMMENFASSUNG

Spuren von Zink, Eisen und Blei in hochreinem Kobalt können im Bereich

0·5–2 p.p.m. quantitativ durch Extraktion oder Ionenaustausch abgetrennt und dann bestimmt werden. Zink wird aus 2 *M* salzsaurem Medium mit einem Gemisch von Tri-*n*-octylamin und Trichloräthylen extrahiert, Eisen wird mit Methylisobutylketon und Amylacetat (1+1) aus kaliumchlorathaltiger 8 *M* Salzsäure extrahiert. Blei wird in 0.3 *M* Bromwasserstoffsäure durch den Anionenaustauscher Dowex 1-X8 zurückgehalten. Nach Abtrennung wird Zink spektrophotometrisch als Dithizonat, Eisen spektrophotometrisch mit Bathophenanthrolin und Blei durch Atomabsorptions spektrophotometrie bestimmt.

BIBLIOGRAPHIE

1 TRAN VAN DANH, J. SPITZ ET C. MATHIEN, *Anal. Chim. Acta*, 36 (1966) 204.
2 TRAN VAN DANH, J. SPITZ ET J. P. TARDIF, *Anal. Chim. Acta*, 42 (1968) 341.
3 G. UNY, M. BRULE ET J. SPITZ, *Anal. Chim. Acta*, 44 (1969) 29.
4 L. E. SCROGGIE ET J. A. DEAN, *Anal. Chim. Acta*, 21 (1959) 282.
5 E. B. SANDELL, *Colorimetric Determination of Traces of Metals*, Interscience, New York, 1959.
6 A. R. GALHER, R. M. HAMMER ET R. C. SHUBERT, *Anal. Chem.*, 33 (1961) 1937.
7 A. CLAASSEN ET L. BASTINGS, *Z. Anal. Chem.*, 160 (1958) 403.
8 K. J. MCNAUGHT, *Analyst*, 67 (1942) 97.
9 T. ANDERSEN ET A. B. KNUTSEN, *Acta Chem. Scand.*, 16 (1962) 849.
10 F. W. E. STRELOW ET F. VON S. TOERIEN, *Anal. Chem.*, 38 (1966) 545.
11 E. KLAKL ET J. KORKISCH, *Talanta*, 16 (1969) 1177.
12 G. UNY, J. NGUEA LOTTIN, J. P. TARDIF ET J. SPITZ, *Spectrochim. Acta*, à paraître.

Analytica Chimica Acta
Elsevier Publishing Company, Amsterdam
Printed in The Netherlands

EXTRACTION OF METALS BY LONG-CHAIN ALKYLAMMONIUM SALTS

PART II. HYDRATION OF TRILAURYLMETHYLAMMONIUM THIOCYANATE OR CHLORIDE

J. F. DESREUX*
Chimie Analytique, Université de Liège au Sart Tilman, B-4000 Liège (Belgium)

(Received July 3rd, 1970)

In recent years, quaternary ammonium salts have been successfully used in liquid–liquid extraction[1,2] but the chemical properties of these extractants have not yet been studied in great detail. In the first paper of this series[3], the hydration of carbon tetrachloride solutions of a series of long-chain alkylammonium salts was discussed, and it was concluded that water does not seem to play any role in the aggregation of the tertiary amine salts. In order to verify this hypothesis with quaternary ammonium salts, the association between water and two compounds, trilaurylmethylammonium chloride and thiocyanate (TLMA·Cl and TLMA·SCN), was studied. The former was chosen because, according to the previous results[3], the amount of water is comparatively high; TLMA·SCN was chosen because of the possibilities of hydration studies by three methods, infrared and n.m.r. spectroscopy and titrations of water.

EXPERIMENTAL

The preparation of the ammonium salts and the experimental methods used were described earlier[3]. All measurements were made at 25°. On account of the importance of water extraction in the organic phase and its sensitivity to any temperature change, both phases were allowed to separate by gravity or were centrifuged very carefully at a temperature as near as possible to the equilibration temperature.

Carbon tetrachloride was used as diluent in all experiments.

HYDRATION OF TRILAURYLMETHYLAMMONIUM THIOCYANATE

The infrared spectrum of the fundamental stretching-vibration region of water is shown in Fig. 1. As has been pointed out previously, these bands are characteristic of water associated to a strong base[3,4]. The appearance of a new broad and intense OH-stretching vibration band about 300 cm^{-1} lower than that of free water in carbon tetrachloride (ν_3 at 3706 cm^{-1}) clearly indicates the formation of an hydrogen bond in this system.

One can distinguish in the spectra a sharp band called the "free OH band"

---

[*] Aspirant au Fonds National de la Recherche Scientifique.

and a broad band called the "associated OH band" which are attributed to the following stretching modes:

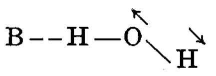

"free"

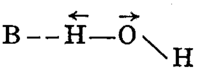

"associated"

The broad band, caused by water associated with TLMA·SCN, is not perfectly symmetrical, but its shape is not modified by changes in salt concentration. The third, less intense, band corresponds to the overtone of the bending vibration.

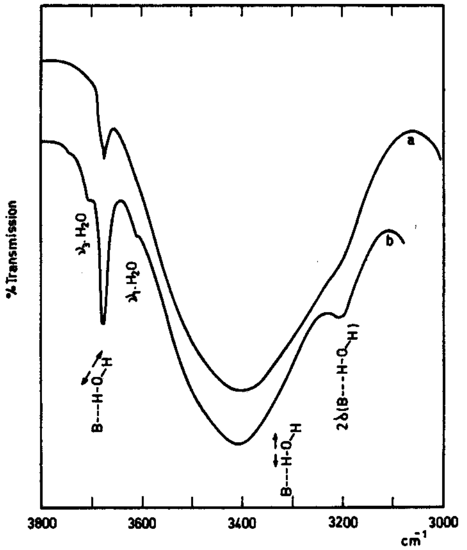

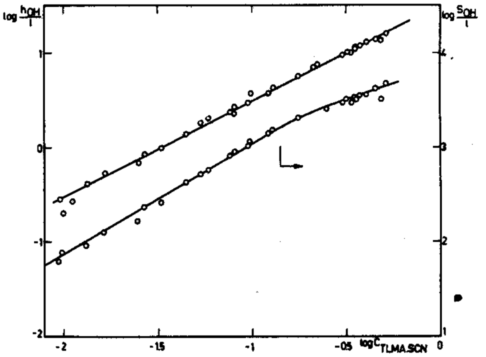

Fig. 1. The OH stretching region for water-saturated carbon tetrachloride solutions of: (a) TLMA·Cl, (b) TLMA·SCN.

Fig. 2. The integrated absorbance (S_{OH}) of the associated OH band and the absorbance at the maximum (h_{OH}) of the free OH band *vs.* the total concentration $[B]_T$ of TLMA·SCN for water-saturated solutions in CCl_4.

In exactly the same manner as before for TLA·HCl[3], the investigation was based on measurement of the integrated absorbance between 3650 cm^{-1} and 3150 cm^{-1} for the associated OH band (S_{OH}), the absorbance at the maximum of the peak of the free OH band (h_{OH}), and the amount of water associated with the salt, $[H_2O]_T - [H_2O]$ (where $[H_2O]_T$ is the total concentration of water in the organic phase and $[H_2O]$ is the solubility of water in the diluent carbon tetrachloride, taking into account the molar volume of the ammonium salt)[5]. The infrared experimental data are given in Fig. 2. On a bilogarithmic plot, straight lines with slopes of 1.2 (S_{OH}) and 1.0 (h_{OH}) are obtained in nearly the whole concentration range studied. In Fig. 3, the water content of the organic phase is plotted against the TLMA·SCN concentration in carbon tetrachloride. Here again, a straight line with a slope of 0.92 in a linear scale and with a slope of 1.0 in a bilogarithmic scale, is obtained. As has been noted previously[3], polymeric complexes through water hydrogen bonds between ammonium salts molecules in the organic phase would influence the shape of the broad infrared water band and the observed slopes in Figs. 2 and 3. Such phenomena have been brought to light by ROLAND AND DUYCKAERTS[6,7] for some phosphorus compounds.

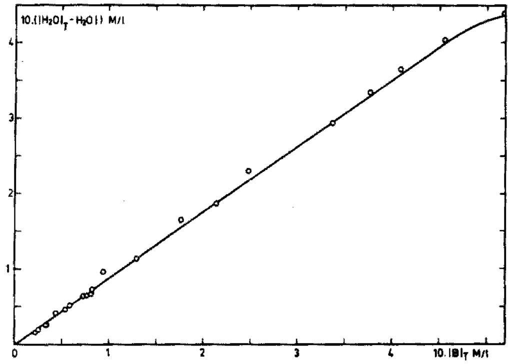

Fig. 3. Extraction of water by TLMA·SCN in carbon tetrachloride at 25°. $[B]_T$: total concentration of amine salt, $[H_2O]_T - [H_2O]$: excess water in the organic solution.

Thus, it is concluded that water does not play a role in the aggregation of TLMA·SCN. It has already been shown[3] that if there are several simultaneous equilibria of the type:

$$B\cdot(H_2O)_n + H_2O \rightleftharpoons B\cdot(H_2O)_{n+1} \qquad K'_{n,n+1} = \frac{[B\cdot(H_2O)_{n+1}]}{[B\cdot(H_2O)_n]} \tag{1}$$

$$B\cdot(H_2O)_{n+1} + H_2O \rightleftharpoons B\cdot(H_2O)_{n+2} \qquad K'_{n+1,n+2} = \frac{[B\cdot(H_2O)_{n+2}]}{[B\cdot(H_2O)_{n+1}]} \tag{2}$$

$$B\cdot(H_2O)_{n+k-1} + H_2O \rightleftharpoons B\cdot(H_2O)_{n+k} \qquad K'_{n+k-1,n+k} = \frac{[B\cdot(H_2O)_{n+k}]}{[B\cdot(H_2O)_{n+k-1}]} \tag{3}$$

where n may have integral values from 0 to n and k may have integral values from 1 to k, the general equation for water extraction is:

$$[H_2O]_T - [H_2O] = [B]_T$$

$$\left\{n + \frac{K'_{n,n+1} + 2K'_{n,n+1}\cdot K'_{n+1,n+2} + \ldots + k\,K'_{n,n+1}\ldots K'_{n+k-1,n+k}}{1 + K'_{n,n+1}\cdot K'_{n+1,n+2} + \ldots + K'_{n,n+1}\ldots K'_{n+k-1,n+k}}\right\} \tag{4}$$

where $[B]_T$ is the total concentration in ammonium salt. It is not possible to conclude, from the linear relationship in Fig. 3, that TLMA·SCN is found only in the form of a monohydrate. A similar conclusion must be drawn from the infrared spectra if all types of associated or free OH bands have the same extinction coefficients. However, as will be discussed later, the results obtained by Karl Fischer titrations and by infrared and n.m.r. spectroscopy are only consistent if one assumes that the monohydrate, TLMA·SCN·H_2O, is the major species in solution.

If the equilibrium:

$$TLMA\cdot SCN + H_2O \rightleftharpoons TLMA\cdot SCN\cdot H_2O$$

is considered, the pertinent equations for water extraction and for infrared data are[3]:

$$[H_2O]_T - [H_2O] = [B]_T \frac{K'_{0,1}}{l + K'_{0,1}} \tag{5}$$

$$\frac{h_{OH}}{\varepsilon_h\, l} = [B]_T \frac{K'_{0,1}}{1 + K'_{0,1}} \tag{6}$$

$$\frac{S_{OH}}{\varepsilon_S\, l} = [B]_T \frac{K'_{0,1}}{1 + K'_{0,1}} \tag{7}$$

where l is the thickness of the cell and ε_h and ε_S are the absorption coefficients of the two bands, then the following values can be calculated: $K'_{0,1} = 12.2$; $\varepsilon_h = 37$ M^{-1} l cm^{-1}; $\varepsilon_S = 19100$ M^{-1} l cm^{-2}.

The calculated ε_h value is rather different from the one obtained for TLA·HCl[3]. Measurements on other ammonium salts, however, indicated that ε_h is not a constant.

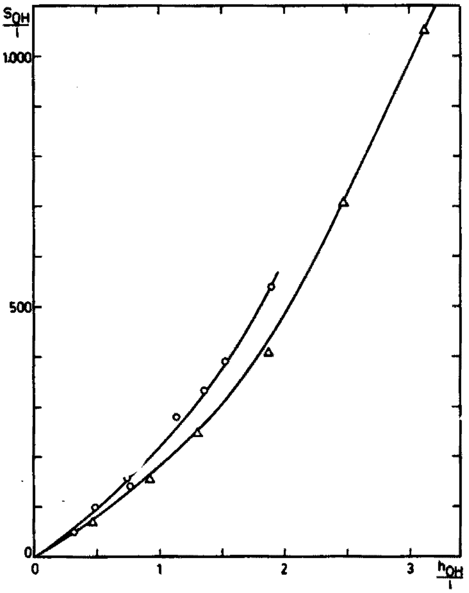

Fig. 4. Study of two solutions of TLMA·SCN which are not saturated with water. (△) $1.02\cdot 10^{-1}$ *M*, (○) $7.06\cdot 10^{-2}$ *M*.

In addition, four different solutions of constant concentration in ammonium salt ($5.01\cdot 10^{-2}$, $7.06\cdot 10^{-2}$, $1.02\cdot 10^{-1}$, $3.54\cdot 10^{-1}$ *M*) but with different water concentration were studied. In no case was a linear relationship between h_{OH} and S_{OH} (Fig. 4) observed, as would have been expected if the monohydrate were the only species in solution. This phenomenon, which could be expected for the last solution ($3.54\cdot 10^{-1}$ *M*) is absolutely unexpected for the first three solutions which were chosen in the concentration range where eqn. (5) above seems to be verified for water-saturated solutions. As seen in Fig. 5, it is the absorbance of the associated OH band which varies linearly with the water concentration.

Apparently, the monohydrate, TLMA·SCN·H_2O, is not the only species in solution. However, these results were not obtained under the same conditions as the previous results, since these concern solutions which are not saturated with water. Therefore, and because of the basicity of TLMA·SCN, complexes of different types, could exist, for instance:

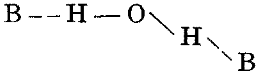

In fact, the infrared spectra of TLMA·SCN solutions with a low water content show a shoulder near 3500 cm^{-1} (Fig. 6). Numerous attempts to interpret the results quantitatively on the basis of simple equilibria were unsuccessful. It is believed, therefore, that this abnormal behaviour does not allow the conclusion that there exist, at least in large amounts, in the saturated solutions other complexes than the monohydrate TLMA·SCN·H_2O. This hypothesis was supported by n.m.r. spectroscopy.

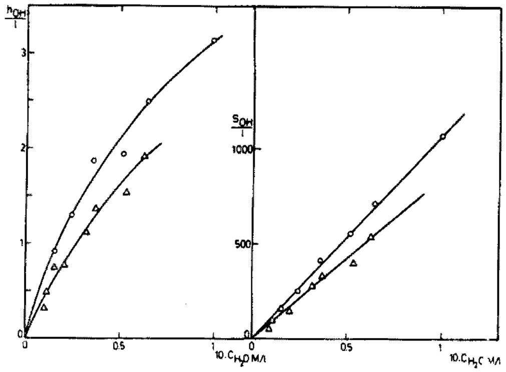

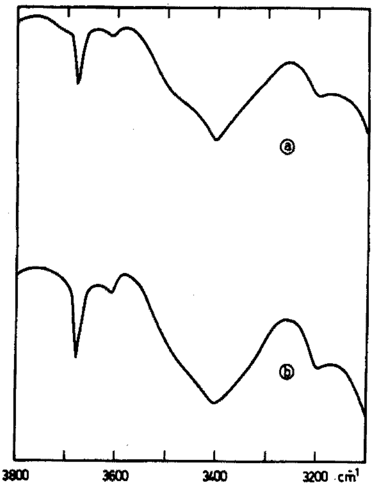

Fig. 5. Influence of water on the infrared spectra of two solutions which are not saturated with water. (○) 1.02·10^{-1} *M*, (△) 7.06·10^{-2} *M*.

Fig. 6. The OH stretching region for two partially hydrated solutions of TLMA·SCN. (a) [TLMA·SCN] = 7.06·10^{-2} *M*, [H_2O] = 9.9·10^{-3} *M*; (b) [TLMA·SCN] = 1.02·10^{-1} *M*, [H_2O] = 7·10^{-3} *M*.

As has been pointed out previously[3], the water peak shows the characteristics of an hydrogen bond, *i.e.* a downfield shift when the solution is made more concentrated (Fig. 7) or when the temperature is decreased. If it is assumed that, in the hydrogen bond, there are only rapid exchanges, then the observed peak is the mean of the chemical shifts of all OH groups. Since water is a monomer in carbon tetrachloride[8], it is possible to write, assuming the existence of only the monohydrate:

$$\delta = \delta_{H_2O} \cdot \frac{2[H_2O]}{2[H_2O]_T} + \delta_h \cdot \frac{[B \cdot H_2O]}{2[H_2O]_T} + \delta_S \frac{[B \cdot H_2O]}{2[H_2O]_T} \qquad (8)$$

where δ is the observed chemical shift with tetramethylsilane as external reference and δ_{H_2O}, δ_h and δ_S correspond respectively to the chemical shift of free water, of the free OH bond and of the associated OH bond. A similar equation has been used for the hydration of acetone in 1,2-dichlorethane[9]. The value measured for δ_{H_2O}, -1.95 p.p.m. at 25°, is in good agreement with the one given by HINDMANN[10] recalculated for a TMS reference.

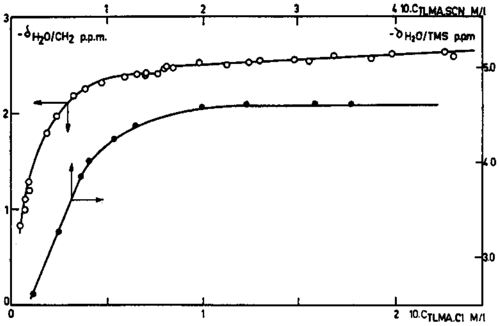

Fig. 7. Chemical shift of water associated with: (●) TLMA·SCN, (○) TLMA·Cl.

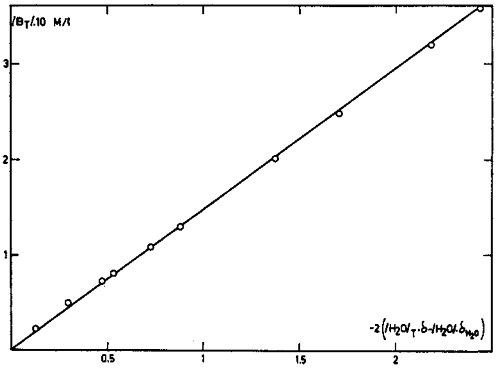

Fig. 8. N.m.r. study of the hydration of TLMA·SCN.

Equation (8) above may also be written in the form:

$$2([H_2O]_T \cdot \delta - [H_2O] \cdot \delta_{H_2O}) = (\delta_h + \delta_S) \cdot \frac{K'_{0,1}}{1 + K'_{0,1}} \cdot [B]_T \qquad (9)$$

As can be seen from Fig. 8, this equation is verified over the entire concentration range. The value of $(\delta_h + \delta_S)$ can be determined from the value of δ for the plateau in Fig. 7. For concentrated solutions the following equations are verified:

$$\delta \simeq (\delta_h + \delta_S)\frac{[\mathrm{B \cdot H_2O}]}{2[\mathrm{H_2O}]_\mathrm{T}} \simeq \frac{(\delta_h + \delta_S)}{2}, \tag{10}$$

since the amount of associated water is much greater than the solubility of water in the diluent. From eqn. (10) and from the value of the slope in Fig. 8, it can be calculated that:

$$(\delta_h + \delta_S) = -7.38 \text{ p.p.m./TMS}$$

$$K'_{0,1} = 11.7$$

The value of the equilibrium constant is in good agreement with the one obtained before by the Karl Fischer titrations assuming monohydrate formation. Such agreement would not be the case if any other complexes existed in significant amounts.

HYDRATION OF TRILAURYLMETHYLAMMONIUM CHLORIDE

As shown in Fig. 1 and as pointed out earlier[3], the free OH band is very weak, whereas the associated OH band is intense and broad. In fact, it is too intense to allow quantitative measurements over any large concentration range. Indeed, interference fringes were obtained when the thickness of the cells was reduced. More-

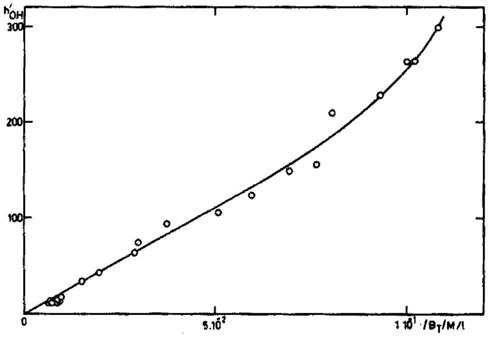

Fig. 9. Extraction of water by carbon tetrachloride solutions of TLMA·Cl at 25°.

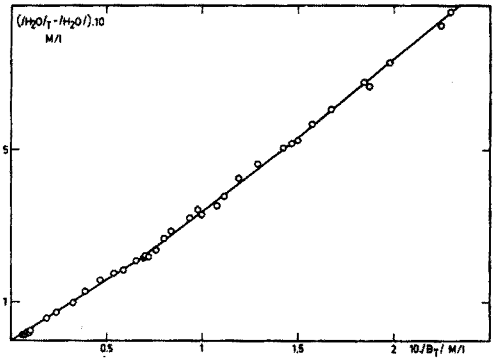

Fig. 10. The absorbance at the maximum of the associated OH band (h'_{OH}) *vs.* the total concentration $[\mathrm{B}]_\mathrm{T}$ of TLMA·Cl for water-saturated solutions.

over, the exact surface of the band was rather difficult to estimate and it seemed better to measure the absorbance at the maximum of the associated OH band (h'_{OH}). This simplification was checked for TLMA·SCN and found to be valid, although it was certainly less accurate.

The experimental results are presented in Figs. 7, 9 and 10. In Fig. 9, it is possible to distinguish two curves: a straight line of slope 3.15 and a curve of very weak curvature for $[\mathrm{TLMA\cdot Cl}]_T > 7\cdot 10^{-2}$ M. Aggregates between several hydrated complexes do not seem to exist in the diluted solutions since a linear relationship is obtained. However, it is not possible to assign a definite formula to the polyhydrates present in the organic phase since many combinations will satisfy eqn. (4).

However, it can be deduced from the value of the slope obtained in Fig. 9 that at least the following equilibrium exists in solution:

$$\mathrm{B\cdot(H_2O)_3 + H_2O \rightleftharpoons B\cdot(H_2O)_4} \qquad (11)$$

The curvature which appears for the more concentrated solutions in Fig. 9 could be explained by variations of activity coefficients or by extraction of water by polymeric species. The latter hypothesis allows the observed results to be explained but both processes probably occur.

If it is assumed that equilibrium (11) above is the major one in the diluted solutions ($K'_{3,4} = 0.715$), the following two equilibria can explain the curve shape of Fig. 9 for TLMA·Cl $> 7\cdot 10^{-2}$ M:

$$\mathrm{B\cdot(H_2O)_3 + H_2O \rightleftharpoons B\cdot(H_2O)_4} \qquad K'_{3,4} = \frac{[\mathrm{B\cdot(H_2O)_4}]}{[\mathrm{B\cdot(H_2O)_3}]} \qquad (12)$$

$$\mathrm{2B\cdot(H_2O)_4 + H_2O \rightleftharpoons B_2\cdot(H_2O)_9} \qquad K'_D = \frac{[\mathrm{B_2\cdot(H_2O)_9}]}{[\mathrm{B\cdot(H_2O)_4}]^2} \qquad (13)$$

From these equations, one calculates that:

$$\log\,[\mathrm{B_2\cdot(H_2O)_9}] = 2\log\,[\mathrm{B\cdot(H_2O)_4}] + \log K'_D \qquad (14)$$

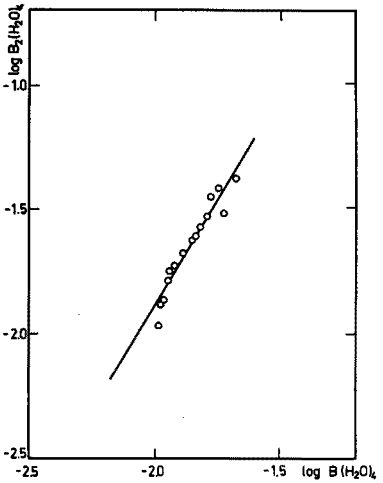

Fig. 11. Existence of a dimer in the concentrated TLMA·Cl solutions.

$$[\mathrm{B}\cdot(\mathrm{H_2O})_4] = \{\tfrac{9}{2}\,[\mathrm{B}]_\mathrm{T} - ([\mathrm{H_2O}]_\mathrm{T} - [\mathrm{H_2O}])\}\cdot 2\,K'_{3,4}/(3+K'_{3,4}) \qquad (15)$$

$$[\mathrm{B_2}\cdot(\mathrm{H_2O})_9] = \tfrac{1}{3}\{[\mathrm{H_2O}]_\mathrm{T} - [\mathrm{H_2O}] - 3[\mathrm{B}]_\mathrm{T} - [\mathrm{B}\cdot(\mathrm{H_2O})_4]\} \qquad (16)$$

Equation (14) is well verified, as is shown in Fig. 11 ($K'_\mathrm{D} = 130\ M^{-1}$).

However, it should be reiterated that some other explanations are certainly possible; only one of the more obvious ones has been considered. I.r. and n.m.r. spectroscopy are consistent with the water titration experiments. In Fig. 10, a curvature appears for $[\mathrm{TLMA\cdot Cl}]_\mathrm{T} > 7\cdot 10^{-2}\ M$ and around the same concentration, a "hump" in the chemical shift curve of the water peak is observed (Fig. 7). Such n.m.r. discontinuities have been pointed out in the literature[11].

Neither the i.r. nor the n.m.r. spectra allow a definite formula to be ascribed to the complexes. Figures 7 and 10 cannot be interpreted in a quantitative manner because there are too many unknowns. It can be proposed, however, that the chloride ion is associated with a "water polymer" in which there remain only a few free OH bonds (since the intensity of the peak attributed to these bonds is very weak). MOHR *et al.*[4] have proposed such a type of complex for the fluoride ion.

Very few papers deal with the aggregation of quaternary ammonium salts. Cryoscopic measurements by COPENHAFER AND KRAUS[12] with solutions of some short-chain quaternary ammonium salts in benzene have shown that the degree of association may be as high as 20. BAC[13], in a study of tricaprylmethylammonium nitrate, found a dimer for benzene solutions around $5\cdot 10^{-2}\ M$ and a trimer existing up to $4\cdot 10^{-1}\ M$. GOOD AND SRIVASTAVA[14] have shown that tricaprylammonium chloride in toluene is a monomer at $2\cdot 10^{-2}\ M$. In more concentrated solutions, it dimerizes rapidly and at $5\cdot 10^{-2}\ M$, higher polymers were found. Finally, since quaternary ammonium salts are less saturated molecules than tertiary amines, the former are probably more associated[15]. Such an aggregation would certainly exist in the lower part of our curves ($[\mathrm{TLMA\cdot Cl}]_\mathrm{T} < 7\cdot 10^{-2}\ M$). Thus, water bridges between quaternary ammonium salts do not seem to be the major factor of polymer formation. The dimer which allows the experimental results to be explained certainly exists with much higher polymers owing to dipole–dipole interactions. However, in the most concentrated range, water seems to interact from one polymer to another.

In conclusion, although water is not the main factor in the aggregation of quaternary ammonium salts, it may not be neglected in aggregation measurements of the most hydrated salts.

The financial support provided by the Fonds National de la Recherche Scientifique and the Institut Interuniversitaire des Sciences Nucléaires is gratefully acknowledged. The author expresses his sincere thanks to Prof. G. DUYCKAERTS for helpful suggestions and to Dr. J. R. PETERSON for help with the English manuscript.

SUMMARY

The hydration of carbon tetrachloride solutions of two quaternary ammonium salts has been investigated by Karl Fischer titrations and by i.r. and n.m.r. spectroscopy. Trilaurylmethylammonium thiocyanate seems to exist mainly as a monohydrate and the associated water does not seem to play a role in the aggregation of the salt, at least in water-saturated solutions. On the other hand, trilaurylmethyl-

ammonium chloride is found in the form of several polyhydrated species in which water does influence the aggregation but certainly much less than expected from dipole–dipole interactions. Thus water cannot be neglected in aggregation measurements of quaternary ammonium salts.

RÉSUMÉ

On a étudié l'hydratation du thiocyanate et du chlorure de trilaurylméthylammonium en solution dans le tétrachlorure de carbone par la méthode de Karl Fischer et par spectroscopie i.r. et r.m.n. Pour le premier de ces composés, l'eau ne semble pas jouer de rôle dans l'agrégation du sel. Par contre, pour le second, on ne peut négliger la présence de l'eau dans les mesures d'agrégation.

ZUSAMMENFASSUNG

Die Hydratbildung von Trilaurylmethylammonium-thiocyanat und -chlorid in Tetrachlorkohlenstoff wurde nach Karl Fischer und durch i.r.- und k.m.r.-Spektroskopie untersucht. Wasser scheint bei der Aggregatbildung des Thiocyanates keine Rolle zu spielen, bei der des Chlorids kann man seinen Einfluss jedoch nicht vernachlässigen.

REFERENCES

1 E. Horwitz, L. Sauro and C. Bloomquist, *J. Inorg. Nucl. Chem.*, 29 (1967) 2033.
2 F. L. Moore, *Anal. Chem.*, 41 (1969) 1658.
3 J. F. Desreux, *Anal. Chim. Acta*, 52 (1970) 207.
4 S. Mohr, W. Wilk and G. Barrow, *J. Amer. Chem. Soc.*, 87 (1965) 3048.
5 W. Müller and G. Duyckaerts, *Euratom Report*, 2246e (1965).
6 G. Roland and G. Duyckaerts, *Spectrochim. Acta*, 24A (1968) 529.
7 G. Roland and G. Duyckaerts, *Spectrochim. Acta*, 22 (1966) 793.
8 T. Lin, S. Christian and H. Affsprung, *J. Phys. Chem.*, 71 (1967) 968.
9 T. Lin, S. Christian and H. Affsprung, *J. Phys. Chem.*, 69 (1965) 2980.
10 J. Hindman, *J. Chem. Phys.*, 44 (1966) 4582.
11 J. Pople, W. Schneider and H. Bernstein, *High-Resolution Magnetic Resonance*, McGraw-Hill, New York, 1959.
12 D. Copenhafer and C. Kraus, *J. Amer. Chem. Soc.*, 73 (1951) 4557.
13 R. Bac, *Radiochim. Acta*, 9 (1968) 130.
14 M. Good and S. Srivastava, *J. Inorg. Nucl. Chem.*, 27 (1965) 2429.
15 R. Diamond, in *Solvent Extraction Chemistry*, North Holland, Amsterdam, 1967, p. 349.

Analytica Chimica Acta
Elsevier Publishing Company, Amsterdam
Printed in The Netherlands

SPECTROPHOTOMETRIC DETERMINATIONS OF IRON(III), MOLYBDENUM(VI) AND VANADIUM(V) IN PRESENCE OF EACH OTHER AND OTHER IONS WITH 1-(2-CARBOXY-4-SULPHONATOPHENYL)-3-HYDROXY-3-PHENYLTRIAZENE AS REAGENT

A. K. MAJUMDAR AND D. CHAKRABORTI
Department of Inorganic and Analytical Chemistry, Jadavpur University, Calcutta-32 (India)

(Received June 25th, 1970)

The triazenes, such as 3-hydroxy-1,3-diphenyltriazene[1] and 3-hydroxy-1-*p*-chlorophenyl-3-phenyltriazene[2] find applications as analytical reagents for the gravimetric determinations of copper, palladium and nickel. The latter reagent has also been found suitable for the gravimetric determination of titanium; since the titanium complex is not of any definite composition, ignition to the oxide as the weighing form is essential. The complexes derived from the *o*-chloro analogue are less stable, but if the chloro group at the *ortho*-position is substituted by a carboxy group, the resultant molecule, 1-(*o*-carboxyphenyl)-3-hydroxy-3-phenyltriazene, becomes an effective reagent for the direct gravimetric determination of titanium[3]. It is also a good spectrophotometric reagent for the extraction and determination of iron(III), titanium(IV) and vanadium(V) in presence of each other and of other ions[4].

The metal complexes of all the above reagents can be extracted by organic solvents, and by such extractions some selectivity can be achieved. However, a water-soluble reagent is more advantageous for general analytical work, because various complexing agents can then be employed to mask the effect of foreign ions. In this paper, the methods developed for the spectrophotometric determination of iron(III), molybdenum(VI) and vanadium(V) in presence of each other and of other ions, with the use of a new reagent 1-(2-carboxy-4-sulphonatophenyl)-3-hydroxy-3-phenyltriazene (sodium salt) are described. Curiously, in contrast to the earlier reagent[3,4], this reagent does not give any coloured reaction with titanium in acidic medium, whereas the earlier reagent does not react with molybdenum(VI).

With iron(III) at pH 3.3–4.5, the reagent forms a bluish violet complex which, with maximum absorbance at 410 nm, obeys Beer's law from 0.5–12 p.p.m. of iron; the optimum concentration range[5] is 1–12 p.p.m. The complex contains, as determined by conventional methods[6,7], a metal:reagent ratio of 1:2, and the instability constant is $3.48 \cdot 10^{-8}$. The sensitivity[8] of the reaction is 0.0108 μg Fe cm^{-2} with the molar absorptivity of 5275.

The yellow-green molybdenum(VI) complex of the reagent formed at pH 3.0–4.2 shows maximum absorbance at 405 nm. It obeys Beer's law from 1–12 p.p.m. with the optimum range from 2–12 p.p.m. of molybdenum. The coloured species, with a sensitivity of 0.0207 μg Mo cm^{-2} and a molar absorptivity of 4812, contains a metal: reagent ratio of 1:2, whose instability constant is in the order of $2.526 \cdot 10^{-7}$.

The yellow complex of vanadium(V) obtained at pH 3.0–6.5 shows maximum absorbance at 405 nm and the coloured system at this wavelength follows Beer's law from 0.5–6.0 p.p.m. The optimum range of concentration is 1–6 p.p.m. of vanadium(V). The metal combines with the reagent in a 1 : 1 ratio with a dissociation constant of the order of $2.11 \cdot 10^{-4}$. The reaction sensitivity is 0.0078 μg V cm^{-2} and the molar absorptivity is 6623.

EXPERIMENTAL

Apparatus and solutions

A Unicam SP 600 spectrophotometer with 1-cm cells and a Cambridge pH meter were used for the measurements of the absorbances and pH values of the solutions, respectively.

Twice-distilled water was used in all solution preparations.

A standard iron(III) solution was prepared by dissolving AnalaR iron(III) chloride in 0.1 *M* hydrochloric acid. The solution was standardized by the classical tin(II) chloride–potassium dichromate method[9].

Molybdenum(VI) and vanadium(V) solutions were prepared from their ammonium salts (AnalaR) by the addition of dilute ammonia solution as required. The solutions were standardized, respectively, by the gravimetric method with 8-hydroxyquinoline[9] and by titration with permanganate[10].

Weaker solutions of the metal ions, when required, were prepared by proper dilution.

The reagent was prepared as 0.5% and 0.25% (w/v) solutions in water.

Solutions of other diverse ions were prepared by dissolving analytical-grade chlorides, sulphates or nitrates of cations in water or dilute hydrochloric acid, and the sodium or potassium salts of the anions in water.

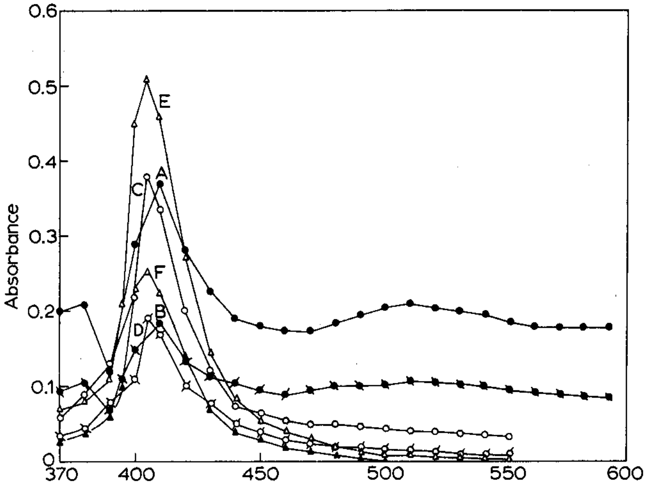

Fig. 1. Absorbance curves. (A) Fe(III) 4 p.p.m. (●); (B) Fe(III) 2 p.p.m. (●); (C) Mo(VI) 8 p.p.m. (○); (D) Mo(VI) 4 p.p.m. (ø); (E) V(V) 4 p.p.m. (△); (F) V(V) 2 p.p.m. (▲).

Absorbance curves

Iron(III). To the iron solution (100 or 50 μg of Fe) in a 50-ml beaker, add 3 ml of the reagent (0.5% w/v) solution, and adjust the pH with dilute hydrochloric acid to 3.5–4.0. Afterwards, transfer the solution to a 25-ml volumetric flask, dilute to the mark with water, mix thoroughly and measure the absorbance of the bluish violet complex against the reagent solution as blank. Curves A and B in Fig. 1 show that the absorbances of the colour systems, corresponding to 4 and 2 p.p.m. of iron(III), are maximal at 410 nm.

Molybdenum(VI). Mix the solution containing 200 or 100 μg of molybdenum(VI) with 7 ml of the reagent (0.25% w/v) and add 10 ml of distilled water. Add dilute hydrochloric acid to adjust the pH to about 3.5. Dilute with water to 25 ml in a volumetric flask, and measure the absorbance against the reagent solution as blank. The yellowish green complex was found to have maximum absorbance at 405 nm (curves C and D in Fig. 1).

Vanadium(V). Mix the solution containing 100 or 50 μg of vanadium(V) with 3 ml of the reagent solution (0.25% w/v) and 10 ml of distilled water. Adjust the pH of the solution to about 4, dilute to 25 ml in a volumetric flask, and measure the absorbance. The absorbance spectra (curves E and F in Fig. 1) show maximum absorbance at 405 nm.

RESULTS AND DISCUSSION

Effect of pH, reagent and time

The colour intensities of the systems remain the same in the pH ranges 3.3–4.5 for iron(III), 3.0–4.2 for molybdenum(VI) and 3.0–6.5 for vanadium(V). The intensity increases if the pH of the iron(III) system is taken above 4.5, but for the systems with molybdenum(VI) and vanadium(V), the intensity decreases if the pH is raised above 4.2 and 6.5, respectively.

For the complete development of the colour intensity, 4 p.p.m. of iron(III) requires 3 ml of 0.5% (w/v) reagent solution, whereas the optimal amounts of the reagent solution (0.25% w/v) for 8 p.p.m. of molybdenum(VI) and 4 p.p.m. of vanadium(V) are, respectively, 7 and 3 ml.

The colour of iron(III) system is stable for 12 h while those of molybdenum(VI) and vanadium(V) are stable for 20 and 15 h, respectively.

Beer's law, optimum range, photometric errors, sensitivity and molar absorptivity

The iron, molybdenum and vanadium colour systems obey Beer's law over the ranges 0.5–12.0 p.p.m., 1–12 p.p.m., and 0.5–6.0 p.p.m. and the optimum concentration ranges as obtained from the steepest slope of the curves drawn on plotting percentage absorbances against log concentration as discussed by RINGBOM[5] are, respectively, 1–12, 2–12, and 1–6 p.p.m. (Fig. 2).

The percentage relative errors per 1% absolute photometric error[11] for the systems are 2.66% for iron(III); 2.68% for molybdenum(VI) and 2.74% for vanadium(V). The sensitivities, log $I_0/I = 0.001$, calculated as described by SANDELL[8], are 0.0108 μg cm^{-2} for iron(III), 0.0207 μg cm^{-2} for molybdenum(VI), and 0.0078 μg cm^{-2} for vanadium(V) with molar absorptivities as 5275, 4812 and 6623, respectively.

Composition of the complexes

The composition of the iron, molybdenum and vanadium complexes was determined by the modified Job's method of continuous variation[6] and by the mole ratio method[7].

In the first method, equimolar solutions of the metal ion and reagent were

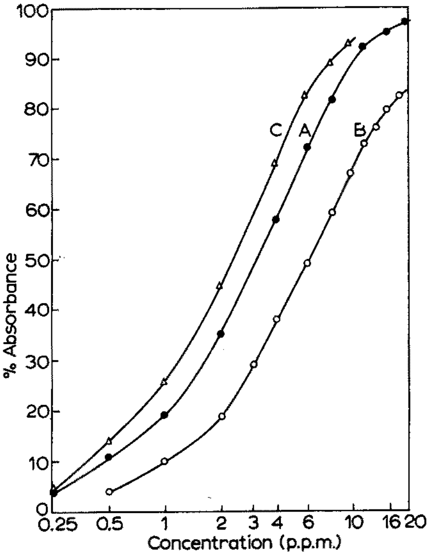

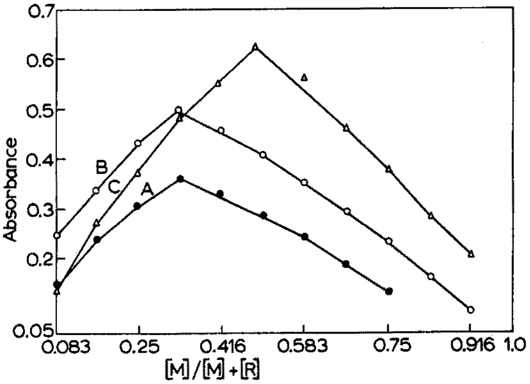

Fig. 2. Ringbom plots. (A) Fe(III); (B) Mo(VI); (C) V(V).

Fig. 3. Composition by Job's method (equimolar). (A) [Fe(III)] = [reagent] = $1 \cdot 10^{-3}$ *M*; (B) [Mo(VI)] = [reagent] = $1.5 \cdot 10^{-3}$ *M*; (C) [V(V)] = [reagent] = $5 \cdot 10^{-4}$ *M*.

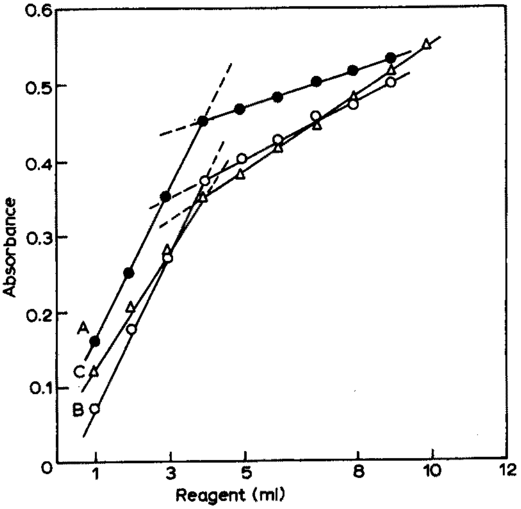

Fig. 4. Composition by mole ratio method. (A) [Fe(III)] = [reagent] = $2.5 \cdot 10^{-3}$ *M*, 2 ml of Fe(III) solution used; (B) [Mo(VI)] = [reagent] = $2.5 \cdot 10^{-3}$ *M*, 2 ml of Mo(VI) solution used; (C) [V(V)] = [reagent] = $5 \cdot 10^{-4}$ *M*, 4 ml of V(V) solution used.

mixed in complementary proportions to a total volume of 12 ml. After suitable adjustment of the pH values, the mixtures were diluted to 25 ml with distilled water and their absorbances were measured at 410 nm for iron(III), and at 405 nm for molybdenum(VI) and vanadium(V). The peaks of the curves plotted (Fig. 3) show that iron(III) and molybdenum(VI) combine with the reagent in the ratio 1:2, while vanadium (V) maintains a ratio of 1:1 with the reagent.

The mole ratio method (Fig. 4) allowed these compositions to be confirmed in all cases.

Degree of dissociation and instability constants

The values of α, the degree of dissociation, were calculated from HARVEY AND MANNING's equation[12]. The instability constants evaluated from the equation $K=(m\,\alpha\,c)^m(n\,\alpha\,c)^n/c(1-\alpha)$, where $m=n=1$ for vanadium(V) and $m=1$, $n=2$ for iron(III) and molybdenum(VI) are given in Table I.

TABLE I

INSTABILITY CONSTANTS OF 1-(2-CARBOXY-4-SULPHONATOPHENYL)-3-HYDROXY-3-PHENYLTRIAZENE COMPLEXES.

Complex	E_m	E_s	c	α	K
Fe(III)	0.50	0.45	$2.5\cdot10^{-3}$	0.1	$5.5\cdot10^{-8}$
Mo(VI)	0.50	0.37	$2.5\cdot10^{-3}$	0.26	$4.5\cdot10^{-7}$
V(V)	0.55	0.35	$5.0\cdot10^{-4}$	0.364	$1.0\cdot10^{-4}$

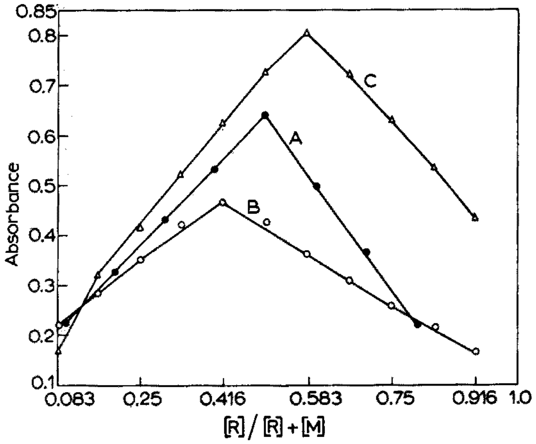

Fig. 5. Job's method for dissociation constants. (A) [Fe(III)]$=1.0\cdot10^{-3}$ *M*, [reagent]$=2.5\cdot10^{-3}$ *M*; (B) [Mo(VI)]$=1.0\cdot10^{-3}$ *M*, [reagent]$=2\cdot10^{-3}$ *M*; (C) [V(V)]$=0.5\cdot10^{-3}$ *M*, [reagent]$=1.0\cdot10^{-3}$ *M*.

The dissociation constants of the complexes were also evaluated from a study of the absorbances of the complementary mixtures of non-equimolar solutions of the metal ions and the reagent (Fig. 5). The colour of the solutions were developed as described previously. The dissociation constants were calculated from the equation of MAJUMDAR AND SEN[13]. The results are given in Table II.

TABLE II

DISSOCIATION CONSTANTS OF COMPLEXES

Metal concentration (·10^3 *M*)		*Reagent concentration* (·10^3 *M*)	*m*	*n*	*p*	*x*	*K at 31°*
Fe(III)	1.0	2.5	1	2	2.5	0.5	$3.48 \cdot 10^{-8}$
Mo(VI)	1.0	2.0	1	2	2	0.58	$2.5 \cdot 10^{-7}$
V(V)	0.5	1.0	1	1	2	0.42	$2.1 \cdot 10^{-4}$

Effect of various ions

To evaluate the tolerance limits for different ions, solutions containing 4 p.p.m. of iron(III), 8 p.p.m. of molybdenum(VI) or 4 p.p.m. of vanadium(V) in acidic medium were prepared with varying amounts of other ions; the procedures followed for the absorbance measurements were as described above. Absorbances differing by 0.005 from the required value were considered to represent interferences.

Phosphate, fluoride, oxalate, citrate, EDTA, tartrate and thiosulphate, form complexes in acidic medium with iron(III) and hence must be absent during the determination of iron(III). The tolerance limits, given in p.p.m. in parentheses, for other ions are: Al^{3+}(20), UO_2^{2+}(200), Mg^{2+}(300), Hg^{2+}(160), Ce^{3+}(200), WO_4^{2-}(20), Zn^{2+}(200), Th^{4+}(80), Ca^{2+}(160), Ti^{4+}(100), Be^{2+}(200), Sr^{2+}(200), As^{3+}(100), Pt^{4+}(200), Cr^{3+}(100), La^{3+}(40), Mn^{2+}(80), Cd^{2+}(360), Ba^{2+}(400), Ni^{2+}(20) and Co^{2+}(30). Copper(II), palladium(II), molybdate and vanadate interfere by forming coloured complexes.

For the molybdenum system, phosphate, fluoride, oxalate, citrate, EDTA and tartrate interfere as do Pd^{2+}, V^{5+}, Cu^{2+} and Fe^{3+} which form coloured products. The tolerance limits of other ions, given in parentheses in p.p.m. are: WO_4^{2-} (80), Ni^{2+}(30), Mn^{2+}(100), Co^{2+}(40), Al^{3+}(30), UO_2^{2+}(160), Mg^{2+}(250), Hg^{2+}(120), Ce^{3+}(50), Zn^{2+}(240), Th^{4+}(40), Ca^{2+}(100), Ti^{4+}(80), Be^{2+}(200), Sr^{2+}(250), As^{3+}(160), Pt^{4+}(200), La^{3+}(50), Cr^{3+}(80), Cd^{2+}(160) and Ba^{2+}(400). Thiosulphate does not interfere.

In the vanadium(V) colour system only EDTA, oxalate, Pd^{2+}, Cu^{2+} and Fe^{3+} interfere and hence must be absent. The system is unaffected by the presence of the following ions, the tolerance limits of which are given in p.p.m. in parentheses: citrate(200), tartrate (200), F^-(>400), PO_4^{3-}(>400), Th^{4+}(200), Zn^{2+}(200), Ce^{3+}(40), Mg^{2+}(240), UO_2^{2+}(200), Al^{3+}(20), Hg^{2+}(150), Mn^{2+}(80), WO_4^{2-}(100), Ca^{2+}(120), Ti^{4+}(100), Be^{2+}(200), Sr^{2+}(200), Cd^{2+}(100), Ba^{2+}(300), As^{3+}(120), Pt^{4+}(160), La^{3+}(30), Cr^{3+}(40). Thiosulphate does not interfere. Nickel(II) and cobalt(II) interfere if the absorbances are measured above pH 4.5, but below pH 4.5 they have no effect. Molybdenum(VI), however, can be tolerated upto 80 p.p.m. if measurements are made at pH 6.3–6.5.

Li^+, Na^+, K^+, Br^-, I^-, Cl^-, SCN^- have no interference in any of the three systems.

Determination of iron(III), molybdenum(VI) and vanadium(V) in presence of each other

Procedures for the determination of these three ions in presence of each other were developed with the use of complexing agents, *e.g.* thiosulphate for iron(III) and sodium fluoride for both molybdenum(VI) and iron(III). The colour intensities for the molybdenum(VI) and vanadium(V) systems were measured at 410 nm, because at this wavelength, the absorption of the reagent itself was less than that observed at 405 nm.

Procedure. Dilute the solution containing all three metal ions to a definite volume in a calibrated flask. Take an aliquot of the solution in a 50-ml beaker, mix with about 5 ml of the reagent solution (0.5% w/v) and adjust to pH 3.5–4.0. Transfer the solution to a 25-ml flask, dilute to volume with distilled water and measure the absorbance at 410 nm against the reagent solution as blank. This gives the amount of the total metal ions (A) present in the aliquot.

To another aliquot, add 5 ml of a 1% (w/v) sodium thiosulphate pentahydrate solution and then follow the above procedure, except that the pH of the solution should be adjusted to 3.0–3.7. This gives the total amount (B) of molybdenum and vanadium present in the aliquot.

In the same way, to another aliquot add 5 ml of a 2% (w/v) sodium fluoride solution and then proceed as above with adjustment of pH to 3.0–6.5. From this, only the amount of vanadium (C) present is obtained. By subtracting (C) from (B), and (B) from (A), the respective amounts of molybdenum and iron are obtained.

The results obtained for various concentrations of the three ions in mixtures are shown in Table III.

TABLE III

SIMULTANEOUS DETERMINATION OF IRON(III), MOLYBDENUM(VI) AND VANADIUM(V)

Amount present (p.p.m.)	*Fe(III) found (p.p.m.)*	*Mo(VI) found (p.p.m.)*	*V(V) found (p.p.m.)*
2.0 Fe(III) 2.0 Mo(VI) 2.0 V(V)	1.947	1.929	2.00
1.0 Fe(III) 2.0 Mo(VI) 3.0 V(V)	0.967	1.982	2.98
3.0 Fe(III) 2.0 Mo(VI) 2.0 V(V)	3.02	2.04	1.946
1.0 Fe(III) 4.0 Mo(VI) 2.0 V(V)	0.972	4.03	2.00

SUMMARY

1-(2-Carboxy-4-sulphonatophenyl)-3-hydroxy-3-phenyltriazene is reported as an excellent spectrophotometric reagent for the determination of iron(III), molybdenum(VI) and vanadium(V). At pH values of 3.3–4.5, 3.0–4.2 and 3.0–6.5, iron(III), molybdenum(VI) and vanadium(V) form bluish violet, yellowish green and yellow complexes with maximum absorbances at 410, 405 and 405 nm, respectively. Beer's law is valid, with optimum ranges of 1–12 p.p.m. for iron(III), 2–12 p.p.m. for molybdenum(VI), and 1–6 p.p.m. for vanadium(V); the percentage relative errors are 2.66, 2.68 and 2.74, respectively. Iron(III) and molybdenum(VI) form 1:2 complexes with the reagent, and vanadium(V) forms a 1:1 complex; the instability constants of the complexes are of the order 10^{-8}, 10^{-7} and 10^{-4}, respectively. Effects of other anions and cations on the colour systems are listed, and a procedure for the determination of iron, molybdenum and vanadium in presence of each other is described.

RÉSUMÉ

Le 1-(2-carboxy-4-sulfophényl)-3-hydroxy-3-phényltriazène est présenté comme un excellent réactif spectrophotométrique pour le dosage du fer(III), du molybdène(VI) et du vanadium(V). Aux pH 3.3–4.5, 3.0–4.2 et 3.0–6.5, le fer(III), le molybdène(VI) et le vanadium(V) forment des complexes (violet bleu, vert jaune et jaune, respectivement), avec absorption maximum à 410, 405 et 405 nm. La loi de Beer s'applique de 1 à 12 p.p.m. pour le fer(III), 2 à 12 p.p.m. pour le molybdène(VI) et 1 à 6 p.p.m. pour le vanadium(V). Le pourcentage d'erreur relative est respectivement de 2.66, 2.68 et 2.74. Fer(III) et molybdène(VI) avec ce réactif forment des complexes 1:2, vanadium(V) des complexes 1:1. Les constantes d'instabilité de ces complexes sont respectivement 10^{-8}, 10^{-7} et 10^{-4}. On examine également l'influence d'autres anions et cations. Une méthode est proposée pour le dosage du fer, du molybdène et du vanadium, les unes en présence des autres.

ZUSAMMENFASSUNG

1-(2-Carboxy-4-sulfonatophenyl)-3-hydroxy-3-phenyltriazen ist ein ausgezeichnetes spektrophotometrisches Reagenz für die Bestimmung von Eisen(III), Molybdän(VI) und Vanadin(V). Eisen(III) bildet bei pH 3.3–4.5 einen bläulich-violetten, Molybdän(VI) bei pH 3.0–4.2 einen gelblich-grünen und Vanadin(V) bei pH 3.0–6.5 einen gelben Komplex. Die maximalen Extinktionen liegen bei 410, 405 und 405 nm. Das Beersche Gesetz ist gültig; die optimalen Bereiche sind 1–12 p.p.m. für Eisen(III), 2–12 p.p.m. für Molybdän(VI) und 1–6 p.p.m. für Vanadin(V); die prozentualen relativen Fehler sind 2.66, 2.68 und 2.74. Eisen(III) und Molybdän(VI) bilden mit dem Reagenz 1:2-Komplexe, Vanadin(V) bildet einen 1:1-Komplex. Die Instabilitätskonstanten der Komplexe sind in der Grössenordnung 10^{-8}, 10^{-7} und 10^{-4}. Die Einflüsse anderer Anionen und Kationen auf die gefärbten Systeme sind untersucht worden. Es wird ein Verfahren für die Bestimmung von Eisen, Molybdän und Vanadin nebeneinander beschrieben.

REFERENCES

1 N. C. Sogani and S. C. Bhattacharyya, *Anal. Chem.*, 28 (1956) 81.
2 N. C. Sogani and S. C. Bhattacharyya, *Anal. Chem.*, 28 (1956) 1616.
3 A. K. Majumdar and S. C. Saha, *Anal. Chim. Acta*, 40 (1968) 299.
4 A. K. Majumdar and S. C. Saha, *Anal. Chim. Acta*, 44 (1969) 85.
5 A. Ringbom, *Z. Anal. Chem.*, 115 (1938/39) 332.
6 J. Job, *Compt. Rend.*, 180 (1925) 928; *Ann. Chim. (Paris)*, 9 (1928) 113.
7 J. H. Yoe and A. K. Jones, *Ind. Eng. Chem., Anal. Ed.*, 16 (1944) 111.
8 E. B. Sandell, *Colorimetric Determination of Traces of Metals*, 3rd Edn., Interscience, New York, 1959.
9 A. I. Vogel, *A Text Book of Quantitative Inorganic Analysis*, 3rd Edn., Longmans Green, London, 1962.
10 G. Charlot and D. Bezier, *Quantitative Inorganic Analysis*, 3rd Edn., John Wiley, New York, 1957.
11 G. H. Ayres, *Anal. Chem.*, 21 (1949) 652.
12 A. E. Harvey, Jr. and D. L. Manning, *J. Am. Chem. Soc.*, 72 (1950) 4488; 74 (1952) 4744.
13 A. K. Majumdar and B. Sen, *Anal. Chim. Acta*, 8 (1953) 369.

Anal. Chim. Acta, 53 (1971) 127–134

Analytica Chimica Acta
Elsevier Publishing Company, Amsterdam
Printed in The Netherlands

DETERMINATION OF CHLORINE IN POLYPROPYLENE AFTER SODIUM HYDROXIDE REFLUXING

R. J. NADALIN AND M. L. THEODORE
Westinghouse Research Laboratories, Pittsburgh, Pa. 15235 (U.S.A.)

(Received July 16th, 1970)

Polypropylene is used in various applications by the Westinghouse Electric Corporation. Since the properties of this material are dependent on a low concentration of chlorine, determination of the total chlorine content of the polypropylene is essential.

The oxygen bomb procedure[1] used for determination of the total chlorine content of polymeric materials is well suited for chlorine contents greater than 10 p.p.m. but, owing to the limitation on sample size, is marginal for samples with contents less than 10 p.p.m. Consequently, an alternative method was needed for the polypropylene samples which might contain less than 10 p.p.m. chlorine.

Only a few studies have been reported for the determination of chlorine in polypropylene[2-4]. The determination of chlorine in other polymeric materials, however, has been accomplished in various ways. In most methods, the chlorine is first freed from the polymer and is determined in a second step.

For freeing the chlorine from the polymeric matrix, the following methods have been reported: fusion with sodium peroxide[5-8], with sodium[9-11], with sodium carbonate[12], with a mixture of sodium carbonate and sodium peroxide[13,14], or with a mixture of sodium carbonate, potassium carbonate and magnesium oxide[15]; combustion in oxygen in a bomb[1], in a heated tube[16-19], or in a Schöniger flask[20-22]; ashing with a flux[23]; pyrolysis[24-27], or heating in a stream of inert gas[28]; oxidative acid attack in a sealed[29] or in a closed system[30]; alkaline refluxing[31] with dioxane and ethylene glycol[32,33], with acetone[34], or with methanol[1]; and Soxhlet extraction with ether[35].

From all of these procedures, the liberated chlorine is obtained as chloride ion in an alkaline solution and is usually determined by an argentimetric titration, either by the Volhard or a potentiometric procedure. Colorimetric procedures, for either chloride[2,4] or silver[23], have been used for determining trace amounts of chlorine in polymers.

X-Ray fluorescence[36,37] and neutron activation[38,39] methods have also been reported for chlorine determination in certain polymers.

Many of the above methods are not suitable for the routine determination of trace amounts of chlorine in polypropylene because of the inert character of this polymer and because of the sample size limitations and/or the high chlorine blank inherent in many of these methods.

The problem of the determination of trace amounts of hydrolyzable chlorine in insulating liquids had been previously considered in this laboratory, and a sodium hydroxide reflux method for hydrolyzable chlorine has been developed[40]. A similar method, but followed by titration of the excess base, has also been used as an industrial procedure[41] to obtain the hydrolyzable chlorine content of epoxy resins. The chlorine content of the polypropylene is derived from the metallic chlorides used in the catalytic polymerization of the polymer. The chlorine may be substituted into the polymer molecule itself or simply trapped as inorganic catalyst. The sodium hydroxide reflux method would free the chlorine occurring in either of these ways.

The proposed method consists of extraction of the sample by a mixture of methanolic sodium hydroxide and xylene under reflux conditions followed by a potentiometric titration of the chloride in the extracted solution with standard silver nitrate solution after addition of acetone to reduce the solubility of the silver chloride. Since the reliability of the potentiometric chloride titration is well established, the present work was confined to the study of finding convenient and reliable conditions for the quantitative extraction of the chlorine from the polypropylene.

EXPERIMENTAL

Apparatus

Beckman Expandomatic pH Meter with a silver chloride-coated silver electrode and a calomel electrode filled with potassium nitrate solution.

Reagents

Analytical-reagent grade chemicals were used throughout.

Standard silver nitrate solution, 0.01 M. Dissolve 1.699 g of silver nitrate in 1 l of chloride-free deionized water, and standardize against reagent-grade sodium chloride dried for 2 h at 600°.

Wash water. Chloride-free deionized water. No turbidity should be obtained when tested with silver nitrate.

Procedure

Carefully cut the polypropylene into small pieces, using plastic gloves and tweezers for all handling. Weigh a 5-g sample to the nearest mg, and transfer it to a 300-ml flat-bottom reflux flask with 24/40 Ts joints, fitted with a water-cooled condenser. Add 67 ml of xylene and 33 ml of methanolic sodium hydroxide (0.1 *M*). Heat the mixture and reflux for 2 h after the start of boiling. After cooling, decant the solution into a 250-ml beaker using 100 ml of acetone to rinse the flask and sample, and add 3.0 ml of 1+1 nitric acid. Place the electrodes and glass-coated magnetic stirring bar in the solution, and, while stirring continuously, titrate the chloride content of the solution with a standard 0.01 *M* silver nitrate solution added from a 5-ml microburette. After each titrant addition of 0.02 or 0.01 ml near the end-point, measure the potential to 1 mV after waiting for equilibrium. Also titrate a reagent blank using 0.01-ml titrant additions. Establish the end-point graphically to 0.001 ml, by taking the midpoint of the steepest part of the titration curve obtained by plotting the potential *vs.* the volume of titrant added. The blank determination is very important for precise low chloride determination, and the utmost care must be taken in handling the sample and cleaning the apparatus to insure no chloride contamination.

RESULTS AND DISCUSSION

The xylene swells and partially dissolves the polypropylene, but the sodium hydroxide which reacts with chlorine is not soluble in xylene. Methanol, however, dissolves the sodium hydroxide and when heated is miscible with xylene. The possibility of completely dissolving the sample in xylene and then adding the methanolic sodium hydroxide was tried. However, this treatment resulted in the precipitation of the polypropylene in such a way that the solution could not be decanted, and low chlorine results were obtained after filtration. This approach was abandoned.

TABLE I

CONCENTRATION OF SODIUM HYDROXIDE *vs.* RECOVERY OF CHLORINE

(Reflux solution, 67 vol. % xylene, 33 vol. % methanolic NaOH; reflux time, 2 h)

M NaOH	0.01	0.01	0.03	0.03	0.05	0.10
Cl recovery (%)	110	92	97	100	105	110

TABLE II

XYLENE–METHANOL RATIO OF REFLUX SOLUTION *vs.* RECOVERY OF CHLORINE

(Reflux solution, 0.033 M NaOH; reflux time, 2 h)

Xylene (vol. %)	67	50	33
Alc. NaOH (vol. %)	33	50	67
Cl recovery (%)	97	89	89

TABLE III

REFLUX TIME *vs.* RECOVERY OF CHLORINE

(Reflux solution, 67 vol. % xylene, 33 vol. % methanolic NaOH, 0.033 M NaOH; reflux time, 2 h)

Time (h)	0.5	1.0	1.5	2.0
Cl recovery (%)	19	27	50	112

TABLE IV

VOLUME OF REFLUX SOLUTION *vs.* RECOVERY OF CHLORINE

(Conditions as for Table III)

Volume (ml)	100	150
Cl recovery (%)	119	112

The recovery of chlorine under various experimental conditions was studied. The following factors were investigated: normality of sodium hydroxide in mixture, ratio of xylene to methanolic sodium hydroxide, refluxing time, and volume of refluxing solution. The polypropylene used for this study was analyzed by the oxygen bomb procedure numerous times, and the average value obtained was used as the total chlorine content to which the values obtained by the reflux method were compared. The results of these experiments are shown in Table I through IV. There are several sets of conditions for which quantitative chlorine extraction is achieved. The most convenient conditions which gave complete recovery of chlorine, were found to be a 2-h extraction time with 100 ml of an extracting solution consisting of 67 vol. % xylene and 33 vol. % methanolic sodium hydroxide which has a total sodium hydroxide concentration of 0.033 *M*.

Repetitive determination of the chlorine content of several samples was carried out using this procedure. The results are summarized in Table V.

TABLE V

RESULTS OF REPETITIVE CHLORINE ANALYSES

Sample	*Average chlorine found (p.p.m.)*	*Standard deviation (p.p.m.)*	*Range (p.p.m.)*	*No. of detns.*
A	27.8	2.7	8	12
B	10.4	2.1	6	7

TABLE VI

COMPARISON OF CHLORINE RESULTS

Sample	*Oxygen bomb (p.p.m. Cl)*	*Reflux method (p.p.m. Cl)*
A	25, 26, 27	27.8 (aver. of 12)
B	10	10.4 (aver. of 7)
C	20	17, 16
D	67	69
E	13, 14	12, 12

Since no polypropylene samples were available for which the total chlorine content was known with certainty, it was not possible to determine the accuracy of the reflux method. However, several polypropylene samples were analyzed by both the oxygen bomb and the sodium hydroxide reflux methods. As is shown in Table VI, the methods give equivalent results.

Conclusions

The sodium hydroxide reflux extraction method is a reliable procedure for determining the total chlorine content of polypropylene. The estimated standard deviation of this method at the 10 and 28 p.p.m. chlorine levels was found to be 2.1 and 2.7 p.p.m.

The authors thank Dr. F. P. BYRNE for his helpful ideas and criticism and Mr. D. EVANCHO for performing some of the determinations.

SUMMARY

A sodium hydroxide reflux method for freeing the trace chlorine content of polypropylene before argentimetric titration of the chloride is presented. The estimated standard deviation of this method was found to be 2.1 and 2.7 p.p.m. at the 10 and 28 p.p.m. chlorine levels, respectively.

RÉSUMÉ

On propose un dosage de traces de chlore dans un polypropylène, par titrage argentimétrique du chlorure libéré par un traitement à l'hydroxyde du sodium, à reflux. La déviation standard estimée pour cette méthode est de 2.1 à 2.7 p.p.m. pour des teneurs en chlore de 10 et 28 p.p.m. respectivement.

ZUSAMMENFASSUNG

Es wird eine Rückflussmethode mit Natriumhydroxid für die Freisetzung der Chlorspuren in Polypropylen beschrieben. Das Chlorid wird argentometrisch titriert. Die Standardabweichung dieser Methode wurde zu 2.1 und 2.7 p.p.m. bei Gehalten von 10 bzw. 28 p.p.m. Chlor gefunden.

REFERENCES

1 *ASTM D 1638.*
2 V. Negina, E. Krasheninnokova, A. Mikhailini, K. Ratnikova and M. Dokuchaeva, *Zh. Analit. Khim.*, 22 (1967) 1552.
3 P. Maltese and L. Clementini, *Materie Plastiche*, 30 (1964) 803.
4 P. Maltese, L. Clementini and A. Mario, *Chim. Ind. (Milan)*, 49 (1967) 1070.
5 *ASTM D 1303 55.*
6 H. Sotobayzshi, *PB Report 152, 218*, 1962.
7 T. Koide, T. Kubota and Y. Umezawa, *J. Soc. Rubber Ind. Japan*, 24 (1951) 295.
8 J. Haslam and W. Suppet, *J. Soc. Chem. Ind. (London)*, 67 (1948) 33.
9 G. Petukhov and T. Guseva, *Zavodsk. Lab.*, 29 (1963) 806.
10 E. Schroder and R. Waurick, *Plaste Kautschuk*, 7 (1960) 9.
11 E. Meachan, T. Parks and H. Laitinen, *J. Polymer Sci.*, 1 (1946) 247.
12 M. Raman, G. Misra, S. Iyer and K. Balakrishna, *Indian J. Technol.*, 3 (1965) 234.
13 K. Stoeckhert, *Kunststoffe*, 37 (1947) 53.
14 G. Esposito, *Chem. Abstr.*, 55 (1959) 1060.
15 E. Khoroshzya, G. Kovrigina and L. Eliseeva, *Zavodsk. Lab.*, 30 (1964) 1450.
16 W. Phillips, *Plastics (London)*, 12 (1948) 587.
17 P. Henicksmen, E. VanKooten, R. Gardiner and W. Ashley, *U.S. At. Energy Comm., LA 2362*, 1959.
18 E. Seefield and J. Robertson, *Anal. Chim. Acta*, 23 (1960) 301.
19 M. Lardera, *Materie Plastiche*, 22 (1956) 804.
20 J. Fertig, *J. Appl. Polymer Sci.*, 2 (1959) 125.
21 J. Haslam, J. Hamilton and D. C. M. Squirrell, *J. Appl. Chem. (London)*, 10 (1960) 97.
22 J. Haslam, J. Hamilton and D. C. M. Squirrell, *Analyst*, 85 (1960) 556.
23 I. Ubaldina and F. Capizza-Maitan, *Chim. Ind. (Milan)*, 37 (1955) 779.
24 B. Cox and W. Criddle, *Brit. Plastics*, 37 (1964) 148.
25 D. Gurvich, V. Balandina, M. Palkina, I. Yurevskaya and M. Noskova, *Zavodsk. Lab.*, 32 (1966) 409.
26 K. Thinius, *Chem. Tech. (Berlin)*, 4 (1952) 44.
27 A. Tribot and R. Simon, *Chim. Anal. (Paris)*, 32 (1950) 31.
28 N. Parlashkevich, R. Gribkova, V. Bildina and T. Ivanovskaya, *Plasticheskie Massy*, 6 (1961) 55.
29 H. Homma and S. Emoto, *Chem. Abstr.*, 55 (1960) 26510.
30 J. Bather, *Analyst*, 81 (1956) 536.
31 *ASTM D 1726 62T.*
32 J. Urbanski and S. Iwanska, *Chem. Anal. (Warsaw)*, 9 (1964) 11.
33 L. Kalinina and M. Barulina, *Chem. Abstr.*, 59 (1963) 8935.
34 L. Kalinina and M. Barulina, *Plasticheskie Massy*, 6 (1961) 62.
35 J. Haslam and W. Suppet, *J. Appl. Chem. (London)*, 1 (1951) 112.
36 G. Smith and R. Maute, *Anal. Chem.*, 34 (1962) 1733.
37 G. Vos, *NASA Doc. N64-16926*, 1964.
38 J. Pauly and F. Girandi, *Bull. Soc. Chim. France*, (1963) 244.
39 V. Guinn, *Proc. Use Short-lived Radioisotope Reactors Seminar, Vienna*, 2 (1962) 3.
40 F. P. Byrne and K. W. Guardipee, *Mater. Res. & Std.*, 2 (1962) 825.
41 *Private communication*, Dow Chemical Co., Midland, Mich.

Analytica Chimica Acta
Elsevier Publishing Company, Amsterdam
Printed in The Netherlands

FEASIBILITY AND ERROR IN LINEAR EXTRAPOLATION TITRATION PROCEDURES

DONALD ROSENTHAL AND GEORGE L. JONES, JR.
Department of Chemistry, Clarkson College of Technology, Potsdam, N.Y. 13676 (U.S.A.)
AND
ROBERT MEGARGLE
Department of Chemistry, University of Missouri, Columbia, Mo. 65201 (U.S.A.)

(Received May 28th, 1970)

There are many titration procedures in which some property is measured which is proportional to the concentration of reactants and/or products. Usually the end-point is determined from the intersection of the straight lines obtained before and after the end-point when the measurements are plotted *versus* volume of titrant. Conductometric[1], amperometric[2,3], photometric[4] and dielectrometric[5] titrations are examples of the types of procedures in common use.

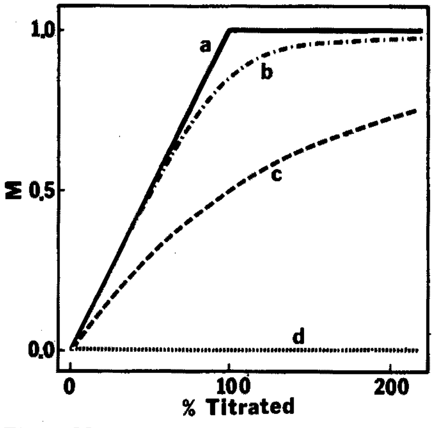

Fig. 1. Measurement *vs.* % titrated for the titration reaction $C + T \rightleftarrows P$.
(a) The titration reaction proceeds completely from left to right ($KC_t = \infty$); (b) the titration reaction proceeds somewhat less than completely ($KC_t = 40$); (c) the titration reaction proceeds rather incompletely ($KC_t = 2$); (d) the titration reaction does not proceed ($KC_t = 0$).

When the titration reaction does not proceed quantitatively from left to right, the experimental measurements will deviate from the "ideal" straight lines. These deviations will be particularly large near the stoichiometric point. In some instances, it may be possible to extrapolate the two straight lines obtained using *some* of the data before and after the stoichiometric point (Fig. 1, curve b). In other instances it may be difficult or impossible to distinguish two straight lines (Fig. 1, curves c and d).

Methods have been described which can be employed when the simple extrapolation procedure is not satisfactory[3,6–8]. This paper considers three principal topics: the conditions which must prevail to obtain reasonable accuracy with the extrapolation procedure, the theoretical error in such titrations when there is no significant error in the measurements, and the effect of measurement errors.

THEORY

The stoichiometric equation for the titration of a constituent, C, by a titrant, T, to yield products, P, can be represented

$$c\,\mathrm{C}+t\,\mathrm{T}\rightarrow p\,\mathrm{P} \tag{1}$$

The reaction may involve precipitation, oxidation–reduction, complexation, or salt formation by an acid and base. The measurement, M, is conductance, $1/R$, in conductometric titration; current, I, in amperometric titrations; absorbance, A, in photometric titrations and dielectric constant, ε [or $(\varepsilon-1)/(\varepsilon-2)$][5] in dielectrometric titrations. In general

$$M = b_1\,[\mathrm{C}]+b_2[\mathrm{T}]+b_3[\mathrm{P}]+b_4 \tag{2}$$

This equation expresses the linear relationship between the concentration of each species and the measurement being made. b_1, b_2, and b_3 are proportionality constants. The constant b_4 represents the contribution of non-reacting constituents in the original solution to the measurement. In some instances there may be an additional term which is proportional to the amount of titrant which has been added. For example, in the conductometric titration of sodium acetate by hydrochloric acid, the b_4 term represents the contribution of sodium ion to the conductance, and there will also be a term representing the contribution of chloride ion which will depend upon the amount of titrant added.

The nature of the titration curve will depend upon the following data.

(*a*) The formation constant for the titration reaction

$$K = \frac{[\mathrm{P}]^p}{[\mathrm{C}]^c\,[\mathrm{T}]^t} \tag{3}$$

For simplicity, any differences between activities and concentrations will be ignored, and K will be regarded as a concentration type equilibrium constant. (For precipitation, aqueous neutralization and analogous reactions which involve heterogeneous equilibria or the formation of solvent, eqns. (3) and (4) do not apply. This case will be considered in a subsequent publication.)

(*b*) The initial concentration, C_t, of the constituent, being determined.

(*c*) The values of the proportionality constants b_1, b_2, and b_3 and the constant term b_4.

It is assumed that:

(*i*) the concentration equilibrium constant, K, and the proportionality constants b_1, b_2 and b_3 are constant under the conditions of the titration;

(*ii*) the titrant is sufficiently concentrated that the volume of titrant added does not appreciably alter the total volume of the solution or the titrant is generated coulometrically without any significant volume change;

(*iii*) only one reaction occurs.

To simplify considerations further, a definite stoichiometry of $c=t=p=1$ will be considered for the reaction presented in eqn. (1).

$$K = \frac{[\mathrm{P}]}{[\mathrm{C}]\,[\mathrm{T}]} \tag{4}$$

If C_t represents the total concentration of the constituent which was initially present, at each point in the titration

$$C_t = [\mathrm{C}] + [\mathrm{P}] \tag{5}$$

If g represents the fraction of the stoichiometric amount of titrant which has been added, the "total concentration of titrant", T_t, is given by

$$T_t = [\mathrm{T}] + [\mathrm{P}] = g\,C_t \tag{6}$$

Substituting eqns. (5) and (6) into eqn. (4):

$$K = \frac{[\mathrm{P}]}{(C_t-[\mathrm{P}])\,(T_t-[\mathrm{P}])} = \frac{[\mathrm{P}]}{(C_t-[\mathrm{P}])\,(g\,C_t-[\mathrm{P}])} \tag{7}$$

Solving eqn. (7) for [P]

$$[\mathrm{P}] = \tfrac{1}{2}\,\{C_t+T_t+K^{-1} - [(C_t+T_t+K^{-1})^2-4\,C_t\,T_t]^{\frac{1}{2}}\} \tag{8}$$

where the square root is a positive number. The other root of the quadratic gives a product concentration greater than C_t or T_t, which is physically meaningless.

Substituting $g\,C_t$ for T_t (eqn. 6) and rearranging yields

$$[\mathrm{P}]/C_t = \tfrac{1}{2}\,\{1+g+K^{-1}C_t^{-1} - [(1+g+K^{-1}C_t^{-1})^2-4\,g]^{\frac{1}{2}}\} \tag{9}$$

Each term in this equation is unitless since $[\mathrm{P}]/C_t$, g, and KC_t are unitless. The fraction of constituent which has been converted to product, $[\mathrm{P}]/C_t$, at any point in the titration (g value) depends upon KC_t. An increase in the concentration of the constituent being determined, C_t, has the same effect on the shape of the titration curve as an increase in the equilibrium constant. If the titration reaction (eqn. 1) proceeds

TABLE I

PERCENT DEVIATION FROM COMPLETE REACTION FOR VARIOUS VALUES OF KC_t

(Percent deviation = 100 $(X-[\mathrm{P}]/C_t)/X$; $X=g$ for 0 to 100% and X = 1.0 for greater than 100 %)

KC_t	*Percent titrated (100 g)*										
	5	*10*	*20*	*80*	*90*	*100*	*110*	*120*	*180*	*190*	*200*
0	100	100	100	100	100	100	100	100	100	100	100
10	9.48	9.90	10.85	21.27	24.02	27.02	23.17	20.00	10.00	9.16	8.44
50	2.06	2.17	2.42	7.20	9.66	13.18	9.36	6.92	2.37	2.12	1.92
100	1.04	1.10	1.23	4.12	6.07	9.51	5.91	4.00	1.22	1.09	0.98
200	0.523	0.552	0.620	2.24	3.63	6.82	3.56	2.20	0.616	0.549	0.495
500	0.210	0.222	0.249	0.954	1.70	4.37	1.68	0.946	0.249	0.221	0.199
800	0.131	0.138	0.156	0.606	1.12	3.47	1.11	0.603	0.156	0.138	0.125
1000	0.105	0.110	0.125	0.487	0.915	3.11	0.908	0.486	0.125	0.111	0.100
5000	0.021	0.022	0.025	0.099	0.195	1.40	0.195	0.099	0.025	0.022	0.020
10000	0.010	0.011	0.012	0.049	0.098	0.991	0.098	0.049	0.012	0.011	0.010
∞	0	0	0	0	0	0	0	0	0	0	0

quantitatively from left to right and two straight lines are obtained for the titration, $[P]/C_t$ will be equal to g before the stoichiometric point and to 1 after the stoichiometric point. It can be seen from eqn. (9) that this will be so when KC_t is very large or infinite. Table I presents the percent deviation from complete reaction, g, for various values of KC_t at various percent titrated values (100 g). The Table clearly shows that for g less than 0.9 or greater than 1.10, when KC_t is about 10^4, $[P]/C_t$ deviates less than 0.1 % from the two straight lines obtained when the titration reaction proceeds completely from left to right. It is obvious that the reaction will proceed more completely from left to right. It is obvious that the reaction will proceed more completely when there is a large excess of either the constituent ($g < 1$) or titrant ($g > 1$). The results confirm this conclusion.

An expression for the measurement, M, as a function of the concentration of product, [P], and constituent, C_t, may be obtained by combining eqns. (2), (5) and (6):

$$M = (b_1 C_t + b_2 g C_t + b_4) + (b_3 - b_2 - b_1)\,[P] \tag{10}$$

Rearranging gives:

$$\frac{M - b_4}{C_t} = (b_1 + b_2 g) + (b_3 - b_2 - b_1)\,\frac{[P]}{C_t} \tag{11}$$

The numerator on the left is the difference between the measurement when no titrant has been added and the measurement when the fracion titrated is g. By substituting eqn. (9) for $[P]/C_t$ in eqn. (11), $(M - b_4)/C_t$ can be expressed in terms of proportionality constants, b_i, g and KC_t.

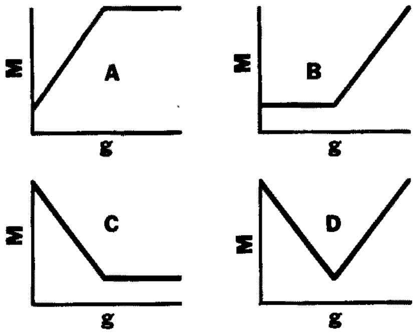

Fig. 2. Titration curves obtained for $KC_t = \infty$ and different relative values of the proportionality constants (eqns. 2 and 10).
(A) $0 = b_2 \leqq b_1 < b_3$, (C) $0 = b_2 \leqq b_3 < b_1$,
(B) $0 \leqq b_1 = b_3 < b_2$, (D) $0 \leqq b_3 < b_1$ and b_2.

The shape of the titration curve will depend upon the relative values of the proportionality constants b_1, b_2 and b_3. Figure 2 presents some of the common titration curves and the relative values of the proportionality constants that produce each curve. Straight lines are drawn indicating that the titration reaction proceeds completely from left to right. Frequently there will be some rounding of the titration curves near the end-point.

In the linear extrapolation titration procedure, measurements are made on the "linear portion" of the titration curves and extrapolated to the point of intersection, which is the estimated equivalence point. The straight line before the end-point can be represented as:

$$M = r_1 g + r_2 \text{ or } M = r_1' V + r_2 \qquad (12)$$

where g is the fraction titrated and V is the volume of titrant.

The straight line after the end-point can be represented as:

$$M = r_3 g + r_4 \text{ or } M = r_3' V + r_4 \qquad (13)$$

Solving eqns. (12) and (13) for the value of g or V where the two lines intersect gives:

$$g_{\text{ep}} = \frac{r_4 - r_2}{r_1 - r_3} \qquad (14)$$

and

$$V_{\text{ep}} = \frac{r_4 - r_2}{r_1' - r_3'} \qquad (15)$$

If the titration reaction proceeds quantitatively, it follows from eqn. (10) that: $r_1 = (b_3 - b_1) C_t$, $r_2 = b_1 C_t + b_4$, $r_3 = b_2 C_t$, and $r_4 = (b_3 - b_2) C_t + b_4$, and g_{ep} is 1. There may be error in g_{ep} caused by error in the measurement from which r_1, r_2, r_3 and r_4 are obtained. But, even if there is no error in the measurements, there can be deviations from the theoretical straight lines for quantitative reactions, because the titration reaction does not proceed completely to product as seen in Table I. Such deviations can result in errors in the titration. $(M - b_4)/C_t$ can be calculated for particular values of KC_t and the proportionality constants over a range of g values (using eqns. 9 and 11). The least squares "straight lines" before and after the end-points can be calculated and the g value at the point of intersection determined. Theoretically, $g = 1$ at the stoichiometric point, so that the percent error in the estimated end-point can be determined. The percent titration error is given by eqn. (16):

$$E_{\text{ti}} = 100\,(g_{\text{ep}} - 1) = 100\,(V_{\text{ep}}/V - 1) \qquad (16)$$

where V is the stoichiometric volume of titrant. The magnitude of the titration error and its dependence on various factors is considered in the next section.

RESULTS AND DISCUSSION

If the experimental error in the measurements is negligible, the titration error will depend only on the error inherent in the extrapolation procedure under the conditions of the titration. This theoretical titration error will vary with the *range*[a] (of g values) and number of data points used to define the two straight lines and the value of KC_t. This error is independent of the values of the constants of eqn. (2), *i.e.*, b_1, b_2, b_3 and b_4 (provided $b_3 = b_1 + b_2$; see eqn. 11).

Figure 3 indicates the effect of the number of data points upon the titration error where data between g ranges of 0.0–0.80 and 1.40–2.20 are used to construct the two lines. Actually the *step* between two points is plotted (0.80, the *interval*, divided by the number of points) as the abscissa in Fig. 3. As the number of points increases (the step decreases) the titration error approaches a limiting value, the "intrinsic theoretical titration error". The intrinsic theoretical titration error was obtained by

---

[a] Range = $\overline{ep} \pm t(SD)_{ep}$ where $\overline{ep}$ = average of Student-estimate end-points and $(SD)_{ep} = [\Sigma(ep_i - \overline{ep})^2/(m - 1)]^{\frac{1}{2}}$; $t = 1.833$ for ten estimates and $t = 2.015$ for five estimates (see results marked with * in Table III).

a linear extrapolation of the error calculated for small steps between points. The straight lines in Fig. 3 represent the extrapolation lines.

In the remainder of this section, the theoretical titration error will refer to the intrinsic or limiting error obtained by such an extrapolation.

Figure 4 summarizes the effect upon the theoretical titration error of KC_t and the ranges used to define the two straight lines. The cusps which occur in the 0–0.6, 1.7–2.3, and 0–0.2, 2.5–2.7 logarithmic plots are due to a change in sign of the error.

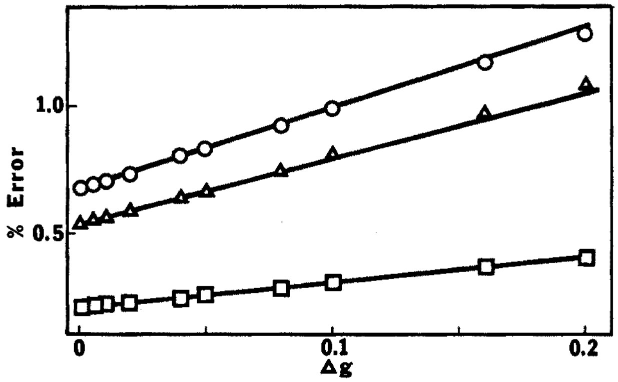

Fig. 3. Effect of the step, Δg, (and number of data points) upon the theoretical percent titration error where data in the range g = 0.0–0.8 and 1.4–2.2 are used. Points represent calculated error ((Δ) for KC_t = 2, (o) for = 20 and (□) for = 200). The straight lines are those used to extrapolate to the intrinsic theoretical titration error, which for KC_t = 2 is 0.533 %, = 20 is 0.672 % and = 200 is 0.201 %.

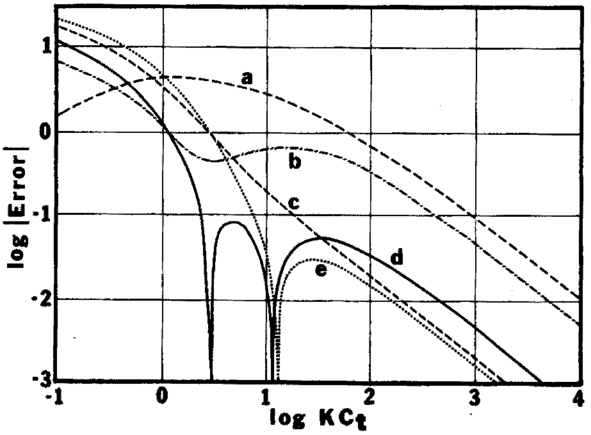

Fig. 4. Logarithm of intrinsic theoretical titration error *vs.* the logarithm of KC_t for different ranges. (a) 0.1–0.9 and 1.1–1.9, (b) 0.0–0.8 and 1.4–2.2, (c) 0.0–0.4 and 2.1–2.5, (d) 0.0–0.6 and 1.7–2.3, and (e) 0.0–0.2 and 2.5–2.7.

The effect of different ranges upon the slopes and intercepts of the two straight lines is shown for KC_t = 10 data in Fig. 5. Note that a judicious choice of range results in relatively small theoretical titration errors (Fig. 5: A 0.039%, B 0.64%, C −2.87%). If different combinations of ranges are employed, the errors can be much larger, *e.g.* in Fig. 5 point D corresponds to −16.6% error and E to + 14.4% error. It is clear that the slope of the least squares straight line varies systematically as the range corresponding to a particular interval is varied. Ranges can be selected so that the theoretical titration error is zero for a particular value of KC_t. As can be seen from Fig. 4, the theoretical titration error varies somewhat with the value of KC_t. Different ranges would have to be selected for each value of KC_t to give zero theoretical titration error. For a given interval, ranges were found which resulted in relatively small theoretical titration errors for KC_t values of 10 or more. These are the ranges 0–0.2, 2.5–2.7; 0–0.4, 2.1–2.5; 0.0–0.6, 1.7–2.3; and 0–0.8, 1.4–2.2 which are used in Fig. 4.

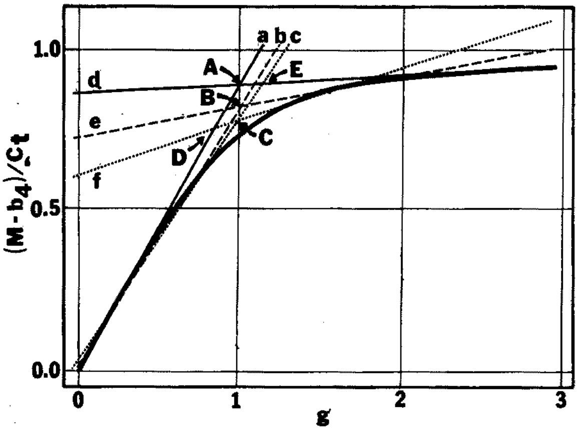

Fig. 5. Titration curve and least squares linear extrapolation lines for data from different ranges for KC_t = 10. Least squares lines using data in the range: (a) 0.0–0.2, (b) 0.0–0.8, (c) 0.1–0.9, (d) 2.5–2.7, (e) 1.4–2.2 and (f) 1.1–1.9. A, B, C, D and E are least squares end-points obtained from some of these lines.

TABLE II

KC_t VALUES CORRESPONDING TO PARTICULAR THEORETICAL TITRATION ERRORS

Ranges	*Theoretical titration error (%)*			
	3	*1*	*0.1*	*0.01*
0–0.2 2.5–2.7	11 (1.5)	42 (3.0)	458 (8.0)	4620 (154)
0–0.4 2.1–2.5	17 (1.2)	62 (2.9)	662 (19)	6670 (201)
0–0.6 1.7–2.3	31 (0.57)	111 (1.2)	1200 (2.4)	12,100 (446)
0–0.8 1.4–2.2	66 (0.41)	277 (1.1)	3310 (446)	33,800 (4850)
0–0.8 1.2–2.0	182 (16)	785 (79)	10,400 (976)	109,000 (9980)

The minimum values of KC_t which result in theoretical titration errors of less than 3%, 1%, 0.1% and 0.01% are presented in parentheses in Table II. For the data presented in this Table and in Figs. 3, 4 and 5, it is presupposed that data from a particular range can be exactly selected. This assumes that the titration stoichiometric point is known, whereas, actually, the end-point must be estimated from the data. One procedure is to estimate an approximate end-point from a plot of the data and then to use this end-point to select the data for the least squares calculations. For example, if data for the ranges 0–0.4 and 2.1–2.5 of the approximate end-point are used to calculate the two least squares lines and the approximate end-point is $g=0.90$, the ranges 0–0.36 and 1.89–2.25 will be used in the least squares procedure. For $KC_t=20$, the theoretical titration error would be -1.60% rather than 0.10%, the titration error if the approximate end-point had been the correct end-point, or $+1.46\%$ if the approximate end-point had been $g = 1.10$.

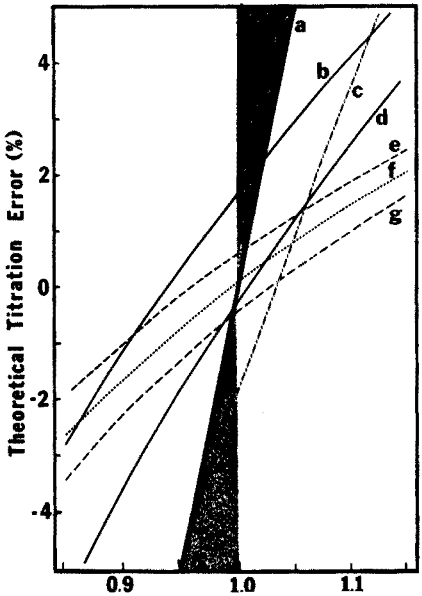

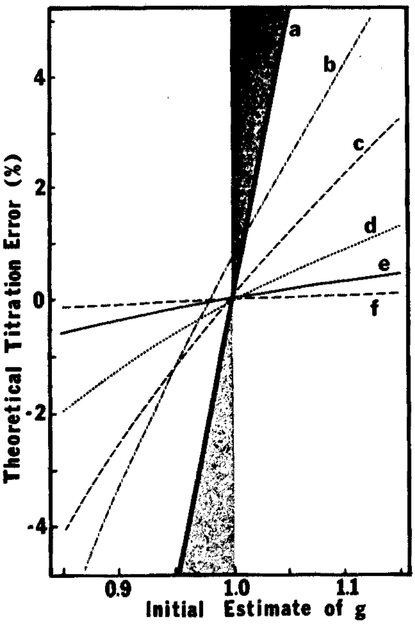

Fig. 6. Least squares intrinsic theoretical percent titration error corresponding to different initial estimates of the end-point for $KC_t = 20$. Results for different ranges corresponding to the interval 0.4 are presented. (a) Iterative limiting, (b) 0.2–0.6 and 1.8–2.2, (c) 0.4–0.8 and 1.2–1.6, (d) 0.2–0.6 and 1.6–2.0, (e) 0.0–0.4 and 2.2–2.6, (f) 0.0–0.4 and 2.1–2.5, and (g) 0.0–0.4 and 2.0–2.4.

Fig. 7. Least squares intrinsic theoretical percent titration error corresponding to different initial estimates of the end-point. Results for different intervals and KC_t values are presented. (a) Iterative limiting line. For $KC_t = 20$, (b) 0.0–0.8 and 1.4–2.2, (c) 0.0–0.6 and 1.7–2.3, and (d) 0.0–0.2 and 2.5–2.7. 0.0–0.6 and 1.7–2.3 (c) $KC_t = 20$, (e) $KC_t = 200$, and (f) $KC_t = 2000$.

The effect of an error in the approximate end-point upon the theoretical titration error obtained by the least squares procedure is shown in Fig. 6 for different ranges where the interval is 0.4. From this Figure it can be seen that if the range 0–0.4 is used to define one line, the range 2.1–2.5 rather than 2.0–2.4 or 2.2–2.6 for the other line results in a theoretical titration error which is closest to zero when the approximate end-point is 1.00. Comparison of the error span from $g=0.85$ to 1.15 associated with the ranges 0–0.4, 2.1–2.5; 0.2–0.6, 1.6–2.0; 0.2–0.6, 1.8–2.2 and 0.4–0.8, 1.2–1.6 reveals that 0–0.4, 2.1–2.5 is the most desirable range corresponding to an interval of 0.4. The best range corresponding to intervals of 0.2, 0.6 and 0.8 was evaluated in a similar manner. The theoretical titration error corresponding to different estimated approximate end-points for these best ranges are plotted in Fig. 7 for a KC_t value of 20. The effect of different KC_t values on this error is shown for the ranges 0–0.6 and 1.7–2.3 in this Figure.

From Figs. 6 and 7 it is clear that the intrinsic theoretical titration error will depend upon the accuracy of the approximate end-point. The values of KC_t not in parentheses in Table II represent the minimum values which will yield a theoretical titration error of less than 3%. 1%, 0.1% and 0.01% if the approximate end-point corresponds to a value of g between 0.85 and 1.15. Table III presents the span of error foı the extrapolation procedure with different ranges and estimates between g values of 0.85 and 1.15 for different values of KC_t.

To determine the accuracy with which the approximate end-points can be estimated, five different titration curves were constructed[9] in which 51 points were plotted at equally spaced intervals between 0–167%, 0–250%, 0–300%, 0–400% and 0–600% titrated for each of eleven KC_t values between 2 and 10,000. For each plot the abscissa was labelled from 0 to 2.00 in intervals of 0.04 and the ordinate was labelled 0 to 1.00 in intervals of 0.01. Points were plotted to the nearest abscissa and ordinate interval. Some plots were prepared in duplicate. These plots were divided between five students. Each student was asked to estimate the end-point using a ruler and pencil. The average, standard deviation and range at the 90% level of certainty (*t* test) were calculated. An error of 3% merely due to the crudeness of the computer plots was anticipated. The ranges of the student estimated end-points at the 90% level are presented in Table III. From these results it appears the approximate end-point can be estimated to within 85% to 115% of the correct values for KC_t values somewhat greater than 20. The results in parentheses represent the span of theoretical percent titration errors corresponding to the 90% level range of student estimated end-points.

From the data in Table III, if KC_t is 20 and the ranges 0–0.2 and 2.5–2.7 are employed, the theoretical titration error corresponding to an initial end-point estimate of 0.85 or 1.15 of the true value is -1.93 or 1.27%. If the initial estimate were 1.00, the least squares theoretical titration error would be only -0.027%. It is obvious from Figs. 6 and 7, that for the "best ranges", the better the estimate of the end-point, generally, the smaller the theoretical titration error.

Suppose the initial least squares end-point is used as the basis of another least squares end-point calculation and this process is repeated several times until convergence to a final estimated end-point, would the resulting estimate be better than the initial estimate? How large would be the error in the final estimated end-point?

For the KC_t values and ranges represented in Figs. 6 and 7, the final theoretical titration error obtained by such an iteration procedure corresponds to the ordinate at the point of intersection of the appropriate curve with the dashed line in Figs. 6 and 7. The dashed line is the locus of points for which the theoretical titration error (ordinate) is equal to the error in the estimate of the end-point (from the abscissa), *i.e.* T.T.E. $= 100$ (E.E. -1) where T.T.E. is the ordinate and E.E. the abscissa in Figs. 6 and 7. If the initial estimate is on the dashed line, the initial estimate of the end-point will be equal to the least squares end-point. In all other cases the iteration procedure will converge to this point.

If the initial estimate of the end-point corresponds to a point on one of the curves

TABLE III

THEORETICAL PERCENT TITRATION ERROR CORRESPONDING TO STUDENT ESTIMATED END-POINTS (IN

KC_t	*Range of student estimated end-points at 90 % level*	*Span of theoretical* E_{tl} *(%)*	
		0.0–0.2 *2.5–2.7*	*0.0–0.4* *2.1–2.5*
2	34.8–170.8*	− 6.64 to 8.96 (−52.8 to 27.4)	− 8.34 to 10.23 (−56.1 to 34.9)
5	75.6–140.2	− 5.00 to 4.38 (− 9.39 to 9.40)	− 6.37 to 5.93 (−11.7 to 13.2)
10	82.5–121.8	− 3.29 to 2.40 (− 3.99 to 3.28)	− 4.35 to 3.62 (− 5.28 to 4.94)
20	92.1–116.9	− 1.93 to 1.27 (− 0.93 to 1.41)	− 2.64 to 2.06 (− 1.21 to 2.28)
40	95.6–107.0	− 1.05 to 0.66 (− 0.28 to 0.32)	−1.47 to 1.11 (− 0.33 to 0.58)
60	96.5–109.6*	− 0.72 to 0.44 (− 0.16 to 0.29)	− 1.02 to 0.76 (− 0.17 to 0.52)
80	98.0–105.8*	− 0.55 to 0.33 (− 0.075 to 0.13)	− 0.78 to 0.58 (− 0.064 to 0.26)
100	96.3–104.0*	− 0.44 to 0.27 (− 0.10 to 0.071)	− 0.63 to 0.47 (− 0.12 to 0.15)
200	97.9–103.3*	− 0.22 to 0.13 (− 0.033 to 0.028)	− 0.33 to 0.24 (− 0.28 to 0.066)
400	94.9–102.6*	− 0.11 to 0.068 (− 0.036 to 0.010)	− 0.16 to 0.12 (− 0.044 to 0.028)
1,000		− 0.046 to 0.027	− 0.066 to 0.048
2,000		− 0.023 to 0.014	− 0.033 to 0.024
5,000		− 0.0092 to 0.0054	− 0.013 to 0.0097
10,000	95.6–101.9	− 0.0046 to 0.0027 (− 0.0013 to 0.00026)	− 0.0067 to 0.0049 (− 0.0015 to 0.0088)

* See footnote a on p. 145.

which is in the shaded area of Figs. 6 or 7, the initial estimate would be more accurate than the final iteration titration end-point.

Final iteration titration errors for different ranges and different KC_t values are summarized in Table IV. Examination of the results in Table IV and Figs. 6 and 7 shows that, for sufficiently large KC_t values the final theoretical titration error will be small and the choice of ranges used may not be very important. However, for small values of KC_t the least squares theoretical titration error and the final iterative titration error may be large if the ranges are not judiciously chosen. If for particular ranges and KC_t value the least squares titration error is zero corresponding to an estimated end-point of 1.00, the final iterative theoretical titration error is zero. In general, a different range would be required to produce zero error for a different KC_t value.

There are some ranges which are obviously not satisfactory from this point of view, *e.g.* 0–0.8 and 1.2–2.0 (see Table IV). Other ranges may be satisfactory for

PARENTHESES) OR ESTIMATES OF 85 % TO 115 % OF CORRECT END-POINT

0.0–0.6	*0.0–0.8*	*0.0–0.8*
1.7–2.3	*1.4–2.2*	*1.2–2.0*
−11.1 to 10.5	−12.0 to 12.2	−18.4 to 5.54
(−59.6 to 42.2)	(−61.4 to 51.0)	(−64.9 to 44.5)
− 8.81 to 7.24	−10.0 to 9.89	−16.0 to 4.80
(−15.3 to 17.8)	(−17.6 to 24.2)	(−23.6 to 19.8)
−6.41 to 5.07	− 7.93 to 7.95	−13.4 to 4.23
(− 7.68 to 7.13)	(− 9.55 to 11.1)	(−15.2 to 7.63)
− 4.16 to 3.24	− 5.66 to 5.94	−10.4 to 3.49
(− 1.98 to 3.62)	(− 2.44 to 6.58,	(− 6.45 to 4.21)
− 2.45 to 1.91	− 3.68 to 4.10	− 7.52 to 2.62
(− 0.58 to 0.96)	(− 0.54 to 2.22)	(− 3.15 to 0.40)
− 1.74 to 1.36	− 2.76 to 3.18	− 6.04 to 2.12
(− 0.31 to 0.91)	(− 0.19 to 2.19)	(− 2.15 to 0.95)
− 1.35 to 1.06	− 2.21 to 2.61	− 5.11 to 1.79
(− 0.11 to 0.46)	(− 0.097 to 1.23)	(− 1.41 to 0.13)
− 1.10 to 0.86	− 1.85 to 2.23	− 4.45 to 1.56
(− 0.20 to 0.27)	(− 0.12 to 0.83)	(− 1.51 to 0.16)
− 0.58 to 0.45	− 1.02 to 1.31	− 2.81 to 0.95
(− 0.048 to 0.12)	(− 0.058 to 0.43)	(− 0.67 to 0.13)
− 0.29 to 0.23	− 0.54 to 0.73	− 1.70 to 0.18
(− 0.077 to 0.052)	(− 0.078 to 0.20)	(− 0.55 to 0.098)
− 0.12 to 0.094	− 0.22 to 0.32	− 0.82 to 0.24
− 0.06 to 0.047	− 0.11 to 0.16	− 0.45 to 0.13
− 0.024 to 0.019	− 0.046 to 0.067	− 0.20 to 0.052
− 0.012 to 0.0095	− 0.023 to 0.034	− 0.10 to 0.026
(− 0.0026 to 0.0177)	(− 0.0120 to 0.0078)	(− 0.022 to 0.0055)

many KC_t values, *e.g.* 0–0.6 and 1.7–2.3 (see Table IV and Fig. 7). The possibility exists of using this iterative procedure in the analysis of data by computer or on-line control and analysis of the titration. In order to perform the iterative analysis, interpolation may be necessary. A second titration, designed on the basis of the results of the first titration, may yield a smaller titration error.

Effect of error in measurements and a small number of data points

The results summarized in Tables II, III and IV indicate the relationship between KC_t and the titration error under conditions where measurement errors do not contribute significantly to the titration error, and where an estimate of the titration error is made from suitable least squares calculations. Measurement errors frequently are important in practical titrations. These are reflected in errors in the slopes and intercepts of the least squares straight lines, *i.e.* r_1, r_2, r_3 and r_4. The mag-

TABLE IV

FINAL ITERATION THEORETICAL PERCENT TITRATION ERRORS FOR SIX, ELEVEN AND AN INFINITE NUMBER OF POINTS ON EACH LINE

KC_t	*0.0–0.2* *2.5–2.7*			*0.0–0.4* *2.1–2.5*			*0.0–0.6* *1.7–2.3*			*0.0–0.8* *1.4–2.2*			*0.0–0.8* *1.2–2.0*		
	6	*11*	∞	*6*	*11*	∞	*6*	*11*	∞	*6*	*11*	∞	*6*	*11*	∞
5	0.55	0.53	0.51	1.05	0.93	0.80	0.49	0.15	−0.19	3.16	2.29	1.42	−20.0	−20.0	−20.0
10	0.078	0.063	0.048	0.43	0.36	0.27	0.44	0.21	−0.031	2.60	1.95	1.31	−10.0	−10.0	−10.0
20	−0.013	−0.021	−0.030	0.21	0.16	0.11	0.35	0.21	0.058	1.99	1.52	1.07	−5.0	−5.0	−5.0
200	−0.0061	−0.0070	−0.0080	0.021	0.016	0.010	0.062	0.042	0.021	0.40	0.31	0.22	−0.50	−0.50	−0.50
1000	−0.0013	−0.0015	−0.0017	0.0043	0.0032	0.0020	0.013	0.0090	0.0046	0.089	0.069	0.048	−0.10	−0.10	−0.10

nitude of the resulting titration error is given by the expression[10]:

$$(\Delta g_{\mathrm{ep}})^2 =$$

$$\sum_{\nu=1}^{4}\left(\frac{\partial g_{\mathrm{ep}}}{\partial r_\nu}\right)^2(\Delta r_\nu)^2+2\left(\frac{\partial g_{\mathrm{ep}}}{\partial r_1}\right)\left(\frac{\partial g_{\mathrm{ep}}}{\partial r_2}\right)\Delta(r_1 r_2)+2\left(\frac{\partial g_{\mathrm{ep}}}{\partial r_3}\right)\left(\frac{\partial g_{\mathrm{ep}}}{\partial r_4}\right)\Delta(r_3 r_4) \tag{17}$$

where $(\Delta r_\nu)^2$ is the estimated error in each of the least squares constants squared. The last two terms in eqn. (17) compensate for the fact that the errors in r_1 and r_2, and r_3 and r_4 are not independent. The partial derivatives are evaluated by differentiation of eqn. (14). The errors in r_1 and r_3 can be calculated from the expressions[11]:

$$(\Delta r_1)^2=(\Delta M)^2/\Sigma(x_{\mathrm{m}}-\bar{x})^2 \tag{18}$$

$$(\Delta r_3)^2=(\Delta M)^2/\Sigma(x_{\mathrm{n}}-\bar{x}')^2 \tag{19}$$

where x_{m} and $\bar{x}$ refer to all data used in obtaining the least squares straight line before the end-point and x_{n} and $\bar{x}'$ to data after the end-point. $(\Delta M)^2$ is the square of the error in the measurements. $(\Delta r_2)^2$ and $(\Delta r_4)^2$ can be calculated from the expressions[11]:

$$(\Delta r_2)^2=(\Delta M)^2\ \Sigma x_{\mathrm{m}}^2/\,k\ \Sigma(x_{\mathrm{m}}-\bar{x})^2 \tag{20}$$

$$(\Delta r_4)^2=(\Delta M)^2\ \Sigma x_{\mathrm{n}}^2/k'\ \Sigma(x_{\mathrm{n}}-\bar{x}')^2 \tag{21}$$

where k and k' are the number of data points used in calculating the least squares line before and after the end-point, respectively.

$$\Delta(r_1r_2)=-\bar{x}\ (\Delta M)^2/\Sigma(x_{\mathrm{m}}-\bar{x})^2 \tag{22}$$

$$\Delta(r_3r_4)=-\bar{x}'\ (\Delta M)^2/\Sigma(x_{\mathrm{n}}-\bar{x}')^2 \tag{23}$$

Substituting the partial derivatives and eqns. (18)–(23) into eqn. (17):

$$(\Delta g_{\mathrm{ep}})^2=\frac{(\Delta M)^2}{(r_1-r_3)^2}\left[\frac{g_{\mathrm{ep}}^2-2g_{\mathrm{ep}}\,\bar{x}+\Sigma x_{\mathrm{m}}^2/k}{\Sigma(x_{\mathrm{m}}-\bar{x})^2}+\frac{g_{\mathrm{ep}}^2-2g_{\mathrm{ep}}\,\bar{x}'+\Sigma x_{\mathrm{n}}^2/k'}{\Sigma(x_{\mathrm{n}}-\bar{x}')^2}\right] \tag{24}$$

The error in volume of titrant can be expressed by an equation analogous to eqn. (24), except that r_1', r_3' (eqns. (12) and (13)) and V_{ep} are substituted for r_1, r_3 and g_{ep}. For the volume error calculation, x would refer to the volume rather than the fraction titrated at each point used in the least squares calculations. In each individual instance eqn. (24) can be used to estimate the titration error caused by errors in the measurements.

Consider the situation where measurements (*e.g.* of absorbance) vary between zero and one and the least squares lines are represented by one of the plots presented in Fig. 2. $(r_1-r_3)^2=1$ in titrations A, B or C, and $=4$ in Titration D. Assuming that ΔM is 0.01, and g_{ep} and (r_1-r_3) are 1, Fig. 8 indicates how the titration error varies with the number of titration points used to define each of the two least squares lines for data from different ranges. Data points from 3 to 101 at equally spaced intervals in each range are considered in the Figure. In any routine manual procedure it is not reasonable to make 202 measurements, 101 on each of the two titration lines. Figure 8 indicates that, for data taken from the ranges 0–0.9 and 1.1–2.0 under the conditions specified, 22 measurements must be made to introduce an error of less than 1% from measurement errors.

TABLE V

LEAST SQUARES LINEAR EXTRAPOLATION END-POINT ERROR CAUSED BY MEASUREMENT ERRORS (M.E) AND THE THEORETICAL TITRATION ERROR (T.T.E.) MEASUREMENT ERROR OF 0.01, AND $(r_1-r_3)^2 = 1$ FOR VERY LARGE KC_t VALUES

(11 points are used for each line)

KC_t	*0–0.2, 2.5–2.7*				*0–0.4, 2.1–2.5*				*0–0.6, 1.7–2.3*			
	M.E.	*T.T.E.*			*M.E.*	*T.T.E.*			*M.E.*	*T.T.E.*		
	$\Delta M = 0.01$	*0.85*	*1.00*	*1.15*	$\Delta M = 0.01$	*0.85*	*1.00*	*1.15*	$\Delta M = 0.01$	*0.85*	*1.00*	*1.15*
5	11.60	−4.99	0.369	4.41	6.52	−6.34	0.554	6.04	3.12	−8.74	0.071	7.51
20	9.48	−1.93	−0.019	1.28	4.06	−2.62	0.137	2.13	2.30	−4.15	0.158	3.48
50	9.05	−0.86	−0.021	0.53	3.83	−1.20	0.059	0.94	2.12	−2.04	0.117	1.73
100	8.91	−0.44	−0.013	0.27	3.75	−0.63	0.031	0.49	2.05	−1.11	0.073	0.95
200	8.83	−0.23	−0.0069	0.14	3.70	−0.32	0.016	0.25	2.02	−0.58	0.041	0.50
500	8.79	−0.092	−0.0029	0.055	3.68	−0.13	0.0064	0.10	2.00	−0.24	0.018	0.21
1000	8.78	−0.046	−0.0015	0.027	3.67	−0.066	0.0032	0.051	1.99	−0.12	0.0090	0.11
2000	8.77	−0.023	−0.00075	0.014	3.67	−0.033	0.0016	0.025	1.99	−0.061	0.0045	0.053
5000	8.76	−0.0092	−0.00030	0.0055	3.67	−0.013	0.00065	0.010	1.99	−0.024	0.0018	0.021
10000	8.76	−0.0046	−0.00015	0.0027	3.66	−0.0066	0.00032	0.0051	1.99	−0.012	0.00092	0.011
∞	8.76	0.0	0.0	0.0	3.66	0.0	0.0	0.0	1.99	0.0	0.0	0.0

KC_t	*0–0.8, 1.4–2.2*				*0–0.8, 1.2–2.0*			
	M.E.	*T.T.E.*			*M.E.*	*T.T.E.*		
	$\Delta M = 0.01$	*0.85*	*1.00*	*1.15*	$\Delta M = 0.01$	*0.85*	*1.00*	*1.15*
5	2.26	−9.99	0.756	10.4	2.11	−16.0	−4.87	5.20
20	1.47	−5.68	0.924	6.53	1.43	−10.6	−2.56	3.97
50	1.40	−3.23	0.706	4.11	1.25	− 7.02	−1.38	2.80
100	1.34	−1.92	0.475	2.67	1.18	− 4.84	−0.80	1.95
200	1.30	−1.08	0.285	1.63	1.14	− 3.19	−0.44	1.25
500	1.28	−0.47	0.129	0.78	1.12	−1.75	−0.19	0.63
1000	1.27	−0.24	0.067	0.43	1.11	− 1.07	−0.097	0.35
2000	1.27	−0.12	0.034	0.23	1.10	− 0.64	−0.049	0.19
5000	1.27	−0.049	0.014	0.093	1.10	− 0.31	−0.020	0.077
10000	1.27	−0.025	0.00070	0.047	1.10	− 0.17	−0.010	0.039
∞	1.27	0.0	0.0	0.0	1.10	0.0	0.0	0.0

If the error is to be further reduced, the error in the measurements must be reduced or $(r_1-r_3)^2$ must be increased. Thus, if ΔM were reduced to 0.001, the ordinate in Fig. 8 would be one-tenth the value indicated. If the conditions of Titration C, where $(r_1-r_2)^2=4$, could be found, then the errors plotted in Fig. 8 would be half those shown. For titrations B–D, if b_2 and b_4 are zero in eqn. (2), the minimum value of the measurements is zero at the end-point. It is possible that conditions could be found where $(r_1-r_3)^2$ would be much larger, and the error due to measurement errors much reduced. For example, in photometric titrations a different wavelength may be available where the molar absorptivities would be much greater. Every situation must be analyzed individually. The ordinate in Fig. 8 is for $\Delta M/|r_1-r_3|=0.01$. This Figure could be used for the ranges shown for other values of $\Delta M/|r_1-r_3|$ by multiplying the ordinate by an appropriate factor.

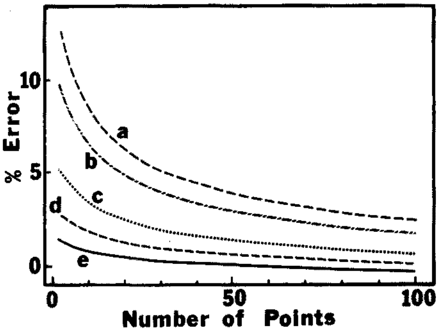

Fig. 8. Percent titration error corresponding to an error in measurement of 0.01 *vs.* number of data points to define each least squares line. The error is calculated using eqn. (24) with $(r_1-r_3)^2 = 1$ and $g_{ep} = 1$. For ranges: (a) 0.0–0.2 and 2.5–2.7, (b) 0.0–0.2 and 2.0–2.2, (c) 0.0–0.4 and 2.1–2.5, (d) 0.0–0.6 and 1.7–2.3, and (e) 0.0–0.9 and 1.1–2.0.

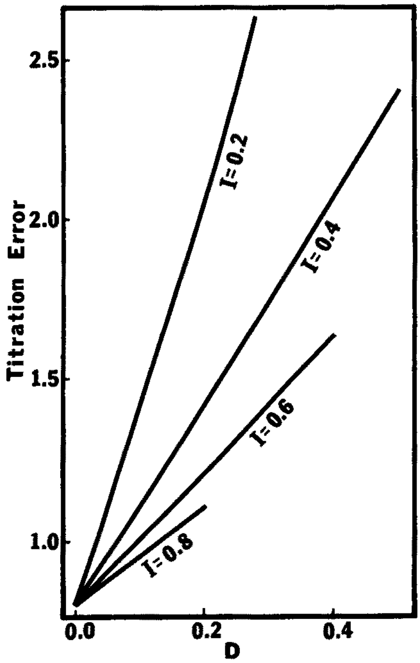

Fig. 9. Effect of the magnitude of the extrapolation distance, D, and the interval, I, upon the percent titration error due to measurement errors of 0.01 with $(r_1-r_3)^2$ and g_{ep} values of 1. Eleven experimental points at equally spaced steps were assumed in calculating each of the two titration lines. The error was calculated from eqn. (24).

A small uncertainty in slope and intercept is amplified into a large uncertainty in the extrapolated end-point, particularly if extrapolation is over a great distance. This accounts for the trends for different ranges which can be seen from Fig. 8. Figure 9 shows the effect of the extrapolation distance with 11 points on each line, a ΔM value of 0.01, and (r_1-r_3) and g_{ep} values of one.

TABLE VI

LEAST SQUARES EXTRAPOLATION PERCENT ERROR AND TITRATION ERROR

(Six points are used for each line)

	0–0.2, 2.5–2.7				*0–0.4, 2.1–2.5*				*0–0.6, 1.7–2.3*			
	M.E.	*T.T.E.*			*M.E*	*T.T.E.*			*M.E.*	*T.T.E.*		
KC_t	$\Delta M = 0.01$	*0.85*	*1.00*	*1.15*	$\Delta M = 0.01$	*0.85*	*1.00*	*1.15*	$\Delta M = 0.01$	*0.85*	*1.00*	*1.15*
5	14.55	—4.98	0.385	4.43	6.52	—6.30	0.623	6.07	3.93	—8.67	0.612	7.77
20	11.88	—1.92	—0.012	1.30	5.10	—2.61	0.175	2.19	2.90	—4.13	0.265	3.69
50	11.35	—0.85	—0.017	0.54	4.80	—1.20	0.053	0.97	2.67	—2.04	0.177	1.87
100	11.17	—0.44	—0.011	0.27	4.70	—0.63	0.041	0.51	2.59	—1.11	0.107	1.03
200	11.08	—0.23	—0.0060	0.14	4.65	—0.32	0.021	0.26	2.54	—0.58	0.057	0.55
500	11.02	—0.091	—0.0025	0.055	4.62	—0.13	0.0059	0.10	2.52	—0.24	0.024	0.23
1000	11.00	—0.046	—0.0013	0.028	4.61	—0.066	0.0030	0.052	2.51	—0.12	0.012	0.11
2000	11.00	—0.023	—0.00066	0.014	4.60	—0.033	0.0015	0.026	2.50	—0.061	0.0060	0.058
5000	10.99	—0.0092	—0.00026	0.0055	4.60	—0.013	0.00086	0.011	2.50	—0.024	0.0024	0.023
10000	10.99	—0.0046	—0.00013	0.0028	4.60	—0.0066	0.00030	0.0053	2.50	—0.012	0.0013	0.012

	0–0.8, 1.4–2.2				*0–0.8, 1.2–2.0*			
	M.E.	*T.T.E.*			*M.E.*	*T.T.E.*		
KC_t	$\Delta M = 0.01$	*0.85*	*1.00*	*1.15*	$\Delta M = 0.01$	*0.85*	*1.00*	*1.15*
5	2.86	—9.90	1.017	10.8	2.69	—16.0	—4.68	5.58
20	1.85	—5.70	1.174	7.09	1.82	—10.8	—2.45	4.43
50	1.78	—3.30	0.889	4.62	1.59	— 7.34	—1.33	3.24
100	1.70	—1.99	0.603	3.09	1.50	— 5.20	—0.78	2.32
200	1.65	—1.13	0.364	1.94	1.45	— 3.56	—0.43	1.54
500	1.62	—0.49	0.166	0.96	1.42	— 2.06	—0.19	0.79
1000	1.61	—0.26	0.087	0.53	1.41	— 1.32	—0.097	0.45
2000	1.61	—0.13	0.045	0.28	1.40	— 0.82	—0.049	0.24
5000	1.60	—0.053	0.018	0.12	1.40	— 0.41	—0.020	0.10
10000	1.60	—0.026	0.0091	0.060	1.39	— 0.23	—0.010	0.051

The calculations of Figs. 8 and 9 assume that the titration reaction proceeds quantitatively from left to right, *i.e.* $r_1 - r_3 = 1$ and the measurement changes by one in going from $g = 0$ to $g = 1$. If KC_t decreases, $r_1 - r_3$ will decrease (see Fig. 1) and the end-point error from measurement error (M.E.) will increase. Table V illustrates the effect upon the error of a variation in KC_t value where there are 22 data points, 11 on each of the two titration lines. Table VI presents the results of similar calculations for 12 data points, 6 on each of the two titration lines.

Also, these Tables present the theoretical titration error (T.T.E.) where 11 and 6 points are used to define each of the least squares lines, and the initial end-point estimate corresponds to 0.85, 1.00 and 1.15 of the stoichiometric point. From the results summarized it is clear that the end-point error from measurement errors does not change significantly unless KC_t values are less than 500. Comparison of the theoretical titration error with the intrinsic (limiting) theoretical titration error presented in Table III and Fig. 4 shows that for the ranges 0–0.2 and 2.5–2.7 the absolute value of the theoretical error for 6 and 11 points on each line is less than the limiting error for KC_t values of 20 or less. For the other ranges the theoretical error is larger than the limiting error generally, by a factor of less than 2 (or 3) for 11 (or 6 points) on each line for KC_t values of 50 or greater.

For titrations described by the conditions outlined in Tables V and VI the measurement error will be more important than the theoretical titration error except for very small KC_t values and the range 0–0.8 and 1.2–2.0. The measurement error under these conditions would have to be very much reduced before the theoretical titration error contributed significantly to the overall titration error. The iterative procedure suggested previously would only be useful where the theoretical titration error contributes significantly to the total error. Table IV summarizes the final iterative error for 6, 11 and an infinite number of points on each line.

Each situation should be evaluated individually. The Tables, Figures and ideas presented in this paper should be useful in such an evaluation. Conditions should be selected for minimizing the important sources of error.

While in this paper a titration involving the reaction of each mole of constituent with one mole of titrant to produce one mole of salt has specifically been considered, a similar analysis could be performed of titrations involving other stoichiometries.

The authors wish to thank Professor HERBERT DAVID, Department of Statistics, Iowa State University for some useful comments on various aspects of this paper and B. BEACH, J. T. CLARK, E. ETZ, G. FRICKE and D. RIVERS for estimating end-points from the computer plots.

SUMMARY

Errors are considered for titration procedures in which a least squares linear extrapolation of data before and after the end-point is performed to estimate the end-point. The error caused by the titration reaction not proceeding to completion is considered. The effect of the formation constant, concentration of constituent, the range of the data used, the number of data points employed and the initial visual estimate of the end-point is discussed. Also, the titration error caused by error in the measurements is calculated.

RÉSUMÉ

Les auteurs ont effectué une étude sur les possibilités d'extrapolation linéaire lors d'analyse par titrage, ainsi que les erreurs qui en résultent. On examine l'influence de la constante de formation, de la concentration des constituants, du nombre et de la position des points considerées, et de l'estimation visuelle initiale du point final. On tient compte également de l'erreur due aux mesures.

ZUSAMMENFASSUNG

Es werden die Fehler von Titrationsverfahren betrachtet, bei denen für die Ermittlung des Endpunktes die Messwerte vor und hinter dem Endpunkt nach der Methode der kleinsten Quadrate linear extrapoliert werden. Es wird der Fehler betrachtet, der durch eine unvollständig ablaufende Titrationsreaktion hervorgerufen wird. Der Einfluss von Bildungskonstante, Konzentration des Bestandteils, Bereich der verwendeten Messwerte, Anzahl der gebrauchten Messpunkte und der ersten visuellen Ermittlung des Endpunktes wird diskutiert. Es wird auch der durch Messfehler bedingte Titrationsfehler berechnet.

REFERENCES

1 H. T. S. Britton, in W. G. Berl, *Physical Methods in Chemical Analysis, Vol. II,* Academic Press, New York, 1951, pp. 52–106.
2 J. T. Stock, *Amperometric Titrations,* Interscience, New York, 1965.
3 L. Meites, *Polarographic Techniques,* Interscience, New York, 1965.
4 H. B. Headridge, *Photometric Titrations,* Pergamon Press, Oxford, 1961.
5 R. Megargle, G. Jones and D. Rosenthal, *Anal. Chem.,* 41 (1969) 1214.
6 J. R. Dean and W. E. Harris, *Anal. Chem.,* 40 (1968) 1177.
7 E. Grunwald, *Anal. Chem.,* 28 (1956) 1112.
8 A. Langer and D. P. Stevenson, *Ind. Eng. Chem., Anal. Ed.,* 14 (1942) 770.
9 G. H. Fricke, *Subroutine Graph,* IBM Contributed Program 360D–08.6.008.
10 H. H. Ku, *J. Res. Natl. Bur. Std.,* 70 C (1966) 263.
11 N. R. Draper and H. Smith, *Applied Regression Analysis,* John Wiley, New York, 1966, p. 55.

Analytica Chimica Acta
Elsevier Publishing Company, Amsterdam
Printed in The Netherlands

USE OF RAPID A.C. POLAROGRAPHY FOR THE EVALUATION OF COMPLEXES OF SPARINGLY SOLUBLE SALTS

APPLICATION TO LEAD(II)–FLUORIDE AND LEAD(II)–CHLORIDE–FLUORIDE SYSTEMS

A. M. BOND
Department of Inorganic Chemistry, University of Melbourne, Parkville 3052, Victoria (Australia)
(Received July 16th, 1970)

Very little information is available on the stability constants of sparingly soluble metal ion-complex systems[1,2]. This is not surprising because most of the common methods of detection of complex formation break down in the presence of precipitation or else they are not applicable below the level of solubility where the concentration of ligand or metal ion remaining after precipitation is too low for complex detection.

Thus for sparingly soluble systems, frequently only the solubility product is known and in any calculations required on such systems complex formation has to be neglected. The exceptions to this general statement are those sparingly soluble salts which are soluble in high (excess) ligand concentrations such as $PbCl_2$, $PbBr_2$ and PbI_2, etc.[1] and for which meaningful measurements can be made over the region in which the system is soluble.

In rare cases where a particular method retains its applicability in spite of precipitation or for systems in which measurements can be made below the solubility level[2], then the possibility of obtaining data exists. However, to date, stability constant measurements on sparingly soluble systems have in general presented a difficult problem, and any means by which this problem may be circumvented should be capable of yielding valuable data.

Mesaric and Hume[3] have shown that if complex formation is rapid and precipitation is kinetically slow, then the polarographic method for detection of complexes[4] is valid. Using conventional d.c. polarography, they successfully measured the sparingly soluble lead(II)–fluoride system. Their results were recently confirmed by Bond and Hefter[2].

The conventional d.c. polarographic method, with its natural drop time of between 2 and 8 seconds requires a considerable potential scan time to record a complete polarogram and cannot be applied to complex detection unless a reasonably high concentration of electroactive metal ion complex remains in solution for at least 5 min after the complex ion system is prepared[5].

The present author has shown that a.c.[6] and rapid polarographic techniques[5] can be used for determination of stability constants of complex ion systems. The rapid method which employs extremely short drop times and fast potential scan rates, when combined with the a.c. technique, should be capable of yielding all the required data for complex detection within about 20 sec[5], and if complete precipitation (below the level of detection of the a.c. method) does not occur before this time interval, any sparingly soluble complex ion system should be resolvable if it is reversibly reduced at the dropping mercury electrode.

In this work, the sparingly soluble lead(II)-fluoride system measured by MESARIC AND HUME has been re-studied in detail by rapid a.c. polarography and with the same technique the lead(II)-chloride-fluoride system has been measured, apparently for the first time. Lead chlorofluoride is a sparingly soluble complex and often has been used as a means for the gravimetric determination of fluoride[7].

In 1964, no information was available on mixed chlorofluoride complexes or any other mixed fluoride complexes[1], let alone mixed fluoride complex systems of sparingly soluble systems, and no information on such systems seems to have been reported since then. The lead(II)-chloride-fluoride system should therefore be an extremely useful example to test the predicted applicability of rapid a.c. polarography to the study of sparingly soluble systems[5] and at the same time provide valuable new information on mixed fluoride complexes.

EXPERIMENTAL

All solutions were prepared from reagent-grade chemicals. Lead(II) solutions were prepared from lead(II) nitrate and fluoride and chloride solutions from their sodium salts.

All solutions were thermostatted at $(25 \pm 0.1)^\circ$ and de-aerated with argon.

The pH of all solutions was adjusted to 5.0 ± 0.2, where the presence of HF and HF_2^- may be neglected as may the formation of lead(II)-hydroxy complexes.

The ionic strength of all solutions was maintained at 1.0 with sodium perchlorate.

Polarograms were obtained with a Metrohm Polarecord E261. A.c. polarography was done with the Metrohm a.c. Modulator E393 with an a.c. voltage of 10 mV, r.m.s. at 50 Hz. Rapid polarographic techniques and a controlled drop time of 0.16 sec were achieved with a Metrohm Polarographie Stand E354. For the a.c. polarography a three-electrode system was used with tungsten as the third or auxiliary electrode. Silver/silver chloride was used as the reference electrode.

Procedure for the lead(II)-fluoride system

Into the polarographic cell a solution of lead(II) and sodium perchlorate were added, calculated so that after later addition of fluoride, the initial concentration of lead(II) would be $4 \cdot 10^{-4} M$ and the ionic strength would be 1.0. This solution was then degassed. An aliquot of degassed fluoride solution was then added to give the desired fluoride concentration. Immediately on addition of the fluoride, a rapid a.c. polarogram was recorded, commencing at a potential of -0.25 V *vs.* the Ag/AgCl electrode, and scanning in the negative direction at a d.c. rate of 0.5 V min^{-1}.

Procedure for the lead(II)-chloride-fluoride system

The same method of obtaining a.c. polarograms was used, except that the initial solution in the polarographic cell was calculated so that after addition of an aliquot of fluoride, the initial concentration of lead(II) would be $4 \cdot 10^{-4}$ *M*, the ionic strength 1.0 and the concentration of chloride 0.2 *M*. The various concentrations of fluoride used are shown in the appropriate Tables.

The fluoride-selective electrode (Orion Model 94-08) was used to monitor the free fluoride concentration where stated. Potentials of this electrode were measured with a Metrohm potentiograph E336A, relative to a Ag/AgCl reference electrode.

THEORY

For polarographic reduction of a metal ion species at the dropping mercury electrode, the half-wave potential, $E_{\frac{1}{2}}$, should be independent of metal ion concentration in any given environment, provided that the electrode reaction is reversible and the ionic strength is maintained constant for all measurements.

For the conventional d.c. method applied to lead(II) in 1 *M* sodium perchlorate, the electrode reaction was shown to be reversible by plots of $E_{\mathrm{d.e.}}$ *vs.* log $i/(i_{\mathrm{d}}-i)$, which were linear and had a slope very close to the theoretical value of 29.6 mV for a reversible 2-electron reduction. It was also confirmed that $E_{\frac{1}{2}}$ was independent of lead(II) concentration. Plots of lead(II) concentration *versus* i_{d} were linear over the range 10^{-5}–$10^{-3}M$ and the electrode reaction was diffusion-controlled. With the rapid d.c. method, no change was observed in the characteristics of the electrode reaction, compared with the conventional d.c. method, and the electrode reaction remained reversible.

For a.c. polarography, the peak potential, E_{s}, is equal to $E_{\frac{1}{2}}$ for reversible electrode processes; experimentally, close agreement was obtained. The half-width of the a.c. polarogram, with both rapid and conventional techniques, was (49 ± 1) mV (uncompensated for *IR* drop) and E_{s} was found to be independent of lead(II) concentration in 1 *M* perchlorate. The a.c. electrode process is therefore also reversible and a.c. polarography can be used for examination of the complex ion systems of lead(II), provided that irreversibility is not caused by chloride or fluoride complexation. The a.c. wave-height, $i_{\mathrm{d}}\sim$, in 1 *M* perchlorate was linearly proportional to the lead(II) concentration up to $5 \cdot 10^{-4}\,M$ with both the rapid and conventional methods. In the presence of fluoride, precipitation occurred and $i_{\mathrm{d}}\sim$ of course decreased. The half-width of the a.c. waves, however, remained close to the reversible value. In complexing media, and even in the presence of precipitation, the electrode reaction was therefore still reversible. Thus E_{s} should be independent of lead(II) concentration and can be evaluated accurately for any particular environment, as the value will be independent of the change of lead(II) concentration occurring via precipitation. If complex formation is extremely rapid and occurs before the kinetically slower precipitation process, then the measured E_{s} values can be used to solve the complex ion system. Changes in concentration of ligand resulting from precipitation can be neglected as the analytical concentration of ligand is initially in a vast excess to that of lead(II) and is effectively unaltered. With these approximations sufficient data are available for determination of the complex system in the normal manner.

As the electrode reaction remains reversible under conditions of rapid polarography, the $E_{\frac{1}{2}}$ and E_{s} values obtained can be used advantageously compared with conventional methods[5,6]. However, because of the more rapid recording possible with the a.c. method[5] and for other reasons[6], the rapid a.c. E_{s} values were used for the sparingly soluble systems in preference to rapid d.c. $E_{\frac{1}{2}}$ values.

TABLE I

DECREASE IN $i_d\sim$ AND [Pb(II)] WITH INCREASING FLUORIDE CONCENTRATION EXPERIMENTALLY OBSERVED AND CALCULATED FROM EQUILIBRIUM CONDITIONS FOR $K_s=[Pb^{2+}][F^-]^2=2.5\cdot10^{-7}$

(Initial $[Pb(II)]=4\cdot10^{-4}$ *M*)

[F⁻] (M)	*$i_d\sim$ (µA)*	*[Pb(II)] in solution at time of measurement (M)*	*[Pb(II)] in solution at equilibrium calculated from K_s (M)*
0.000	1.32	$4.0\cdot10^{-4}$	$4.0\cdot10^{-4}$
0.032	1.31	$4.0\cdot10^{-4}$	$2.4\cdot10^{-4}$
0.080	1.30	$3.9\cdot10^{-4}$	$3.9\cdot10^{-5}$
0.196	1.15	$3.5\cdot10^{-4}$	$6.5\cdot10^{-6}$
0.392	0.475	$1.4\cdot10^{-4}$	$1.6\cdot10^{-6}$
0.588	0.410	$1.2\cdot10^{-4}$	$7.3\cdot10^{-7}$
0.800	0.055	$1.7\cdot10^{-5}$	$3.9\cdot10^{-7}$

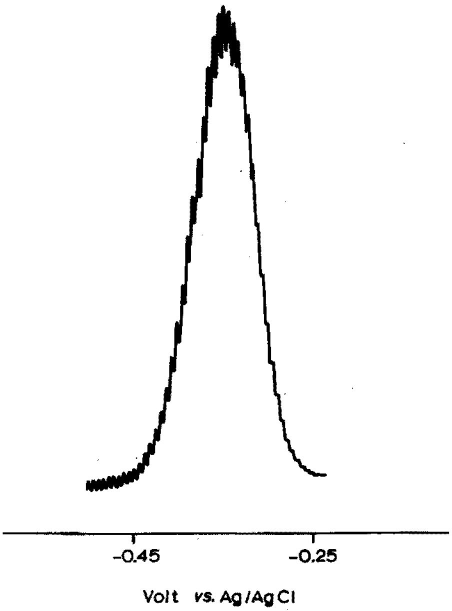

Fig. 1. Rapid a.c. polarogram of lead(II) with or without precipitation.

From solubility data, it can be shown that at precipitation equilibrium the concentration of lead(II) remaining in solution in the lead(II)–fluoride system would be too low to detect. The solubility product for sparingly soluble lead fluoride[3],

$$K_s=[Pb^{2+}]\,[F^-]^2$$

is reported as being $2.5\cdot10^{-7}$ under similar conditions used in this work. Thus, with a concentration of 1 *M* sodium fluoride the equilibrium concentration of lead(II) would be about $2.5\cdot10^{-7}$ *M*, which is well below the level of detection by rapid a.c. polarography (*ca.* 10^{-5} *M*).

Table I shows the measured $i_d\sim$ values and the approximate concentrations of lead(II) at the point of measurement calculated from a calibration curve in 1 M perchlorate, compared with the equilibrium concentrations expected if the above solubility product is applicable and complex formation is neglected. It can be seen that precipitation is kinetically quite slow and that solubility equilibrium is certainly not reached within the time interval of the polarographic experiment. Furthermore, no significant change in lead(II) concentration occurs during the recording of a rapid a.c. polarogram. Figure 1 shows a typical a.c. polarogram measured in the presence of precipitation. The shape is completely unaffected by precipitation, which would not happen if the lead(II) concentration changed considerably during the recording of the polarogram.

The same considerations apply to the lead(II)–chloride–fluoride system as given for lead(II)–fluoride, and "normal" polarograms could be recorded on all solutions, again indicating that little change occurred in the lead(II) concentration during the short scan time. The precipitation of lead chlorofluoride in the system was also observed to be kinetically slow and had similar characteristics to that for lead fluoride.

It is estimated, therefore, that if complex formation is rapid, and E_s is independent of metal ion concentration, then the complexes of a sparingly soluble system can be determined by rapid a.c. polarography if the metal ion concentration remains greater than 10^{-5} M for the 20 sec necessary for the recording.

The reproducibility of the rapid E_s value for lead(II) in 1 M perchlorate was found to be slightly better than 1 mV. The reproducibility was virtually unaltered by the precipitation of lead fluoride or chlorofluoride, which suggests that physical interaction of the mercury drop with the precipitate caused no significant interference to the mercury drop during its 0.16-sec growth time.

For the lead(II)–fluoride system, the equation of DEFORD AND HUME[4] is valid with one minor modification[3]. The usual equation[4] can be expressed as:

$$\begin{aligned} F_0(X) &= \sum_{j=0}^{j} \beta_j[\mathrm{F}^-]^j \\ &= \text{antilog}\left\{0.4343\,\frac{nF}{RT}\,[(E_{\frac{1}{2}})_f-(E_{\frac{1}{2}})_c]+\log\frac{I_f}{I_c}\right\} \end{aligned} \tag{1}$$

where the subscripts f and c refer to the free and complexed lead(II) ions, respectively. Other symbols are those used conventionally. $F_0(X)$ is introduced to represent the experimentally measured right-hand side of the equation.

The term log I_f/I_c, normally measured as log $(i_d)_f/(i_d)_c$ had to be omitted in the presence of precipitation[3], as changes in i_d other than those caused by complex formation occur. As I_f and I_c are usually very similar, this should be a good approximation.

For a.c. polarography, the lead(II)–fluoride system can be solved by the expression

$$\begin{aligned} F_0(X) &= \sum_{j=0}^{j} \beta_j[\mathrm{F}^-]^j \\ &= \text{antilog}\ 0.4343\,\frac{nF}{RT}\,[(E_s)_f-(E_s)_c] \end{aligned} \tag{2}$$

again omitting the term log I_f/I_c. This equation can be solved graphically in the normal way[4] and as described previously[5,6].

In the presence of two ligands, chloride and fluoride, an equation proposed by SCHAAP AND MCMASTERS[8] can be applied to mixed ligand complex formation. This equation can be written as:

$$F_0(X) = 1 + \sum_{j=1}^{j}\beta_j[\mathrm{F}^-]^j + \sum_{k=1}^{k}\alpha_k[\mathrm{Cl}^-]^k + \sum_{l=1,m=1}^{l,m}\gamma_{l,m}[\mathrm{F}^-]^l[\mathrm{Cl}^-]^m$$
$$= \text{antilog } 0.4343\,\frac{nF}{RT}\,[(E_s)_t - (E_s)_c]$$

where β_j are the stability constants of fluoride complexes from the equilibria

$$\mathrm{Pb}^{2+} + j\mathrm{F}^- \overset{\beta_j}{\rightleftharpoons} \mathrm{PbF}_j{}^{(2-j)+}$$

α_k are the stability constants of chloride complexes from the equilibria

$$\mathrm{Pb}^{2+} + k\mathrm{Cl}^- \overset{\alpha_k}{\rightleftharpoons} \mathrm{PbCl}_k{}^{(2-k)+}$$

and $\gamma_{l,m}$ are the stability constants for the mixed chloro–fluoro system:

$$\mathrm{Pb}^{2+} + l\mathrm{F}^- + m\mathrm{Cl}^- \overset{\gamma_{l,m}}{\rightleftharpoons} \mathrm{PbCl}_m\mathrm{F}_l{}^{(2-m-l)+}$$

As it is already known from other data that three major lead complexes of chloride[1,9] and two of fluoride exist[2,3], the equation for mixed complexes can be simplified to

$$F_0(X) = 1 + \alpha_1[\mathrm{Cl}^-] + \alpha_2[\mathrm{Cl}^-]^2 + \alpha_3[\mathrm{Cl}^-]^3$$
$$+ (\beta_1 + \gamma_{11}[\mathrm{Cl}^-])[\mathrm{F}^-] + \beta_2[\mathrm{F}^-]^2 \qquad (3)$$

if it is assumed that the only mixed complex of lead(II) is the 1:1 complex, PbClF. If other mixed complexes exist, then additional terms must be added.

If all measurements are made at constant chloride concentrations, then in terms of constants A, B and C, eqn. (3) becomes

$$F_0(X) = A + B[\mathrm{F}^-] + C[\mathrm{F}^-]^2 \qquad (4)$$

which is of the same mathematical form as for the lead(II)–fluoride system. Thus the mixed system can be solved in a similar way to lead(II)–fluoride for the constants A, B and C as follows.

A plot of $F_0(X)$ *vs.* $[\mathrm{F}^-]$ should be curved with an intercept at $[\mathrm{F}^-]=0$ of A. A plot of $F_1(X) = (F_0(X) - A)/[\mathrm{F}^-]$ *vs.* $[\mathrm{F}^-]$ should be a straight line of slope C and intercept B. A plot of $F_2(X) = (F_1(X) - B)/[\mathrm{F}^-]$ *vs.* $[\mathrm{F}^-]$ should be a straight line parallel to the concentration axis, and have a constant value equal to C.

The values of A should be consistent with the value $1 + \alpha_1[\mathrm{Cl}^-] + \alpha_2[\mathrm{Cl}^-]^2 + \alpha_3[\mathrm{Cl}^-]^3$, B will be equal to $(\beta_1 + \gamma_{11}[\mathrm{Cl}^-])$ from which γ_{11} can be evaluated, and C should be equal to β_2. The values of A and C provide a useful check on the solution of the mixed complex system.

RESULTS AND DISCUSSION

The lead(II)–fluoride system

Table II shows the data for the lead(II)–fluoride system obtained at 25° and ionic strength 1.0. Table II and the graphical method of analysis shown in Fig. 2

indicate that two fluoride complexes of lead(II) exist with β_j values of 25 ± 5 (β_1 for PbF^+) and 350 ± 30 (β_2 for PbF_2), respectively.

These values are in reasonable agreement with those reported earlier[2,3], after allowing for differences in temperature and ionic strength.

The lead(II)–chloride–fluoride system

Table III and Fig. 3 show the data and calculation method for the lead(II)–chloride–fluoride system. It can be seen that the data fit the equation given pre-

TABLE II

ANALYSIS OF $F_j(X)$ FUNCTIONS FOR THE LEAD(II)–FLUORIDE SYSTEM

[F⁻] (M)	$-E_s$ *(V vs. Ag/AgCl)*	$F_0(X)$	$F_1(X)$	$F_2(X)$
0.000	0.3314	1.000	—	—
0.032	0.3449	2.860	—	—
0.080	0.3528	5.290	53.63	358
0.128	0.3609	9.940	69.83	350
0.196	0.3685	17.99	86.70	315
0.392	0.3854	66.99	168.4	366
0.588	0.3942	133.0	224.5	339
0.800	0.4040	284.4	354.3	412

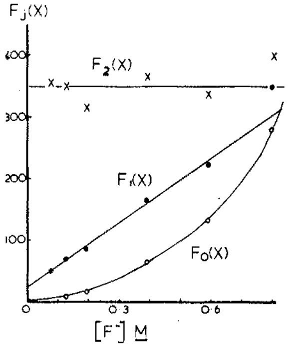

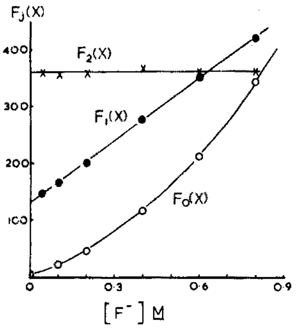

Fig. 2. Analysis of the $F_j(X)$ functions for the lead(II)–fluoride system.

Fig. 3. Analysis of the $F_j(X)$ functions for the lead(II)–chloride–fluoride system.

TABLE III

ANALYSIS OF $F_j(X)$ FUNCTIONS FOR THE LEAD(II)–CHLORIDE–FLUORIDE SYSTEM

($(E_{\frac{1}{2}})_t = -0.3314$ V *vs.* Ag/AgCl; [NaCl] = 0.2 *M*)

[F⁻] (M)	$-E_s$ *(V vs. Ag/AgCl)*	$F_0(X)$	$F_1(X)$	$F_2(X)$
0.00	0.3314	—	—	—
0.04	0.3619	10.77	144.3	358
0.10	0.3709	21.67	166.7	367
0.20	0.3804	45.50	202.5	363
0.40	0.3924	115.6	276.3	366
0.60	0.4000	209.7	341.2	352
0.80	0.4061	336.2	414.0	355

viously assuming that the complex PbClF is formed. A is experimentally calculated from the $F_0(X)$ plot as 5. α values obtained from previous work[9] for the lead(II)–chloride system were $\alpha_1=15$ ($PbCl^+$), $\alpha_2=15$ ($PbCl_2$) and $\alpha_3=80$ ($PbCl_3^-$). Thus, for a chloride concentration of 0.2 M, A, where $A=1+\alpha_1[Cl^-]+\alpha_2[Cl^-]^2+\alpha_3[Cl^-]^3$, is calculated to be 5.2.

C is experimentally calculated as being 360 from the $F_2(X)$ plot which is parallel to the fluoride concentration axis. This value is in excellent agreement with the value of $\beta_2=350$ for PbF_2 obtained above.

B was found to have a value of 130 from the intercept of the linear $F_2(X)$ plot. Since $B=(\beta_1+\gamma_{11}[Cl^-])$, then a value of $\gamma_{11}=525$ is obtained for the complex PbClF, assuming that $\beta_1=25$ for the complex PbF^+ as determined above.

The value of 525 for the mixed complex can obviously only be assumed to be an order of magnitude but evidence is provided which strongly supports the existence of the PbClF complex.

As a further check, the presence of mixed chloride–fluoride complexes of lead(II) were examined in a qualitative manner with the fluoride ion-selective electrode. The potential of a 10^{-5} M fluoride solution in 1 M perchlorate was measured. Addition of lead(II) to this solution altered the potential, as lead fluoride complexes were formed and the fluoride activity was lowered. Addition of chloride to the system caused a further change in potential consistent with a further decrease of fluoride activity. As conditions were chosen to be well below the solubility level of PbF_2, $PbCl_2$ or PbClF, the only explanation is that a mixed chloride–fluoride complex is formed, which provides qualitative verification of the polarographic evidence.

A.c. polarography of the lead(II) complex system in the presence of oxygen

For a.c. polarography, it has been claimed[11] that measurements can be made without degassing to remove oxygen. However, an a.c. polarogram of lead(II) in 1 M perchlorate solution shows two very distinct peaks if oxygen is not removed. The first peak occurs at almost the same E_s value as in a degassed solution and can be attributed to the normal electrode reaction. The second wave can be attributed to lead hydroxy complexes[10] which are quite strong[1], the hydroxide coming from the electroreduction of oxygen, although no a.c. wave was observed for oxygen alone at the instrument sensitivities used. When degassing was carried out, the second peak attributed to the hydroxy complex, gradually disappeared and the height of the first peak increased proportionally; on complete degassing only one peak was obtained as in Fig. 1.

In the presence of fluoride or chloride, marked changes in the effect of oxygen occurred and at high halide concentrations only one wave was observed in both degassed and non-degassed solutions. In 1 M sodium chloride the wave observed in the presence of oxygen was *ca.* 100 mV more negative than the corresponding wave obtained after degassing, and its shape was asymmetrical and markedly dependent on the lead(II) concentration. Obviously, the interaction of the products of the oxygen electrode reaction with the lead(II)–chloride complex system must be complicated. The results show, however, that it would be impossible to study lead(II) complexes in the presence of oxygen. This finding is in agreement with previous experience for a cadmium(II)–fluoride system[6]. It seems likely that degassing is unnecessary only when no interference occurs from hydroxide formation, which does not often happen.

SUMMARY

Rapid a.c. polarographic methods possess certain advantages in studies of complex ions of sparingly soluble systems involving reversible electrode processes. The sparingly soluble lead(II)–fluoride system, studied previously, was re-examined in detail by the rapid a.c. method; excellent agreement was obtained with earlier values. The mixed complex system lead(II)–chloride–fluoride was then evaluated. The complex PbClF was detected and a stability constant of 525 was obtained at an ionic strength of 1.0 and 25°. The general need for eliminating oxygen in a.c. polarography is discussed.

RÉSUMÉ

Les méthodes polarographiques rapides, à courant alternatif, présentent certains avantages pour l'étude de complexes dans des systèmes relativement peu solubles, comprenant des processus d'électrode réversible. Le système fluorure de plomb, étudié préalablement, a été réexaminé en détail par cette méthode. Les résultats obtenus concordent très bien avec les valeurs déjà trouvées. On a ainsi décélé le complexe PbClF; une constante de stabilité de 525 est obtenu, à une force ionique de 1.0 à 25°. On examine également la necessité d'éliminer l'oxygène en polarographie c.a.

ZUSAMMENFASSUNG

Methoden der Rapid-Wechselstrompolarographie haben gewisse Vorteile bei der Untersuchung von Komplexionen von wenig löslichen Systemen, die reversible Elektrodenprozesse enthalten. Das früher bearbeitete wenig lösliche Blei(II)–Fluorid-System wurde ausführlich mit der Rapid-Wechselstrom-Methode erneut untersucht; es wurde ausgezeichnete Übereinstimmung mit früheren Werten erhalten. Dann wurde das gemischte Komplexsystem Blei(II)–Chlorid–Fluorid ausgewertet. Es wurde der Komplex PbClF nachgewiesen und eine Stabilitätskonstante von 525 bei Ionenstärke 1.0 und 25° erhalten. Die allgemeine Notwendigkeit der Eliminierung von Sauerstoff bei der Wechselstrompolarographie wird diskutiert.

REFERENCES

1 *Stability Constants of Metal-Ion Complexes*, Special Publication No. 17, The Chemical Society, London, 1964.
2 A. M. BOND AND G. HEFTER, *Inorg. Chem.*, 9 (1970) 1021.
3 S. S. MESARIC AND D. N. HUME, *Inorg. Chem.*, 2 (1963) 788.
4 D. D. DEFORD AND D. N. HUME, *J. Am. Chem. Soc.*, 73 (1951) 5321.
5 A. M. BOND, *J. Electroanal. Chem.*, 23 (1969) 277.
6 A. M. BOND, *J. Electroanal. Chem.*, 20 (1969) 223.
7 C. A. HORTON, in I. M. KOLTHOFF AND P. J. ELVING, *Treatise on Analytical Chemistry, Part II, Vol. 7*, Interscience, New York, 1961, p. 257.
8 W. B. SCHAAP AND D. L. MCMASTERS, *J. Am. Chem. Soc.*, 83 (1961) 4699.
9 A. M. BOND AND G. HEFTER, Unpublished work, University of Melbourne, 1969–70.
10 B. BREYER, F. GUTMAN AND S. HACOBIAN, *Australian J. Sci. Res.*, A3 (1950) 567.
11 S. L. GUPTA AND M. K. CHATTERJEE, *J. Electroanal. Chem.*, 8 (1964) 245; *Rev. Polarog. (Kyoto)*, 14 (1967) 198.

Analytica Chimica Acta
Elsevier Publishing Company, Amsterdam
Printed in The Netherlands

ETUDE ANALYTIQUE DES NICKELATES DE SODIUM ET DE BARYUM

MICHELINE VILTANGE

Laboratoire de Recherches Microanalytiques, Ecole Nationale Supérieure de Chimie, 11 rue Pierre-et-Marie-Curie, Paris 5e (France)

(Reçu le 24 juin 1970)

Poursuivant l'étude des réactions à l'état solide du peroxyde de sodium sur divers oxydes métalliques[1], nous exposons ici les résultats obtenus par chauffage de cet agent chimique en présence de l'oxyde de nickel. Des travaux sur les nickelates de sodium, préparés par voie sèche, sont connus. Glemser et Einerhand[2] ont préparé le nickelate(III) $NaNiO_2$ (Na:Ni:O actif = 1:1:0.5) par fusion d'un mélange de peroxyde de sodium et de soude dans un creuset de nickel. Dyer et coll.[3] ont utilisé la soude seule et un courant d'oxygène comme agent d'oxydation pour obtenir la même substance. Wallace et Fleck[4] sont parvenus à un corps plus oxydé $Na_2Ni_5O_{15}$ (Na:Ni:O actif = 0.4:1:1.8) en incorporant 5% de peroxyde de sodium au mélange d'oxyde de nickel et de soude. Klemm et coll.[5] ont atteint, vers 400°–500°, une phase de composition $Na_{1.5}NiO_{2.5}$ (Na:Ni:O actif = 1.5:1:0.75) qui se transforme à plus haute température en $NaNiO_2$. Butyutskii et Khitrova[6] ont étudié par rayons X le composé $Na_{0.2}NiO_{1.8}$ (Na:Ni:O actif = 0.2:1:0.7). La diversité des substances susceptibles d'être obtenues nous a donc conduit à étudier la réaction, dans l'air, du peroxyde de sodium sur NiO par les méthodes habituellement utilisées, thermogravimétrie, analyse thermique différentielle, puis à soumettre les produits recueillis à l'analyse chimique et à l'examen par spectrographie d'absorption infrarouge pour les identifier et mettre en évidence quelques-unes de leurs propriétés.

TECHNIQUES UTILISÉES

Le peroxyde de sodium (Prolabo) avait une teneur de 1.30 atome d'oxygène actif et de 2.46 atomes de sodium par 100 g de produit brut non chauffé. L'oxyde de nickel, vert-jaune, de pureté voisine de la composition stoechiométrique, a été préparé par chauffage jusqu'à 800° de l'hydroxyde, lui-même obtenu par décomposition à l'ébullition de nitrate de nickel ammoniacal. Un second échantillon (Prolabo) de couleur vert foncé a également été utilisé. Son comportement a été sensiblement le même que celui du premier.

Thermogravimétrie

Les mélanges de poudres ont été chauffés dans des creusets de porcelaine Staatlich disposés dans le four d'une thermobalance Adamel à enregistrement photographique, pour les expériences qui se sont déroulées dans l'air, ou électronique pour celles qui ont été effectuées sous courant gazeux, à titre de contrôle. La montée de la température était de 300° h^{-1}.

Analyse thermique différentielle

L'analyseur thermique différentiel de Mazières, construit par Bureau de Liaison, a servi à l'étude des variations de température développées au sein des mélanges ne pesant que quelques dixièmes de milligramme. Le four n'a pas été chauffé au-dessus de 400° afin que la soude, toujours présente dans le peroxyde, ne déborde pas du micro-creuset d'alumine et n'attaque pas la sonde de platine. Sur les enregistrements, nous retrouvons aux températures inférieures à 200° les phénomènes précédemment étudiés[7] qui traduisent seulement l'évolution thermique des hydrates, peroxydrates, percarbonates, impuretés inévitables du peroxyde de sodium.

Spectrographie d'absorption infrarouge.

Les spectres ont été enregistrés entre 200 et 4000 cm^{-1} sur un spectromètre Beckman IR 12, à double faisceau. Des lamelles de CsI, CsBr et NaCl ont servi à confectionner les cuves. Les poudres ont été généralement mêlées à de la vaseline pour augmenter leur homogénéité.

RÉACTION $Na_2O_2 + NiO$

Thermogravimétrie et analyse thermique différentielle

Quelle que soit la valeur du rapport molaire Na_2O_2:NiO choisi (1:1 à 4:1), le mélange, chauffé dans l'air, commence à se colorer en noir à partir de 210°–230°, tandis qu'on observe une faible augmentation de poids et un léger dégagement de chaleur qui se poursuivent jusque vers 400° pour les mélanges relativement pauvres

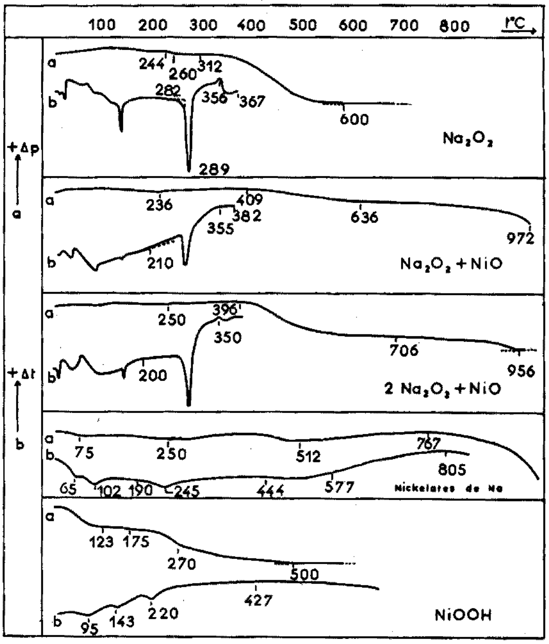

Fig. 1. Courbes thermogravimétriques (a) et d'analyse thermique différentielle (b) de Na_2O_2, des mélanges de Na_2O_2 et de NiO, des nickelates de sodium après lavage à l'eau et séchage à la température ordinaire et du produit d'hydrolyse de ceux-ci.

en peroxyde (1:1 et 2:1); pour les autres (3:1 et 4:1), un départ d'oxygène commence vers 360° ainsi qu'un effet endothermique (Fig. 1). Rappelons que le peroxyde de sodium, seul, se décompose entre 310° et 600° environ. Le retard observé dans le dégagement d'oxygène jusqu'à 360° ou 400° laisse supposer soit une inhibition de la décomposition du peroxyde, soit l'oxydation de l'oxyde de nickel. La deuxième hypothèse justifierait la coloration noire du contenu du creuset. Si le pic de fusion de la soude se dessine toujours à partir de 282°, celui de la transformation $Na_2O_{3,6} \rightarrow Na_2O_2$ n'est plus observé: le superoxyde, NaO_2, contenu dans le peroxyde à la température ordinaire ou le premier terme de sa dégradation, $Na_2O_{3,6}$, doit donc entrer en réaction avec NiO avant 280°.

La perte de poids du système qui commence vers 400° se poursuit jusque vers 1000°. Sur les courbes de chauffage des mélanges 1:1, on observe la présence d'un point d'inflexion vers 640° et sur les autres (2:1 à 4:1), un ralentissement de la perte de poids entre 680° et 820°. Par chauffage en thermostat vers 620°–650°, un poids constant est atteint quel que soit le rapport molaire initial. On calcule à partir de ces courbes ATG que 0.5 atome d'oxygène actif environ est encore fixé sur chaque mole de NiO initial, ceci pour les rapports 2:1 à 4:1 qui nous le verrons, assurent un rendement de 100%. A ce stade, le nickel se trouve donc bien sous une valence égale ou équivalente à 3.

Les courbes ATG ne renseignent pas ensuite sur la température à partir de laquelle la réduction totale de ce composé est réalisée: dès 850°, la décomposition du carbonate de sodium intervient en effet.

Des mélanges ont été chauffés également dans l'azote ou dans l'oxygène

TABLEAU I

TEMPÉRATURES LIMITES DE LA DÉCOMPOSITION DE Na_2O_2 DANS DIVERS GAZ

Gaz	*Composition initiale*	*Temp. de début de décomposition*	*Temp. finale de décomposition*	*Composition calculée du résidu*
Air	Na_2O_2	310	593	$\frac{\text{O actif}}{\text{Ni total}} = \frac{0.5}{1}$
	$1.5\ Na_2O_2 + NiO$	434	680–820	
Azote	Na_2O_2	312	750	$\frac{\text{O actif}}{\text{Ni total}} = \frac{0.478}{1}$
	$1.5\ Na_2O_2 + NiO$	460	683	
Oxygène	Na_2O_2	300	735	$\frac{\text{O actif}}{\text{Ni total}} = \frac{0.52}{1}$
	$1.5\ Na_2O_2 + NiO$	575	900	

TABLEAU II

GAIN DE POIDS OBSERVÉ ENTRE 230 ET 400° PAR CHAUFFAGE DYNAMIQUE DE MÉLANGES DE Na_2O_2 + NiO ET RAPPORTÉ AU POIDS INITIAL DE NiO

Rapport molaire	*Atmosphère*	*Gain de poids (%)*
1:1	air	0.77 à 1.3
1.25:1	air	1
1.5:1	air	1.5 à 2.1
1.5:1	oxygène	1
2:1	air	1.6 à 2.3
4:1	air	2.9

(Tableau I). Au cours du chauffage dynamique dans l'oxygène, l'oxyde de nickel seul ne semble pas en capter, tout au moins dans la limite de la précision des mesures. Rappelons que Besson n'a pas observé de modification du réseau cristallin de NiO entre 200° et 420°[8]. Par contre, en présence de peroxyde de sodium (rapports 1:1 et 2:1), une absorption superficielle se mesure entre 300° et 500°. Son importance paraît liée à la teneur en peroxyde du mélange (Tableau II). En conséquence, le faible gain de poids observé dans l'air est dû à une absorption d'oxygène en plus de celle d'anhydride carbonique qui est habituellement observée dans tout système comportant du peroxyde ou de l'oxyde de sodium. Coué[9] a constaté que l'addition d'ions étrangers (en l'occurence Li^+) stimulait l'adsorption de l'oxygène sur NiO. De son côté, Charman et coll.[10] a montré que des ions du nickel(III) existaient déjà dans les oxydes divalents non stoechiométriques. Enfin, Brown[11] a obtenu l'oxyde le plus réactif par calcination de l'oxalate, précisément à 450°.

Analyses chimiques

Des résidus de chauffage obtenus vers 730° ou par maintien en thermostat à 600°–650° sont traités par le mélange oxalate–acide sulfurique dont l'excès est dosé en retour par le permanganate. Pour tous les rapports molaires supérieurs à 1.5:1, l'oxydation de NiO est complète, un demi-atome d'oxygène s'est bien fixé sur chaque mole de NiO (Tableau III).

TABLEAU III

VALEURS DE LA TENEUR EN OXYGÈNE ACTIF, DÉTERMINÉES PAR OXYDIMÉTRIE, POUR DIFFÉRENTS MÉLANGES DE PEROXYDE DE SODIUM ET D'OXYDE DE NICKEL, APRÈS CHAUFFAGE EN THERMOSTAT VERS 600°–700°

O actif initial / *Ni total*	*O actif résiduel* / *Ni total* *(calculs)*	*O actif résiduel* / *Ni total* *(oxydimétries)*	*Remarques*
0.98:1	0.48:1	0.405:1	double dosage
1.33:1	0.51:1	0.508:1 ± 0.003:1	dosage direct
1.71:1	0.48:1	0.497:1	dosage direct
1.94:1	0.49:1	0.48:1 ± 0.04:1	double dosage
2.04:1	0.45:1	0.488:1 ± 0.003:1	dosage direct
2.77:1	0.62:1	0.495:1 ± 0.003:1	dosage direct
4.51:1	0.52:1	0.53:1	double dosage

Il est à remarquer que le catalyseur (H_2SO_4–$CuSO_4$) du dosage gazométrique de l'oxygène actif, par la méthode précédemment mise au point, est sans action sur le produit obtenu vers 600°–700°: une gazométrie du mélange chauffé à une température comprise entre 400° et 600°, suivie d'une oxydimétrie à l'oxalate, permet donc de doser sélectivement d'abord la quantité de peroxyde de sodium en excès puis la quantité de nickel(III) formé. Cette dernière est à peine inférieure à celle obtenue par une oxydimétrie directe, en ce qui concerne les produits portés à 600°–700°.

Les calculs s'accordent assez bien avec les résultats expérimentaux du Tableau IV. Les écarts s'expliquent surtout par la carbonatation partielle du milieu.

Le lavage à l'eau distillée du produit obtenu à 600°–700° permet, d'après divers auteurs, d'obtenir le nickelate, $NaNiO_2$, qui s'hydrolyse facilement en NiOOH et $Ni(OH)_2$. En effet, le dosage de la soude libre, dans divers résidus lavés puis cen-

TABLEAU IV

BILAN DE LA CONSOMMATION DE L'OXYGÈNE ACTIF DU PEROXYDE DE SODIUM CHAUFFÉ À DIFFÉRENTES TEMPÉRATURES AVEC NiO, PAR PLUSIEURS MÉTHODES

$t°$	*20*	*220*	*304*	*402*	*417*	*501*	*635*
$\frac{\text{O actif initial}}{\text{NiO total}}$	1:0	1:0	1.65:1	1.66:1	1.63:1	1.73:1	1.46:1
$n_{\text{gazometrique}}$ [a]	2.60	2.20 ± 0.02	2.03	1.51	1.36 ± 0.03	1.17	0
$\frac{\text{O actif résiduel}}{\text{NiO total}}$ (par gazométrie)			1.22	0.97	0.85	0.78	0
$\frac{\text{O actif résiduel}}{\text{NiO total}}$ (par oxydimétrie)			0.100	0.43		0.468	0.508
$\frac{\text{O actif résiduel}}{\text{NiO total}}$ (pertes d'après courbes ATG)			0	0	0	0.05	0.684
Pertes en oxygène et CO_2, entre 20 et 200°			0.25	0.25	0.25	0.26	0.22
$\frac{\text{O actif total}}{\text{NiO total}}$ (gazo+oxydi+ATG+pertes entre 20 et 200°)			1.57	1.65		1.564	1.412
Ecarts % avec $\frac{\text{O actif initial}}{\text{NiO total}}$			−4.8	−0.6			−3.4
Rendement d'oxydation de NiO(%)			20	84		87	100

[a] $n_{\text{gazometrique}}$ = nombre de valences grammes d'oxygène actif rapportées à 100 g de peroxyde de sodium et déterminées par gazométrie.

trifugés, indique par différence des valeurs du rapport R = (Na combiné : Ni total) très dispersées, bien que les dosages oxydimétriques ultérieurs accusent une conservation à peu près quantitative de l'oxygène actif. Nous avons alors procédé par tâtonnements successifs en suivant la variation de pH des suspensions dans l'eau pour un volume donné de celle-ci et un poids donné des mélanges initiaux. Il a été ainsi possible d'isoler des résidus de R compris entre 2.24 et 1.16 par cette méthode très grossière, il est vrai, puisque plusieurs phénomènes secondaires interviennent aussi: présence d'ions carboniques, adsorption d'ions libres Na^+ par les composés du nickel en particulier. De l'examen des résultats obtenus, il semble que la valeur de R diminue quand la température de chauffage en thermostat et surtout la durée de celui-ci augmentent: par exemple, $R = 1.47$ pour 1½ h à 639°, 1.16 pour la même durée à 660°, 1.38 pour 2 h à 640°. Une extraction des ions sodium non combinés par le butanol primaire a laissé un résidu de composition telle que $R = 1.9 \pm 0.2$ (50 min à 649°).

La dispersion des résultats fait penser soit à la formation de composés d'addition de Na_2O et de Ni_2O_3 ou d'un nickelate de sodium, soit à un mélange de plusieurs nickelates, tels que $NaNiO_2$ (ou $Na_2Ni_2O_4$) et $Na_4Ni_2O_5$, ce dernier par analogie avec

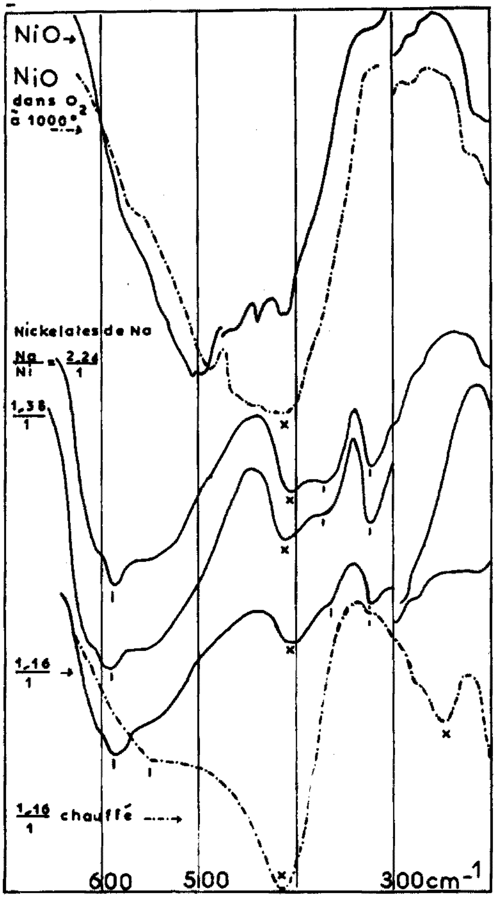

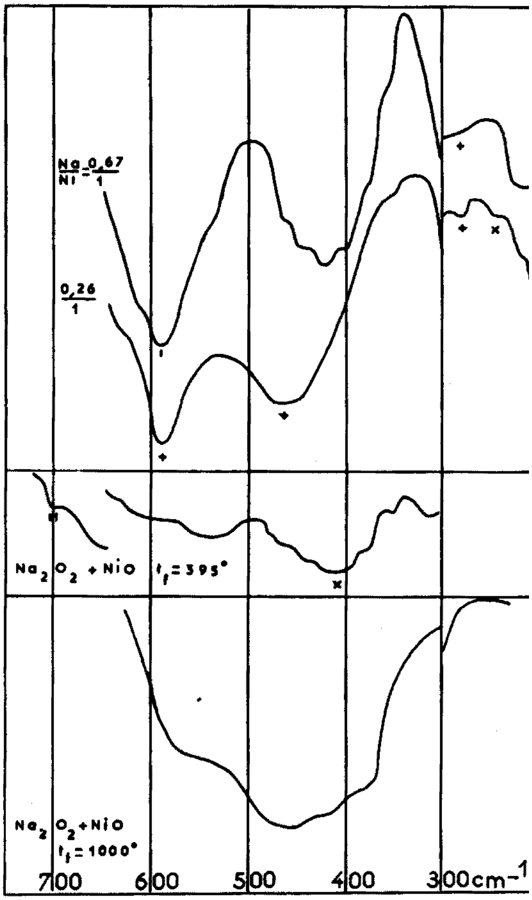

Fig. 2a. Spectres d'absorption infrarouge entre 200 et 650 cm^{-1} de NiO, de NiO après chauffage dans l'oxygène à 1000°, des nickelates de sodium de composition Na:Ni=2.24:1, 1.38:1, 1.16:1 et 1.16:1 soumis à un second chauffage à 740°.

Fig. 2b. Spectres d'absorption infrarouge des produits de lavage des nickelates de sodium de composition Na:Ni = 0.67:1 et 0.26:1 obtenue par dosage du mélange Na_2O_2 + NiO après chauffage à 395° et 1000°.

le nickelate de baryum, $Ba_2Ni_2O_5$, préparé par action de BaO_2 sur NiO[12]. La spectrographie d'absorption infrarouge devrait éclaircir cette question.

Spectrographie d'absorption infrarouge

Spectres de composés divalents du nickel. Le maximum de la bande d'absorption de NiO, entre 400 et 500 cm^{-1}, se pointe vers 488 cm^{-1} (Fig. 2 a). Il se déplace à 410–430 cm^{-1} par chauffage jusqu'à 470° dans l'air aussi bien qu'à 1000° dans l'oxygène, tandis qu'apparaît un épaulement vers 575 cm^{-1}.

L'hydroxyde de nickel absorbe à 3645–3580 cm^{-1} (ν_{OH}), 523 cm^{-1} (δ_{OH}), 350 cm^{-1} (γ_{OH}) et 462 à 475 cm^{-1} ($\nu_{Ni(II)-O}$)[13].

Spectres des résidus de chauffage entre 600 et 740° des mélanges de Na_2O_2 et de NiO. L'aspect des spectres des produits lavés avec précaution, puis analysés, montre des différences liées surtout à l'hydrolyse partielle qui peut se produire, plutôt qu'à la teneur en ions sodiques, pour une température de chauffage déterminée. Ainsi, tous les produits préparés vers 630–650° présentent des bandes d'absorption à 610–585–560 cm^{-1}, 400–405 cm^{-1}, 370–380 cm^{-1} (épaulement) et 320 cm^{-1}. Par chauffage du résidu de $R=1.16$ jusqu'à 740°, c'est-à-dire à une température inférieure à sa décomposition, la bande de 405 cm^{-1} se déplace jusqu'à 410–420 cm^{-1} et s'amplifie considérablement; il en apparaît une autre à 250 cm^{-1} alors que celles de 560 et de 320 cm^{-1} sont très affaiblies. Deux formes (A) et (B) de nickelates existent, dont les bandes caractéristiques sont les suivantes*:

(A)	610–585–560, f F af		370–380, 320 cm^{-1} e m	
(B)		405–420 TF		250 cm^{-1} af

L'intensité de la bande de 405–420 cm^{-1} augmente bien avec la valeur de la température finale de chauffage par exemple à 713°, ce qui dénote un mélange de (A) et de (B) dans la plupart des résidus.

Notons que l'absorption de 370–380 cm^{-1} ne peut être confondue avec la vibration γ_{HO} de $Ni(OH)_2$ de 350 cm^{-1}. Pour les résidus de R supérieurs à 1:1, on peut supposer qu'ils se présentent sous la forme de combinaisons de Na_2O dans le nickelate (A), soit $NaNiO_2$, soit $Na_2Ni_2O_4$.

Toutes les bandes décrites pour (A) et (B) disparaissent par chauffage à 950°–1000°. Elles sont donc caractéristiques de l'état d'oxydation des nickelates de sodium. Avec une assez bonne précision, il est possible de déterminer celui-ci par comparaison de leurs nombres d'onde avec ceux des vibrations de valence des composés du fer. On sait en effet que les fréquences caractéristiques des groupements XO_4 varient avec la masse atomique du métal X et avec le degré d'oxydation de celui-ci[14]. En prenant comme bases de comparaison pour les ferrates et les ferrites:

$\nu_{3\,\mathrm{Fe(VI)-O_4}} = 780$–$850$ cm^{-1} [15]

$\nu_{3\,\mathrm{Fe(V)-O_4}}$ ou $\nu_{3\,\mathrm{Fe(IV)-O_4}} = 700$ cm^{-1} [15]

$\nu_{3\,\mathrm{Fe(III)-O_4}} = 570$ cm^{-1} [16] et 550–650 cm^{-1} [17] pour les ferrites du type spinelle inverse, on voit que la vibration de valence antisymétrique de $Ni(III)-O_4$ peut se situer légèrement au-dessus de 570 cm^{-1}, dans la mesure où un tel groupement existe et possède la configuration d'un tétraèdre régulier ou peu déformé. Cette valeur se situe bien dans l'une des régions d'absorption du nickelate (A), à 585–560 cm^{-1}.

TARTE[17] a montré que les groupements $Fe(III)-O_6$ et $Cr(III)-O_6$ des composés complexes absorbaient respectivement entre 300 et 400 cm^{-1} d'une part, 300 et 450 cm^{-1} d'autre part, c'est-à-dire à des fréquences plus basses que celles des tétraèdres isolés $Fe(III)-O_4$ et $Cr(III)-O_4$ (550–650 cm^{-1}) selon une loi générale que l'on retrouve également chez les germanates[18] et les stannates[19]. La bande forte de 420 cm^{-1} du nickelate (B), qui n'a pas encore perdu d'oxygène au cours de son deuxième chauffage, doit s'attribuer alors à la vibration de valence d'une liaison $Ni(III)-O$ hexacoordinée. A 250 cm^{-1} se situerait sa vibration de déformation.

On pourrait se demander si la bande de 405 cm^{-1} n'est pas, elle aussi, caracté-

---

* F= fort, TF = très fort, f = faible, af = assez faible, e = épaulement.

ristique de (A), dont le spectre ressemblerait alors à celui de spinelles inverses tels que $NiFe_2O_4$ (587 et 396 cm^{-1}): dans la même espèce, on décèlerait des groupements NiO_4 et NiO_6. Nous verrons plus loin que la transformation (A) $\rightarrow$ (B) ne se localise pas dans un domaine restreint de températures au-delà de 650°. Donc l'hypothèse de la présence simultanée de nickelates (A) et (B) dès 600°–650° paraît plus admissible.

La bande de 320 cm^{-1} du nickelate (A) dont l'intensité est affectée par le chauffage, tout comme celle de 585 cm^{-1}, peut être δ_{NiO_4}.

Dyer et coll.[3] ont montré que la forme basse température du nickelate de sodium trivalent, $NaNiO_2$, obtenue par chauffage à 650° puis à 850° pendant quatre jours était isomorphe de $NaFeO_2$ et monoclinique avec deux molécules par maille. Le nickel y est précisément hexacoordiné à l'oxygène. Il y a une certaine analogie également entre le spectre de (B) et celui de l'oxyde divalent chauffé dans l'air à 450° aussi bien qu'à 1000° dans l'oxygène dont un maximum d'absorption se dessine vers 410–430 cm^{-1}, bien que sur la courbe thermogravimétrique, on ne décèle pas de gain de poids sensible. Cela confirme l'existence de centres actifs Ni(III) superficiels reconnus par de nombreux auteurs.

Spectres des produits d'hydrolyse du nickelate de sodium. L'hydrolyse assez poussée conduit à des résidus contenant toujours un peu de sodium (R=0.67 puis 0.241 par exemple). Labat[20] a confirmé que, sous l'action de l'eau, $NaNiO_2$ se transformait en NiOOH-γ et $Ni(OH)_2$. Sur les spectres étudiés, on retrouve effectivement des bandes de ce dernier, très faibles. En outre, on observe une absorption à 585 cm^{-1}, moins étalée que pour les nickelates (A), ainsi qu'à 280, 435–60, 1035–975 et 3400 cm^{-1}.

L'absorption de la région de 3400 cm^{-1} indique l'existence de vibrations ν_{OH} ou ν_{H_2O} peu liées. La première hypothèse entraîne les attributions suivantes: δ_{OH} vers 1000 cm^{-1}, γ_{OH} vers 450 cm^{-1}, en accord d'une part avec les positions des vibrations planes et gauches reconnues pour les groupements relativement libres de nombreux composés chimiques, d'autre part avec celles des hydroxydes naturels XOOH. Pour la goethite α-FeOOH, par exemple, $\nu_{OH}=3090$ cm^{-1}, $\delta_{OH}=893$ et 797 cm^{-1} et $\gamma_{OH}=465$ cm^{-1} [13].

La seconde hypothèse ne semble pas devoir être retenue car la vibration δ_{H_2O} qu'on devrait attendre est rarement observée vers 1600–1650 cm^{-1}. Donc $\nu_{OH}=3400$ cm^{-1}, $\delta_{OH}=1035$–975 cm^{-1} et $\gamma_{OH}=430$–460 cm^{-1}.

La bande de 585 cm^{-1} de ce produit d'hydrolyse doit être une vibration de valence Ni(III)–O. Rappelons que pour la goethite, on observe à 580 cm^{-1} une absorption due à l'atome métallique[13]. Il n'est pas possible d'affirmer que la liaison Ni–O soit encore tétracoordinée: la relative faiblesse de la liaison OH pourrait conférer à NiOOH une structure un peu différente, plus proche de l'oxyde Ni_2O_3. Nous savons en effet que Fe_2O_3 se présente sous forme d'un réseau tridimensionnel d'octaèdres vibrant entre 550 et 600 cm^{-1}, précisément dans la même région que les sites tétraédriques isolés[17].

Spectres des résidus de chauffage à 400° des mélanges de Na_2O_2 et de NiO. Klemm et coll.[5] ont envisagé que vers 400° il se substituait une certaine quantité d'ions Na^+ et O^{2-} dans le réseau des atomes nickel(III), ce qui entraînerait le passage d'une petite quantité de ces derniers à la valence 4.

Les cuves du produit dont la température a été arrêtée à 400° ont été confectionnées en atmosphère d'argon à cause de leur extrême avidité pour l'eau. Après broyage, les grains présentent une couleur marron qui rappelle celle de MnO_2 tandis que les nickelates de sodium sont noirs. Les bandes se situent à 700 cm^{-1} (TF), 530 cm^{-1} (f et large (l), elle est produite par une impureté du peroxyde de sodium en excès), 400 cm^{-1} (l, af). Celles de 700 et de 400 cm^{-1} sont compatibles avec l'existence de liaisons Ni(IV) – O et Ni(III) – O. Il est regrettable qu'il n'ait pas été possible de chauffer les creusets à plus de 400° dans les expériences d'ATD. Car, si vers 400° la masse réagissante contient un composé tétravalent du nickel, même en faible quantité, on devrait pouvoir observer sa décomposition à plus haute température.

ÉTUDE PAR THERMOGRAVIMÉTRIE ET ANALYSE THERMIQUE DIFFÉRENTIELLE DU NICKELATE DE SODIUM ET DE NiOOH

Les nickelates de sodium de $R = 2.24$ et 1.161 possèdent des courbes semblables. Au-dessus de 500°, un net dégagement de chaleur ne s'accompagne que d'un faible gain de poids. On l'attribue à la décomposition des composés de (A) en nickelate (B) et à l'absorption de CO_2 par l'oxyde de sodium libéré. Au-delà de 750°, l'oxygène actif est libéré. Ces produits conservés en tubes n'échappent pas à une hydrolyse lente qui se traduit par une faible perte de poids avant 200° et de petits pics endothermiques entre 60° et 97°, 97° et 123°, 208° et 360°.

Dès 45°, NiOOH perd de l'eau en quantité variable avec absorption de chaleur. Un palier oblique s'étale ensuite entre 120° et 177° avant une seconde perte de poids (sensiblement 17 g par atome de nickel) qui traduit la décomposition en oxyde divalent. Elle est accompagnée d'un pic endothermique (A = 200°, D = 220°). Il rappelle celui de la courbe ATD de α-FeOOH dont le maximum se situe vers 260°–270° [21]. Toute perte de poids ultérieure, entre 700° et 1000° est due à la présence éventuelle de nickelate et de carbonate de sodium.

RÉACTION $BaO_2 + NiO$

Par chauffage dynamique dans l'air, un mélange de BaO_2 et de NiO dans la proportion 1.5:1 garde son poids constant jusqu'à 640° (BaO_2 chauffé dans les mêmes conditions se décompose entre 450° et 800° environ). A 905°, alors que la perte de poids n'est pas encore terminée, on observe un net gain de poids qui cesse à 990° et représente le tiers de la perte mesurée entre 640° et 905° (Fig. 3).

Le peroxyde de baryum ne présente pas ce phénomène quand il est chauffé seul dans l'air ou dans l'oxygène (température de décomposition dans ce dernier gaz = 690° à 1000°). Le mélange $BaO_2 + NiO$, dans l'oxygène, reprend entre 945° et 990° seulement un-cinquième du poids perdu entre 665° et 945°, soit 0.1 atome d'oxygène par mole de NiO de la prise d'essai. Si le four est mis en thermostat à 990°, au bout d'un certain temps, on observe une seconde perte, très légère (le tiers du poids gagné). De tels phénomènes n'ont pas été observés avec le peroxyde de sodium.

BaO_2 se décompose dans l'air dès 380° en absorbant de la chaleur (Fig. 3). Pour le mélange $BaO_2 + NiO$ un dégagement de chaleur s'observe de 260° à 624°. Une dépression endothermique traduit ensuite le dégagement d'oxygène, puis elle est suivie au-delà de 915° d'un phénomène exothermique correspondant à la capture d'oxygène.

On peut donc localiser le début de la réaction entre BaO_2 et NiO vers 260°, sensiblement à la même température que pour le mélange $Na_2O_2 + NiO$. Le retard au dégagement d'oxygène, au cours de la production de nickelate est plus important, deux cent degrés au lieu d'une centaine.

Le mélange chauffé dans l'air à 580° possède des bandes (Fig. 4) à 595 cm^{-1}, 495 cm^{-1} (excès de NiO), 415 cm^{-1} (m), 310 cm^{-1} (f) et 280 cm^{-1} (f), comparables à celles du spectre du nickelate de sodium (A). L'intensité des bandes de 595 et 415 cm^{-1} diminue quand la température atteint 850° puis 900°, le résidu étant alors vert-foncé, puis elle augmente à nouveau, particulièrement celle de 415 cm^{-1} (forme B). Cela montre bien qu'à 990° la poudre contient davantage de nickel(III) qu'à 900°.

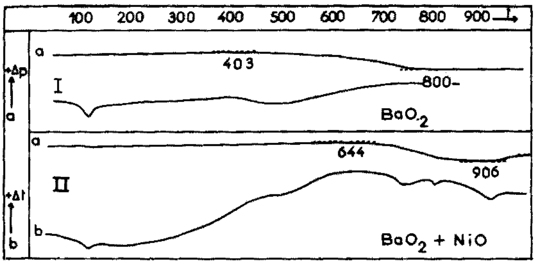

Fig. 3. Courbes de thermogravimétrie (a) et d'analyse thermique différentielle (b) de BaO_2 et de BaO_2 + NiO.

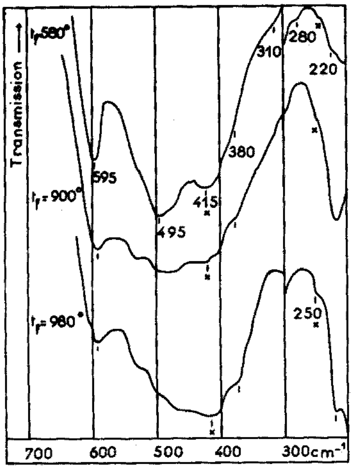

Fig. 4. Spectres d'absorption infrarouge des mélanges de BaO_2 + NiO après chauffage dans l'air à 580°, 900° et 980°,

Rien ne permet d'envisager la formation avant 400° d'un composé plus oxygéné. Il semble y avoir, comme pour les composés sodiques, un équilibre entre les formes (A) et (B), la seconde étant prédominante à haute température.

RÉSUMÉ

L'étude de la réaction du peroxyde de sodium sur NiO a montré qu'entre 200° et 400° environ, il se formait partiellement une substance très instable qui peut posséder la valence IV, en plus de centres actifs Ni(III) en situation octaédrique. Vers 600° à 750°, des composés d'addition de Na_2O avec le nickelate(III), où le nickel se trouve à la fois tétra- et hexacoordiné, évoluent par chauffage vers l'espèce à sites uniquement octaédriques avant la décomposition en un mélange d'oxydes de sodium et de nickel divalent. L'action ménagée de l'eau froide provoque la formation d'un produit d'hydrolyse, NiOOH, analogue aux composés correspondants du fer, mais à liaisons OH plus faibles.

SUMMARY

A study of the reaction of sodium peroxide with nickel oxide has shown that between 200° and 400°, a very unstable compound containing nickel(IV) as well as nickel(III) central atoms in an octahedral configuration is formed. At 600–750°, addition compounds of Na_2O and nickelate(III), in which nickel appears to be both tetra- and hexacoordinated, change on heating to a species containing only octahedral sites, before decomposition to a mixture of sodium oxide and nickel(II) oxide. The action of cold water leads to formation of a hydrolysed product, NiOOH, analogous to similar iron compounds but containing weaker OH bonding.

ZUSAMMENFASSUNG

Die Reaktion zwischen Natriumperoxid und Nickeloxid wurde untersucht. Zwischen 200 und 400° werden eine sehr instabile Nickel(IV) enthaltende Verbindung ebenso wie Nickel(III)-Zentralatome in oktaedrischer Konfiguration gebildet. Bei 600–750° gehen Additionsverbindungen von Na_2O und Nickelat(III) mit sowohl vierfach als auch sechsfach koordiniertem Nickel beim Erhitzen in eine Spezies mit nur oktaedrischer Anordnung über. Danach erfolgt Zersetzung zu einem Gemisch von Natriumoxid und Nickel(II)-oxid. Kaltes Wasser hydrolysiert zu NiOOH in Analogie zu ähnlichen Eisenverbindungen, jedoch mit schwächerer OH-Bindung.

BIBLIOGRAPHIE

1 M. VILTANGE, *Anal. Chim. Acta*, 42 (1968) 259; *Chim. Anal. (Paris)*, 51 (1969) 378.
2 O. GLEMSER ET J. EINERHAND, *Z. Anorg. Allgem. Chem.*, 261 (1950) 26, 43.
3 L. D. DYER, B. S. BORIE ET G. P. SMITH, *J. Amer. Chem. Soc.*, 76 (1954) 1499.
4 T. WALLACE ET A. FLECK, *J. Chem. Soc.*, 119 (1921) 1839.
5 H. BADE, W. BRONGER ET W. KLEMM, *Bull. Soc. Chim. France*, (1965) 1124.
6 P. N. BITYUTSKII ET V. I. KHITROVA, *Kristallografiya, Soviet Phys. Cryst.*, 13 (1969) 867.
7 M. VILTANGE, *Anal. Chim. Acta*, 39 (1967) 491.
8 J. BESSON, *Ann. Chim. (Paris)*, 2 (1947) 527.
9 J. COUÉ, *Thèse*, Lyon, 1963, d'après J. L. RIVAIL, *J. Chim. Phys., Phys.-Chim. Biol.*, 62 (1965) 619.
10 H. B. CHARMAN, R. M. DELL ET S. S. TEALE, *Trans. Faraday Soc.*, 59 (1963) 453.
11 R. A. BROWN, *J. Amer. Ceram. Soc.*, 48 (1965) 627.
12 J. J. LANDER ET L. A. WOOTEN, *J. Amer. Chem. Soc.*, 73 (1951) 2452.
13 C. CABANNES, *Ann. Chim. (Paris)*, 5 (1960) 905.
14 C. DUVAL ET J. LECOMTE, *Bull. Soc. Franç. Minéral. Crist.*, Avril-Juin (1949) 245.
15 N. BECARUD, *Thèse Doctorat*, Paris, 1965.
16 R. D. WALDRON, *Phys. Rev.*, 99 (1955) 1727.
17 P. TARTE, *Compt. Rend.*, 254 (1962) 2008; P. TARTE ET R. COLLONGUES, *Ann. Chim. (Paris)*, 9 (1964) 135.
18 J. P. LABBÉ, *Ann. Chim. (Paris)*, 10 (1965) 1.
19 T. DUPUIS ET V. LORENZELLI, *Compt. Rend.*, 262 (1966) 489.
20 J. LABAT, *Ann. Chim. (Paris)*, 9 (1964) 399.
21 S. NOBUOKA, K. ADO ET A. TAKAHASHI, *Bull. Gov. Ind. Res. Inst. Osaka*, 19 (1968) 312.

Analytica Chimica Acta
Elsevier Publishing Company, Amsterdam
Printed in The Netherlands

SHORT COMMUNICATIONS

Determination of iodine in the p.p.m. range in rocks*

Methods for the determination of iodine have been surveyed by ZAK[1]. Popular methods include those based on: (1) the catalytic effect of iodide on the oxidation of arsenic(III) by cerium(IV), (2) the color intensity of iodine in various solvents, (3) the color intensity of the tri-iodide ion, and (4) the color intensity of the iodo–starch complex. Sensitivity is enhanced in the last three methods by use of an amplification reaction wherein iodide is first converted to iodate and then made to react with added iodide to produce a 6-fold increase in the iodine liberated. To realize maximum sensitivity it is generally required for all methods that iodine be separated from the matrix material, preferably by distillation.

The catalytic methods require careful control of conditions; they are affected by the constituents of a sample and as a result are not uniformly successful without time-consuming separations. Those methods that depend on the amplification iodate–iodide reaction are not entirely without problems, for the excess of oxidant used to convert iodide to iodate must be completely destroyed, under conditions that will not reduce iodate. The iodate–iodide reaction is sensitive to pH and there is a tendency, because of induced reactions or air oxidation of the iodide added, for more iodine to be liberated than indicated by the stoichiometry of the reaction. For these reasons it seemed desirable to avoid the iodate—iodide reaction and to measure the iodine coming only from the sample.

The need for a simple method for determining iodine in geological materials has become increasingly important. For environmental studies, a rapid method that would delineate "highs" in rocks and soils was needed in regional surveys being undertaken by the U.S. Geological Survey. This paper describes such a method. The procedure provides for the presence of various forms of iodine such as iodide or iodate bound inorganically or iodide bound organically. The chemical reactions involved are:

$$I^-, IO_3^- \xrightarrow[\substack{\text{Alk.} \\ \text{KMnO}_4}]{} IO_3^- \xrightarrow[\substack{H_2SO_4 \\ SnSO_4}]{} I^- \xrightarrow[\text{NaNO}_2]{} I_2$$

The iodine is extracted into carbon tetrachloride and determined spectrophotometrically.

The original sample is decomposed by sintering with a mixture of sodium carbonate, potassium carbonate, and magnesium oxide. Magnesium oxide aids in the destruction of organic matter and retains most of the silica as insoluble magnesium silicate when the sinter is leached with water and the solution is filtered. The filtrate containing iodide and iodate is the starting point for the reactions noted above. Approximately 1 p.p.m. of iodine can be determined as a lower limit on a 1-g sample and at least 1 mg of bromide and 25 mg of chloride can be tolerated without interference. With a minor change in procedure at least 10 mg of bromide can be tolerated.

---

* Publication authorized by the Director, U.S. Geological Survey.

Apparatus and reagents

A Beckman Model DU spectrophotometer with 5-cm cells of 2.5 cm^3 volume (American Instrument Co., Silver Spring, Maryland) was used.

Flux. Mix together 400 g each of sodium and potassium carbonates and 100 g of magnesium oxide.

Standard iodide solutions (1, 10, and 100 µg ml^{-1}). Prepare a stock solution from dry reagent-grade potassium iodide and from this prepare standards by successive dilutions.

Tin(II) sulfate (approximately 0.3 N). Stir 3.22 g of tin(II) sulfate in 50 ml of water. Cool in an ice bath and then while stirring add 40 ml of (1+1) sulfuric acid. Filter through a medium-porosity paper and adjust the volume of the filtrate to 100 ml. Add 2 g of mossy tin.

Procedure

Mix a 1-g sample with 4.5 g of flux in a nickel crucible and heat uncovered for 1–1.5 h in a small furnace at 750°. Leach the sinter with 30–40 ml of water overnight, covered, on a steam bath. When the sinter disintegrates, remove the crucible and wash, adding the washes to the main solution. Heat and break all lumps with a glass rod. Filter on a 9-cm medium-porosity filter paper and wash the residue with hot water. Reject the residue.

Evaporate the solution on a hot plate to *ca.* 20 ml. Add 3 drops of 0.3 *N* potassium permanganate solution (some manganate may form) and heat to near boiling for about 1 min. Cool in an ice bath. Add (1+1) sulfuric acid dropwise while stirring until the solution is just acid. Neutrality is judged when a drop of sulfuric acid causes no effervescence and is confirmed by applying a small drop of the solution to litmus paper. Add 3.5 ml of (1+1) sulfuric acid in excess and stir vigorously to allow most of the carbon dioxide to escape.

Add tin(II) sulfate solution dropwise while stirring until the permanganate is decolorized, and add 1 ml in excess. After 1 min add 1 ml of aqueous 0.4 *M* sodium nitrite solution and stir briefly. After another minute add 1 ml of aqueous 4% (w/v) urea solution and mix. Transfer the solution without undue delay to a 60-ml separatory funnel. After 1 min extract with 3 ml of carbon tetrachloride added by pipette, shaking the mixture for 1 min. Drain the iodine extract into a dry 5–10 ml beaker, which acts to hold back water droplets and then transfer the solution to a 10 × 75-mm test tube. Cover loosely with a Teflon stopper. After 15 min measure the absorbance of the extract in a 5-cm cell at 517 nm against carbon tetrachloride in a matched cell. Determine the iodine concentration by reference to a calibration curve relating net absorbance to iodine concentration.

A procedural blank should be run with each new batch of prepared flux. The calibration curve is prepared by taking standard iodide or iodate solutions, adjusting the volume to 25 ml with water, adding 1 pellet of sodium hydroxide, and proceeding with the permanganate oxidation and subsequent steps of the procedure.

Results and discussion

Decomposition of sample. The flux composition suggested provides for decomposition of samples containing up to approximately 65% silica. Samples containing more silica require proportionally more magnesia to retain silica in the insoluble form but no change is necessary in the amounts of other flux ingredients. The amounts of silica escaping into the filtrate cause no problems. Fusions are best made in nickel crucibles, with 99.9% alumina ceramic a second choice. Low and erratic recoveries of iodine were noted with platinum crucibles possibly as the result of the sequestering action of platinum on iodide, or the interference of soluble platinum corrosion products in the oxidation–reduction reactions of the procedure. Temperatures above 800° lead to losses of iodine by volatilization.

Oxidants and reductants. Conversion of iodide to iodate by alkaline permanganate ensures that no iodine is lost during the vigorous evolution of carbon dioxide accompanying acidification of the carbonate solution. The conversion of iodate to iodide at microgram levels proved difficult and of the many reductants tried only tin(II) sulfate gave immediate quantitative reduction. The conversion of iodide to iodine is also critical in that the oxidant used must have little tendency to further oxidize the iodine to a positive oxidation state. A number of oxidants proved useful and from these sodium nitrite was selected.

Reagent concentrations. The conditions selected call for the extraction of iodine from a total volume of 30 ml formed after addition of the various reagents. There is a comfortable latitude in the concentration of reagents that can be used. For example, half or twice the amount of sulfuric acid causes no problems. Also, the distribution ratio is high enough so that the total volume of the aqueous phase can be changed up or down by 40% without significant effect (< 5%) on the recovery of iodine. Table I presents six combinations of reagent amounts tested which permit quantitative recovery of iodine when 3.5 ml of sulfuric acid in excess is used. Of course, enough sodium nitrite should be used to oxidize the tin(II) sulfate and to provide a sufficient excess to liberate iodine.

TABLE I

COMBINATIONS OF REAGENT AMOUNTS YIELDING QUANTITATIVE RECOVERY OF IODINE

Excess 0.3 N $SnSO_4$ (ml)	*0.4 N $NaNO_2$ (ml)*	*4% urea (ml)*
1.0, std.	1.0, std.	1.0, std.
0.5	1.0	1.0
0.5	2.0	2.0
1.0	2.0	2.0
2.0	2.0	2.0
2.0	4.0	4.0

Standard curve. A plot of iodine absorbance against wavelength (420–600 nm) yields a bell-shaped curve with absorbance peaking at 517 nm. The standard curve relating net absorbance to iodine concentration is a straight line up to an iodine concentration of 35 p.p.m., the maximum tested. The sensitivity according to Sandell's definition is 0.33 μg cm^{-2}.

Effects of bromide and chloride. At least 1 mg of bromide and 25 mg of chloride can be tolerated without change in the procedure. With more of each, low results are obtained, probably as a result of oxidation of iodine to the positive monovalent state as, for example, in iodine monochloride[2].

At least 10 mg of bromide and 25 mg of chloride can be tolerated if the bromide is oxidized to bromine and then volatilized. The presence of bromine is made evident by its color during the acidification step after alkaline permanganate oxidation. Here more permanganate is added a drop at a time, waiting after each drop for the bromine to form and for the permanganate to bleach. When the bromide is completely titrated, one drop of permanganate is added in excess. The solution is then brought to the boil and boiled for a full minute to expel the bromine. Some manganese dioxide may precipitate at the same time. The analysis is then continued with the addition of tin(II) sulfate and with subsequent steps of the general procedure.

Volatility of iodine. After liberation of iodine with sodium nitrite, extraction of the iodine into carbon tetrachloride should proceed without undue delay, to minimize losses from the volatility of iodine. For example, when 20-μg amounts of iodide were converted to iodine as in the procedure, 70% of the iodine was recovered when the solution before extraction was allowed to stand in an open 50-ml beaker for 30 min at room temperature (25°), and 45% was similarly recovered from an open 100-ml beaker. Comparable iodine losses from open beakers were observed for dilute sulfuric acid solutions of iodine prepared from elemental iodine, but no losses were evident from closed containers. There were also no losses of iodine from carbon tetrachloride solutions allowed to stand for 1 h in open 10 × 75 mm test tubes.

TABLE II

DETERMINATION OF IODINE IN SHALE AND LIMESTONE—MEANS AND STANDARD DEVIATIONS

Sample	*No. of detns.*	*Mean (p.p.m.)*	*Std. dev. (p.p.m.)*
Procedural blank	9	0.1	0.08
Limestone	14	2.67	0.31
Limestone + 10 p.p.m. I^-	9	12.7	0.66
Shale	2	0.0	—
Shale + 10 p.p.m. I^-	11	9.8	0.34

Test of procedure. Iodine was determined repetitively in a shale and a limestone both directly and after the addition of 10 μg of iodide to each. The results are summarized in Table II. It would seem that at least 1 p.p.m. of iodine can be determined as a lower limit on a 1-g sample and that somewhat higher concentrations should be determinable within a relative error of 10%.

U.S. Geological Survey,
Washington, D.C. (U.S.A.)

F. S. GRIMALDI
M. M. SCHNEPFE

1 B. ZAK, *Iodine*, in D. F. BOLTZ (Ed.), *Colorimetric Determination of Nonmetals*, Interscience New York, 1958, pp. 197–230.
2 J. K. JOHANNESON, *Anal. Chem.*, 30 (1958) 1535.

(Received June 18th, 1970)

Analytica Chimica Acta
Elsevier Publishing Company, Amsterdam
Printed in The Netherlands

Comparison of the trifluoroacetyl and trimethylsilylether derivatives for gas chromatography of steroids

The use of trifluoroacetyl derivatives for the isolation and characterization of natural hydroxy compounds has been demonstrated in various investigations. Trifluoroacetyl derivatives of carbohydrates[1,2], terpenols[3,4], flavonoids, nucleosides[5] and, particularly, steroids[6] are suitable for g.l.c. and g.l.c.–m.s. investigations and also for structure determination by ^{19}F-n.m.r. These derivatives are suitable for routine work because of their fast preparation, short retention times and sensitivity for electron capture detectors. Thus, a comparison of the gas-chromatographic behavior of trifluoracetyl and trimethylsilyl steroid derivatives of biological origin on various columns seemed to be advisable in order to test the most suitable conditions. So far very few papers deal with the applicability of trifluoroacetyl derivatives for g.l.c. investigations of hydroxyl compounds[7–9].

Experimental

The retention data were obtained on a Hewlett-Packard, Model 5750 gas chromatograph equipped with a hydrogen flame ionization detector. Three Pyrex glass columns were packed with Gas-Chrom Q 100–120 mesh (Applied Science Laboratories, Inc., Pa.) and coated with the stationary phases OV-17 (1 %), OV-1 (3 %) and XE-60 (1 %) (Applied Science Laboratories, Inc.). The temperature of the inlet system was 235°, and the temperatures of the columns were 200°, 210°, 220°, 225°, 230° and 235°. Nitrogen was used as carrier gas with a flow rate of 50 ml min^{-1}.

The trimethylsilylethers were obtained by dissolving the steroid (0.1–0.5 mg) in 0.1 ml of chloroform (E. Merck AG, Darmstadt) and adding 0.1 ml of hexamethyldisilazane and 5 drops of trimethylchlorosilane (Merck) to the mixture. After a reaction time of 12 h the solutions were evaporated to dryness and dissolved in 0.05 ml of chloroform for injection. The trifluoroacetates of steroids were prepared[6] by dissolving a 0.1–0.5 mg sample of steroid in a few drops of carbon tetrachloride (Merck) and adding 0.5 ml of trifluoroacetic anhydride (Schuchardt, Munich) distilled over P_4O_{10}; the resulting solution was injected after 10 min. Every measurement was repeated twice.

The retention indices of a compound[10] give the position of a peak in a chromatogram. In order to determine these indices, *n*-alkanes with even numbers of carbon atoms from C_{18} to C_{32} (EGA-Chemie, Steinheim) were used as reference standards. The advantage of the Kováts indices is that the reference system, *e.g.* methane 100, ethane 200, butane 400, decane 1000, etc., does, by definition, not depend on the liquid phase used. The indices of two successive *n*-alkanes are interpolated. Plotting the indices *versus* the number of carbons always yields a straight line. Before and after measuring the steroid samples, the mixture of *n*-alkanes was injected in order to obtain reproducible results.

Results and discussion

The Kováts indices of trimethylsilyl- and trifluoroacetyl-steroids determined on the stationary phases OV-1 and OV-17 are presented in Table I. Table II shows the retention data relative to 16α-methylpregnenolone, of the same derivatives obtained on the stationary phases OV-1, OV-17 and XE-60.

A comparison of the Kováts indices of the steroid derivatives clearly shows that

TABLE I

KOVÁTS INDICES OF TRIFLUOROACETYL (TFA) AND TRIMETHYLSILYL (TMSi) STEROID DERIVATIVES[a]

	OV-17 (1 %) at 210°		*OV-1 (3 %) at 225°*	
	TFA[b]	*TMSi*[c]	*TFA*[d]	*TMSi*[e]
Estrone(*1*)	2682	2952	2392	2578
Estradiol(*2*)	2527	2868	2353	2660
Estriol(*3*)	2476	3048	2340	2870
1-Methyl-6α, 7α-dihydroxyestrone(*4*)	2418	2968	2520	2744
Androst-5-en-3β-ol(*5*)	2304	—	2201	—
5α-Dihydrotestosterone(*6*)	2719	2840	2452	2564
5β-Dihydrotestosterone(*7*)	2670	2772	2420	2528
Androsterone(*8*)	2621	2712	2372	2458
Epiandrosterone(*9*)	2688	—	2436	2560
Testosterone(*10*)	2454	2910	2352	2628
Dehydroepiandrosterone(*11*)	2670	2798	2405	2524
6β-Hydroxy-3α, 5α-cycloandrostan-17-one(*12*)	2650	2530	2404	2308
Androst-5-ene-3β,17β-diol-16-one(*13*)	2742	2970	2512	2760
Pregnanediol(*14*)	2602	2798	2488	2744
Pregnenolone(*15*)	2824	2968	2564	2700
16α-Methylpregnenolone(*16*)	2772	2914	2584	2714
3β-Hydroxy-17αH-Δ^5-aetianic acid(*17*)	2812	2924	2576	2690
11α-Hydroxyprogesterone(*18*)	2702	3088	2550	2710

[a] For systematic names of steroids, see end of Table II.
[b-e] For column conditions, see end of Table II.

the retention times of the trifluoroacetyl compounds in all cases are much shorter, the only exception being 3α, 5α-cyclo-6-hydroxyandrostan-17-one (*12*). The indices on the OV columns were also calculated at temperatures of 200° (OV-17) and 235° (OV-1); however, the values changed only slightly (1–2 %) and are therefore not included. As *n*-paraffins with a higher number of carbon atoms (C_{34}–C_{40}) were not available the Kováts indices could not be calculated. Instead the relative retention data for columns with the stationary phase XE-60 are presented. As a reference compound, the derivatives of the not naturally occurring steroid 16α-methylpregnenolone (*16*) were chosen.

A comparison of the absolute retention times of the trifluoroacetyl derivatives with the trimethylsilyl derivatives shows that the trifluoroacetylated compounds have much shorter retention times on OV-17 and OV-1 columns. Thus the absolute retention times (in min) for the trifluoroacetyl and trimethylsilyl derivatives on the OV-17 column at 210° for certain compounds are as follows:

	Trifluoroacetyl	*Trimethylsilyl*
Estrone(*1*)	8.03	20.02
Estradiol(*2*)	4.54	14.85
5α-Dihydrotestosterone(*6*)	9.04	13.45
Testosterone(*10*)	3.53	17.35
Dehydroepiandrosterone(*11*)	7.59	12.30

However, when XE-60 is used as stationary phase, the absolute retention time of the trimethylsilyl derivatives is often smaller than that of the trifluoroacetyl derivatives. With increasing numbers of trifluoroacetylated hydroxyl groups on the steroid skeleton, the Kováts indices and the absolute retention times on the OV-1 and OV-17

TABLE II

RELATIVE RETENTION TIMES FOR TRIMETHYLSILYL ETHERS AND TRIFLUOROACETYL ESTERS OF STEROIDS (RELATIVE TO 16α-METHYLPREGNENOLONE)[a]

	OV-17 at 210°		*OV-1 at 225°*		*XE-60 at 220°*	
	TFA[b]	*TMSi*[c]	*TFA*[d]	*TMSi*[e]	*TFA*[f]	*TMSi*[g]
Estrone(*1*)	0.71	1.06	0.56	0.66	0.97	1.24
Estradiol(*2*)	0.40	0.78	0.49	0.85	0.52	0.53
Estriol(*3*)	0.33	1.49	0.47	1.61	0.70	0.80
1-Methyl-6α, 7α-dihydroxyestrone(*4*)	0.27	1.21	0.82	1.09	1.52	1.31
Androst-5-en-3β-ol(*5*)	0.18	—	0.30	—	0.22	—
5α-Dihydrotestosterone(*6*)	0.80	0.71	0.67	0.56	1.21	0.91
5β-Dihydrotestosterone(*7*)	0.66	0.56	0.61	0.63	1.09	0.76
Androsterone(*8*)	0.57	0.45	0.52	0.46	0.79	0.56
Epiandrosterone(*9*)	0.72	—	0.63	0.57	0.98	0.60
Testosterone(*10*)	0.31	0.91	0.48	0.78	0.42	1.30
Dehydroepiandrosterone(*11*)	0.67	0.65	0.60	0.60	0.85	0.92
6β-Hydroxy-3α, 5α-cycloandrostan-17-one(*12*)	0.65	0.24	0.58	0.29	0.32	0.38
Androst-5-ene-3β, 17β-diol-16-one(*13*)	0.87	1.13	0.80	1.15	1.80	1.02
Pregnanediol(*14*)	0.52	0.62	0.76	0.80	0.63	0.45
Pregnenolone(*15*)	1.15	1.12	0.97	0.96	1.26	1.09
16α-Methylpregnenolone(*16*)	1.00	1.00	1.00	1.00	1.00	1.00
3β-Hydroxy-17αH-Δ^5-aetianic acid(*17*)	1.10	1.04	0.98	0.93	1.06	0.77
11α-Hydroxyprogesterone(*18*)	0.78	1.73	0.92	0.96	1.24	—

[a] Systematic names of steroids:
1 = 1, 3, 5(10)-Estratriene-3-ol-17-one.
2 = 1, 3, 5(10)-Estratriene-3, 17β-diol.
3 = Estratriene-1, 3, 5(10)-triol-(3, 16α, 17β).
4 = 1-Methyl-1, 3, 5(10)-estratriene-3, 6α, 7α-triol-17-one.
5 = Androst-5-en-3β-ol.
6 = 5α-Androstan-17β ol-3-one.
7 = 5β-Androstran-17β-ol-3-one.
8 = 5α-Androstan-3α-ol-17-one.
9 = 5α-Androstan-3β-ol-17-one.
10 = Androst-4-en-17β-ol-3-one.
11 = Androst-5-en-3β-ol-17-one.
12 = 6β-Hydroxy-3α, 5α-cycloandrostan-17-one.
13 = Androst-5-ene-3β, 17β-diol-16-one.
14 = 5β-Pregnane-3α, 20α-diol.
15 = Pregn-5-en-3β-ol-20-one.
16 = 16α-Methyl-5-pregnen-3β-ol-20-one.
17 = 3β-Hydroxy-17αH-Δ^5-aetianic acid.
18 = Pregn-4-ene-11α ol-3, 20-dione.

[b-g] Column conditions for Tables I and II. Columns 77 feet, 100–120 mesh Gas-Chrom Q, 3.5 mm i.d., nitrogen flow rates 50 ml min^{-1}.
[b] 1 % OV-17, 210°; 16α-methylpregnenolone(*16*): 11.25 min.
[c] 1 % OV-17, 210°; 16α-methylpregnenolone(*16*): 18.95 min.
[d] 3 % OV-1, 225°; 16α-methylpregnenolone(*16*): 18.25 min.
[e] 3 % OV-1, 225°; 16α-methylpregnenolone (*16*): 23.5 min.
[f] 1 % XE-60, 220°; 16α-methylpregnenolone(*16*): 3.65 min.
[g] 1 % XE-60, 220°; 16α-methylpregnenolone(*16*): 3.76 min.

columns decrease. This is demonstrated by comparing the absolute retention data of estradiol (OV-1, 9 min; OV-17, 4.54 min) with those of estriol (OV-1, 7.84 min; OV-17, 3.71 min). In the case of the trimethylsilyl derivatives, these results are reversed.

The steroisomers 5α- and 5β-dihydrotestosterone (*6*, *7*) can be separated on all three columns at different temperatures as their trimethylsilyl as well as their trifluoroacetyl derivatives; the 5α-dihydrotestosterone derivatives are eluted later than those of the 5β-isomer. Trifluoroacetylated androsterone (*8*; axial 3-OH) is eluted faster than trifluoroacetylated epiandrosterone (*9*; equatorial 3-OH).

The relative response factors for the trifluoroacetyl derivatives of androsterone, aetiochol anolone and dehydroepiandrosterone are superior to those of the trimethylsilyl derivatives of the corresponding steroids by factors of 1.30, 1.41 and 1.54, respectively, with the flame ionization detector. In general, the relative retention of closely related steroids is smaller for trifluoroacetyl derivatives than for trimethylsilyl derivatives, in agreement with previous reports[11].

Attempts are now being made to explore the advantages of the trifluoroacetyl derivatives concerning short retention time and high response factors for the determination and structure elucidation of biologically occurring steroids, especially in the paediatric age group, where many steroid-like substances have been found[12], but their structures have not yet been fully confirmed.

We are grateful to E. Merck (Germany) and F. Hoffmann-La Roche (Switzerland) for providing steroid samples, and to the Deutsche Forschungsgemeinschaft for financial assistance. Two of us (G. B. and W. V.) thank the Fonds der Chemischen Industrie and the Deutsche Forschungsgemeinschaft for financial support.

Chemisches Institut der Universität,
Wilhelmstrasse 33,
D-74 Tübingen (D.B.R.)

WOLFGANG VOELTER
GÜNTHER JUNG
EBERHARD BREITMAIER
GERHARD BOUCHON
ERNST BAYER

Universitätskinderklinik, Tübingen (D.B.R.)

DEREK GUPTA

1 G. JUNG, W. VOELTER, E. BREITMAIER AND E. BAYER, *Tetrahedron Letters*, 43 (1969) 3785; *Liebigs Ann. Chem.*, 734 (1970) 136.
2 G. JUNG, H. PAUSCHMANN, W. VOELTER, E. BREITMAIER AND E. BAYER, *Chromatographia*, 3 (1970) 26.
3 E. BREITMAIER, G. JUNG, W. VOELTER AND E. BAYER, *Tetrahedron*, 26 (1970) 2053.
4 G. SCHNEIDER, E. BREITMAIER, G. JUNG AND W. VOELTER, *Tetrahedron*, 26 (1970) in press.
5 W. VOELTER, G. JUNG AND E. BREITMAIER, unpublished results.
6 E. BREITMAIER, W. VOELTER, G. JUNG AND E. BAYER, *Angew. Chem.*, 82 (1970) 82; *Angew. Chem. Intern. Edn. Engl.*, 9 (1970) 75; *Steroids*, 15 (1970) 275; *Organic Magnetic Resonance*, 2 (1970) 251.
7 B. A. KNIGHTS, *J. Gas Chromatogr.*, 2 (1964) 160; *Advan. Gas Chromatogr., Proc. Int. Symp. 4th*, 1967, p. 135.
8 W. J. A. VANDEN HEUVEL, B. G. CREECH AND E. C. HORNING, *Anal. Biochem.*, 4 (1962) 191.
9 E. C. HORNING, M. G. HORNING, N. IKEKAWA, E. M. CHAMBAZ, P. U. JAAKONMAKI AND C. J. W. BROOKS, *Advan. Gas Chromatogr.*, (1967) 122.
10 A. WEHRLI AND E. KOVÁTS, *Helv. Chim. Acta*, 42 (1959) 2 709.
11 E. C. HORNING, W. J. A. VANDEN HEUVEL AND B. G. CREECH, *Methods of Biochemical Analysis, Vol. XI*, Interscience, New York, 1967, p. 105.
12 D. GUPTA AND J. M. TANNER, *Nature*, 203 (1964) 187.

(Received July 10th, 1970)

Analytica Chimica Acta
Elsevier Publishing Company, Amsterdam
Printed in The Netherlands

Simultaneous gravimetric determination of aluminium and chromium in chrome ores

Aluminium is a common constituent of many ores, but few rapid and accurate gravimetric methods are available for its determination. In the analysis of chrome ores, aluminium, chromium and silica are brought into solution by alkali fusion and aluminium is generally determined as its hydroxide in the presence of chromium(VI) after silica has been separated. Incomplete separation from silica and difficulties in washing the aluminium hydroxide free of chromate are some of the drawbacks of this method.

It is well known that chromium(III) and aluminium(III) can be precipitated from homogeneous solution as their oxinates, and the method has been used for gravimetric determination of these elements[1-3]. MERRITT AND WALKER[4] studied the qualitative use of 8-hydroxyquinaldine (2-methyloxine) as a reagent for several metal ions and reported that chromium(III) is precipitated but aluminium is not. RAJAGOPALA RAO[2] studied extensively the homogeneous precipitation of chromium by 2-methyloxine and suggested this reagent for the determination of chromium in presence of aluminium. Based on the combined precipitation of chromium and aluminium by oxine and the selective precipitation of chromium by 2-methyloxine, the method described below allows the simultaneous determination of chromium and aluminium; precipitation is done from homogeneous solution to obtain precipitates of improved physical characteristics. The method has been applied to the analysis of chromium and aluminium in chrome ores.

Reagents and samples

All reagents used were of analytical grade.

Standard chromium and aluminium solutions. A 0.1 *N* potassium dichromate solution was used as a source for chromium. A standard solution of aluminium(III) was prepared by dissolving 47.5 g of potassium aluminium sulphate, $Al_2(SO_4)_3\,K_2SO_4\cdot 24\,H_2O$ in 1 l of water.

Chrome ore. A British Chemical Standard chrome ore, No. 308 (41.5 % Cr_2O_3 and 19.4% Al_2O_3) was used.

Combined precipitation of aluminium and chromium

Acidify 5–10 ml of 0.1 *N* dichromate solution with 1 ml of 2 *M* hydrochloric acid, add 0.2 g of sodium sulphite and stir to dissolve the solid. Add 25 ml of aqueous 40% (w/v) urea solution and 20 ml of 2% (w/v) oxine reagent in 2 *M* acetic acid. Dilute to about 100 ml with water and heat on a boiling water bath. Precipitation starts in about 15 min and is complete after 2 h. Filter the precipitate through a sintered glass crucible (porosity 3), wash with hot water 5–6 times, dry at 120° for 1 h and weigh. The value obtained represents the combined weight of chromium and aluminium oxinates.

Precipitation of chromium in presence of aluminium

Mix 5–10 ml of 0.1 *N* dichromate solution and 1–5 ml of standard aluminium solution, acidify with 1 ml of 2 *M* hydrochloric acid, add 0.2 g of sodium sulphite and stir to dissolve the solid. Add 20 ml of aqueous 40% (w/v) urea solution, 1–2 g of sodium potassium tartrate and 8 ml of 2% (w/v) 2-methyloxine reagent in 2 *M* acetic acid. Dilute to about 100 ml and heat on a boiling water bath. Precipitation starts in 30–45 min and is complete after 2 h. Filter the precipitate through a sintered glass crucible (porosity 3) while it is hot, wash with hot water, dry at 120° for 1 h and weigh as $Cr(C_{10}H_8NO)_3$. The value gives directly the amount of chromium present in the sample.

Procedure for chrome ore

Weigh about 0.5 g of the ore and fuse it with sodium peroxide–hydroxide mixture in a nickel crucible[5]. Extract the melt by leaching with water and filter. Make up the filtrate which contains chromium, aluminium and silica to 250 ml. The residue should completely dissolve in hot concentrated hydrochloric acid; residual black particles indicate incomplete fusion. Determine chromium and aluminium in an aliquot of the filtrate after neutralising with dilute acid as described above.

Because some aluminium may remain with the residue after fusion, it is often necessary to analyse aluminium in the residue. Dissolve the residue in hydrochloric acid and separate the iron as oxinate below pH 3.5. Precipitate aluminium as oxinate at pH 5 and weigh as $Al(C_9H_6NO)_3$.

Results and discussion

The results for chromium and aluminium in a synthetic mixture (Table I) clearly indicate the suitability of the method for the simultaneous gravimetric determination of aluminium and chromium. Combined precipitation of aluminium and chromium by oxine is quantitative under the conditions described. Precipitation of chromium with 2-methyloxine is simple, accurate and free from interference of aluminium. Thus, aluminium can be determined accurately by difference. Alternatively, chromium can be estimated by any of the known titrimetric methods and the value of aluminium obtained by difference.

TABLE I

DETERMINATION OF ALUMINIUM AND CHROMIUM IN SYNTHETIC MIXTURES

Sl. no.	*Taken (mg)*		*Wt. of combined oxinates of Al and Cr (mg)*	*Wt. of Cr $(C_{10}H_8NO)_3$ (mg)*	*Found (mg)*		*Difference*	
	Cr_2O_3	*Al_2O_3*			*Cr_2O_3*	*Al_2O_3*		
(1)	*(2)*	*(3)*	*(4)*	*(5)*	*(6)*	*(7)*	*(6)−(2)*	*(7)−(3)*
1	12.68	4.05	116.3	87.6	12.60	3.96	−0.08	−0.09
2	12.68	10.40	174.0	87.8	12.68	10.33	−0.00	−0.07
3	6.34	26.00	272.6	43.7	6.31	25.79	−0.03	−0.21
4	12.68	5.20	127.6	87.6	12.60	5.22	−0.08	+0.02
5	6.34	5.20	87.6	43.7	6.31	5.26	−0.03	+0.06

Though oxine can react either with chromium(VI) or chromium(III) to form the complex $Cr(C_9H_6NO)_3$, the precipitate obtained by direct reaction of oxine with chromium(VI) is bulky and difficult to filter; it may even pass through the filter. A prior reduction to chromium(III) was therefore necessary. Reduction with sodium sulphite is simple and the resultant precipitates are in an easily filterable crystalline form. The presence of sulphite, sulphate and sodium ions had no adverse effect on the gravimetric procedure. In the precipitation of chromium with 2-methyloxine in presence of aluminium, addition of tartrate is recommended to prevent any possible precipitation of aluminium hydroxide.

Chrome ores are generally associated with silica, magnesium and small quantities of calcium and barium. Precipitation of chromium and aluminium was carried out by the described procedures in presence of 0.05–1 g of calcium, magnesium and barium in the form of their chlorides or nitrates and of silica as sodium silicate. None of these elements interfered. The analysis of aluminium and chromium in presence of silica in solution is a noteworthy feature of this method. The precipitates obtained in all the cases are easily filtered and washed free of impurities.

TABLE II

DETERMINATION OF CHROMIUM AND ALUMINIUM IN A STANDARD CHROME ORE SAMPLE

Sl. no.	*Cr_2O_3(%)*[a]		*Al_2O_3(%)*[b]	
	Found	*Error*	*Found by difference*	*Error*
1	41.36	−0.14	19.37	−0.03
2	41.45	−0.05	19.42	+0.02
3	41.52	+0.02	19.38	−0.02
4	41.42	−0.08	19.36	−0.04
	Av. 41.44		Av. 19.38	

[a] Certified value 41.50 %.
[b] Certified value 19.40 %.

The results of the analysis of a British Chemical Standard certified sample of chrome ore (Table II) show that the values of chromium and aluminium obtained by the present method are the certified figures.

We express our thanks to Mr. G. S. CHOUDHURY, Director, for keen interest and encouragement, and Professor M. N. SASTRI, Andhra University, for a sample of 8-hydroxyquinaldine. The technical assistance of Mr. DIBAKAR PRADHAN is acknowledged.

Regional Research Laboratory,
Bhubaneswar-4 (India)

J. RAJAGOPALA RAO
B. R. SANT

1 M. KITANO, K. YAMAGATA AND Y. YAMAZATTI, *Nippon Kagaku Zasshi*, 90 (2) (1969) 190.
2 J. RAJAGOPALA RAO, *Ph.D. Thesis*, 1969, Andhra University, Waltair, India.
3 K. E. STUMPF, *Z. Anal. Chem.*, 138 (1953) 30.
4 L. L. MERRITT, JR. AND J. K. WALKER, *Ind. Eng. Chem., Anal. Ed.*, 16 (1944) 387.
5 L. S. THEOBALD, *Analyst*, 67 (1942) 287.

(Received July 20th, 1970)

Analytica Chimica Acta
Elsevier Publishing Company, Amsterdam
Printed in The Netherlands

The use of lens masks to improve sensitivity in atomic absorption spectrophotometry

Rann and Hambly[1] investigated the atom distribution in a laminar-flow air–acetylene flame for twelve elements, and found a considerable concentration of atoms at the centre of the flame. They showed that the sensitivity of atomic absorption could be improved for several elements by using a pinhole mask with a 1-mm aperture, as the light path is restricted to the "atom-rich" part of the flame. However, the 1-mm mask cut off approximately 99% of the incident light, giving a poor signal-to-noise ratio. Jaworowski *et al.*[2], in an early investigation of the nitrous oxide–acetylene flame, also used a pinhole aperture in a study of chromium and vanadium. They found no increase in sensitivity for these elements, and explained this as being due to the narrow nitrous oxide–acetylene flame and the different optical system of their Perkin-Elmer instrument. However, Sprague and Slavin[3] noted that a single mask is used on the Perkin-Elmer model 303, to limit the size of the optical beam through the flame, and that this increases sensitivity for molybdenum. The Boling burner[4] is designed to improve sensitivity by presenting a wider flame and therefore a larger cross-sectional area of atom-rich flame to the detector. Sprague and Slavin[3] claimed increases in sensitivity of up to 100% for calcium, chromium and molybdenum in the air–acetylene flame, using this burner on a Perkin-Elmer model 303.

This communication confirms Rann and Hambly's finding, and demonstrates that a simple arrangement of masks can give significantly improved sensitivity for many determinations.

Experimental

Instrumentation. A Techtron model AA5 atomic absorption spectrometer, fitted with a Jarrell-Ash ½ meter Ebert monochromator type 82–025, was used. Two lens masks of 6 mm diameter (as supplied by Techtron for flame emission work) were used to constrict the aperture of the condensing lenses.

Lamps. All lamps were of the Varian/Techtron 40-mm type, with the exception of gallium, indium, mercury and selenium, which were supplied by Jarrell-Ash. The mercury lamp was argon-filled; all other lamps were neon-filled.

Burners. Techtron titanium grooved burners were used, as shown in Table I.

Solutions. In most cases the solutions were prepared from the pure metal, and were present as the chloride in 2 % hydrochloric acid. Gold, silver, platinum and palladium were in 10% hydrochloric acid; lead and mercury were in 2% nitric acid.

TABLE I

USE OF BURNERS

Type	*Slot length (mm)*	*Slot width (mm)*	*Flames*	*Abbreviation in Table II*
AB50	60	0.5	Nitrous oxide/acetylene	NOA
AB51	100	0.5	Air/acetylene	AA
			Air/hydrogen	AH
AB52	100	1.0	Nitrogen/hydrogen/entrained air	NHA
			Air/methyl isobutyl ketone	MA

TABLE II

A COMPARISON OF SENSITIVITIES WITH AND WITHOUT LENS MASKS

Element	*Wavelength (nm)*	*Lamp current (mA)*	*Slit (μm)*	*Burner[a] height (mm)*	*Flame[b] adjustment*	*Flame[c] mixture*	*Sensitivity[c] without masks*	*Sensitivity[c] with masks*	*% Improvement in absorbance*
Ag	328.07	5	50	0.5	L	AA	0.051	0.047	9
Al	309.27	10	50	2.5	R	NOA	1.07	1.02	5
Au	242.30	10	100	0.5	L	AA	0.28	0.23	18
		10	100	2.0	—	MA	0.043	0.039	11
Ba	553.55	10	50	2.5	R	NOA	2.16	1.87	21
Bi	223.06	10	100	2.5	M	AA	0.37	0.32	14
Ca	422.67	5	50	2.5	R	NOA	0.042	0.028	50
Cd	228.80	5	50	0.5	L	AA	0.036	0.034	6
Co	240.73	15	50	0.5	L	AA	0.111	0.100	11
		15	50	0.5	L	NOA	0.34	0.27	28
Cr	357.87	10	50	5.0	R	AA	0.106	0.077	38
		10	50	2.5	R	NOA	0.128	0.113	13
Cu	324.75	5	50	0.5	L	AA	0.079	0.071	11
		5	50	0.5	L	NOA	0.184	0.161	14
Fe	248.33	10	50	2.5	M	AA	0.114	0.098	16
		10	50	2.5	M	NOA	0.56	0.50	11
Ga	287.42	10	100	1.0	VR	AH	1.43	1.17	22
		10	100	2.5	R	NOA	1.10	1.00	10
Ge	265.16	10	50	2.5	VR	NOA	1.32	1.18	12
Hg	253.65	3	100	0.5	L	AA	3.84	3.20	20
		3	100	5.0	M	NHA	2.03	1.72	18
In	303.94	5	100	1.0	M	AA	0.48	0.42	15
Mg	285.21	10	50	0.5	L	NOA	0.0052	0.0050	5
Mn	279.48	10	50	2.5	M	AA	0.056	0.050	12
		10	50	2.5	M	NOA	0.126	0.107	18
Mo	313.26	10	50	5.0	VR	AA	0.46	0.34	35
		10	50	2.5	VR	NOA	0.29	0.24	23
Ni	232.00	10	100	0.5	L	AA	0.092	0.078	18
		10	100	0.5	L	NOA	0.24	0.22	6
Pb	217.00	10	50	0.5	L	AA	0.21	0.18	18
Pd	244.29	10	100	0.5	L	AA	0.152	0.131	16
Pt	265.95	10	100	0.5	L	AA	1.22	1.12	9
Sb	217.58	10	50	2.5	M	AA	0.42	0.38	11
Se	196.03	15	200	2.5	M	AA	0.56	0.47	18
		15	200	5.0	M	NHA	0.160	0.143	12
Si	251.61	10	150	6.0	VR	NOA	2.17	1.42	52
Sn	224.61	10	200	2.5	VR	NOA	1.22	1.14	7
		10	200	2.5	M	AA	3.41	2.82	21
		10	200	5.0	M	NHA	0.22	0.19	13
Sr	460.73	10	50	2.5	R	NOA	0.123	0.100	23
Te	214.28	10	100	2.5	M	AA	0.27	0.24	15
Ti	364.27	15	50	5.0	VR	NOA	3.17	2.75	15
V	318.40	10	50	5.0	R	NOA	0.72	0.65	11
Zn	213.86	10	100	0.5	L	AA	0.012	0.011	4

[a] The burner height is measured as the distance between the burner top and the optical path, *i.e.*, the point at which the burner top starts to intercept the light beam.
[b] L = lean; M = medium; R = rich; VR = very rich.
[c] μg ml^{-1} for 1 % absorption.

Results and discussion

The lens masks have been used on Techtron instruments (models AA4 and AA5) for the past two years in the routine analysis of mining and metallurgical samples, and have provided some improvement in sensitivity for every element and in every flame investigated (Table II). This improvement may be as low as 5%, but can be 50%. With recent advances in the design of hollow-cathode lamps, the problems of poor signal-to-noise ratio are not serious, and, in particular, the fact that most lamps have cathodes of less than 4 mm diameter means that there is considerably less attenuation when masks are used than was the case with 10-mm cathodes. Typically, two 6-mm diameter lens masks transmit 50% of the signal received with no masks in position. Alignment of the hollow-cathode lamps does become more critical, but this can be overcome by modifying the lamp turret on the instruments to enable precise alignment in the vertical and horizontal planes.

Roan Selection Trust Technical Services,
P. O. Box 1,
Kalulushi (Zambia)

M. A. Hildon
G. R. Sully

1 C. S. Rann and A. N. Hambly, *Anal. Chem.*, 37 (1965) 879.
2 R. J. Jaworowski, R. P. Weberling and D. J. Bracco, *Anal. Chim. Acta*, 37 (1967) 284.
3 S. Sprague and W. Slavin, *Atomic Absorption Newsletter*, 4 (1965) 293.
4 E. A. Boling, *Spectrochim. Acta*, 22 (1966) 425.

(Received July 20th, 1970)

Anal. Chim. Acta, 53 (1971) 192–194

Photometric determination of micro amounts of calcium with arsenazo III

Arsenazo III (1,8-dihydroxynaphthalene-3,6-disulphonic acid-2,7-bis[(azo-2)-phenylarsonic acid]) reacts with many metallic ions to form very stable highly coloured inner-complex salts. The reagent has been widely applied in the spectrophotometric determination of heavy metals such as U, Th, Zr, etc., but its reactions with di- and trivalent light metals have been less studied.

In the work described here, it was found that arsenazo III formed a blue 1:1 complex with calcium(II). The absorbance spectrum showed two maxima at 595–600 nm and 650–655 nm. In the pH range studied (3–10), maximum absorbance was observed at pH 9, and the sensitivity was excellent, but better selectivity was found at pH 5–6. Small amounts of calcium(II) could then be determined in the presence of 100-fold amounts of magnesium(II) and manganese(II); the method was applied for the analysis of magnesite.

Reagents and apparatus

Arsenazo III solution. An aqueous 10^{-3} *M* solution was prepared by weighing the reagent (Fluka). Its actual concentration was determined to be $0.73 \cdot 10^{-3}$ *M* by the method of Nemodruk[1].

Calcium chloride solution. A 10^{-2} *M* solution was prepared by dissolving calcium carbonate (Shering-Kahlbaum, p.a.) in reagent-grade hydrochloric acid; it was standardized compleximetrically.

Reagent-grade $MgSO_4 \cdot 7H_2O$, $Mn(NO_3)_2 \cdot 6H_2O$, $FeSO_4 \cdot 7H_2O$, $FeCl_3 \cdot 6H_2O$ and $Al(NO_3)_3 \cdot 9H_2O$ were used to prepare solutions of diverse ions. Buffer solutions pH 3–10 were prepared as described by KOLTHOFF[2] from analytical-grade reagents.

Absorbance spectra were obtained with a SF-10 spectrophotometer (USSR). Photometric determinations were carried out with a FEK-56 photometer (USSR). A pH meter (L. Seibold, type GNE) with a glass electrode served for pH control of the solutions.

Preliminary study of the calcium(II)–arsenazo III complex

The reaction of calcium(II) with arsenazo III was studied in the pH range 3–10 in order to establish the optimal conditions for complex formation. As can be seen from Fig. 1, complex formation begins at pH 3–4 and maximum absorbance is achieved at pH 9. These spectra have two well defined peaks at 600 nm and 650 nm. The peaks shift by ± 5 nm depending on the pH of the solution. The absorbance of the reagent was also followed at different pH. In acidic media, arsenazo III has an absorbance maximum at 540 nm but the maximum shifts to 566 nm at pH 6–10. A plot of the difference between the absorbances of the reagent and the calcium(II) complex as a function of pH (Fig. 2) showed that the maximum difference occurs at pH 9 for 650 nm and at pH 8–9 for 600 nm.

As is known from previous work[3], arsenazo III forms only 1:1 complexes with the divalent cations. This was confirmed by measuring the spectra of solutions containing a 100-fold excess of calcium(II) at pH 9, or a 10-fold excess of the reagent at pH 9 and 4.2; the spectra showed the same two peaks in all cases. The molar absorptivity of the complex was determined under the optimal conditions, *i.e.* at pH 9, with different amounts of calcium(II) and nearly 10-fold excesses of arsenazo III for ionic strength $\mu = 0$. Values of 20000 at 600 nm and 28000 at 650 nm were found.

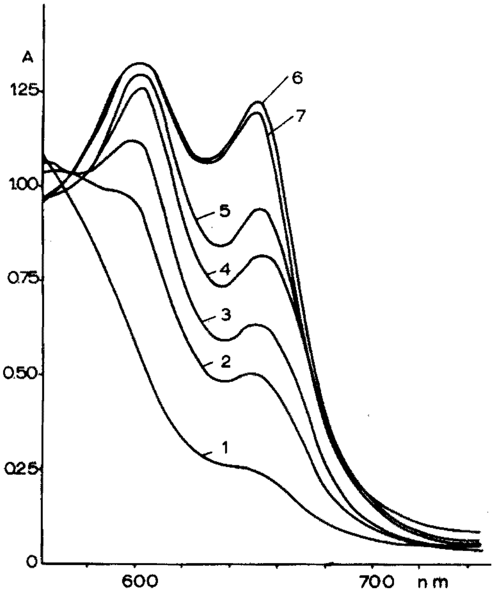

Fig. 1. Dependence of absorbance spectra on the acidity. $C_{Ca} = 2.19 \cdot 10^{-4}$ *M*, $C_{\text{arsenazo III}} = 1.46 \cdot 10^{-5}$ *M*; pH: (1) 3.1, (2) 4.2, (3) 5.5, (4) 7.0, (5) 8.0, (6) 9.0, (7) 10.0.

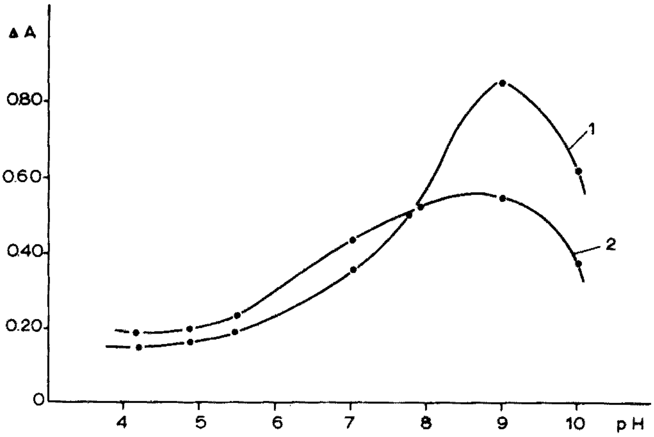

Fig. 2. Difference between the absorbance of the complex and the reagent at 650 nm (1) and at 600 nm (2).

Reaction of arsenazo III with other ions

As has been shown by SAVVIN[4], the molar absorptivities of the complexes of arsenazo III with the various elements depend on the ionic radii of the elements. The colour reactions for a group of divalent cations are observed at $r >$ 0.1 nm, and for trivalent cations at $r >$ 0.081 nm. Accordingly, magnesium(II), cadmium(II), aluminium(III), etc. should not form complexes with arsenazo III. However, when the interferences of these ions were investigated, it was found that magnesium(II), for example, formed a blue-coloured complex with maximum absorbance at 597 nm in the

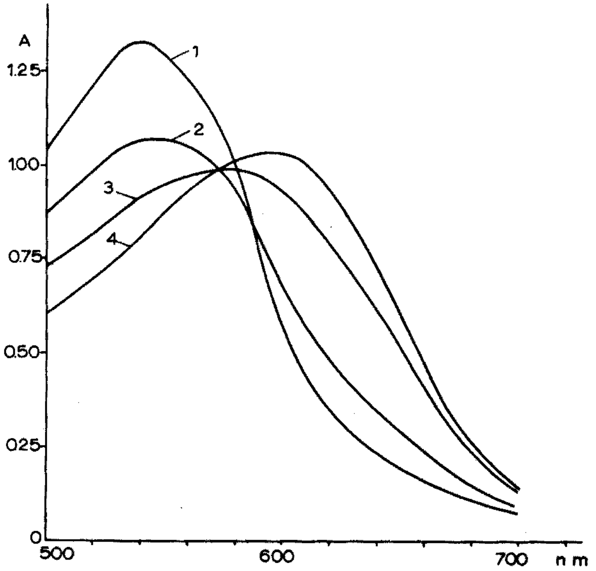

Fig. 3. Complex formation of magnesium with arsenazo III. $C_{Mg} = 4.0 \cdot 10^{-3}$ M, $C_{\text{arsenazo III}} = 1.46 \cdot 10^{-5}$ M; pH: (1) 5.95, (2) 7.0, (3) 8.0, (4) 9.0.

more basic range (Fig. 3), although no complex formation occurred at pH 4–6. Similar investigations with the other ions again showed greater selectivity in slightly acidic media.

The data obtained indicated that it should be possible to determine micro amounts of calcium(II) in the presence of some other ions in slightly acidic media. The reaction was therefore studied in detail at pH 5.5. At this acidity magnesium(II) and manganese(II) do not form complexes with arsenazo III, but in the presence of Zn(II), Cd(II), Al(III) and Fe(II) ions the wavelength of maximum absorbance of the reagent shifts about 20 nm (Fig. 4); iron(III) forms a dark-brown precipitate.

Photometric determination of calcium(II)

The recommended procedure for determination of small amounts of calcium(II) in the presence of magnesium(II) and manganese(II) is as follows.

Procedure. To the calcium(II) solution add 10.0 ml of $0.73 \cdot 10^{-4}$ *M* arsenazo III dissolved in acetate buffer pH 5.5 and dilute to 25 ml with water in a volumetric flask. After 30 min, measure the absorbance at 600 nm (FEK-56, orange filter) in 30-mm cells against a reagent blank treated in the same way.

The choice of 600 nm as the wavelength for measurement is clear from Fig. 2. Beer's law was found to be followed in the range 0.030–1.50 μg Ca ml^{-1}. At pH 5.5, calcium can be determined in presence of 100-fold amounts of magnesium and manganese(II) if absolute amount of calcium(II) does not exceed 25 μg (1 μg ml^{-1}). The method could therefore be applied to the determination of calcium(II) in magnesite.

Analysis of magnesite

Dissolve the sample (0.1–0.2 g) by heating with 10 ml of (1+9) hydrochloric

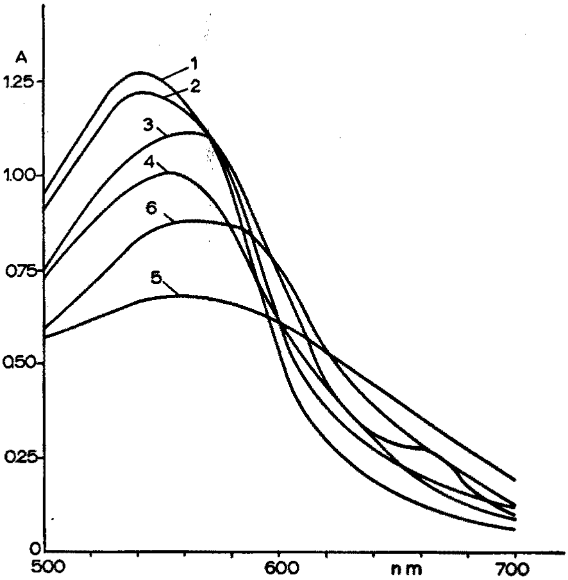

Fig 4. Absorbance spectra of arsenazo III and of its complexes at pH 5.5. $C_{\text{arsenazo III}} = 1.46 \cdot 10^{-5}$ *M*, $C_{\text{Me}^{n+}} = 4.0 \cdot 10^{-3}$ *M*. (1) Arsenazo III, (2) + Mn(II), (3) + Cd(II), (4) + Zn(II), (5) + Fe(II), (6) + Al(III).

acid (Merck). Separate iron and aluminium as follows. Add 1–2 drops of concentrated hydrogen peroxide to convert iron(II) to iron(III) and destroy the excess of peroxide by gentle boiling. Cool and neutralize with solid sodium carbonate. Dissolve the initial hydroxide precipitate in 1–2 drops of concentrated hydrochloric acid, heat to boiling and precipitate with 15 ml of aqueous 25% (w/v) hexamethylenetetramine solution. Heat on a water-bath to coagulate the precipitate, filter and wash with a warm 0.5% solution of hexamethylenetetramine. Complete separation of aluminium(III) and iron(III) was thus achieved. Collect the filtrate and washings in a 100-ml volumetric flask. Use aliquots of this solution for determination of calcium(II) by the recommended procedure.

TABLE I

DETERMINATION OF CALCIUM IN MAGNESITE

No.	*Magnesite taken (g)*	*Aliquots (ml)*	*Calcium found*[a] *(μg Ca ml^{-1})*	*Calcium found (% CaO)*
1	0.1026	5.0	0.78	0.53
2	0.1002	5.0	0.76	0.53
3	0.1048	5.0	0.78	0.52
4	0.0997	5.0	0.82	0.57
5	0.0997	3.0	0.45	0.53
6	0.2015	3.0	0.97	0.56
7	0.2006	3.0	0.95	0.55

Average value of Ca = 0.54% CaO
Standard deviation = ± 0.02% CaO

[a] Average of 3 determinations on separate aliquots.

A calibration curve was plotted for the range 0.25–1.25 μg Ca ml^{-1} from pure calcium chloride solution without any of the preliminary treatments. The solutions obtained were red-violet in colour and were stable for several days. By statistical methods[5], the sensitivity of the reaction at pH 5.5 was found to be 0.04 μg Ca ml^{-1}.

The results obtained for magnesite are shown in Table I.

Department of Chemistry,
University of Sofia,
Sofia 26 (Bulgaria)

V. MICHAYLOVA
P. ILKOVA

1 A. A. NEMODRUK, *Zh. Analit Khim.*, 22 (1967) 629.
2 I. M. KOLTHOFF, *Acid–Base Indicators*, Academic Press, New York, 1937.
3 S. B. SAVVIN, *Talanta*, 8 (1961) 673.
4 S. B. SAVVIN, *Arsenazo III*, Atomizdat, Moscow, 1966, p. 43.
5 K. DOERFEL, *Beurteilung von Analysenverfahren und Ergebnissen*, Springer-Verlag, Berlin, 1962.

(Received July 2nd, 1970)

Analytica Chimica Acta
Elsevier Publishing Company, Amsterdam
Printed in The Netherlands

The measurement of pH in acid fluoride solutions and evidence for the existence of $(HF)_2$

The measurement of hydrogen ion concentration in acid fluoride solutions is complicated by the presence of molecular HF. In this paper the effect of hydrofluoric acid on the glass electrode is examined, and it is shown that the quinhydrone electrode is suitable for the measurement of pH under acid fluoride conditions where the glass electrode gives erroneous readings. The results obtained in concentrated HF solutions can be accounted for if the presence of a dimer $(HF)_2$ is assumed.

It is well known that hydrogen fluoride attacks silica (and glass) according to the overall reaction

$$4HF(g) + SiO_2(s) \rightarrow SiF_4(g) + 2H_2O$$

In solution, fluorosilicic acid, H_2SiF_6, is formed, though the details of the mechanisms are not fully understood. In view of these facts, the operation of the glass electrode may be affected by the presence of hydrogen fluoride. Dole *et al.*[1] found that whereas fluoride ions caused no error in glass electrode pH readings, momentary immersion in a 1 *M* potassium fluoride solution at pH 4.14 gave large errors, and subsequent measurements in alkaline solutions showed greatly increased "alkaline errors". These authors suggested that glass electrodes should not, therefore, be used in fluoride solutions where the concentration of molecular hydrogen fluoride exceeds 10^{-4} *M*.

The hydrogen electrode, or a cell suggested by Broene and De Vries[2]

$$\text{Pb (5\% amalgam)}, PbF_2(s) \mid HF, NaF \mid H_2(g)$$

appear, however, to be suitable for acid fluoride solutions. Industrially, the antimony electrode has found some use. The utility of the quinhydrone electrode as a hydrogen ion indicator for these systems has been investigated in the present work.

Experimental

The quinhydrone electrode was prepared as recommended by Ives and Janz[3]. Polypropylene beakers were used, and no glass components entered the solutions, which were purged with oxygen-free nitrogen. The reference calomel electrode was an Orion Model 90-01 with an HF-resistant epoxy resin body. Cell potentials were recorded to ±0.1 mV on the expanded scales of a Pye Model 290 pH meter. Steady readings were obtained within 1 min for all solutions at 26°. The quinhydrone electrode was calibrated against potassium tetraoxalate (pH 1.68), potassium hydrogen phthalate (pH 4.01), and a phosphate buffer (pH 6.99), the coefficient $\Delta mV/\Delta pH$ being 59.25 at 26° (theoretical 59.37).

Results

To establish whether there was any reaction between fluoride or hydrogen fluoride and quinhydrone (which is a 1:1 molecular compound of quinone and hydroquinone), the fluoride ion concentration was monitored with an Orion fluoride electrode Model 94-09. A 10^{-2} *M* sodium fluoride solution of pH 5.90 was prepared and 1.6 g of quinhydrone per litre was added. No change in the measured fluoride activity was observed. The measurement was repeated on a 10^{-1} *M* sodium fluoride solution, adjusted to pH 2.5 with hydrochloric acid, containing, therefore, about 0.05 moles of molecular hydrogen fluoride per litre. Again no change in the measured fluoride activity occurred. Any reaction between fluoride or hydrogen fluoride and quinhydrone in solution is therefore not significant.

The response of a glass electrode (Pye-Ingold Model 201-E07) was then compared with that of the quinhydrone electrode. Fluoride solutions of $10^{-2}M$ and $10^{-1}M$ were prepared from recrystallized analytical-grade sodium fluoride. These were gradually acidified by the addition of hydrochloric acid, and the pH values were recorded by both electrodes. The glass electrode was inserted for only 2–4 min at each pH and then withdrawn.

The results are shown in Fig. 1, where pH measured by the glass electrode, pH_G, less that measured by the quinhydrone, pH_Q, is plotted against the concentration of molecular hydrogen fluoride. It is clear that the glass electrode begins malfunctioning when the concentration of hydrogen fluoride exceeds $5 \cdot 10^{-3}$ moles l^{-1}. It was noted that pH_G increased over 10 sec from about the correct pH to a much higher value.

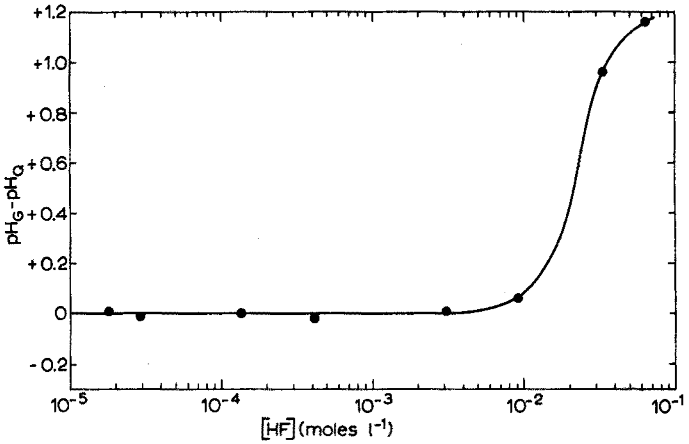

Fig. 1. The measurement of pH in acid fluoride solutions; comparison of glass and quinhydrone electrodes.

The pH values above which the glass electrode can be safely used, *i.e.* where $[HF] \leqq 5 \cdot 10^{-3}M$, are listed below.

Solution	*pH above which glass electrode can be used*
Hydrofluoric acid	2.8
NaF $10^{-2}M$	2.1
NaF $10^{-1}M$	4.1
NaF 1 M	4.9

These findings show that Vanderborgh's[4] determination of K_1 for hydrogen fluoride with a glass electrode is quite acceptable, because all his data were obtained below the critical pH.

The quinhydrone electrode was then used to study the equilibria in sodium fluoride solutions, under conditions where the glass electrode is unsuitable. The results were explained in terms of the following equilibrium constants:

$$K_1: \quad H^+ + F^- = HF \tag{1}$$

$$K_2: \quad HF + F^- = HF_2^- \tag{2}$$

$$K_d: \quad 2HF = (HF)_2 \tag{3}$$

The equilibria (1) and (2) are well known (see, for example, Sillén and Martell[5] and Vanderborgh[4]). Smith[6] has characterized the hexamer $(HF)_6$ and the tetramer $(HF)_4$ in hydrogen fluoride *vapour* by i.r. absorption. He found little dimer $(HF)_2$. The existence of HF polymers in *solution* has not previously been reported.

The equilibria (1), (2) and (3) were studied in succession by measurements in sodium fluoride solutions of increasing concentrations. A $10^{-3}M$ solution of sodium fluoride was acidified with hydrochloric acid to give eight solutions of successively decreasing pH (and therefore of increasing ionic strength). Under these circumstances, the amounts of HF_2^- and $(HF)_2$ were negligible, and eqn. (1) can be considered alone; $[H^+]$ and $[F^-]$ were measured directly, and [HF] was calculated from $C_F - [F^-]$ where C_F = initial concentration of NaF, *i.e.* $10^{-3}M$. At 22°, over the ionic strength range 0.0005 to 0.005, $K_1 = (1.46 \pm 0.02) \cdot 10^3$. This is in good agreement with the values of previous workers[2,4].

In $10^{-2}M$ sodium fluoride acidification produces a significant concentration of HF_2^-, and equilibria (1) and (2) must be considered together. Again $[H^+]$ and $[F^-]$ were measured directly, and using the previously determined K_1, [HF] was calculated from $[HF] = K_1[H^+][F^-]$. $[HF_2^-]$ was then calculated from $2[HF_2^-] = C_F - [F^-] - [HF]$ whence $K_2 = [HF_2^-]/[HF][F^-]$. At 23° over the ionic strength range 0.005 to 0.009, the results were fully consistent with a value of $K_2 = 4.3 \pm 0.4$. (The large relative error is caused by using small differences obtained by subtraction between much larger numbers.)

The measurements made in more concentrated acidified sodium fluoride solutions ($10^{-1}M$) were especially interesting. Assuming that the measured values of $[H^+]$ were correct, an assumption justified by the previous results, the decrease in the concentration of free fluoride ions on acidification was found to be distinctly too large to be accounted for by the formation of HF and HF_2^- alone. Various reactions which would further reduce the free fluoride ion concentration were considered, among them the formation of dimer $(HF)_2$, as in eqn. (3). In this case

$$2[(HF)_2] = C_F - [F^-] - [HF] - [HF_2^-] \quad \text{and} \quad K_d = [(HF)_2]/[HF]^2$$

Over the ionic strength range 0.050 to 0.062, K_d remained constant at 2.7 ± 0.3, strongly supporting the existence of the dimer $(HF)_2$. As $(HF)_2$ exists in the solid and vapour states, it is not unreasonable that it should also exist in solution. Furthermore, the data were not consistent with the assumption of the presence of tetramer, hexamer, or species of the type HF_3^{2-}.

Activity coefficient corrections in the dilute solutions used to obtain K_1 are quite small. In the more concentrated solutions in which K_2 and K_d were determined, the activity coefficients in the equilibrium constant expressions tend to cancel, and will have little effect.

The helpful suggestions of Dr. J. A. Kitchener are gratefully acknowledged. I thank the University of Queensland for a Travelling Scholarship, and the Institution of Mining and Metallurgy for a Stanley Elmore Grant.

Imperial College of Science and Technology,
Department of Mining and Mineral Technology,
Royal School of Mines,
London, S.W.7 (England)

L. J. Warren

1 M. Dole, R. M. Roberts and C. E. Holley, *J. Amer. Chem. Soc.*, 63 (1941) 725.
2 H. H. Broene and T. de Vries, *J. Amer. Chem. Soc.*, 69 (1947) 1644.
3 D. J. G. Ives and G. J. Janz, *Reference Electrodes*, Academic Press, New York, 1961, p. 270.
4 N. E. Vanderborgh, *Talanta*, 15 (1968) 1009.
5 L. C. Sillén and A. E. Martell, *Stability Constants of Metal-Ion Complexes*, The Chemical Society Special Publication No. 17, 1964, p. 256.
6 D. F. Smith, *J. Chem. Phys.*, 28 (1958) 1040.

(Received July 12th, 1970)

Preparation, analytical evaluation and applications of a new heterogeneous membrane electrode for copper(II)

Two types of copper(II)-selective membrane electrode have been described: a liquid membrane ion-exchange electrode and a solid-state membrane electrode[1], the latter of which is the more satisfactory[2]. The solid-state electrode comprises a pelletted mixture of copper(II) and silver sulfides. In the present communication, a new type of heterogeneous membrane electrode is described which is selective to copper(II) and is prepared by thermomoulding an organic polymer with a mixture of copper(II) and silver sulfides. An analytical evaluation of this electrode is presented.

Precipitation of sulfides and electrode preparation

Silver and copper sulfides were prepared either by bubbling hydrogen sulfide into a solution containing silver nitrate and copper(II) nitrate in 10^{-2} *M* perchloric acid, or by adding sodium sulfide to neutral solutions; in both cases an excess of sulfide was always added. The membrane electrode was prepared as described previously[3], by thermomoulding the mixture of the copper and silver sulfides with polythene. The weight ratio of polythene to sulfides was about 1:1.

In some experiments, the two sulfides were ground together and mixed with the polymer. In other cases, the mixed sulfides were obtained by simultaneous precipitation and were mixed with the polymer before the thermomoulding in a moulding press.

The membrane was heat-sealed to a polythene tubing; the internal solution was 10^{-3} *M* silver nitrate or 10^{-3} *M* copper(II) chloride and the internal reference electrode was a silver or silver–silver chloride wire. Potentiometric measurements were carried out in the conventional manner by using the membrane electrode and a saturated calomel reference electrode with a Beckman Research pH meter 1019.

Results and discussion

Membrane electrodes prepared as described above proved to be selective for copper(II). Calibration curves obtained by plotting E *vs.* $\log[Cu^{2+}]$ showed, however, that the Nernst equation

$$E = E^0 + 0.0296 \log a_{Cu^{2+}} \qquad (1)$$

held only when the electrodes were made with copper and silver sulfides which had been precipitated simultaneously. When the membranes were prepared by thermomoulding copper sulfide or a mixture of the two sulfides, the theoretical slope was not found. (Fig. 1). The mole ratio of the two cations in the preparation of the mixed sulfides was not critical; when the ratio of silver(I) to copper(II) was varied in the range 30–70%, a slope of 28–30 mV for each decade change in copper(II) concentration was always obtained. No significant difference was found whether the sulfides were precipitated with hydrogen sulfide or with sodium sulfide. The concentration range

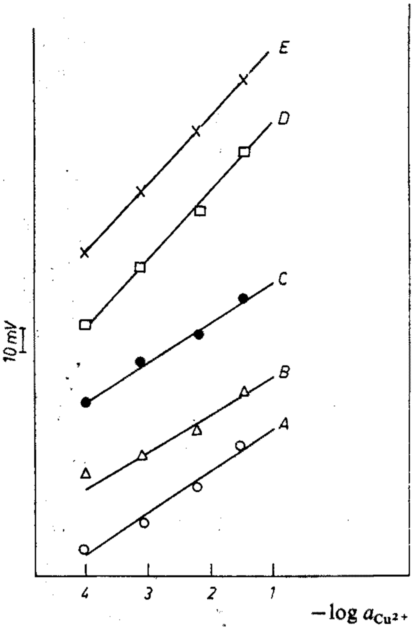

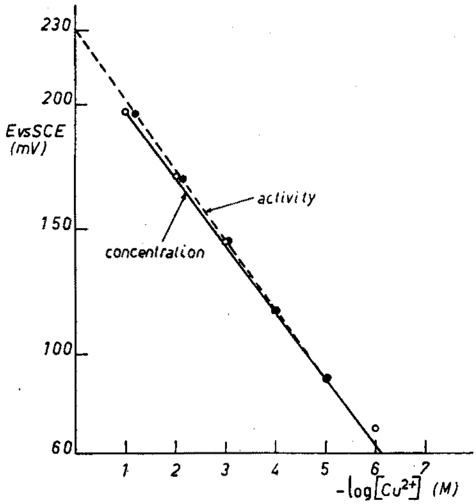

Fig. 1. Calibration curves E *vs.* $\log a_{Cu^{2+}}$ for copper electrodes prepared with membranes of different sulfide composition. All sulfides were precipitated with Na_2S. Copper sulfide and silver sulfide were precipitated separately and mixed mechanically in B, C and D, but precipitated simultaneously from the same solution in E. The curves are shifted along the ordinate axis for graphic presentation. Slopes are expressed as mV per decadic change in concentration. (A) CuS, slope = 16; (B) CuS and Ag_2S (3:1 molar ratio), slope = 15; (C) CuS and Ag_2S (1:1 molar ratio), slope = 19; (D) CuS and Ag_2S (1:3 molar ratio), slope = 24; (E) CuS and Ag_2S (1:1 molar ratio), slope = 29.

Fig. 2. Calibration curve for the copper(II) membrane electrode *vs.* S.C.E. The solutions were prepared by dilution of a standard solution of 0.1 *M* $Cu(NO_3)_2$. The single ion activity coefficients were calculated from the Debye–Hückel theory.

for linear response of this electrode is from 1 M to about 10^{-6} M copper(II) (Fig. 2), but in solutions containing at least 10^{-6} M of total copper, it appears from the titration of copper(II) with EDTA solution (Fig. 3) or with iminodiacetic acid, disodium salt (Fig. 4), that the uncomplexed copper(II) can be measured below 10^{-10} M.

The normal potential E^0. All the reported experiments were carried out with a membrane electrode containing 10^{-3} M copper(II) chloride as the internal solution. A series of 10 membrane electrodes was prepared to measure the normal potential of the half-cell:

$$\mathrm{Ag}\,|\,\mathrm{AgCl}\,|\,\underset{10^{-3}\,M}{\mathrm{CuCl_2}}\,|\,\underset{\text{polythene}}{\mathrm{CuS,\,Ag_2S}}\,|\,\mathrm{Cu^{2+}} \qquad (2)$$

By extrapolation of the calibration curve (Fig. 2) to $\log a_{\mathrm{Cu^{2+}}} = 0$ the normal electrode potential was obtained; it was found to be $+230 \pm 5$ mV *vs.* S.C.E. at room temperature. When the internal solution was replaced by a solution of 10^{-3} M silver nitrate, the normal potential was about +430 mV and slowly decreased with time as the following reaction occurred.

$$2\mathrm{Ag^+} + \mathrm{CuS} \rightarrow \mathrm{Cu^{2+}} + \mathrm{Ag_2S} \qquad (3)$$

The slope of the calibration curves was not affected by the change of the internal solution.

Resistance of membranes. The resistance of the membrane electrodes was measured with a circuit similar to that reported by Eckfeldt and Perley[4].

The resistance increased as the silver sulfide content increased, and higher values were found for the membranes prepared from simultaneously precipitated copper and silver sulfides (Table I).

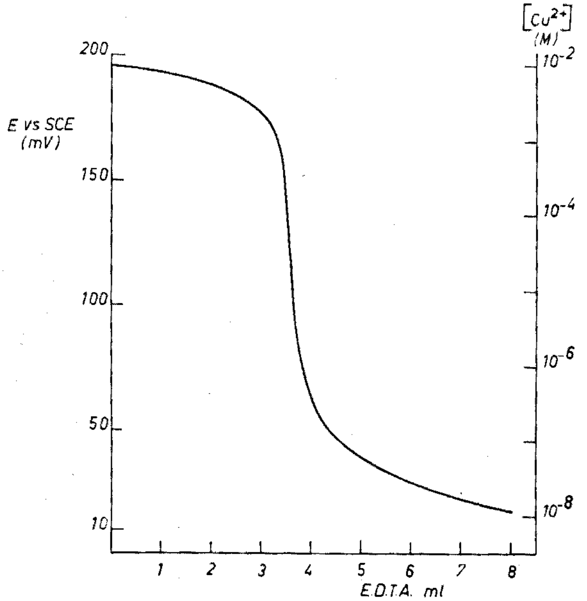

Fig. 3. Potentiometric titration of 40 ml of *ca.* 0.01 M $\mathrm{Cu(NO_3)_2}$ in acetate buffer with 0.1 M EDTA.

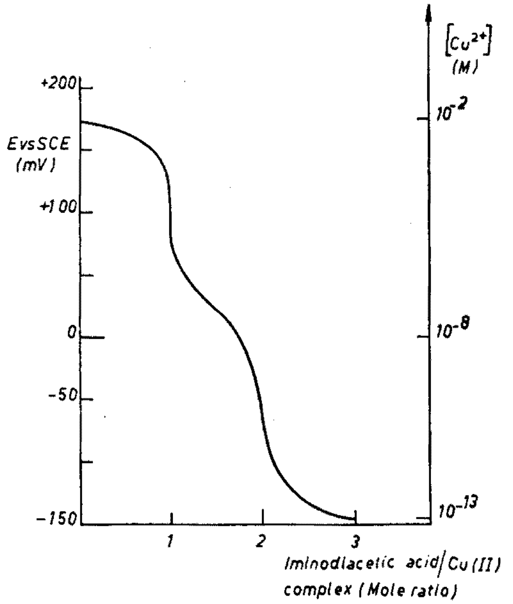

Fig. 4. Potentiometric titration of 50 ml of *ca.* 0.01 *M* $Cu(NO_3)_2$ with 0.1 *M* iminodiacetic acid disodium salt.

TABLE I

RESISTANCE OF MEMBRANES PREPARED FROM DIFFERENT SULFIDE COMPOSITIONS

CuS content of precipitate (mole %)	*Resistance (kΩ)*	*CuS content of precipitate (mole %)*	*Resistance (kΩ)*
100	35	66[b]	70
75[a]	45	50[b]	80
50[a]	55	33[b,c]	130
25[a]	80		

[a] Mechanical mixing of precipitates.
[b] Simultaneous precipitation of sulfides.
[c] A membrane prepared from Ag_2S only, showed a resistance of 250 kΩ.

Electrode selectivity towards cations. The selectivity of this electrode towards the more common cations was investigated. Its behaviour was similar to that of the sulfide electrode[3]; all cations which form sulfides with a solubility product lower than the solubility product of copper(II) sulfide, such as mercury(I), mercury(II) and silver(I), interfere. The electrode response to copper(II) is not affected by lead, zinc, nickel or cobalt ion, or by other ions such as Na^+, K^+, Ca^{2+}, Mg^{2+}; the selectivity constants for these cations are less than 10^{-4}.

Chloride, bromide and iodide interfere when the equilibrium silver ion concentration of the system Ag_2S–CuS–Cu^{2+} is greater than the silver ion concentration from the equilibrium AgCl–Cl^-, AgBr–Br^- or AgI–I^-. For a 10^{-3} *M* copper(II) solution, interference occurred at the following halide concentrations: $[Cl^-] \geqq 10^{-1}$, $[Br^-] \geqq 10^{-4}$, $[I^-] \geqq 10^{-6}$.

Applications

The proposed electrode can be successfully applied as an indicator electrode for copper(II) either by direct potentiometry or in potentiometric titrations. For example, the EDTA titration of copper(II) (Fig. 3) can be done in water or in mixed solvents.

Istituto di Chimica Analitica,
Università di Roma, Roma (Italy)

M. Mascini
A. Liberti

1 J. W. Ross, in R. A. Durst, *Ion-Selective Electrodes*, N.B.S. Spec. Publ. 314, Washington, 1969.
2 G. A. Rechnitz and N. C. Kenny, *Anal. Letters*, 2 (1969) 395.
3 M. Mascini and A. Liberti, *Anal. Chim. Acta*, 47 (1969) 339; 51 (1970) 231.
4 E. L. Eckfeldt and G. A. Perley, *J. Electrochem. Soc.*, 98 (1951) 37.

(Received July 19th, 1970)

Anal. Chim. Acta, 53 (1971) 202–206

A new type of solid-state ion-selective electrodes with insoluble sulphides or halides

The liquid state electrode[1,2] introduced in this laboratory a year ago consists of a graphite cylinder impregnated with a water-immiscible organic solvent and mounted at the end of a plastic tube[3]. It does not include the usual inner reference electrode and aqueous filling solution, and the graphite is directly connected to the potentiometer by means of a steel wire. The ion-sensitive surface of this electrode consists only of the water-immiscible organic liquid adsorbed on the graphite, serving as its conducting support.

Such an electrode is essentially inert unless it has been activated by dissolving a suitable species in the organic phase. Thus, for example, solutions of silver dithizonate in xylene can be used for preparing a silver-selective electrode[4], solutions of valinomycin in mesitylene to produce a potassium-selective electrode, or solutions of iodine in benzene for an iodide-selective electrode[3].

It has recently, and rather surprisingly, been found that compounds which are *not soluble in the organic phase* can also be used to activate the electrode. For example, when silver sulphide is precipitated on the surface of a graphite rod, which is then dried (at 200°) and finally hydrophobized by impregnation with carbon tetrachloride, benzene or mesitylene, an excellent silver ion-sensitive electrode is obtained. Similarly, sulphides of mercury, copper, cadmium, lead, etc. (or their mixtures with silver sulphide) can be successfully used for making ion-selective electrodes responding to these metals (Table I).

A slightly different technique was employed in preparation of silver halide electrodes. Silver chloride, silver bromide or silver iodide (or their mixtures with silver sulphide) were melted, and the graphite rods were impregnated with the melt. The

TABLE I

EXAMPLES OF ION-SENSITIVE ELECTRODES

Ion	*Electroactive species*	*Useful pH-range*[a] *(approx.)*	*Tested pM-range*[b]	*Potential at pH* 3 *and pM* 3 *(mV)*[c]
Hg^{2+}	HgS	2–10	3–5	460
Ag^{+}	Ag_2S	2–10	3–6	430
Cu^{2+}	CuS	3–10	3–6	250
Pb^{2+}	PbS	4–10	3–6	30
Cd^{2+}	CdS	4–10	3–6	−10
I^{-}	AgI	3–10	3–6	−205
Br^{-}	AgBr	3–10	3–5	
Cl^{-}	AgCl	3–10	3–5	

[a] With Nernstian response.

[b] With Nernstian response. Lower limits can certainly be achieved in solutions where metal ions or halides are buffered.

[c] The values given are ±20 mV and were measured *versus* saturated calomel electrode; when necessary, a KNO_3 bridge was used.

treated rods were, after cooling to room temperature, hydrophobized by impregnation with carbon tetrachloride, benzene or mesitylene. These electrodes responded correctly to changes in the respective halide ion activities. Similarly to the known behaviour of the solid-state membrane halide-selective electrodes[5], admixture of silver sulphide reduced the light sensitivity of the electrode.

The ion-selective electrodes made of sulphide and halides described above exhibit a pure Nernstian response for the regions indicated in Table I, are stable during continuous use, have a fast response to changes in ion activity, are robust and have a low electric resistance. However, the electrode properties depend entirely on the method of preparing the precipitates (see, *e.g.*, also ref. 6).

According to present knowledge, it appears that a family of new electrodes may be foreseen. These could possibly be called solid-state electrodes, but they are not conventional membrane electrodes and do not rely on any inner reference system. In contrast to the generally used solid-state membrane electrodes which employ either pure monocrystals or pellets made almost entirely of the electroactive species, the present electrodes utilize only a minute amount of the electroactive species adsorbed on the graphite surface.

The theory and use of these electrodes are being further investigated in this laboratory and will be reported together with experimental details.

Chemistry Department A,
Technical University of Denmark,
Lyngby (Denmark)

J. Růžička
C. G. Lamm

1 J. Růžička and J. Chr. Tjell, *Anal. Chim. Acta*, 49 (1970) 346.
2 J. Růžička, C. G. Lamm and J. Chr. Tjell, *Patent appl. NO 3789/69*, Denmark, and further applications.
3 J. Růžička and K. Rald, *Anal. Chim. Acta*, in press.

4 J. Růžička and J. Chr. Tjell, *Anal. Chim. Acta*, 51 (1970) 1.
5 J. Ross, in R. A. Durst (Ed.), *Proc. Symp. on Ion-Selective Electrodes*, National Bureau of Standards Spec. Publ. No. 367, Washington, 1969 p. 57.
6 A. M. G. Macdonald and K. Tóth, *Anal. Chim. Acta*, 41 (1968) 99.

(Received August 16th, 1970)

Anal. Chim. Acta, 53 (1971) 206–208

Simultane Bestimmung von Plutonium(IV) und Salpetersäure mit Hilfe von Dichte–Leitfähigkeitsmessungen

Bei der Wiederaufarbeitung bestrahlter Kernbrennstoffe ist es von grossem Nutzen, für die laufende Kontrolle wichtiger Prozessgrössen betriebssichere In-line-Messinstrumente zu besitzen. Die gleichzeitige Ermittlung von Dichte und Leitfähigkeit der wässrigen Prozesslösung erlaubt die Simultanbestimmung von Plutonium und Salpetersäure, wenn das Plutonium weitgehend von seinen Begleitelementen abgetrennt ist.

Die Ergebnisse dieser Methode waren voll befriedigend und haben bei uns zu einer Anwendung geführt. Im folgenden wird das zugrunde liegende Eichdia-

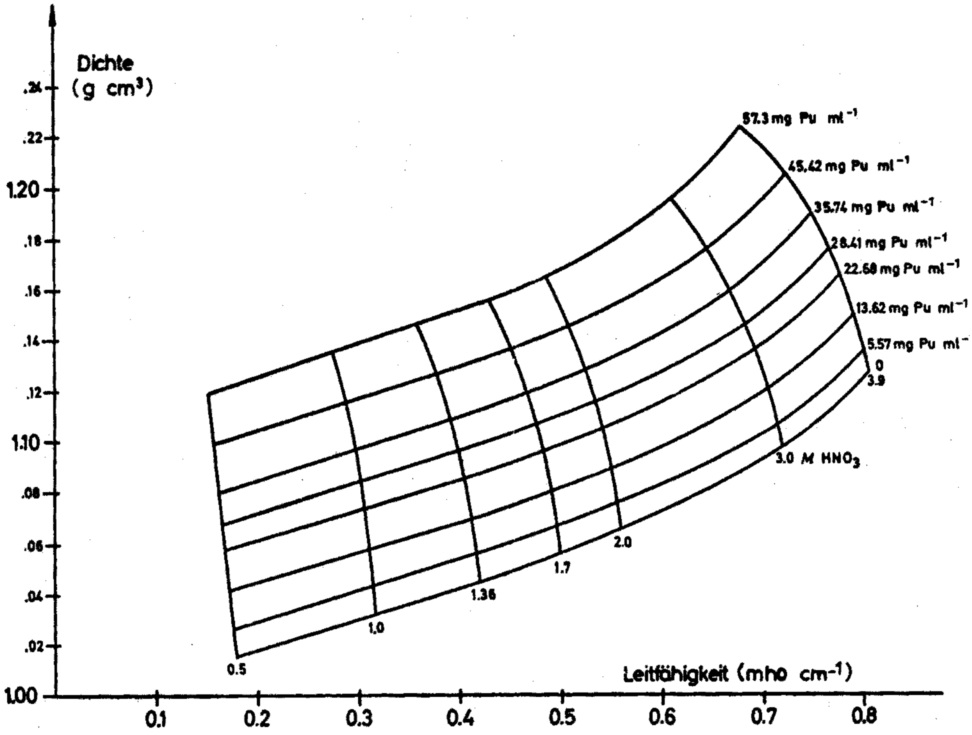

Abb. 1. Dichte–Leitfähigkeit für das System $Pu(NO_3)_4$–HNO_3.

Anal. Chim. Acta, 53 (1971) 208–210

gramm angegeben. Ein ähnliches Diagramm zur Bestimmung von Uran und Salpetersäure wird von Duncombe und Mitarbeitern beschrieben[1].

Experimentelles

Für den interessierenden Konzentrationsbereich von 0–60 g Pu l^{-1} und 0.5–4 *M* Salpetersäure wurde die Abhängigkeit der Dichte und Leitfähigkeit für verschiedene Pu(IV)/HNO_3-Konzentrationsverhältnisse ermittelt. Ausgehend von einer Pu(IV)-Stammlösung (hergestellt nach ref. 2) wurden Lösungen verschiedener Konzentrationen hergestellt. Der Plutoniumgehalt dieser Lösungen wurde röntgenfluoreszensanalytisch nach Ertel und Wettstein[3] bestimmt. Die Salpetersäurekonzentration wurde nach dem Verfahren von Schmieder und Kuhn[2] ermittelt. Die Standardabweichung der Pu-Bestimmung betrug ±1%, die der Säurebestimmung ±1.1%.

Die Dichtemessung wurde mit einem geeichten Pyknometer bei 20° durchgeführt. Der durchschnittliche Fehler betrug ±0.2%. Die Leitfähigkeit der Lösungen wurde mit einer Leitfähigkeitsmesszelle LTA (Fa. WTW, Weilheim) gemessen, nachdem sie zuvor mit KCl-Eichlösungen bei 20° geeicht worden war. Der mittlere Fehler dieser Messungen betrug ±2%. Die erhaltenen Ergebnisse gibt das Netzdiagramm der Abb. 1 wieder, in dem der Zusammenhang von Dichte und Leitfähigkeit für verschiedene Pu- und HNO_3-Konzentrationen deutlich wird.

Testversuche

Zur Ermittlung der Genauigkeit dieses Verfahrens zur Pu/HNO_3-Bestimmung wurde von unbekannten salpetersauren Plutoniumlösungen zunächst deren Konzentrationen nach den oben angegebenen Verfahren titrimetrisch und röntgenfluoreszensanalytisch bestimmt. Danach wurde über eine Dichte–Leitfähigkeits-

TABELLE I

VERGLEICH DER ANALYTISCH BESTIMMTEN KONZENTRATION MIT DEN AUS DEM DIAGRAMM ERMITTELTEN WERTEN

Konzentration analytisch		*Dichte* (*$g\ cm^{-3}$*)	*Leitfähigkeit* (*$mho\ cm^{-1}$*)	*Konzentr. aus Diagr.*		*Fehler Pu* (%)	*Fehler HNO_3* (%)
Pu (*$g\ l^{-1}$*)	*HNO_3* (*$Mol\ l^{-1}$*)			*Pu* (*$g\ l^{-1}$*)	*HNO_3* (*$Mol\ l^{-1}$*)		
9.0	1.11	1.0533	0.3367	9.0	1.09	0	−1.8
18.1	1.23	1.0745	0.3562	19.3	1.17	+6.6	−4.9
27.1	1.34	1.0941	0.3782	28.4	1.29	+4.6	−3.7
36.9	1.45	1.1148	0.4087	37.1	1.44	+0.5	−0.7
45.2	1.56	1.1278	0.4270	43.3	1.56	−4.2	0
53.9	1.68	1.1477	0.4404	51.4	1.75	−4.6	+4.2
58.6	1.74	1.1589	0.4490	57.3	1.80	−2.2	+3.4
47.0	1.70	1.1420	0.4673	46.6	1.80	−0.8	+5.9
18.2	1.83	1.0917	0.4941	19.8	1.74	+8.8	−4.9
10.8	1.76	1.0771	0.5038	10.7	1.77	−0.9	+0.6

messung die Pu- und HNO_3-Konzentration aus dem Diagramm der Abb. 1 abgelesen, wobei linear interpoliert wurde. Ein Vergleich der nach den verschiedenen Methoden gemessenen Werte (Tabelle I) zeigt, dass die maximale Abweichung $+8.8\%$ für Plutonium und $+5.9\%$ für HNO_3 beträgt, bezogen auf die titrimetrisch bzw. röntgenfluoreszensanalytisch ermittelten Werte. Die mittlere Abweichung beträgt $\pm 3.2\%$. Die Genauigkeit der Methode reicht also für eine Betriebsüberwachung aus.

Kernforschungszentrum Karlsruhe,
75 Karlsruhe (Deutschland)
G. Baumgärtel
E. Kuhn

1 E. Duncombe, A. W. Fenton und A. J. Walton, *Proc. 5th Intern. Instr. and Measurements Conf., Stockholm, 1960, Vol. 2,* Academic Press, 1961, pp. 675–704.
2 H. Schmieder und E. Kuhn, *Talanta,* 00 (1969) 691.
3 D. Ertel und W. Wettstein, *Bericht KFK 747,* 1968.

(Eingegangen den 20. Juli, 1970)

Rapid spectrophotometric method for free acid determination in uranyl nitrate and chloride solutions

Though the optical properties of uranium(VI) in nitric acid solutions have been studied in detail[1,2], no successful attempts appear to have been made to use its absorbance for the determination of free acid in such solutions. It has been observed in these laboratories[3] that the absorbance of uranyl nitrate solution increases linearly with increase in acid concentration at the three absorbance maxima at 404, 416 and 426 nm. Based on this observation a rapid spectrophotometric method has been developed for the estimation of free nitric and hydrochloric acids in solutions containing the uranyl ion. The method is applicable for the determination of free acid in the range 0.5–4.0 *M*, unlike the other methods involving complexation of uranium(VI) by oxalate[4] and also automated ion-exchange colorimetry[5] which are useful only for acid concentration of less than 0.1 *M*. The results of these observations are presented in this communication.

Reagents and equipment

Nuclear pure uranyl nitrate and uranyl chloride solutions were used in all experiments. All other chemicals used were of A. R. grade. The uranium content of the solution was determined by the ammonium diuranate method[6] and the free acid was determined potentiometrically[7] as well as by the ion-exchange method.

A Cary-14 automatic recording spectrophotometer was used for scanning the spectra and a Beckman model DU spectrophotometer was employed for measuring the absorbance of solutions.

Method

A series of solutions having the same uranium concentration, C_1 (*e.g.* 20 g l^{-1}), but having different nitric acid concentrations varying from 0.5 *M* to 4.0 *M* were prepared. The absorbances were measured at the three maxima at 404, 416 and 426 nm. The absorbances at these maxima were found to increase linearly with increase in nitric acid concentration[8]. The straight lines obtained were extrapolated to 0.0 *M* nitric acid to obtain the absorbance d_0, of uranyl nitrate solution of concentration C_1, free of nitric acid. The molar absorptivities of uranyl nitrate solutions free of nitric acid were found to be 7.20, 7.97 and 6.19 at 404, 416 and 426 nm respectively. Figure 1 shows typical calibration curves at 404, 416 and 426 nm given as percentage rise in absorbance $[(d_1 - d_0)100/d_0]$, *vs.* nitric acid concentration, where d_1 is the absorbance of uranium solution of concentration, C_1. These calibration curves were used to obtain the free acid in any solution of uranium concentration, C_2, in the following way: the absorbance, d_2, of the solution was measured and from the formula, $d_1 = d_2C_1/C_2$, the absorbance corresponding to concentration, C_1, as well as the percentage rise, were calculated. The free acid in the unknown could then be found by referring to Fig. 1. As can be seen from the Figure, the slope of the straight line at 426 nm is higher than

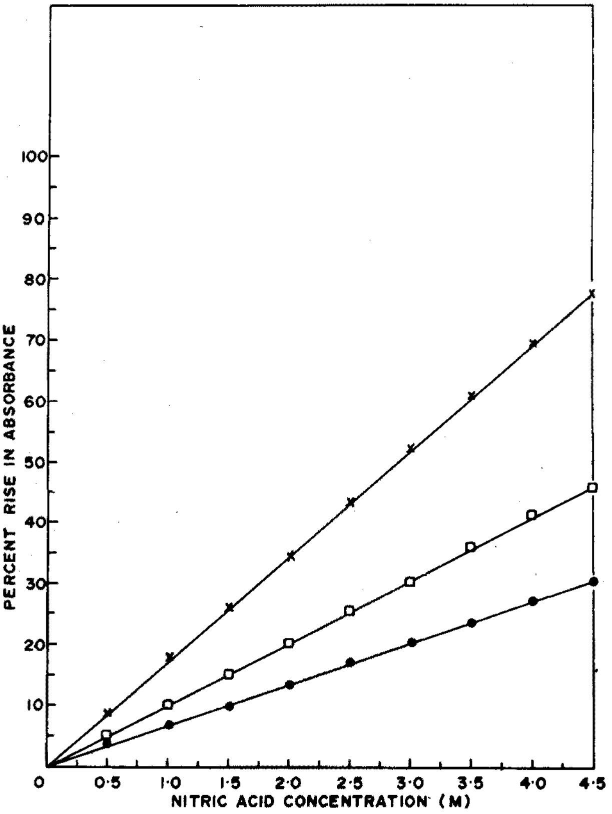

Fig. 1. Calibration curves for free acid at different wavelengths. Uranium concentration, 20 g l^{-1}. (×) 426 nm; (□) 416 nm; (●) 404 nm.

those at the other two wavelengths and accordingly the results were better at this wavelength. Similar results were obtained for the uranyl chloride–hydrochloric acid system and the method works equally well for the determination of hydrochloric acid. Table I gives some typical determinations of free nitric and hydrochloric acids in solutions containing the uranyl ion.

Interferences

Among the interfering ions studied were possible corrosion and fission products like Co(II), Ni(II), Fe(II), Fe(III), Ru(III), Rh(III), Cr(VI) and Ce(IV). The last two ions which have strong absorption in the region 350–450 nm were found to introduce an error of ± 0.1 *M* in the acid determination when they were present upto 0.1% with respect to uranium. The coloured fission products ruthenium(III) and rhodium(III) when present upto 0.25%, and iron(III) upto 5% with respect to uranium, caused no significant error. Iron(III) in amounts larger than 2.5% interfered. Cobalt(II) and nickel(II) upto 5% with respect to uranium caused no error.

Conclusions

The simplicity and reasonable degree of accuracy (± 0.1 *M*) of this method make it attractive for application to industrial process streams such as those in purex processes. The amounts of corrosion and fission products encountered in such streams will not exceed the limits given above and hence will not interfere in the determination. At acidities lower than 0.5 *M*, the increase in absorbance of uranyl ion was small and the results were found to be erroneous, while at acidities greater than 4.0 *M*, the

TABLE I

DETERMINATION OF FREE NITRIC ACID AND HYDROCHLORIC ACID IN URANIUM(VI) SOLUTIONS AT 426 nm

($d_0(HNO_3)^a = 0.52$ for $[U(VI)] = 20.0\ g\ l^{-1}$; $d_0(HCl)^a = 0.29$ for $[U(VI)] = 11.6\ g\ l^{-1}$)

'U' concn. ($g\ l^{-1}$)	*Absorbance*	*Absorbance for C_1 g 'U' l^{-1}*	*% Rise in absorbance w.r.t. d_0*	*Free acid concn. (M)*		*Error*
				Added	*Found*	
$UO_2(NO_3)_2$–HNO_3 system						
5.0	0.143	0.570	9.62	0.5	0.55	+0.05
15.0	0.460	0.613	17.90	1.0	1.03	+0.03
25.0	0.820	0.658	26.54	1.5	1.53	+0.03
15.0	0.560	0.746	43.50	2.5	2.51	+0.01
25.0	1.045	0.835	60.77	3.5	3.50	—
15.0	0.652	0.870	67.50	4.0	3.90	−0.10
UO_2Cl_2–HCl system						
10.0	0.325	0.377	30.0	1.0	1.10	+0.10
15.0	0.563	0.435	50.0	2.0	1.90	−0.10
10.0	0.458	0.532	83.4	3.0	3.10	+0.10
20.0	1.050	0.609	110.0	4.0	4.08	+0.08

[a] Calculated from extinction coefficient at 426 nm.

absorbance maxima shifted to longer wavelengths and the method was not applicable. Though the present method, like conventional methods, requires a prior knowledge of uranium, it offers a simple possibility for continuous monitoring of free acid.

Radiochemistry Division,
Bhabha Atomic Research Centre,
Trombay, Bombay-85 (India)

V. K. Bhargava
E. S. Chandrasekharan
V. K. Rao
R. H. Iyer
M. V. Ramaniah
N. Srinivasan*

1 E. E. Erickson and C. M. Slansky, *N.S.-8*, 1961, p. 83.
2 P. Markl, L. Humblet, H. Wichmann and H. Eschrich, *ETR-221*, 1966.
3 V. K. Bhargava, E. S. Chandrasekharan, R. H. Iyer, V. K. Rao, M. V. Ramaniah and N. Srinivasan, Paper presented at *Convention of Chemists, I.I.T., Kharagpur, Dec. 28–31, 1969.*
4 G. L. Booman, M. C. Elliot, R. B. Kimball, F. O. Cartan and J. E. Rein, *Anal. Chem.*, 30 (1958) 284.
5 R. H. Gaddy and R. S. Dorsett, *Anal. Chem.*, 40 (1968) 428.
6 A. I. Vogel, *A Text Book on Quantitative Inorganic Analysis*, 3rd Edn., Longmans Green, London, 1961, p. 539.
7 C. J. Rodden, *Analytical Chemistry of the Manhattan Project*, McGraw Hill, New York, 1950, p. 214.
8 V. K. Bhargava, E. S. Chandrasekharan, R. H. Iyer, V. K. Rao, M. V. Ramaniah and N. Srinivasan, *BARC report 510* (1970).

(Received July 29th, 1970)

---

* Fuel Reprocessing Division.

Analytica Chimica Acta
Elsevier Publishing Company, Amsterdam
Printed in The Netherlands

ANNOUNCEMENTS

FOURTH EUROPEAN SYMPOSIUM ON FOOD, 1971

The 4th European Symposium on Food with particular reference to progress in food process engineering and in preserving proteins, enzymes and aromas in food, will take place in Prague from July 6 to 9, 1971.

The lectures will be held in the Technical University of Prague, and the conference languages will be English, German and French. The Symposium papers will be published in a volume of the *Dechema-Monographien.*

Further information can be obtained from the Food Working Party, Gesellschaft Deutscher Chemiker, Dr. W. Fritsche, D-6000 Frankfurt, Postfach 119075, Germany.

THIRD INTERNATIONAL CONGRESS OF ABSORPTION SPECTROMETRY AND ATOMIC FLUORESCENCE

Paris
September 27–*October* 1, 1971

The Groupement pour l'Avancement des Méthodes Physiques d'Analyse (GAMS) assisted by Scientific and Industrial Societies is charged with the organisation of the 3rd International Congress of Absorption Spectrometry and Atomic Fluorescence (3rd CISAFA). This congress will take place from September 27 to October 1st 1971 at the Faculté de Pharmacie, 4 avenue de l'Observatoire, Paris VIe.

The congress will be divided into the following sections:

Theory and Methodology
Atomic Fluorescence
Geology
Agriculture
Biology
Metallurgy
Oils and Petroleums
Chemical and Industrial Products
Apparatus and Instrumentation

The titles of communications should be submitted to the Secretariat of the 3rd CISAFA before January 1st 1971, and the summary before April 1st, 1971.

Enquiries on any aspects of the congress should be addressed to: Secrétariat du 3e CISAFA, GAMS, 1, rue Gaston Boissier, Paris XVe, France.

PRELIMINARY ANNOUNCEMENT OF 1971 PITTSBURGH CONFERENCE

The Twenty-second Pittsburgh Conference on Analytical Chemistry and Applied Spectroscopy will be held in Cleveland, Ohio, U.S.A., February 28–March 5, 1971. The headquarters for the meeting will be the Cleveland Convention Center. An estimated 300 papers on all phases of Analytical Chemistry and Spectroscopy will be presented. Symposia on the following subjects are now being arranged.

1. Recent Advances in n.m.r. Spectroscopy
2. Analytical Techniques on the Horizon
3. Pharmaceutical Analysis
4. Trace Atmospheric Contaminants
5. Challenge in the Steel Industry
6. Group Frequencies in Raman Spectroscopy
7. Flame Atomic Absorption and Emission Spectroscopy
8. Liquid Chromatography—New Developments and Applications
9. Coblentz Symposium on Interferometry
10. SSP Award Symposium on Emission Spectroscopy

Papers are *not* restricted to the symposium topics and original papers on *all* phases of analytical chemistry and spectroscopy are invited.

In addition to the program of technical papers, there will be an exhibition of the newest analytical instrumentation. More than 250 companies will display instruments, chemicals and equipment. A complete program of activities for wives and lady attendees at the Conference is also being planned for the 1971 Pittsburgh Conference.

1971 Pittsburgh Conference Chairman
Dr. William G. Fateley
Carnegie-Mellon Univ.,
4400 Fifth Avenue,
Pittsburgh, Pa. 15213, U.S.A.

Exposition Chairman
Charles J. McCafferty
PPG Research Center,
P.O. Box 11472,
Pittsburgh, Pa. 15238, U.S.A.

BOOK ANNOUNCEMENTS

NATIONAL BUREAU OF STANDARDS TECHNICAL NEWS

Reports on the following topics have recently become available:
Improved High-Vacuum Sealing Techniques Devised at NBS (Ref. STR-4102; 1970).
Ion–Molecule Reaction Mass Spectrometer (Ref. STR-4070; 1970).
Improved Accuracy in Thomas-Type One-Ohm Standard Resistor Calibration (Ref. STR-4125; 1970).

Further information on these topics is available from the NBS Office of Technical Information and Publications, National Bureau of Standards, Washington, D.C. 20234, U.S.A.

Galen W. Ewing, *Instrumental Methods of Chemical Analysis*, 3rd Edn., see *Anal. Chim. Acta*, 49 (1970) 605.

This book is now available as a paperback (£ 2.90).

Analytica Chimica Acta
Elsevier Publishing Company, Amsterdam
Printed in The Netherlands

BOOK REVIEWS

G. DRYHURST, *Periodate Oxidation of Diol and other Functional Groups. Analytical and Structural Applications*, Pergamon Press, Oxford, 1970, xii+191 pp., price £3.50

This monograph is the second in a series on organic functional group analysis. A quarter of it is devoted to analytical and practical applications of oxidation by periodate whilst the remainder is concerned with theoretical aspects in the author's belief that analysts should have a clear understanding of the underlying theory and mechanism of this complex reaction. Consequently, there are chapters dealing at length with the theory of the preparation and properties of periodates, the mechanism of periodate oxidation, the anomalous or non-Malapradian oxidations of various organic compounds, many of which contain sulphur and nitrogen, and the use of periodate oxidation in structure determination, such as that of the polysaccharides. Analytical methods are then comprehensively described over 49 pages but it is left to the investigator to decide on an appropriate procedure or to use the text as a guide to the voluminous literature on the subject.

There can be little doubt of the importance of oxidation by periodate; it is one of the most widely studied reactions in organic chemistry, finding multifarious applications, and, in consequence, the literature on the subject is vast. Despite the fact that the determinations of simple diols and of their oxidation products are a relatively simple matter, the mechanism of the reaction is extraordinarily complex and still somewhat controversial. Hence the author's task is a difficult one, but greater emphasis should perhaps have been placed upon practical applications and the choice of suitable procedures. The present state of knowledge is adequately summarised, albeit a little bewilderingly in places, and will be useful information for research workers and analysts, since much of this data have not been summarised previously. However, the author has not been consistent in the use of modern formula and nomenclature and some of the diagrams and mechanisms could have been clearer, hence the book cannot be recommended as an auxiliary text for undergraduate students, but research workers using oxidation by periodate will, undoubtedly, want access to this monograph, as it is a source of valuable information.

L. HOUGH (London)

Infrared Spectroscopy—Its Use in the Coatings Industry, Edited by INFRARED SPECTROSCOPY COMMITTEE, CHICAGO SOCIETY FOR PAINT TECHNOLOGY, Philadelphia, Pa. 19107, 1969, x + 456 pp., price $30.00.

This book is intended to be a comprehensive and modern reference source for spectroscopists in the coatings industry. The early chapters cover the basic theory of infrared spectroscopy and describe in simple terms the development of instrumentation and experimental techniques. The newer sampling techniques, specular reflectance, internal reflection and the use of cesium iodide and KRS-5 plates are mentioned briefly but are not well covered by the bibliography. The chapter on interpretation of qualitative spectra includes specimen interpretations and tables of characteristic absorption frequencies, and shows the advantages and limitations of this analytical technique. The section which describes theoretical aspects of quantitative analysis would be improved if more practical examples were given. A chapter on selected applications completes the text and this is backed up by an extensive bibliography of applications of infrared spectroscopy in the coatings industry.

The major part of the work consists of an extensive catalogue of the infrared spectra of materials used in the U.S. coatings industry, and this section is of international interest. A graduate worker should gain a good introduction to the application of infrared spectroscopy in the coatings industry from the text and the extensive bibliography and the spectra collection would interest any spectroscopist working on such applications.

D. B. BRUCE (Birmingham)

L. S. ETTRE AND W. H. MCFADDEN (Eds.), *Ancillary Techniques of Gas Chromatography*, Wiley–Interscience, New York, 1969, ix+395 pp., Price 165 s.

Recent years have seen a great increase in the coupling of different instrumental or chemical techniques with gas chromatography in order to carry out qualitative analyses of separated eluates. While these techniques are independently well known, there has previously been no general survey of their connexion or interfacing with the gas chromatograph.

The editors, an eminent gas chromatographer and a specialist in instrumental analysis, have remedied this need with a most timely volume in which various authors not only outline each ancillary technique but discuss its applicability and the type of information that it can yield.

The basic principles involved in interfacing are first discussed and there follows a summary of microreaction gas chromatographic techniques. Among the specific ancillary methods discussed, pyrolysis, mass spectrometry and infra-red analysis will probably interest most readers, but many will surely be encouraged in the interfacing of n.m.r., t.l.c. and Raman spectroscopy. Excellent chapters on chemical identification and specific detection are also included.

This is a book which every practising gas chromatographer will wish to possess both as a source volume and as a practical manual.

P. C. UDEN, Birmingham

Anal. Chim. Acta, 53 (1971) 218–219

PAUL G. JEFFERY, *Chemical Methods of Rock Analysis*, International Series of Monographs in Analytical Chemistry, Vol. 36, Pergamon Press Ltd., Oxford, 1970, xv+507 pp., price £7.00.

At least two books dealing with the analysis of geochemical substances have appeared recently, and here we have a third covering much the same subject. It may be that each author has independently felt the need for an up-to-date book on the analysis of rocks and minerals, but now we may be in danger of having too many. This is particularly significant for those who are limited in the number of publications they can buy, and to them a careful assessment of the relative merits of similar publications is important.

The aim of this book is to provide all the practical details necessary for the satisfactory (chemical) determination of major, minor, and trace constituents of silicate rocks and minerals, although extensions of many of the methods described will enable the same procedures, which include flame spectroscopy and atomic-absorption spectrophotometry, to be applied to carbonate and other rocks.

This monograph, written from first-hand experience by a well-known authority on the subject, is comprehensive and deals with the occurrence and determination of nearly sixty elements. The author is to be congratulated on the clarity of his presentation; in the procedural details the carefully selected choice of detail appears to provide adequate information for the successful application of the methods.

W. T. ELWELL (Birmingham)

Anal. Chim. Acta, 53 (1971) 219

R. M. JOHNSON AND I. W. SIDDIQI, *The Determination of Organic Peroxides*, Pergamon Press, Oxford, 1970, ix + 119 pp., price £2.50.

As intermediate products of air oxidation of carbon–hydrogen compounds, and as man-made oxidising and alkylating agents or initiators of free-radical reactions, organic peroxides are of growing interest in various fields of chemistry, including organic synthesis, foodstuffs, pharmaceuticals, fuels, paints, plastics and petrochemicals. Not surprisingly, development of appropriate analytical techniques for peroxides has generally followed independent lines in each field. JOHNSON AND SIDDIQI have collected and reviewed in their monograph information from over 300 published references, covering not only the determination of various types of organic peroxides, but also their separation and identification in mixtures. After two brief introductory chapters in which the novice will find an outline of the uses, structural classification, and reactivity of peroxides, there follows more specialised discussion and description of procedures for titrimetric, colorimetric and polarographic estimation, the interpretation of infrared spectra, and the application of column, paper, thin-layer and gas chromatography.

The book is clearly written and attractively published, but is marred by signs of inadequate proofreading. In addition to trivial errors and inconsistencies, noticeable mainly in the lists of references, it contains examples of confusing ("diperoxides" for dialkyl peroxides) or nonsensical ("2-methyl-but-1-hydroperoxide") organic nomenclature which will mislead the student reader. Some reference numbers (*e.g.* in Table 7.2) have been scrambled and require puzzle-solving ability to follow up. Despite occasional avoidable errors, however, the monograph contains a mass of valuable information and fills a real need. Both the research student and the specialist should find it a useful guide to the applicability of known techniques to their particular problems. The price of the book seems high for its size, but should be recoverable in time saved on literature searching and experimentation with analytical techniques.

A. PAJACZKOWSKI (Welwyn Garden City)

R. C. MACKENZIE (Ed.), *Differential Thermal Analysis*, Vol. 1, Academic Press, London, 1970, xv + 771 pp., price £12.00.

This book is an up-to-date account of the science of differential thermal analysis. Competent authorities from nine countries contribute to a balanced assessment of current thought and status of this field. The book is a must for a novice to the field, and an excellent reference for the current thermal analyst. As a whole, the book is very comprehensible; it has many Tables, Figures and illustrative thermograms. Where useful, pertinent X-ray and thermochemical data are provided in discussing the significance of the thermoanalytical results. It is interdisciplinary, in that various sciences are shown to interrelate in the field of thermal analysis. Excellent ground work is provided for appreciation of the techniques used and the basis for interpretation. For those who are concerned with the direction of development and applications, pertinent conclusions and crystal gazing are provided. Literature references are timely, in that over half date 1960 and later. As a reference book, the user is easily guided by a table of contents for each chapter. There is a good comparison of various instruments, especially useful for someone contemplating the purchase of equipment.

The book is divided into three main sections: *General*, *Inorganic Materials*, and *Organic Materials*. Approximately 15% of the contents deal with organic materials. Therefore, the discussion on the DTA of Organic Materials is relatively weak, in comparison to the inorganic section, which accounts for 60% of the contents.

The *General* section deals with historical background, DTA theory, instrumentation, techniques, and complementary methods. The section on *Inorganic Materials* deals with the DTA of metals and alloys, chalcogenides, oxides and hydroxides, carbonates, simple and complex salts, chlorates and perchlorates, oxysalts, inclusion compounds, and a host of minerals. For each type of material there is a discussion of technique and basis for interpretation. Construction of phase diagrams from DTA curves is well presented. The section on *Organic Materials* deals with the DTA of organic compounds, polymers and biological materials. The discussion of the DTA of biological materials shows the timeliness of this book.

Many principles for methods of analysis, and for interpretation are common to organic and inorganic systems. Therefore, the deficiency on DTA of organic materials is not serious, and the book remains as one of general value to the thermal analyst.

F. NOEL (Sarnia, Ontario)

Thin Layer Chromatography, Edited by E. STAHL, translated by M. R. F. ASHWORTH, 2nd Edn., Allen and Unwin, Ltd., London–Springer Verlag, Berlin, 1969, xxiv + 1041 pp. , price £13.75.

This new edition of *Stahl's Laboratory Manual of Thin-Layer Chromatography* represents a considerable increase in size over the first edition which appeared in 1962. The enormous growth in the literature of TLC in each succeeding year since its inception has given the publishers of this volume the not-inconsiderable problem of keeping the text to a manageable size. As it is, the volume runs to well over 1000 pages.

Professor STAHL has acted as general editor and has contributed chapters on *General Apparatus* and *Special Techniques* in the short *General Section* of the book (200 pages). Other aspects of TLC discussed in this section include *Thin-Layer Electrophoresis, Coupling of GC and TLC, Documentation and Quantitative Evaluation of Thin-layer Chromatograms,* and *Isotope Techniques.*

The much larger special section of the book contains chapters describing the TLC of various types and classes of organic materials, such as terpenes, steroids, vitamins, lipids, alkaloids, indoles, amines and tar bases, synthetic pharmaceutical products, antibiotics, synthetic colouring matters, foodstuffs and their additives, synthetic organic products, plant constituents, amino acids, nucleic acids and sugars. Other chapters consider the use of TLC in chemical diagnosis, the TLC of inorganic ions, and spray reagents. Useful appendices deal with R_F–R_M conversions, a glossary of terms used in TLC in English, French and German, and a list of manufacturers and suppliers of equipment and materials. Extensive author and subject indexes are commendable features of the book.

Professor STAHL has enlisted the help of a number of contributing authors, whose knowledge of specialised TLC separations adds greatly to the authority of this book. It is perhaps unfortunate that publication seems to have been so long delayed since the editor's completion of the manuscript in 1966. Translation has undoubtedly accounted for much of this delay, but Professor ASHWORTH's careful translation is most acceptable and very readable. In such a rapidly expanding field of study, it would have been advantageous to provide supplementary bibliographies which updated the main bibliographies beyond 1966. Nevertheless, this is a most valuable handbook on all aspects of TLC, which should be accessible to all workers concerned with this technique. Its high price rather precludes its purchase by individuals, but most laboratories and institutes with chemical or biochemical interests should possess this standard reference book. This new edition is so much revised and enlarged that it is essentially a new book. Springer's excellent format (much of the book is printed on art paper for better reproduction of the many photographs of chromatograms) completes the impression of a successful production.

W. I. STEPHEN (Birmingham)

D. J. DAVID AND H. B. STALEY (Eds.), *Analytical Chemistry of the Polyurethaues, (Polyurethanes, Part III; High Polymers, Vol. XVI)*, Wiley–Interscience, New York, 1969, xii + 627 pp., price £13.50.

This book forms Part III of a series of volumes on the Polyurethanes. Parts I and II have dealt with the basic chemistry of this class of compounds, but in order to help the reader fully understand the need for the individual analytical methods, the authors of Part III have also considered it necessary to provide a considerable amount of information on the chemistry, preparation and reactions by which the raw materials, intermediates and final polyurethane products are produced. The title of the book, in drawing attention to only one of the salient features of the contents, does not therefore do full justice to the work, which is remarkably comprehensive.

After an introductory chapter the next five chapters are concerned with raw materials such as phosgene, the nitrotoluenes and tolylenediamine; the isocyanates; isocyanate derivatives including urethanes, allophanates, ureas and biurets; polyols; and finally the polyurethanes themselves (62 pages). Each of these chapters or sections within a chapter follows the same general pattern, describing where appropriate the preparation, relevant reactions and the methods used for analysis and characterisation of the product. The polyurethanes are considered in two sections dealing with cellular and non-cellular materials, the latter including cast elastomers, coatings, adhesives and fibres. The volume concludes with some 220 pages summarising in Table-form the physical properties of the isocyanates, and a short but useful chapter on isocyanate toxicity and the determination of toxic concentrations of isocyanates in the atmosphere.

The method of presentation of the introductory and descriptive material makes the subject matter more easily assimilated by the newcomer to this field of technology than it might otherwise have been and the analytical methods are given in sufficient detail to be easily followed. The recommended procedures include both 'wet' methods and modern instrumental techniques such as gas chromatography, ultraviolet, infrared and nuclear magnetic resonance spectroscopy and thermal analysis.

The book is well written, clearly printed and adequately illustrated. The bibliography is extensive and like the parent volume will be of great value to those whose interests concern the analysis of this important class of compounds and their precursers.

D. C. M. SQUIRRELL (Welwyn Garden City)

Selected Readings in Chromatography, Edited by R. J. MAGEE, Commonwealth and International Library of Science, Technology, Engineering and Liberal Sciences, Pergamon Press, Oxford, 1970, vii + 129 pp., price £1.75 (hard cover); £1.25 (flexi-cover).

This modest little volume presents a collection of some of the classical papers on chromatography. TSWETT's original paper (1907) on the separation of the chlorophylls, in which the term "chromatography" is first used, is presented in its original form. This is followed by MARTIN AND SYNGE's paper (1941) on partition chromatography, and KIRCHNER, MILLER AND KELLER's paper (1951) on thin-layer chromatography, which established the great potential of this technique. A classic paper on paper electrophoresis by HAUGAARD AND KRONER (1948) shows the relationship with simple paper chromatography; this leads to a discussion of ion-exchange chromatography and how that technique was used by SEABORG and his colleagues (1954) to establish the chemistry of elements 99 and 100. The final chapter deals with gas chromatography and contains JAMES AND MARTIN's original paper (1951) on the separation of volatile fatty acids.

The tremendous importance of chromatographic methods in analytical processes makes this a valuable little book. In the masses of literature on chromatographic separations, the student all too readily loses the great sense of occasion which surrounds these outstanding original papers, now conveniently brought together. Students and teachers alike will find an absorbing interest in reading these papers on which the whole complex structure of chemical chromatography was founded. The flexi-covered volume may be over-priced for the average student.

W. I. STEPHEN (Birmingham)

VOL. **53** NO. 1 ANALYTICA CHIMICA ACTA JANUARY 1971

CONTENTS

(continued on page 4 of cover)

Continued from inside page of cover

Short Communications

PRINTED IN THE NETHERLANDS